

Mesenchymal Stromal Cells for Kidney Repair

Mesenchymale Stromale cellen voor nierreparatie

Jesús María Sierra Párraga

Copyright © Jesús María Sierra Párraga, the Netherlands, 2020

Cover design and layout: Jesús M. Sierra Parraga

Printing: ProefschriftMaken

The research in this thesis was funded by the Lunbeck Foundation under grant agreement no R198-2015-184.

ISBN 978-94-6380-876-7

All rights reserved. No part of this thesis may be reproduced in any form without written permission from the author or, when appropriate, of the publishers of the publications.

Mesenchymal Stromal Cells for Kidney Repair

Mesenchymale Stromale cellen voor nierreparatie

Thesis

to obtain the degree of Doctor from the

Erasmus University Rotterdam

by command of the

rector magnificus

prof. R.C.M.E. Engels

and in accordance with the decision of the Doctorate Board.

The public defence shall be held on

Tuesday September 1st, 2020 at 15.30 hrs

by

Jesús María Sierra Párraga

born in Córdoba, Spain.

Doctoral Committee

Promotors: Prof. Dr. C. C. Baan

Prof. Dr. B. Jespersen

Other members: Prof. Dr. R. Zietse

Prof. Dr. L. J.W. Van der Laan

Dr. C. K. Holm

Copromotor: Dr. M. J. Hoogduijn

To my family

Table of contents

- Chapter 1** Mesenchymal stromal cells as anti-inflammatory and regenerative mediators for donor kidneys during normothermic machine perfusion.
Stem Cells Dev, 2017, Aug 15;26(16):1162-1170.
- Chapter 2** Concise introduction, aim and outline of the thesis
- Chapter 3** Immunomodulation by Therapeutic Mesenchymal Stromal Cells (MSC) Is Triggered Through Phagocytosis of MSC By Monocytic Cell.
Stem Cells. 2018 Apr;36(4):602-615.
- Chapter 4** Mesenchymal Stromal Cells Are Retained in the Porcine Renal Cortex Independently of Their Metabolic State After Renal Intra-Arterial Infusion.
Stem Cells Dev. 2019 Sep 15;28(18):1224-1235.
- Chapter 5** Reparative effect of mesenchymal stromal cells on endothelial cells after ischemic and inflammatory injury.
(In preparation)
- Chapter 6** Effects of Normothermic Machine Perfusion Conditions on Mesenchymal Stromal Cells.
Front Immunol. 2019 Apr 10; 10:765.
- Chapter 7** Infusing Mesenchymal Stromal Cells into Porcine Kidneys during Normothermic Machine Perfusion: Intact MSCs Can Be Traced and Localised to Glomeruli.
Int. J. Mol. Sci. 2019, 20(14), 3607.
- Chapter 8** Summary and discussion
- Chapter 9** Nederlandse samenvatting
- Chapter 10** Dansk resume
- Chapter 11** Resumen en español
- Appendices** Curriculum vitae
PhD portfolio
List of publications
Acknowledgements

Chapter 1

Mesenchymal stromal cells as anti-inflammatory and regenerative mediators for donor kidneys during normothermic machine perfusion

J.M. Sierra Parraga¹, M. Eijken², J. Hunter³, C. Moers⁴, H. Leuvenink⁴, B. Møller⁵, R.J. Ploeg³, C.C. Baan¹, B. Jespersen⁶, M.J. Hoogduijn¹

¹*Nephrology and Transplantation, Dept. of Internal Medicine, Erasmus MC, University Medical Center, Rotterdam, the Netherlands*

²*Institute of Clinical Medicine, Aarhus University, Denmark*

³*Nuffield Department of Surgical Sciences and Oxford Biomedical Research Centre, University of Oxford, UK*

⁴*Department of Surgery – Organ Donation and Transplantation, University Medical Center Groningen, Groningen, the Netherlands*

⁵*Department of Clinical Immunology, Aarhus University Hospital, Denmark*

⁶*Department of Renal Medicine, Aarhus University Hospital, Aarhus, Denmark*



Abstract

There is a great demand for transplant kidneys for the treatment of end-stage kidney disease patients. To expand the donor pool, organs from older and comorbid brain death donors, so-called expanded criteria donors (ECD), as well as donation after circulatory death donors, are considered for transplantation. However, the quality of these organs may be inferior to standard donor organs. A major issue affecting graft function and survival is ischemia reperfusion injury, which particularly affects kidneys from deceased donors. The development of hypothermic machine perfusion has been introduced in kidney transplantation as a preservation technique and has improved outcomes in ECD and marginal organs compared to static cold storage. Normothermic machine perfusion is the most recent evolution of perfusion technology and allows assessment of the donor organ prior to transplantation. The possibility to control the content of the perfusion fluid offers opportunities for damage control and reparative therapies during machine perfusion. Mesenchymal stromal cells (MSC) have been demonstrated to possess potent regenerative properties via the release of paracrine effectors. The combination of normothermic machine perfusion and MSC administration at the same time is a promising procedure in the field of transplantation. Therefore, the MePEP consortium has been created to study this novel modality of treatment in preparation for human trials. MePEP aims to assess the therapeutic effects of MSC administered ex-vivo by normothermic machine perfusion in the mechanisms of injury and repair in a porcine kidney autotransplantation model.

Introduction

Kidney transplantation is currently the best treatment for end-stage renal disease. However, the success of this treatment depends on the availability and quality of donor kidneys [1] as the number of people on the waiting list to receive an organ keeps rising faster than the availability of donor organs [2]. In 2014, 119,678 transplantations were performed worldwide of which 79,768 were kidney transplants, according to the Global Observatory on Donation and Transplantation. Recent data published by Eurotransplant, National Health Service Blood and Transplant from the UK and the Human Resources and Service Administration from the USA, show that in 2015 141,568 patients were waiting for a transplant in these areas, of which 82% were in need of a kidney transplant.

This situation has resulted in the extension of the minimal criteria required for a person to be a potential donor regarding age and health conditions [3], as well as a more widespread use of donation after cardiac death (DCD) organs. A donor is classified as expanded criteria donor (ECD) by being older than 60 years or older than 50 years and suffering from two out of these three: hypertension, having a cerebrovascular cause of death and a serum creatinine concentration above 1.5 mg/dl at the time of organ donation [4]. Thus, more kidneys will be used for transplantation, thereby reducing the time people have to wait for a kidney, but at the cost of a higher risk of primary nonfunction (PNF) and delayed graft function, as well as inferior graft function and graft survival.

Increase in available kidneys, decrease in quality

Organs from circulatory death donors are increasingly considered for transplantation. DCD organs have a prolonged period of warm ischemia prior to retrieval and higher risk of PNF and poorer organ quality. Delayed graft function defined as need of dialysis occurs in 24% of the transplant recipients in standard criteria donation. Delayed graft function in DCD donors have been reported in up to 52% of the recipients [5] and for ECD donors it is a 70% higher than SCD donation [6]. Primarily, organs from brain death donors are used for transplantation. Brain death induces a massive release of inflammatory cytokines such as tumor necrosis factor α (TNF- α) and IL-6 in the potential donor [7], which is associated with an elevated risk of delayed graft function [8,9]. Donation after brain death is correlated with more rejection and inferior graft survival [10,11] whereas delayed graft function is similar to DCD donation [12].

Chapter 1

Despite increasing the number of kidneys available for transplantation, ECD organs have been shown to have a poorer outcome when compared to standard criteria transplantation [13,14]. Graft function from ECD has been proven to be inferior to kidneys from standard donors [3,6] and combined with lower graft survival this may explain inferior patient survival.

Ischemia reperfusion injury

An inherent problem of organ transplantation regardless of the type of donor is ischemia reperfusion injury (IRI). During ischemia, the lack of nutrients causes metabolic disruption. Lack of oxygen supply stops aerobic metabolism and leads to accumulation of waste products resulting in a toxic environment. The reactivation of cells at the time of reperfusion is accompanied by the formation of reactive oxygen species and an inflammatory response in the organ [15], which is a primary cause of acute kidney injury (AKI) [16]. Both ischemia time and reperfusion can be optimized to reduce oxidative damage and inflammatory response and hence improve organ quality.

Towards improving kidney transplantation outcome

Since ischemia is a major cause of inflammation, new strategies have arisen to improve preservation techniques and reduce the time that organs are starved of nutrients and oxygen. Machine perfusion of donor organs is an alternative to static cold storage, which has been the standard method for preserving organs so far. Machine perfusion involves connecting the kidney to a circuit which will pump and recirculate a perfusion fluid. Machine perfusion can be carried out at different temperatures and settings. Hypothermic machine perfusion (HMP) has been demonstrated to improve the outcome of renal transplantation [17,18]. Normothermic machine perfusion (NMP) has the advantage that kidney function can be assessed during preservation prior to transplantation [19]. Currently, several perfusion conditions are being tested to achieve the best possible outcome such as different temperatures, perfusion characteristics or fluid composition.

Hypothermic machine perfusion

HMP as an alternative to cold storage has been proven to be effective in improving kidney function in animal models through two main postulated mechanisms: preservation of

endothelial function by maintaining the expression of key genes such as eNOS, which improve circulation during reperfusion [20], and reducing the activation of caspases, meaning that HMP may have a protective role on cell apoptosis [21]. Human studies have shown that HMP reduces inflammation by decreasing the secretion of inflammatory cytokines and thus, decreasing the severity of IRI [22].

Normothermic machine perfusion

To further improve the physiological conditions for kidney transplants, NMP has been developed. This technique allows to maintain the metabolic requirements of the organ and reduce the ischemic injury by perfusing it with a fluid at physiological temperature which is supplemented with nutrients and oxygen. This technique is useful to reduce cold ischemia and additionally it offers the possibility of assessing organ viability prior to transplantation [23]. In the only published clinical series, this procedure has been proved to decrease delayed graft function in kidneys, particularly in ECD organs [23,24].

Introduction of other therapies during machine perfusion

NMP offers the possibility of monitoring kidney function and perfusion fluid content can be measured permanently in such a way that it is possible to perform metabolic profiling during perfusion [25,26]. This is translated in the possibility to add other therapies such as pharmacologic treatments in a very controlled manner [27-29]. Drug delivery during machine perfusion has been proven effective in reducing IRI during NMP[30]. Cell therapy is also a very interesting option to be used during ex-vivo perfusion. Mesenchymal stromal cells (MSC) have potential for regeneration and interaction with the immune system [31,32] and could be administered prior to transplantation during NMP.

Mesenchymal stromal cells

MSC are adult stem cells with the ability to differentiate into several cellular lineages [33-35]. They are usually retrieved from bone marrow [36] and adipose tissue [37], but MSC are present in almost every adult tissue [38,39]. The interest in the use of MSC for therapy is based on the easy expansion of these cells in vitro, their regenerative and immunomodulatory effects and low immunogenicity. The lack of expression of MHC class II and low expression of

Chapter 1

MHC class I and co-stimulatory molecules [40] make them poorly recognizable by the adaptive immune system. Several studies have demonstrated that MSC derived from bone marrow and adipose tissue are immunosuppressive and suppress alloreactivity [31,32,41].

MSC, therefore, have been tested and proved to possess regenerative and immunomodulatory properties, and results of preclinical studies qualify them as a very promising therapeutic agent [42], although possible detrimental side effects have still not been fully explored.

MSC as mediators of healing

MSC interact with injured tissue and cells of the immune system in multiple ways. MSC have been shown to release a wide variety of growth factors and immunomodulatory cytokines which change the microenvironment at sites of injury [43] affecting the immune response and tissue regeneration [44-47]. Specifically, stromal cell-derived factor 1 is secreted by endothelial cells (EC) during hypoxic conditions [48] enhancing the recruitment of MSC [48-51]. As a result of oxygen deprivation, EC also secrete hepatocyte growth factor (HGF) [52], which has been shown to increase EC growth [53] and stimulates MSC migration [54]. MSC express the HGF receptor c-met allowing MSC homing to injured endothelium. MSC themselves secrete HGF and via autocrine signaling remain present at the site of injury [54,55]. MSC also help to repair wounds and have anti-fibrotic effects that avoid the formation of scar tissue [56] via paracrine secretion of proangiogenic factors [57] and increasing keratinocyte and fibroblast migration towards injured tissue [58].

In addition, MSC exert angiogenic effects by secreting a variety of growth factors. Simultaneous release of HGF and vascular endothelial growth factor by MSC has been found to reduce endothelial permeability during inflammation [59] and enhance angiogenesis [60]. Moreover, vasculature integrity is protected through angiopoietin-1 interaction with EC [61] while thrombospondin-1 protects platelet-derived growth factor from degradation and therefore enhances angiogenesis [62]. Matrix metalloproteases (MMP) are released under inflammatory conditions [63] and degrade collagen extracellular matrix. MSC inhibit MMP-related tissue disruption by releasing tissue inhibitor of metalloproteases, which bind to MMP in a competitive manner and maintain matrix structure [64].

In addition to their tissue protective and regenerative effects, MSC are potent mediators in reversing inflammatory processes. Several of the immunoregulatory effects of MSC are

potentiated under inflammatory conditions. Expression of inhibitory molecules such as programmed death-ligand 1 on MSC membranes suppress immune cell activation and proliferation [65,66]. Pro-inflammatory macrophage activation is inhibited via secretion of TNF- α stimulated gene 6 by MSC, which at the same time prevents TNF- α secretion from macrophages and reduces inflammation [56]. Furthermore, prostaglandin E2 (PGE2) induces an M1 to M2 macrophage shift, and activates proliferation and survival genes in human umbilical vein endothelial cells [67]. At the same time PGE2 induces Th2 lymphocyte formation [68] and regulatory T-cell proliferation [69,70]. Moreover, MSC inhibit effector T-cell proliferation [31,71,72] by depleting the tryptophan from the medium as a result of indoleamine 2,3-dioxygenase secretion [72-74].

MSC function is also based on cell-to-cell membrane interaction. Mesenchymal and endothelial cell interaction at injured tissue is well documented [75]. Furthermore, crosstalk between MSC and immune cells impair their homing [76,77] and proliferation [78]. MSC express a range of cell surface molecules that enable them to interact with immune and tissue cells. MSC express very late antigen, therefore they can bind to EC via vascular cell adhesion molecule and P-selectin on the surface of endothelial cells [79,80].

Thus, the concerted action of soluble and membrane bound molecules is responsible for the tissue protective and immunoregulatory effects of MSC.

MSC in kidney injury animal models

MSC therapy has the potential to limit IRI-induced damage, to stimulate regenerative activity in the kidney. Multiple studies have tried to prove the beneficial effect of MSC on tissue injury and inflammation in animal models with very promising results. Post-transplantation immune system modulation and IRI-induced AKI animal models have been developed to test the effect of MSC therapy. In a renal allograft transplantation model in rat, intra-arterial MSC injection resulted in improved early kidney function, reduction of lymphocyte infiltration and decreased inflammation-related gene expression [81]. In an IRI model, reduced infiltration of immune cells in the kidney was also observed after MSC infusion [82]. In large-animal models it has been found that administration of MSC improves kidney function after transplantation, restoring the glomerular filtration rate and decreasing tissue inflammation [83,84]. In a renal injury porcine model, administration of MSC resulted in a decreased kidney concentration of TNF- α and IL-1 β and restoration of IL-10 levels [83]. In a cisplatin-induced AKI rhesus monkey

model, MSC infusion through the renal artery seemed to improve renal function and decrease serum creatinine concentration [84].

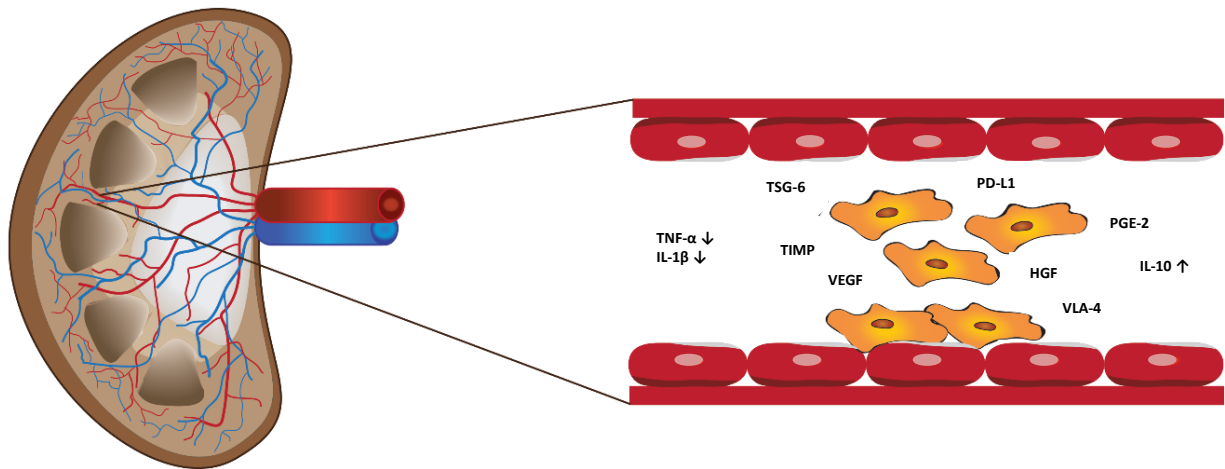


Figure 1. Interaction of MSC with the endothelium. The endothelial cells of the microvasculature of the kidney are the first cells MSC encounter after administration via the renal artery. MSC release a wide variety of anti-inflammatory and regenerative factors, which may interact with endothelial cells by reducing inflammatory responses and stimulate regenerative responses. Molecules present on the membrane of MSC such as PD-L1 and VLA-4 may provide further reparative signals to the endothelium. MSC, mesenchymal stromal cells; PD-L1, programmed death-ligand 1; VLA-4, very late antigen.

Clinical use of MSC in kidney transplantation

The encouraging results from preclinical studies have led to test the safety of MSC therapy as treatment for several conditions [85-87]. Hence, a number of small clinical trials have studied the feasibility and effects of MSC cell therapy focusing on kidney transplant recipients. In these studies, MSC administration showed no deleterious effects on graft or patient survival [31,88,89]. Furthermore, there are indications that MSC treatment modulated the immune response of these patients. This has led to the presumption that the use of MSC might allow reduction of immunosuppressive drugs without elevating the incidence of rejection [88]. However, the administration of MSC as treatment of kidney transplant recipients via intravenous infusion has some practical limitations. Intravenously administered MSC are trapped in the micro-capillaries of the lungs, are not capable of migrating towards injured kidneys [90,91] and may at least theoretically cause pulmonary embolism [92]. Targeted administration of MSC into the kidney in an ex-vivo organ perfusion system offers the possibility to bring MSC in direct contact with injured kidney cells and the possibility of a beneficial effect with a relatively low number of cells.

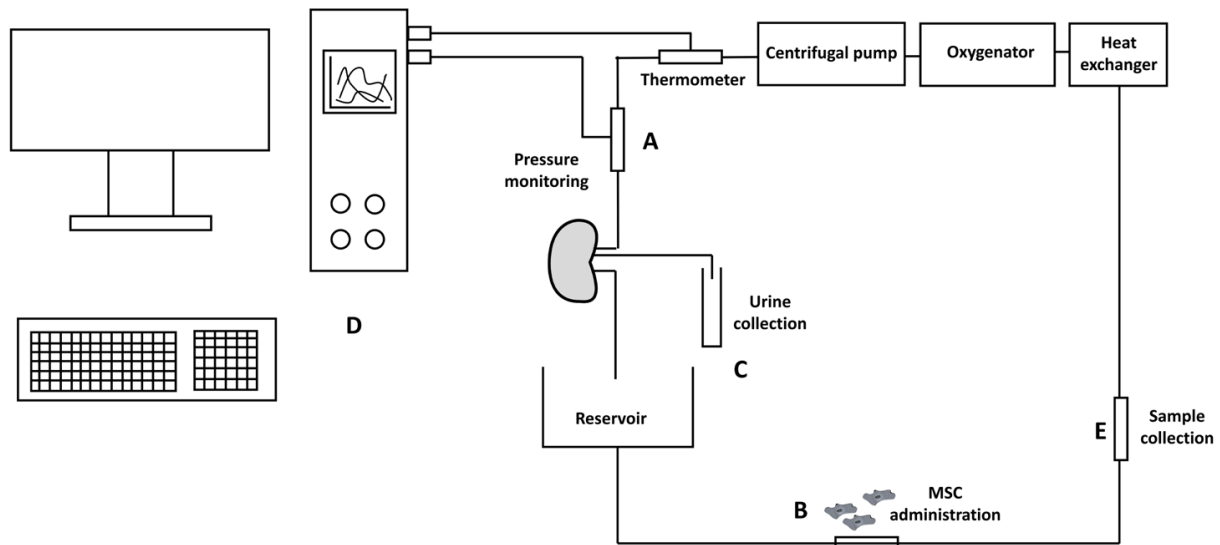


Figure 2. Schematic drawing of a kidney connected to a perfusion machine. The renal artery is connected to a pump and also the ureter is cannulated (A). MSC are added to the perfusion fluid containing oxygen and nutrients (B). From the cannulated ureter, urine is collected for analysis (C). Perfusion pressure, flow, temperature, and oxygen saturation can be continuously monitored (D) and nutrient and waste product concentrations can be frequently sampled (E).

Mesenchymal stem cells in normothermic ex-vivo PERfusion in Pigs: The MePEP Project

MSC therapy has the potential to limit IRI-induced damage, to stimulate regenerative activity in the kidney, and to reduce the use of immunosuppressive drugs in the transplant recipient. Machine perfusion offers the possibility to apply MSC therapy directly to donor kidneys ex-vivo and by-pass the lung barrier. To investigate the use of MSC for this purpose, an international consortium has been created with the goal of developing a pre-transplant therapy based on MSC and NMP to improve the quality of donor kidneys.

Administration of MSC to donor kidneys via machine perfusion (figure 1) delivers MSC directly to the injured organ and possibly in direct contact to injured tissue. The addition of MSC to the perfusion fluid may lead to their adherence to the injured endothelium. This may enable them to interact with endothelial cells both physically [93,94] and via cytokine secretion.

When donor organs are reperfused, the release of reactive oxygen species occurs, leading to organ damage and inflammation [15,95]. NMP in combination with MSC may potentially attenuate the inflammatory processes and regenerate injured tissue, eventually leading to reduced fibrosis and better patient outcomes with improved graft survival [46,56]. Localized secretion of immunomodulatory effectors may be able to modulate the immune response of

Chapter 1

the host after transplantation, decreasing rejection and improving early graft function. Studies within the MePEP project will attempt to resuscitate the kidney before transplantation in order to reduce the severity of IRI and its consequences. In addition, optimal growth conditions and pretreatment of MSC as well as administration of the cells will be studied together with possible side effects in a porcine autotransplantation model.

In summary, the shortage of kidneys for transplantation is leading to the acceptance of lower quality organs for transplantation in an effort to increase the number of transplanted patients and reduce waiting times. The main objective of this research is to develop a procedure based on NMP and MSC to improve the quality of transplanted organs, as well as the reduction of the immune response against the transplanted kidney by the host. If the results from these large animal studies will be favorable, human studies will follow. Ex-vivo MSC therapy could eventually lead to more and better donor kidneys for transplantation and an increase in patient and graft survival, with less use of immunosuppressive drugs.

References

1. Abecassis M, ST Bartlett, AJ Collins, CL Davis, FL Delmonico, JJ Friedewald, R Hays, A Howard, E Jones, AB Leichtman, RM Merion, RA Metzger, F Pradel, EJ Schweitzer, RL Velez and RS Gaston. (2008). Kidney transplantation as primary therapy for end-stage renal disease: a National Kidney Foundation/Kidney Disease Outcomes Quality Initiative (NKF/KDOQIM) conference. *Clin J Am Soc Nephrol* 3:471-80.
2. Hippen B, LF Ross and RM Sade. (2009). Saving lives is more important than abstract moral concerns: financial incentives should be used to increase organ donation. *Ann Thorac Surg* 88:1053-61.
3. Ojo AO. (2005). Expanded criteria donors: process and outcomes. *Semin Dial* 18:463-8.
4. Stratta RJ, MS Rohr, AK Sundberg, G Armstrong, G Hairston, E Hartmann, AC Farney, J Roskopf, SS Iskandar and PL Adams. (2004). Increased kidney transplantation utilizing expanded criteria deceased organ donors with results comparable to standard criteria donor transplant. *Ann Surg* 239:688-95; discussion 695-7.
5. Rao PS and A Ojo. (2009). The alphabet soup of kidney transplantation: SCD, DCD, ECD--fundamentals for the practicing nephrologist. *Clin J Am Soc Nephrol* 4:1827-31.
6. Metzger RA, FL Delmonico, S Feng, FK Port, JJ Wynn and RM Merion. (2003). Expanded criteria donors for kidney transplantation. *Am J Transplant* 3 Suppl 4:114-25.
7. Azarpira N, S Nikeghbalian, K Kazemi, B Geramizadeh, Z Malekpour and SA Malek-Hosseini. (2013). Association of Increased Plasma Interleukin-6 and TNF- α Levels in Donors with the Complication Rates in Liver Transplant Recipients. *International Journal of Organ Transplantation Medicine* 4:9-14.
8. Watts RP, O Thom and JF Fraser. (2013). Inflammatory signalling associated with brain dead organ donation: from brain injury to brain stem death and posttransplant ischaemia reperfusion injury. *J Transplant* 2013:521369.
9. Vergoulas G, P Boura and G Efstathiadis. (2009). Brain dead donor kidneys are immunologically active: is intervention justified? *Hippokratia* 13:205-210.
10. Ponticelli C. (2014). Ischaemia-reperfusion injury: a major protagonist in kidney transplantation. *Nephrol Dial Transplant* 29:1134-40.
11. Yarlagadda SG, SG Coca, RN Formica, Jr., ED Poggio and CR Parikh. (2009). Association between delayed graft function and allograft and patient survival: a systematic review and meta-analysis. *Nephrol Dial Transplant* 24:1039-47.
12. Siedlecki A, W Irish and DC Brennan. (2011). Delayed graft function in the kidney transplant. *Am J Transplant* 11:2279-96.
13. Nagaraja P, GW Roberts, M Stephens, S Horvath, Z Kaposztas, R Chavez and A Asderakis. (2015). Impact of expanded criteria variables on outcomes of kidney transplantation from donors after cardiac death. *Transplantation* 99:226-31.
14. Pascual J, J Zamora and JD Pirsch. (2008). A systematic review of kidney transplantation from expanded criteria donors. *Am J Kidney Dis* 52:553-86.
15. Jang HR, GJ Ko, BA Wasowska and H Rabb. (2009). The interaction between ischemia-reperfusion and immune responses in the kidney. *J Mol Med (Berl)* 87:859-64.
16. Basile DP, MD Anderson and TA Sutton. (2012). Pathophysiology of acute kidney injury. *Compr Physiol* 2:1303-53.

Chapter 1

17. Salvadori M, G Rosso and E Bertoni. (2015). Update on ischemia-reperfusion injury in kidney transplantation: Pathogenesis and treatment. *World Journal of Transplantation* 5:52-67.
18. Moers C, JM Smits, MH Maathuis, J Treckmann, F van Gelder, BP Napieralski, M van Kasterop-Kutz, JJ van der Heide, JP Squifflet, E van Heurn, GR Kirste, A Rahmel, HG Leuvenink, A Paul, J Pirenne and RJ Ploeg. (2009). Machine perfusion or cold storage in deceased-donor kidney transplantation. *N Engl J Med* 360:7-19.
19. Kathis JM, VN Spetzler, N Goldaracena, J Echeverri, KS Louis, DB Foltys, M Stempel, P Yip, R John, I Mucsi, A Ghanekar, D Bagli, L Robinson and M Selzner. (2015). Normothermic Ex Vivo Kidney Perfusion for the Preservation of Kidney Grafts prior to Transplantation. *J Vis Exp*:e52909.
20. Chatauret N, R Coudroy, PO Delpesch, C Vandebrouck, S Hosni, M Scepi and T Hauet. (2014). Mechanistic analysis of nonoxygenated hypothermic machine perfusion's protection on warm ischemic kidney uncovers greater eNOS phosphorylation and vasodilation. *Am J Transplant* 14:2500-14.
21. Zhang Y, Z Fu, Z Zhong, R Wang, L Hu, Y Xiong, Y Wang and Q Ye. (2016). Hypothermic Machine Perfusion Decreases Renal Cell Apoptosis During Ischemia/Reperfusion Injury via the Ezrin/AKT Pathway. *Artif Organs* 40:129-35.
22. Tozzi M, M Franchin, G Soldini, G letto, C Chiappa, E Maritan, F Villa, G Carcano and R Dionigi. (2013). Impact of static cold storage VS hypothermic machine preservation on ischemic kidney graft: inflammatory cytokines and adhesion molecules as markers of ischemia/reperfusion tissue damage. Our preliminary results. *Int J Surg* 11 Suppl 1:S110-4.
23. Nicholson ML and SA Hosgood. (2013). Renal transplantation after ex vivo normothermic perfusion: the first clinical study. *Am J Transplant* 13:1246-52.
24. Hosgood SA and ML Nicholson. (2011). First in man renal transplantation after ex vivo normothermic perfusion. *Transplantation* 92:735-8.
25. Bruinsma BG, GV Sridharan, PD Weeder, JH Avruch, N Saeidi, S Ozer, S Geerts, RJ Porte, M Heger, TM van Gulik, PN Martins, JF Markmann, H Yeh and K Uygun. (2016). Metabolic profiling during ex vivo machine perfusion of the human liver. *Sci Rep* 6:22415.
26. Bon D, N Chatauret, S Giraud, R Thuillier, F Favreau and T Hauet. (2012). New strategies to optimize kidney recovery and preservation in transplantation. *Nat Rev Nephrol* 8:339-47.
27. van Rijt WG, N Secher, AK Keller, U Møldrup, Y Chynau, RJ Ploeg, H van Goor, R Nørregaard, H Birn, J Frøkiaer, S Nielsen, HGD Leuvenink and B Jespersen. (2014). α -Melanocyte Stimulating Hormone Treatment in Pigs Does Not Improve Early Graft Function in Kidney Transplants from Brain Dead Donors. *PLoS ONE* 9:e94609.
28. van Rijt WG, GJ Nieuwenhuijs-Moeke, H van Goor, PJ Ottens, RJ Ploeg and HGD Leuvenink. (2013). Renoprotective capacities of non-erythropoietic EPO derivative, ARA290, following renal ischemia/reperfusion injury. *Journal of Translational Medicine* 11:286-286.
29. Yang B, SA Hosgood, A Bagul, HL Waller and ML Nicholson. (2011). Erythropoietin regulates apoptosis, inflammation and tissue remodelling via caspase-3 and IL-1 β in isolated hemoperfused kidneys. *Eur J Pharmacol* 660:420-30.
30. Hunter JP, SA Hosgood, M Patel, R Rose, K Read and ML Nicholson. (2012). Effects of hydrogen sulphide in an experimental model of renal ischaemia-reperfusion injury. *Br J Surg* 99:1665-71.
31. Roemeling-van Rhijn M, M Khairoun, SS Korevaar, E Liewers, DG Leuning, JN Ijzermans, MG Betjes, PG Genever, C van Kooten, HJ de Fijter, TJ Rabelink, CC Baan, W Weimar, H Roelofs, MJ Hoogduijn and ME Reinders. (2013). Human Bone Marrow- and Adipose Tissue-derived Mesenchymal Stromal Cells are Immunosuppressive In vitro and in a Humanized Allograft Rejection Model. *J Stem Cell Res Ther Suppl* 6:20780.

32. Casiraghi F, N Azzollini, P Cassis, B Imberti, M Morigi, D Cugini, RA Cavinato, M Todeschini, S Solini, A Sonzogni, N Perico, G Remuzzi and M Noris. (2008). Pretransplant infusion of mesenchymal stem cells prolongs the survival of a semiallogeneic heart transplant through the generation of regulatory T cells. *J Immunol* 181:3933-46.
33. Beyer Nardi N and L da Silva Meirelles. (2006). Mesenchymal Stem Cells: Isolation, In Vitro Expansion and Characterization. In: *Stem Cells*. Wobus AM and KR Boheler eds. Springer Berlin Heidelberg, Berlin, Heidelberg. pp 249-282.
34. Krampera M, M Franchini, G Pizzolo and G Aprili. (2007). Mesenchymal stem cells: from biology to clinical use. *Blood Transfusion* 5:120-129.
35. Pittenger MF, AM Mackay, SC Beck, RK Jaiswal, R Douglas, JD Mosca, MA Moorman, DW Simonetti, S Craig and DR Marshak. (1999). Multilineage potential of adult human mesenchymal stem cells. *Science* 284:143-7.
36. Wexler SA, C Donaldson, P Denning-Kendall, C Rice, B Bradley and JM Hows. (2003). Adult bone marrow is a rich source of human mesenchymal 'stem' cells but umbilical cord and mobilized adult blood are not. *Br J Haematol* 121:368-74.
37. Zuk PA, M Zhu, P Ashjian, DA De Ugarte, JI Huang, H Mizuno, ZC Alfonso, JK Fraser, P Benhaim and MH Hedrick. (2002). Human adipose tissue is a source of multipotent stem cells. *Mol Biol Cell* 13:4279-95.
38. da Silva Meirelles L, PC Chagastelles and NB Nardi. (2006). Mesenchymal stem cells reside in virtually all post-natal organs and tissues. *J Cell Sci* 119:2204-13.
39. Hoogduijn MJ, MJ Crop, AM Peeters, GJ Van Osch, AH Balk, JN Ijzermans, W Weimar and CC Baan. (2007). Human heart, spleen, and perirenal fat-derived mesenchymal stem cells have immunomodulatory capacities. *Stem Cells Dev* 16:597-604.
40. Jacobs SA, VD Roobrouck, CM Verfaillie and SW Van Gool. (2013). Immunological characteristics of human mesenchymal stem cells and multipotent adult progenitor cells. *Immunol Cell Biol* 91:32-9.
41. Dahlke MH, M Hoogduijn, E Eggenhofer, FC Popp, P Renner, P Slowik, A Rosenauer, P Piso, EK Geissler, C Lange, D Chabannes, B Mazzanti, S Bigenzahn, P Bertolino, U Kunter, M Introna, A Rambaldi, C Capelli, N Perico, F Casiraghi, M Noris, E Gotti, M Seifert, R Saccardi, HW Verspaget, B van Hoek, A Bartholomew, T Wekerle, HD Volk, G Remuzzi, R Deans, H Lazarus, HJ Schlitt, CC Baan and MS Group. (2009). Toward MSC in solid organ transplantation: 2008 position paper of the MISOT study group. *Transplantation* 88:614-9.
42. Franquesa M, MJ Hoogduijn, ME Reinders, E Eggenhofer, AU Engela, FK Mensah, J Torras, A Pileggi, C van Kooten, B Mahon, O Detry, FC Popp, V Benseler, F Casiraghi, C Johnson, J Ancans, B Fillenberg, O delaRosa, JM Aran, M Roemeling-van Rhijn, J Pinxteren, N Perico, E Gotti, B Christ, J Reading, M Introna, R Deans, M Shagidulin, R Farre, A Rambaldi, A Sanchez-Fueyo, N Obermajer, A Pulin, FJ Dor, I Portero-Sanchez, CC Baan, TJ Rabelink, G Remuzzi, MG Betjes, MH Dahlke, JM Grinyo and SOTSG Mi. (2013). Mesenchymal Stem Cells in Solid Organ Transplantation (MiSOT) Fourth Meeting: lessons learned from first clinical trials. *Transplantation* 96:234-8.
43. Caplan AI and D Correa. (2011). The MSC: an injury drugstore. *Cell Stem Cell* 9:11-5.
44. Caplan AI. (2007). Adult mesenchymal stem cells for tissue engineering versus regenerative medicine. *J Cell Physiol* 213:341-7.
45. Linero I and O Chaparro. (2014). Paracrine effect of mesenchymal stem cells derived from human adipose tissue in bone regeneration. *PLoS One* 9:e107001.
46. Baraniak PR and TC McDevitt. (2010). Stem cell paracrine actions and tissue regeneration. *Regen Med* 5:121-43.

Chapter 1

47. Prockop DJ and JY Oh. (2012). Mesenchymal stem/stromal cells (MSCs): role as guardians of inflammation. *Mol Ther* 20:14-20.
48. Ohnishi H, S Mizuno, Y Mizuno-Horikawa and T Kato. (2015). Stromal cell-derived factor-1 (SDF1)-dependent recruitment of bone marrow-derived renal endothelium-like cells in a mouse model of acute kidney injury. *Journal of Veterinary Medical Science* 77:313-319.
49. Li J, S Liu, W Li, S Hu, J Xiong, X Shu, Q Hu, Q Zheng and Z Song. (2012). Vascular Smooth Muscle Cell Apoptosis Promotes Transplant Arteriosclerosis Through Inducing the Production of SDF-1 alpha. *American Journal of Transplantation* 12:2029-2043.
50. De Becker A and IV Riet. (2016). Homing and migration of mesenchymal stromal cells: How to improve the efficacy of cell therapy? *World J Stem Cells* 8:73-87.
51. Marquez-Curtis LA and A Janowska-Wieczorek. (2013). Enhancing the migration ability of mesenchymal stromal cells by targeting the SDF-1/CXCR4 axis. *Biomed Res Int* 2013:561098.
52. Morishita R, S Nakamura, Y Nakamura, M Aoki, A Moriguchi, I Kida, Y Yo, K Matsumoto, T Nakamura, J Higaki and T Ogihara. (1997). Potential role of an endothelium-specific growth factor, hepatocyte growth factor, on endothelial damage in diabetes. *Diabetes* 46:138-42.
53. Nakano N, R Morishita, A Moriguchi, Y Nakamura, SI Hayashi, M Aoki, I Kida, K Matsumoto, T Nakamura, J Higaki and T Ogihara. (1998). Negative regulation of local hepatocyte growth factor expression by angiotensin II and transforming growth factor-beta in blood vessels: potential role of HGF in cardiovascular disease. *Hypertension* 32:444-51.
54. Neuss S, E Becher, M Woltje, L Tietze and W Jahnen-Dechent. (2004). Functional expression of HGF and HGF receptor/c-met in adult human mesenchymal stem cells suggests a role in cell mobilization, tissue repair, and wound healing. *Stem Cells* 22:405-14.
55. *Stem Cells and Revascularization Therapies*. CRC Press. Taylor & Francis Group.
56. Qi Y, D Jiang, A Sindrilaru, A Stegemann, S Schatz, N Treiber, M Rojewski, H Schrezenmeier, S Vander Beken, M Wlaschek, M Bohm, A Seitz, N Scholz, L Durselen, J Brinckmann, A Ignatius and K Scharffetter-Kochanek. (2014). TSG-6 released from intradermally injected mesenchymal stem cells accelerates wound healing and reduces tissue fibrosis in murine full-thickness skin wounds. *J Invest Dermatol* 134:526-37.
57. Wu Y, L Chen, PG Scott and EE Tredget. (2007). Mesenchymal stem cells enhance wound healing through differentiation and angiogenesis. *Stem Cells* 25:2648-59.
58. Lee DE, N Ayoub and DK Agrawal. (2016). Mesenchymal stem cells and cutaneous wound healing: novel methods to increase cell delivery and therapeutic efficacy. *Stem Cell Res Ther* 7:37.
59. Yang Y, QH Chen, AR Liu, XP Xu, JB Han and HB Qiu. (2015). Synergism of MSC-secreted HGF and VEGF in stabilising endothelial barrier function upon lipopolysaccharide stimulation via the Rac1 pathway. *Stem Cell Res Ther* 6:250.
60. Burlacu A, G Grigorescu, AM Rosca, MB Preda and M Simionescu. (2013). Factors secreted by mesenchymal stem cells and endothelial progenitor cells have complementary effects on angiogenesis in vitro. *Stem Cells Dev* 22:643-53.
61. Zacharek A, J Chen, X Cui, A Li, Y Li, C Roberts, Y Feng, Q Gao and M Chopp. (2007). Angiopoietin1/Tie2 and VEGF/Flk1 induced by MSC treatment amplifies angiogenesis and vascular stabilization after stroke. *J Cereb Blood Flow Metab* 27:1684-91.
62. Belotti D, C Capelli, A Resovi, M Introna and G Taraboletti. (2016). Thrombospondin-1 promotes mesenchymal stromal cell functions via TGFbeta and in cooperation with PDGF. *Matrix Biol* 55:106-116.

63. Xu X, PL Jackson, S Tanner, MT Hardison, M Abdul Roda, JE Blalock and A Gaggari. (2011). A self-propagating matrix metalloprotease-9 (MMP-9) dependent cycle of chronic neutrophilic inflammation. *PLoS One* 6:e15781.
64. Lozito TP and RS Tuan. (2011). Mesenchymal stem cells inhibit both endogenous and exogenous MMPs via secreted TIMPs. *J Cell Physiol* 226:385-96.
65. Luz-Crawford P, D Noel, X Fernandez, M Khoury, F Figueroa, F Carrion, C Jorgensen and F Djouad. (2012). Mesenchymal stem cells repress Th17 molecular program through the PD-1 pathway. *PLoS One* 7:e45272.
66. Wang WB, ML Yen, KJ Liu, PJ Hsu, MH Lin, PM Chen, PR Sudhir, CH Chen, CH Chen, HK Sytwu and BL Yen. (2015). Interleukin-25 Mediates Transcriptional Control of PD-L1 via STAT3 in Multipotent Human Mesenchymal Stromal Cells (hMSCs) to Suppress Th17 Responses. *Stem Cell Reports* 5:392-404.
67. Vasandan AB, S Jahnavi, C Shashank, P Prasad, A Kumar and SJ Prasanna. (2016). Human Mesenchymal stem cells program macrophage plasticity by altering their metabolic status via a PGE2-dependent mechanism. *Sci Rep* 6:38308.
68. Bouffi C, C Bony, G Courties, C Jorgensen and D Noel. (2010). IL-6-dependent PGE2 secretion by mesenchymal stem cells inhibits local inflammation in experimental arthritis. *PLoS One* 5.
69. Hsu WT, CH Lin, BL Chiang, HY Jui, KK Wu and CM Lee. (2013). Prostaglandin E2 potentiates mesenchymal stem cell-induced IL-10+IFN-gamma+CD4+ regulatory T cells to control transplant arteriosclerosis. *J Immunol* 190:2372-80.
70. Plock JA, JT Schnider, W Zhang, R Schweizer, W Tsuji, N Kostereva, PM Fanzio, S Ravuri, MG Solari, HY Cheng, PJ Rubin, KG Marra and VS Gorantla. (2015). Adipose- and Bone Marrow-Derived Mesenchymal Stem Cells Prolong Graft Survival in Vascularized Composite Allograft Transplantation. *Transplantation* 99:1765-73.
71. Crop MJ, CC Baan, SS Korevaar, JN Ijzermans, IP Alwayn, W Weimar and MJ Hoogduijn. (2009). Donor-derived mesenchymal stem cells suppress alloreactivity of kidney transplant patients. *Transplantation* 87:896-906.
72. Yang SH, MJ Park, IH Yoon, SY Kim, SH Hong, JY Shin, HY Nam, YH Kim, B Kim and CG Park. (2009). Soluble mediators from mesenchymal stem cells suppress T cell proliferation by inducing IL-10. *Exp Mol Med* 41:315-24.
73. Kyurkchiev D, I Bochev, E Ivanova-Todorova, M Mourdjeva, T Oreshkova, K Belezmezova and S Kyurkchiev. (2014). Secretion of immunoregulatory cytokines by mesenchymal stem cells. *World J Stem Cells* 6:552-70.
74. Meisel R, A Zibert, M Laryea, U Gobel, W Daubener and D Dilloo. (2004). Human bone marrow stromal cells inhibit allogeneic T-cell responses by indoleamine 2,3-dioxygenase-mediated tryptophan degradation. *Blood* 103:4619-21.
75. Chamberlain G, H Smith, GE Rainger and J Middleton. (2011). Mesenchymal stem cells exhibit firm adhesion, crawling, spreading and transmigration across aortic endothelial cells: effects of chemokines and shear. *PLoS One* 6:e25663.
76. Zanotti L, R Angioni, B Cali, C Soldani, C Ploia, F Moalli, M Garghesha, G D'Amico, S Elliman, G Tedeschi, E Maffioli, A Negri, S Zacchigna, A Sarukhan, JV Stein and A Viola. (2016). Mouse mesenchymal stem cells inhibit high endothelial cell activation and lymphocyte homing to lymph nodes by releasing TIMP-1. *Leukemia* 30:1143-54.
77. Luu NT, HM McGettrick, CD Buckley, PN Newsome, GE Rainger, J Frampton and GB Nash. (2013). Crosstalk between mesenchymal stem cells and endothelial cells leads to downregulation of cytokine-induced leukocyte recruitment. *Stem Cells* 31:2690-702.

Chapter 1

78. Li X, Z Xu, J Bai, S Yang, S Zhao, Y Zhang, X Chen and Y Wang. (2016). Umbilical Cord Tissue-Derived Mesenchymal Stem Cells Induce T Lymphocyte Apoptosis and Cell Cycle Arrest by Expression of Indoleamine 2, 3-Dioxygenase. *Stem Cells Int* 2016:7495135.
79. Ruster B, S Gottig, RJ Ludwig, R Bistrrian, S Muller, E Seifried, J Gille and R Henschler. (2006). Mesenchymal stem cells display coordinated rolling and adhesion behavior on endothelial cells. *Blood* 108:3938-44.
80. Steingen C, F Brenig, L Baumgartner, J Schmidt, A Schmidt and W Bloch. (2008). Characterization of key mechanisms in transmigration and invasion of mesenchymal stem cells. *J Mol Cell Cardiol* 44:1072-84.
81. Koch M, A Lehnhardt, X Hu, B Brunswig-Spickenheier, M Stolk, V Brocker, M Noriega, M Seifert and C Lange. (2013). Isogeneic MSC application in a rat model of acute renal allograft rejection modulates immune response but does not prolong allograft survival. *Transpl Immunol* 29:43-50.
82. Qiu Z, D Zhou and D Sun. (2014). Effects of human umbilical cord mesenchymal stem cells on renal ischaemia-reperfusion injury in rats. *Int Braz J Urol* 40:553-61.
83. Zhu XY, V Urbietta-Caceres, JD Krier, SC Textor, A Lerman and LO Lerman. (2013). Mesenchymal stem cells and endothelial progenitor cells decrease renal injury in experimental swine renal artery stenosis through different mechanisms. *Stem Cells* 31:117-25.
84. Moghadasali R, M Azarnia, M Hajinasrollah, H Arghani, SM Nassiri, M Molazem, A Vosough, S Mohitmafi, M Najarasl, Z Ajdari, RS Yazdi, M Bagheri, H Ghanaati, B Rafiei, Y Gheisari, H Baharvand and N Aghdami. (2014). Intra-renal arterial injection of autologous bone marrow mesenchymal stromal cells ameliorates cisplatin-induced acute kidney injury in a rhesus Macaque mulatta monkey model. *Cytotherapy* 16:734-49.
85. Vega A, MA Martin-Ferrero, F Del Canto, M Alberca, V Garcia, A Munar, L Orozco, R Soler, JJ Fuertes, M Huguet, A Sanchez and J Garcia-Sancho. (2015). Treatment of Knee Osteoarthritis With Allogeneic Bone Marrow Mesenchymal Stem Cells: A Randomized Controlled Trial. *Transplantation* 99:1681-90.
86. Kebriaei P, L Isola, E Bahceci, K Holland, S Rowley, J McGuirk, M Devetten, J Jansen, R Herzig and M Schuster. (2009). Adult human mesenchymal stem cells added to corticosteroid therapy for the treatment of acute graft-versus-host disease. *Biol Blood Marrow Transplant* 15.
87. Bang OY, JS Lee, PH Lee and G Lee. (2005). Autologous mesenchymal stem cell transplantation in stroke patients. *Ann Neurol* 57:874-82.
88. Tan J, W Wu, X Xu, L Liao, F Zheng, S Messinger, X Sun, J Chen, S Yang, J Cai, X Gao, A Pileggi and C Ricordi. (2012). Induction therapy with autologous mesenchymal stem cells in living-related kidney transplants: a randomized controlled trial. *JAMA* 307:1169-77.
89. Perico N, F Casiraghi, M Inrona, E Gotti, M Todeschini, RA Cavinato, C Capelli, A Rambaldi, P Cassis, P Rizzo, M Cortinovia, M Marasa, J Golay, M Noris and G Remuzzi. (2011). Autologous mesenchymal stromal cells and kidney transplantation: a pilot study of safety and clinical feasibility. *Clin J Am Soc Nephrol* 6:412-22.
90. Eggenhofer E, V Benseler, A Kroemer, FC Popp, EK Geissler, HJ Schlitt, CC Baan, MH Dahlke and MJ Hoogduijn. (2012). Mesenchymal stem cells are short-lived and do not migrate beyond the lungs after intravenous infusion. *Frontiers in Immunology* 3:297.
91. Luk F, S de Witte, SS Korevaar, M Roemeling-van Rhijn, M Franquesa, T Strini, S van den Engel, M Gargasha, D Roy, FJ Dor, EM Horwitz, RW de Bruin, MG Betjes, CC Baan and MJ Hoogduijn. (2016). Inactivated mesenchymal stem cells maintain immunomodulatory capacity. *Stem Cells Dev*.
92. Iwai S, I Sakonju, S Okano, T Teratani, N Kasahara, S Yokote, T Yokoo and E Kobayash. (2014). Impact of ex vivo administration of mesenchymal stem cells on the function of kidney grafts from cardiac death donors in rat. *Transplant Proc* 46:1578-84.

MSC Therapy for Kidneys on Machine Perfusion

93. Allen TA, D Gracieux, M Talib, DA Tokarz, MT Hensley, J Cores, A Vandergriff, J Tang, JB de Andrade, PU Dinh, JA Yoder and K Cheng. (2016). Angiopellosis as an Alternative Mechanism of Cell Extravasation. *Stem Cells*.
94. Nassiri SM and R Rahbarghazi. (2014). Interactions of mesenchymal stem cells with endothelial cells. *Stem Cells Dev* 23:319-32.
95. Zhu XY, A Lerman and LO Lerman. (2013). Concise review: mesenchymal stem cell treatment for ischemic kidney disease. *Stem Cells* 31:1731-6.

Chapter 2

**Concise introduction, aim
and outline of the thesis**



Concise introduction

The regenerative properties of MSC could be a therapeutic option against ischemia reperfusion injury and its known detrimental effect on long term graft function in kidney transplantation. To study the possible side-effects and to introduce such a treatment in the clinic in the most rational way, *in-vitro* studies and large animal experiments are needed. The overarching aim of this thesis is to evaluate the feasibility of delivering mesenchymal stromal cells (MSC) to a donor kidney during normothermic machine perfusion (NMP) as a therapeutic strategy to enhance transplantation outcome. The fate of MSC after infusion directly to the kidney and their regenerative properties and performance in NMP conditions were investigated in this thesis.

The delivery of MSC during NMP entails infusion through the renal artery as opposed to intravenous (IV) infusion, which is the preferred route of administration of MSC in most clinical trials. IV infused MSC are known to end up in the lungs and have a short survival and the mechanisms responsible for MSC immunomodulatory and regenerative responses are still unknown. Therefore, the fate of MSC after intrarenal infusion needs to be assessed to examine its safety and renal regenerative and immunoregulatory properties of MSC. Little information is available regarding their effect on repairing hypoxia and reoxygenation injury of the endothelium, which is particularly vulnerable for ischemia reperfusion injury. The endothelium is the first cell type with which MSC interact after infusion. Determination of the mechanisms of action of the regenerative effect of MSC on injured endothelial cells will allow to generate the conditions necessary for efficient administration of MSC during NMP, ensuring MSC survival and function. The effects of MSC delivery to a kidney during NMP will allow to elucidate the fate of MSC after infusion and to assess the effect of the infusion procedure on MSC regenerative properties in order to assess the feasibility of MSC infusion to the kidney during *ex-vivo* perfusion.

Outline of the thesis

In this thesis, the possibility to repair renal injury using targeted MSC therapy during NMP is investigated. Firstly, in **chapter 3** the fate of MSC after intravenous (IV) infusion is tested in a mouse model. The location and survival of infused MSC is examined as well as their interaction with the host immune system. In order to improve the delivery efficiency of MSC to the kidney, in **chapter 4** a more direct and simple delivery route for MSC therapy is tested. MSC are tracked after renal intra-arterial infusion in an ischemia-reperfusion injury porcine model. The lifespan of MSC and the structures where they locate after infusion are explored as well as the mechanism involved in the retention of MSC in the kidney. The suitability of this delivery route to avoid off-target localization of MSC is also assessed by the amount of MSC found in organs other than the kidney.

To determine whether MSC have the capacity to exert a regenerative response on injured endothelial cells, in **chapter 5** the reparative effect of MSC on human umbilical vein endothelial cells (HUVEC) injured by hypoxic and inflammatory insult is evaluated. First, the direct cell-to-cell interaction between these cells and the involved pathways are studied. Next, the effect of MSC on HUVEC injury is assessed as well as the main mechanism of action of MSC. Then, the capacity of MSC to migrate through a layer of endothelial cells toward kidney injury chemokines is examined by *in vitro* experiments.

However, *in vitro* cell culture conditions are far from close to the conditions necessary to infuse MSC during *ex-situ* organ perfusion. In **chapter 6** the effect of suspension conditions, cryopreservation and thawing and exposure to perfusion solution on MSC is studied. The effect of these conditions on the survival, function and regenerative properties of human and porcine MSC is tested in this chapter to evaluate the feasibility of MSC therapy under NMP conditions. Finally, in **chapter 7** MSC are infused to porcine kidneys during NMP for the first time. The distribution of MSC is assessed by histology and MRI scan on the perfused kidney, concomitant with monitoring the hemodynamic and metabolic profile of the kidney during NMP.

Chapters 8 to 11 summarize and discuss the results obtained within this thesis in 4 different languages.

Chapter 3

Immunomodulation by therapeutic mesenchymal stromal cells (MSC) is triggered through phagocytosis of MSC by monocytic cells

Samantha F.H. de Witte^{1*} & Franka Luk^{1*}, Jesus M. Sierra Parraga¹, Madhu Gargsha², Ana Merino¹, Sander S. Korevaar¹, Anusha S. Shankar¹, Lisa O'Flynn³, Steve J. Elliman³, Debashish Roy², Michiel G.H. Betjes¹, Philip N. Newsome⁴⁻⁶, Carla C. Baan¹, Martin J. Hoogduijn¹

¹*Nephrology and Transplantation, Department of Internal Medicine, Erasmus MC, Rotterdam, The the Netherlands;*

²*BioInVision Inc., Mayfield Village, OH, USA;*

³*Orbsen Therapeutics Ltd., Galway, Ireland;*

⁴*National Institute for Health Research Liver Biomedical Research Unit at University Hospitals Birmingham NHS Foundation Trust and the University of Birmingham;*

⁵*Centre for Liver Research, Institute of Immunology and Immunotherapy, University of Birmingham;*

⁶*Liver Unit, University Hospitals Birmingham NHS Foundation Trust, Birmingham*

*Samantha F.H. de Witte and Franka Luk contributed equally to this study



Abstract

Mesenchymal stem or stromal cells (MSC) are under investigation as a potential immunotherapy. MSC are usually administered via intravenous infusion, after which they are trapped in the lungs and die and disappear within a day. The fate of MSC after their disappearance from the lungs is unknown and it is unclear how MSC realize their immunomodulatory effects in their short lifespan. We examined immunological mechanisms determining the fate of infused MSC and the immunomodulatory response associated with it. Tracking viable and dead human umbilical cord MSC (ucMSC) in mice using Qtracker beads (contained in viable cells) and Hoechst33342 (staining all cells) revealed that viable ucMSC were present in the lungs immediately after infusion. Twenty-four hours later, the majority of ucMSC were dead and found in the lungs and liver where they were contained in monocytic cells of predominantly non-classical Ly6Clow phenotype. Monocytes containing ucMSC were also detected systemically. In vitro experiments confirmed that human CD14⁺⁺/CD16⁻ classical monocytes polarized towards a non-classical CD14⁺⁺CD16⁺CD206⁺ phenotype after phagocytosis of ucMSC and expressed programmed death ligand-1 and IL-10, while TNF- α was reduced. ucMSC-primed monocytes induced Foxp3⁺ regulatory T cell formation in mixed lymphocyte reactions. These results demonstrate that infused MSC are rapidly phagocytosed by monocytes, which subsequently migrate from the lungs to other body sites. Phagocytosis of ucMSC induces phenotypical and functional changes in monocytes, which subsequently modulate cells of the adaptive immune system. It can be concluded that monocytes play a crucial role in mediating, distributing and transferring the immunomodulatory effect of MSC.

Introduction

MSC are currently being investigated in various animal models¹⁻⁷ and clinical trials⁸⁻¹³ for their immunotherapeutic potential. Around 700 clinical trials with MSC were registered with clinicaltrials.gov in early 2017. The *in vitro* immunomodulatory properties of MSC are well documented, but their mechanism of action after administration is largely unknown.¹⁴ Administration of MSC is most commonly performed via intravenous infusion, after which they are known to end up in the micro-vasculature of the lungs from where the majority are lost within 24 hours.¹⁵ The assumed short survival of MSC does not appear to interfere with their effectiveness, as beneficial effects of MSC are seen in a variety of settings long after the cells have been cleared.^{12, 16-21} Yet, how MSC modulate the host immune system during their short lifespan is still unclear.

Recently, we observed that inactivation of MSC in which their immunophenotype remained intact while their secretome and active crosstalk with immune cells was disabled, retained the cells' immunomodulatory capacity in a lipopolysaccharide (LPS) sepsis model.²² In this model, the therapeutic effect of MSC appears to be independent of their cellular activity and depends on a mechanism potentially involving recognition and phagocytosis of MSC by monocytic cells.^{22, 23}

Monocytes can induce long-term adaptive immune responses upon differentiation into macrophages; moreover, *in vitro* studies have shown that MSC stimulate monocytes to adapt an anti-inflammatory IL-10 producing phenotype.^{24, 25} In addition, we have recently shown that membrane particles that were generated from MSC are able to modulate the immune response by targeting pro-inflammatory monocytes and inducing apoptosis.²⁶ Furthermore, intravenous administration of MSC has been shown to lead to the induction of regulatory monocytes that are capable of suppressing allo- and autoimmune responses independently of regulatory T cells (Tregs).²⁷

In the present study, we elucidated the fate of infused MSC and their immunomodulatory effects after administration and demonstrated that infused MSC are rapidly cleared through phagocytosis by monocytes. This results in the polarization of monocytes towards an immunosuppressive phenotype, which then impacts on adaptive immune cells. Moreover, MSC-activated monocytes relocate via the systemic route to other body sites, in particular to the liver, thereby distributing their adapted immune status. This suggests that at least part of

the immunomodulatory response seen after infusion of MSC is independent of the cellular activity of MSC.

Materials and methods

Culture expansion of ucMSC

Human umbilical cord tissue was collected from Caesarean section deliveries by Tissue Solutions Ltd. (Glasgow, UK) from healthy donors without known active viral infections. All cord tissue was obtained according to the legal and ethical requirements of the country of collection, with the approval of an ethics committee (or similar body) and with anonymous consent from the donor. Isolation of CD362+ ucMSC was performed as previously described by de Witte et al.^{28, 29} After isolation, cells were counted, seeded for expansion and cryopreserved at passage 2 for shipment to Erasmus Medical Center. Here, ucMSC were cultured in minimum essential medium Eagle alpha modification (MEM- α ; Sigma-Aldrich, St Louis, MO, USA) containing 2 mM L-glutamine (Lonza, Verviers, Belgium), 1% penicillin/streptomycin solution (P/S; 100IU/ml penicillin, 100IU/ml streptomycin; Lonza) and supplemented with 15% fetal bovine serum (FBS; Lonza) and 1 ng/ml basic fibroblast growth factor (bFGF) (Sigma-Aldrich) and kept at 37°C, 5% CO₂ and air O₂. The medium was refreshed once a week and ucMSC were passaged using 0.05% trypsin-EDTA (Life technologies, Paisley, UK) at ~80-90% confluence. UcMSC were used in experiments between passage 3-6.

Generation of conditioned medium

For the generation of conditioned medium from ucMSC, 100,000 ucMSC were seeded per 6 wells plate well in 2 ml of standard culture medium. Medium was refreshed the following day. UcMSC were cultured for 3 days in the same medium, whereafter medium was collected and centrifuged for 10min at 3000RPM to remove cell debris and stored at -80 °C until further use.

Labeling ucMSC with Qtracker 605 beads, Hoechst33342 and PKH26

For in vivo tracking experiments of viable and dead cells using CryoViz imaging, ucMSC were dual labeled with Qtracker 605 beads (Life technologies) and Hoechst33342 (ThermoFisher, Bleiswijk, the Netherlands) as these labels were properly detected by the available detectors. UcMSC were labeled with Qtracker 605 beads according the manufacturer's instructions. Qtracker beads are actively taken up and contained within viable cells, while they disperse

when cells die (Supplementary figure 1). After labeling, ucMSC were thoroughly washed to remove any beads that were not internalized. Subsequently, ucMSC were incubated with Hoechst33342 (1 µg/ml), which binds to DNA and remains bound even after cells die. For monocyte phagocytosis experiments, ucMSC were labeled with the membrane dye PKH26 (PKH26 Red Fluorescent Cell Linker Kit, Sigma-Aldrich, Zwijndrecht, the Netherlands) according to the manufacturer's instructions.

Mice

Healthy male C57BL/6 mice (8 weeks old) were purchased from Charles River (Germany). The mice had free access to food and water and were kept at a 12-hour light-dark cycle. Animal housing conditions and all procedures were carried out in strict accordance with current EU legislation on animal experimentation. All procedures were approved by the Institutional Committee for Animal Research (protocol EMC No. 127-12-14).

Cell tracking by CryoViz imaging

Healthy male C57BL/6 mice were infused with ucMSC (150,000 ucMSC / 200 µl PBS) that were dual labeled with Qtracker 605 beads and Hoechst33342 via tail vein injections. Five minutes, 24 and 72 hours after ucMSC infusion, the mice were euthanized with carbon dioxide. Subsequently, whole mice were embedded in mounting medium for Cryotomy (O.C.T. compound, VWR Chemical, Amsterdam, The Netherlands), frozen in liquid nitrogen and stored at -80 °C until shipment to BioInVision, OH, USA, for imaging. At BioInVision 3D anatomical and molecular fluorescence videos were generated with CryoViz™ technology. The signals of Qtracker 605 beads and Hoechst33342 are spectrally separated from each other. Hence, a combination of hardware (optical filters) and software (machine learning based cell detector) was used to differentiate between them. UcMSC positive for Qtracker605 beads were detected by the fluorescent signal that arises from clustered beads present in viable cells. Non-viable ucMSC are not capable of containing the beads intracellular and as a consequence the beads will disperse and the signal may no longer be picked up. Hoechst33342, in contrast, is present in viable and dead cells, but its signal is not detected in live ucMSC as the Qtracker605 signal outshines the Hoechst33342 signal. As a result, the Hoechst33342 signal is detected only in dead ucMSC. Cell counts for Qtracker 605 positive cells (live ucMSC) and Hoechst33342 positive cells (dead ucMSC) were quantified using imaging algorithms by BioInVision Inc.

Detection of ucMSC phagocytosis by monocytes in vivo

The mice were infused via the tail vein with PKH26-labeled ucMSC (150,000 ucMSC/200ul PBS). 24 hours after the ucMSC infusion, the mice were sacrificed by cervical dislocation and the lungs, blood and liver were harvested. The lungs and livers were digested by collagenase type IV (0.5mg/ml, Life Technologies, Paisley, UK) for 30 minutes at 37 °C to obtain a single cell suspension. Red blood cells were lysed with red blood cell lysis buffer (ThermoFisher) and the cells suspensions were then washed with FACS buffer (PBS+0.1% BSA +0.1% sodium azide). Single cell suspensions of lung tissue and heparinized whole blood (100 µL) were stained for CD11b-APC, Ly6C-Bv450BD (both BD Biosciences, San Jose, CA, USA), CD45-Pe-Cy7, CX3CR1-PERCPCy5.5 (all Biolegend) and lung cells were stained in addition for CD68-PE (Biolegend) for 30 minutes at 4 °C. The blood samples were subsequently lysed for 10 minutes with Lyse/Fix buffer (BD Biosciences) and washed twice with FACS buffer. Liver samples were stained for CD11b-APC, Ly6C-Bv450, CD45-Pe-Cy7 and CLEC4F-PE (kindly provided by Xifeng Yang, Biolegend) for 30 minutes at 4 °C. Samples were then washed with FACS buffer and measured on a FACSCanto II flow cytometer.

Detection of phagocytosis of ucMSC by human immune cells

Human peripheral blood samples were collected from healthy volunteers. 50,000 PKH26-labeled ucMSC were added to 200 µl whole blood for 1h, 4h and 24h in polypropylene tubes at 37°C, 5% CO₂ and air O₂. In addition, peripheral blood mononuclear cells (PBMC) were isolated from blood by density gradient centrifugation using Ficoll-Paque (GE healthcare). Monocytes were isolated from PBMC via the positive selection of CD14⁺ cells by MACS using CD14 microbeads (Miltenyi, Bergisch Gladbach, Germany), according to the manufacturer's recommendations. Subsequently, 200,000 monocytes were co-cultured with 50,000 PKH26-labeled ucMSC for 1h, 4h and 24h in polypropylene tubes in RPMI medium supplemented with 2 mM L-glutamine, 1% P/S and 10% heat-inactivated FBS at 37°C, 5% CO₂ and air O₂.

Whole-blood or isolated monocytes incubated with ucMSC were stained for CD14-Pacific Blue (BD Biosciences), CD15-FITC (BD Biosciences) and CD45-APC (BD Biosciences) or CD14-Pacific Blue (BD Biosciences), CD16-FITC (Bio-Rad, the Netherlands), CD90-APC (BD Biosciences), HLA-DR-Amcyan (BD Biosciences), PD-L1-PeCy7 (BD Biosciences), CD206-Pacific Blue (BD Biosciences), CD163-FITC (Bio-rad antibodies) and Via-Probe (BD Biosciences) respectively, for

30 minutes at 4 °C. Whole-blood samples were then fixed and red blood cells lysed for 10 minutes at 4 °C with BD FACS Lysing solution (BD Biosciences). Samples were washed and measured on a FACSCanto II flow cytometer with FACSDiva software (BD Biosciences).

Detection of monocyte phenotype shift due to phagocytosis ucMSC or cytokines secreted by ucMSC

CD14⁺ selected monocytes were cultured in 50% ucMSC conditioned medium or co-cultured with ucMSC at a 4:1 ratio in standard culture medium for 24 hours. Subsequently, samples were stained for CD45-APC, CD14-Pacific Blue and CD16-FITC or CD90-APC (BD Biosciences), PD-L1-PeCy7, CD206-Pacific Blue and CD163-FITC, for 30 minutes at 4 °C. Samples were washed and measured on a FACSCanto II flow cytometer with FACSDiva software (BD Biosciences).

Confocal microscopy imaging of ucMSC phagocytosis by monocytes

Monocytes were isolated from PBMC via positive selection of CD14⁺ cells as described above and labeled with PKH67 (PKH67 Green Fluorescent Cell Linker Kit, Sigma-Aldrich) for 10 min at 37 °C. The monocytes were cultured at 37 °C on gelatin-coated glass slides for 1h and 16h in the presence of PKH26 labeled ucMSC at a 1:4 ratio (ucMSC:monocytes) in RPMI medium supplemented with 2 mM L-glutamine, 1% P/S and 10% heat-inactivated FBS. As a negative control, monocytes were co-cultured with ucMSC for 16 hours at 4 °C.

Confocal microscopy analysis of phagocytosis of PKH26-labeled ucMSC by monocytes was carried out on a Leica TCS SP5 confocal microscope (Leica Microsystems B.V., Eindhoven, the Netherlands) equipped with Leica Application Suite – Advanced Fluorescence (LAS AF) software, DPSS 561 nm lasers, using a 60 X (1.4 NA oil) objective. The microscope was equipped with a temperature-controlled incubator (incubator settings: 37 °C and 5% CO₂). Images were processed using ImageJ 1.48 (National Institutes of Health, Washington, USA).

Addition of ucMSC primed monocytes to mixed lymphocyte reaction

CD14⁺ monocytes were isolated from PBMC via MACS separation as described above. To prime CD14⁺ monocytes, the cells were co-cultured for 24 hours with ucMSC at a 1:4 ratio (ucMSC:monocytes). Thereafter, ucMSC were manually separated from monocytes using

Chapter 3

biotin anti-human CD73 (clone AD2, Biolegend Inc., San Diego, CA, USA) and MagniSort Streptavidin Positive Selection Beads (MSPB-6003, eBioscience, Affymetrix Inc, San Diego, CA, USA) and the EasySep™ Magnet (StemCell technologies, Germany). The obtained untouched primed monocytes showed a purity of >98% (Supplementary figure 2).

Primed and non-primed monocytes (10,000) were added to mixed lymphocyte reactions (MLR) of 50,000 carboxyfluorescein succinimidylester (CFSE)-labeled PBMC (autologous to monocytes) and 50,000 γ -irradiated (40 Gy) HLA-mismatched PBMC in RPMI supplemented with 2 mM L-glutamine, 1% P/S and 10% heat-inactivated FBS. After 7 days, PBMC were harvested and stained for 30 min at room temperature with CD3-PERCP (BD Biosciences), CD4-Pacific Blue (Biolegend Inc.), CD8-APC-Cy7 (BD Pharmingen), CD25-PE-Cy7 (BD Pharmingen) and CD127-PE (BD Pharmingen). In addition, intracellular staining for Foxp3 (eBiosciences) was performed with anti-human FoxP3-APC staining kit (BD Biosciences). Cell proliferation was determined by CFSE dilution, measured on a FACSCanto II flow cytometer (BD Biosciences).

Real time qPCR

mRNA was isolated from primed and non-primed monocytes using the High Pure RNA Isolation Kit (Roche). Complement DNA was synthesized from 500ng mRNA with random primers (Promega Benelux B.V., the Netherlands). Quantitative gene expression was determined using TaqMan Gene Expression Assays-on-demand for IL1 β (Hs00174097.m1), IL6 (Hs00174131.m1), IL8 (Hs00174114.m1), IL10 (Hs00174086.m1), TGF β (Hs00171257.m1) and TNF α (Hs99999043.m1; all Applied Biosystems, Foster City, CA). Results were expressed as copy number.

Statistical Analysis

Statistical analysis was performed by unpaired t-tests using Prism software v5.04 (GraphPad Software Inc. La Jolla, CA). P values of <0.05 were considered significant.

Results

UcMSC accumulate in the lungs after intravenous infusion

To investigate the bio-distribution of intravenously infused ucMSC, cells were dual labeled with Qtracker605 beads and Hoechst33342 prior to infusion to enable detection of live and dead ucMSC in vivo, respectively. Live ucMSC were identified by Qtracker605 signal

(Qtracker605 signal outshines the Hoechst33342 signal), whereas dead ucMSC were detected by Hoechst33342 signal. Detection of Qtracker605 signal 5 minutes post infusion revealed that the majority of ucMSC were alive and present in the lungs (Figure 1A, E). In addition, few dead ucMSC were observed in the lungs and liver as detected by Hoechst33342 signal (Figure 1B, E).

Dead ucMSC re-localize to the liver prior to their disappearance

At 24 hours post-infusion, a large decrease in the number of live ucMSC was observed in the lungs (Figure 1C, E). The number of dead cells in the lungs was however increased and interestingly, there was an accumulation of dead ucMSC in the liver (Figure 1D-E). No living ucMSC were detected in the liver and by 72 hours post-infusion, minimal numbers of cells were detected, which were all dead (Figure 1E).

UcMSC are phagocytosed and re-distributed by host innate immune cells

To examine how ucMSC disappear from the lungs and reappear in the liver 24 hours after infusion, whole blood, lungs and liver were harvested from mice that were infused with 150,000 PKH26-labeled ucMSC, single cell suspensions were prepared and stained for leukocyte markers and analyzed by flow cytometry. PKH26⁺ cells were found in the lungs (3.4±0.13% of total cells), blood (0.7±0.05%) and liver (2.9±0.11%) (Figure 2A-B). In the cell suspensions from lungs and blood, PKH26⁺ cells were mostly CD11b⁺⁺, whereas in the liver, PKH26 signal was mostly found in CD11b⁺ cells (Figure 2A, C), indicating that ucMSC were phagocytosed by host-innate immune cells. A minority of PKH26⁺ cells in the lungs were CD68⁺CD11b⁺ lung-resident macrophages (12.6±1.0%), whereas 32.1±0.9% were CX3CR1⁺CD11b⁺⁺ blood-derived monocytes and 47.5±1.1% were SSC⁺⁺CD11b⁺⁺ neutrophils (Figure 2A, D). In the blood, 89.3±1.3% of PKH26⁺ cells were CX3CR1⁺CD11b⁺⁺ monocytes and 5.7±0.7% were neutrophils (Figure 2A, E). In the liver, PKH26⁺ cells were mainly CLEC4F⁺CD11b⁺ Kupffer cells (83.8±0.4%), whereas 3.8±0.15% were CLEC4F⁻CD11b⁺⁺ and 10.1±0.5% were neutrophils (Figure 2A, F).

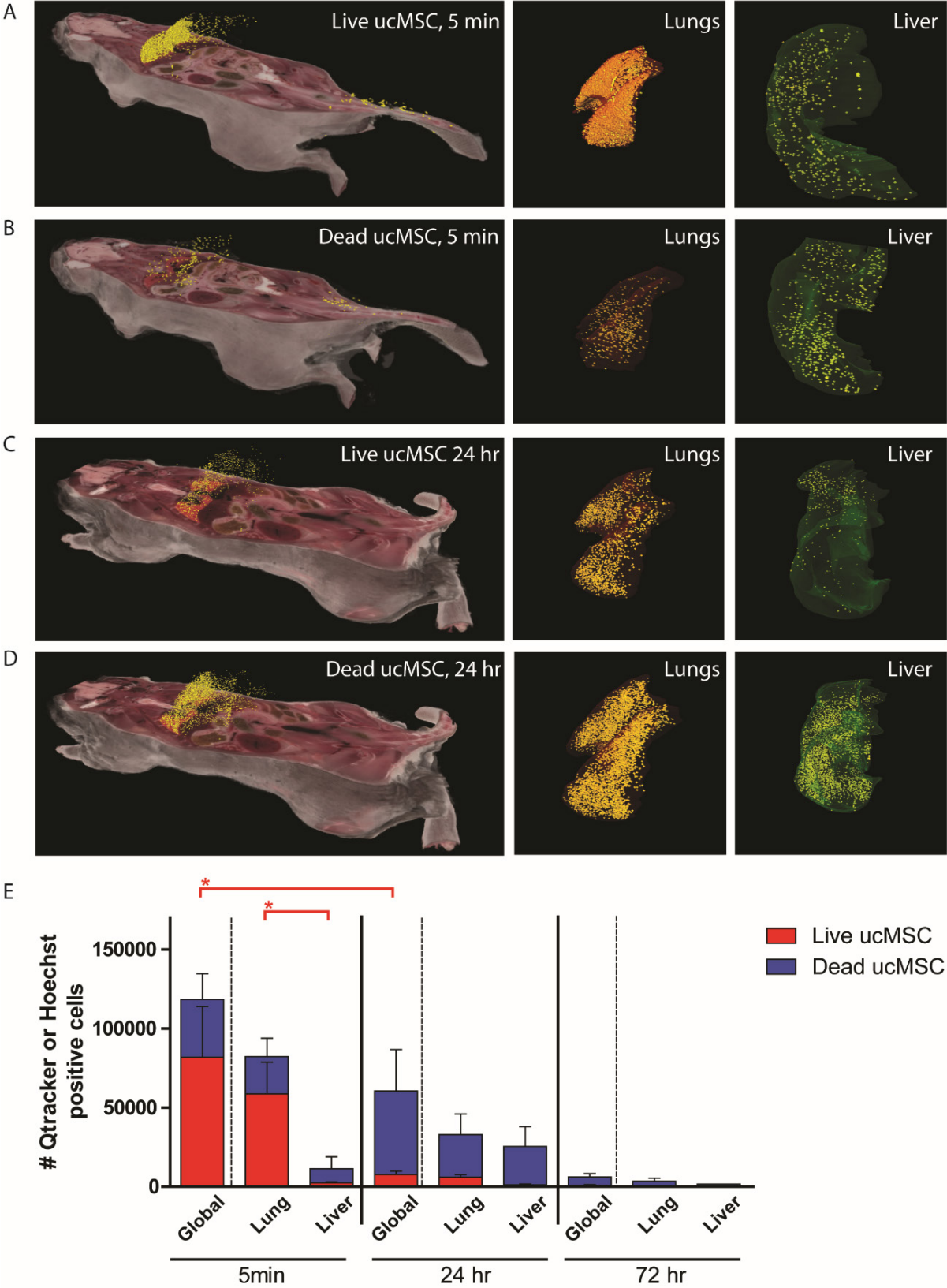


Figure 1. UcMSC strand in the lungs after infusion and re-localize to the liver prior to their disappearance. CryoViz images (left: whole body, middle: lungs, right: liver) of mice after tail vein infusion of 150,000 live ucMSC. (A) Qtracker 605 bead signal, corresponding to live ucMSC 5 min post ucMSC infusion and (B) Hoechst33342 signal, corresponding to dead ucMSC 5 min post ucMSC infusion. (C) Qtracker 605 bead signal 24h post ucMSC infusion and (D) Hoechst33342 signal 24h post ucMSC infusion. Scale bar in full body image of mouse (left), 1 cm;

scale bar in image of lungs (middle), 5mm; scale bar in image of liver (right), 5 mm. (E) Number of Qtracker 605 bead (red) positive live ucMSC and Hoechst33342 (blue) positive dead ucMSC at 5 min, 24h and 72h post ucMSC infusion, globally, in the lungs and in the liver. Results are shown as means \pm SEM (n=6). * indicates significant difference ($p < 0.05$).

Monocytes express a regulatory phenotype after phagocytosis of ucMSC

Thus, monocytes and neutrophils contribute to the clearing of infused ucMSC. In addition to their phagocytic activity, monocytes may play immune-activating as well as immune-regulatory roles. To examine the function of monocytes that phagocytosed ucMSC, PKH26+ monocytes in lung, blood and liver cell suspensions were subdivided into classical (pro-inflammatory) and non-classical (anti-inflammatory) monocytes, based on their expression of Ly6C (Figure 3A). In addition, CD68, CDX3CR1 or CLEC4F were used to indicate lung resident macrophages, blood circulating monocytes and Kupffer cells, respectively. In the lungs, non-classical blood circulating monocytes (Ly6C-CD68-) are the biggest population within the PKH+ cells (Figure 3B). Next, lung resident macrophages make up a big portion. In the blood, the majority of PKH+ monocytes demonstrate a non-classical Ly6C- CX3CR1+CD11b+ phenotype (Figure 3B). Furthermore, PKH+ cells in the liver consist mainly out of Kupffer cells (CLEC4F+) followed by monocytes with a non-classical Ly6C-CLEC4F-) phenotype (Figure 3B).

ucMSC are actively phagocytosed by monocytes in vitro

To further study the interaction of ucMSC with human innate immune cells, PKH26-labeled ucMSC were added to human whole blood in vitro. After 24h of incubation, $21 \pm 8\%$ of CD45+CD15+ neutrophils and $91 \pm 3\%$ of CD45+CD14+ monocytes had become positive for PKH26 (Figure 4A), thereby confirming the results from the in vivo experiments. In contrast, no significant uptake of ucMSC was measured in CD45+ SSClow lymphocytes at all time points (Supplementary figure 3). PKH26-labeled ucMSC were subsequently incubated with human blood-derived CD14+ monocytes. Nearly all monocytes became positive for PKH26 within 24h as measured by flow cytometry ($19 \pm 2\%$ at 1h, $34 \pm 3\%$ at 4h and $92 \pm 1\%$ 24h) (Figure 4B).

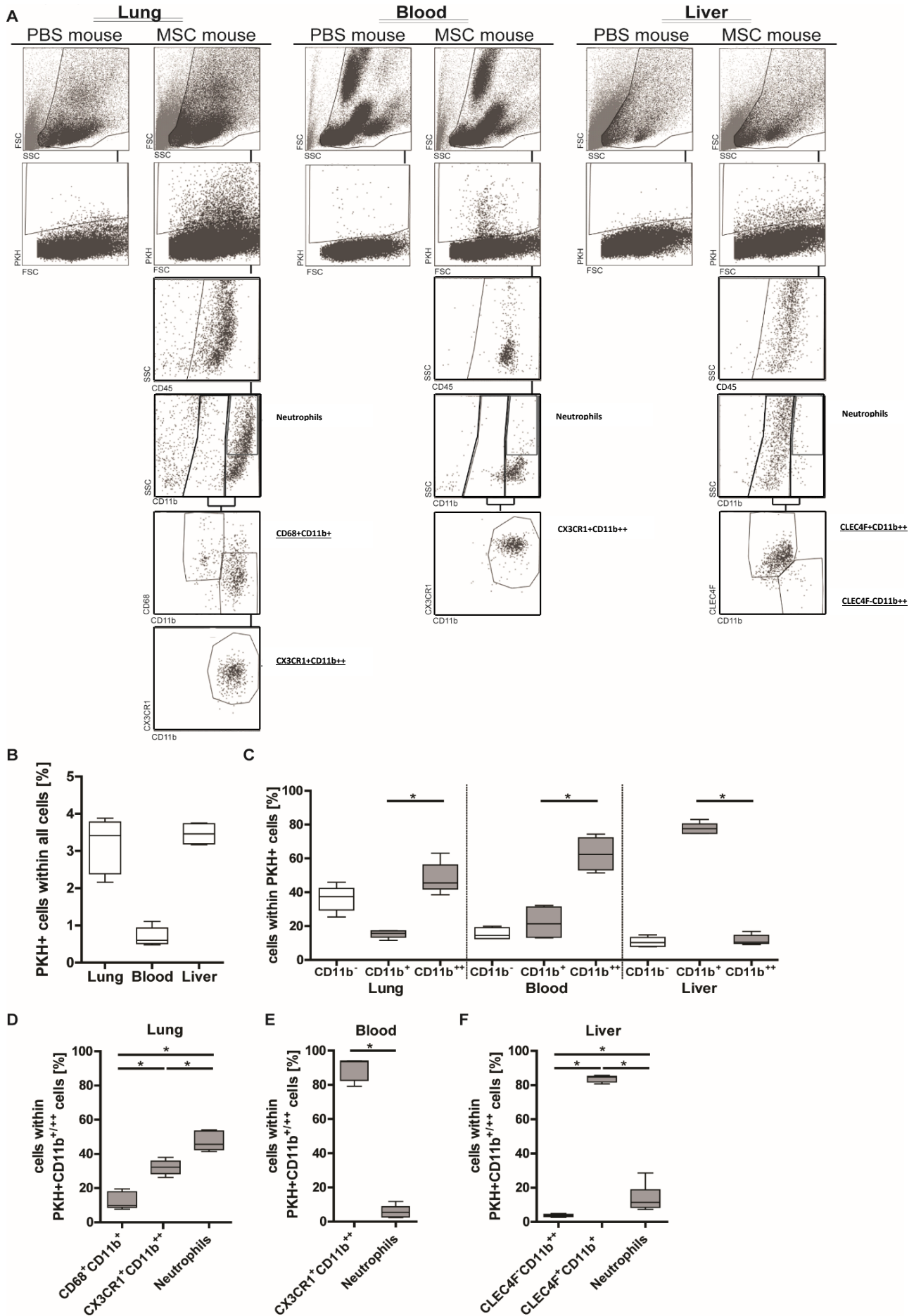


Figure 2. UcMSC are phagocytosed after infusion by host immune cells and distributed to blood and liver. PKH26-labeled ucMSC were administered to mice via the tail vein and after 24h cells of the lungs, blood and liver were analyzed by flow cytometry. (A) Gating strategy for lungs, blood and liver cell suspensions to investigate the origin of PKH26 signal based on CD11b, CX3CR1, CD68 and CLEC4F expression of PKH26+ cells. (B) Proportion of PKH26+ cells in the lungs, blood and liver. (C) Proportion of CD11b+, CD11b++ and CD11b- PKH26+ cells in the lungs, blood and liver. (D) Proportion of lung resident macrophages (CD68+CD11b+), circulating monocytes (CX3CR1+CD11b++) and neutrophils (SSChighCD11b+) of PKH26+CD11b+/++ cells in the lungs. (E) Proportion of CX3CR1+CD11b++ and neutrophils in PKH26+CD11b+/++ cells in the blood. (F) Proportion of CLEC4F-CD11b++, CLEC4F+CD11b+ (Kupffer cells) and neutrophils in PKH26+CD11b+/++ cells in the liver. Results are shown as means \pm SEM (n=5). * indicates significant difference (p<0.05).

To visualize the phagocytosis of ucMSC by human monocytes, serial confocal images of co-cultures of PKH67-labeled monocytes and PKH26-labeled ucMSC were produced. It was observed that monocytes actively migrated towards ucMSC within 1h (Figure 4C). Monocytes with internalized fragments of PKH26-labeled ucMSC were observed 3h after the start of the co-cultures (Figure 4D). At 16h, the majority of monocytes contained PKH26-labeled ucMSC fragments (Figure 4E). In the control co-culture, which was left at 4 °C for 16h, no phagocytosis of ucMSC by monocytes was observed (Figure 4F), demonstrating that phagocytosis of ucMSC by monocytes is an active process.

Phagocytosis of ucMSC activates monocytes and induces polarization

UcMSC are rapidly recognized and phagocytosed by human monocytes. To investigate whether phagocytosis of ucMSC affects monocyte properties, expression of PD-L1, CD90, IL-6, IL-1 β , IL-8, TGF- β , TNF- α and IL-10 was analyzed. Monocytes significantly upregulated cell surface expression of PD-L1 (from 40 \pm 9% to 73 \pm 3%, p<0.05) and CD90 (from 21 \pm 4% to 47 \pm 3%, p<0.05) after 24h of co-culturing with ucMSC (Figure 5A-B). Moreover, mRNA expression levels of IL-1 β , IL-6, IL-8, IL-10 and TGF β significantly increased in the presence of ucMSC, whereas expression of pro-inflammatory TNF- α decreased (Figure 5C).

Skewing of monocytes by phagocytosis of ucMSC differs from skewing by ucMSC conditioned medium

Monocytes that have phagocytosed ucMSC exhibit a different phenotype than prior to phagocytosis. To investigate whether this is caused by factors secreted by ucMSC or by phagocytosis of ucMSC, monocytes were cultured in ucMSC conditioned medium or co-cultured with ucMSC. After 3 days the phenotype of monocytes (CD14, CD16, CD163, CD206, CD90 and PD-L1 expression) was analyzed. CD14, CD16, CD90 and PD-L1 expression by

Chapter 3

monocytes that phagocytosed ucMSC or monocytes that were cultured in ucMSC conditioned medium was similar (Figure 5F).

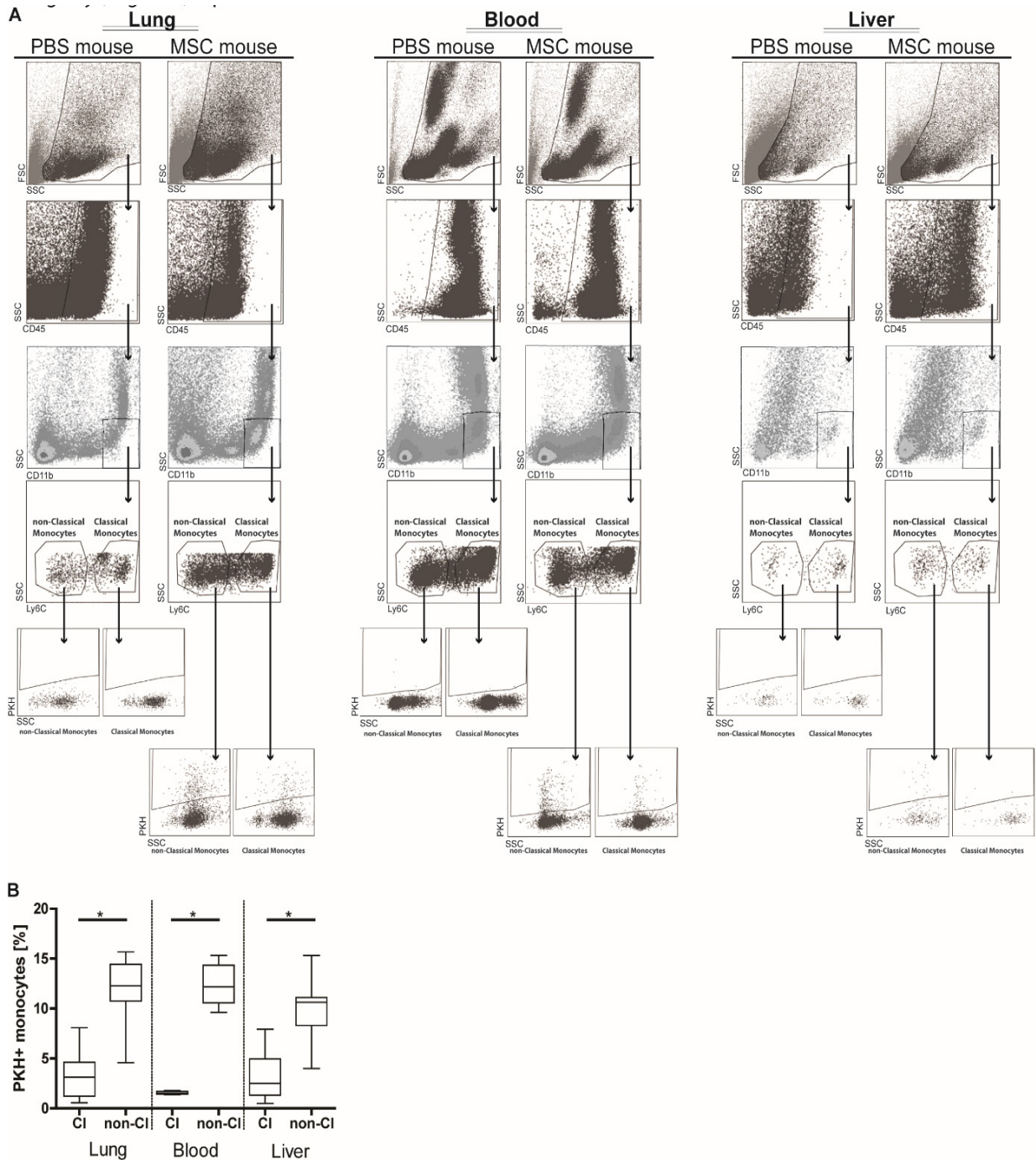


Figure 3. Monocytes that have phagocytosed ucMSC predominantly express a Ly6C- regulatory phenotype. (A) Representative flow cytometry plots of PKH positive classical (pro-inflammatory) and non-classical (anti-inflammatory) monocytes based on SSC and CD11b and Ly6C expression in the lungs, blood and liver. Non-classical monocytes are predominantly positive for PKH26 signal (indicating phagocytosis of MSC). **(B)** Distribution of PKH positive cells in the lungs, blood and liver 24h after PBS or ucMSC infusion. Results are shown as means \pm SEM (n=3 PBS mice and n=5 ucMSC mice). * indicates significant difference (p<0.05).

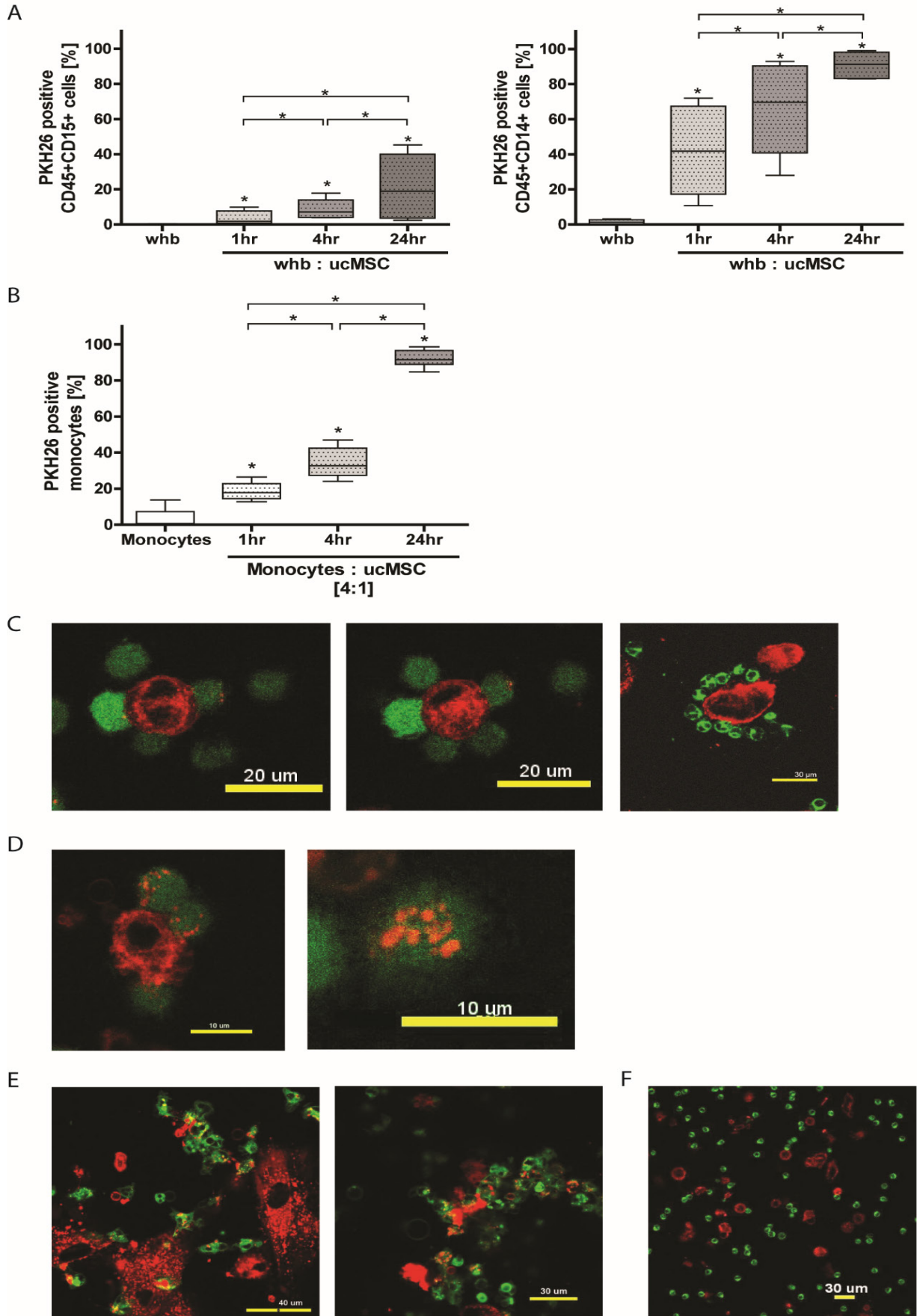


Figure 4. UcMSC are phagocytosed by human monocytes in vitro. (A) Frequency of PKH26+ neutrophils (left) and monocytes (right) after addition of PKH26+ ucMSC to human whole blood. An increase in PKH26+ neutrophils and monocytes can be observed over time. (B) Percentage of PKH26+ monocytes after co-culture of isolated CD14+ monocytes with PKH26+ ucMSC. (C) Confocal images 1h after adding PKH26+ ucMSC (red) to PKH67+ monocytes (green). (D) UcMSC are phagocytosed by monocytes and fragments of ucMSC are visible intracellularly. (E) Overview image of co-culture at 16h. (F) Image of co-culture kept at 4 °C for 16h, showing a lack of phagocytosis of ucMSC by monocytes, indicating phagocytosis is an active process. Results are shown as means \pm SEM (n=3). * indicates significant difference ($p < 0.05$).

However, in contrast to monocytes that phagocytosed ucMSC, monocytes cultured in ucMSC conditioned medium did not upregulate CD163 expression, nor CD206 expression (Figure 5F). The percentage of monocytes expressing CD163-CD206+ was significantly higher when monocytes phagocytosed ucMSC ($31,6 \pm 3\%$) compared to when they are cultured in ucMSC conditioned medium ($5,3 \pm 2\%$). Likewise, significantly more monocytes expressed CD163+CD206+ after phagocytosis of ucMSC ($9,4 \pm 2\%$) compared to after culturing in ucMSC conditioned medium ($1,9 \pm 1\%$).

Monocytes primed by ucMSC induce regulatory T cells

Upon phagocytosis of ucMSC, monocytes are activated and polarized towards an immune regulatory phenotype. We investigated whether these primed monocytes would subsequently alter the adaptive immune response in vitro. UcMSC primed and unprimed monocytes were added to mixed lymphocyte reactions, in which the responder cells were autologous to the added monocytes. Addition of ucMSC primed monocytes led to a significant increase in Foxp3+ regulatory T cells from $8.9 \pm 2\%$ to $13 \pm 2\%$ of CD4+CD25hiCD127- cells (Figure 6A-B). In contrast, addition of ucMSC primed monocytes to the mixed lymphocyte reaction led to a significant reduction in activated CD4+ T cells (Foxp3-CD4+CD25hiCD127-). Finally, the ratio of Foxp3+/Foxp3- CD4+CD25hiCD127- T cells increased from 0.1 to 0.2 upon addition of ucMSC primed monocytes (Figure 6B).

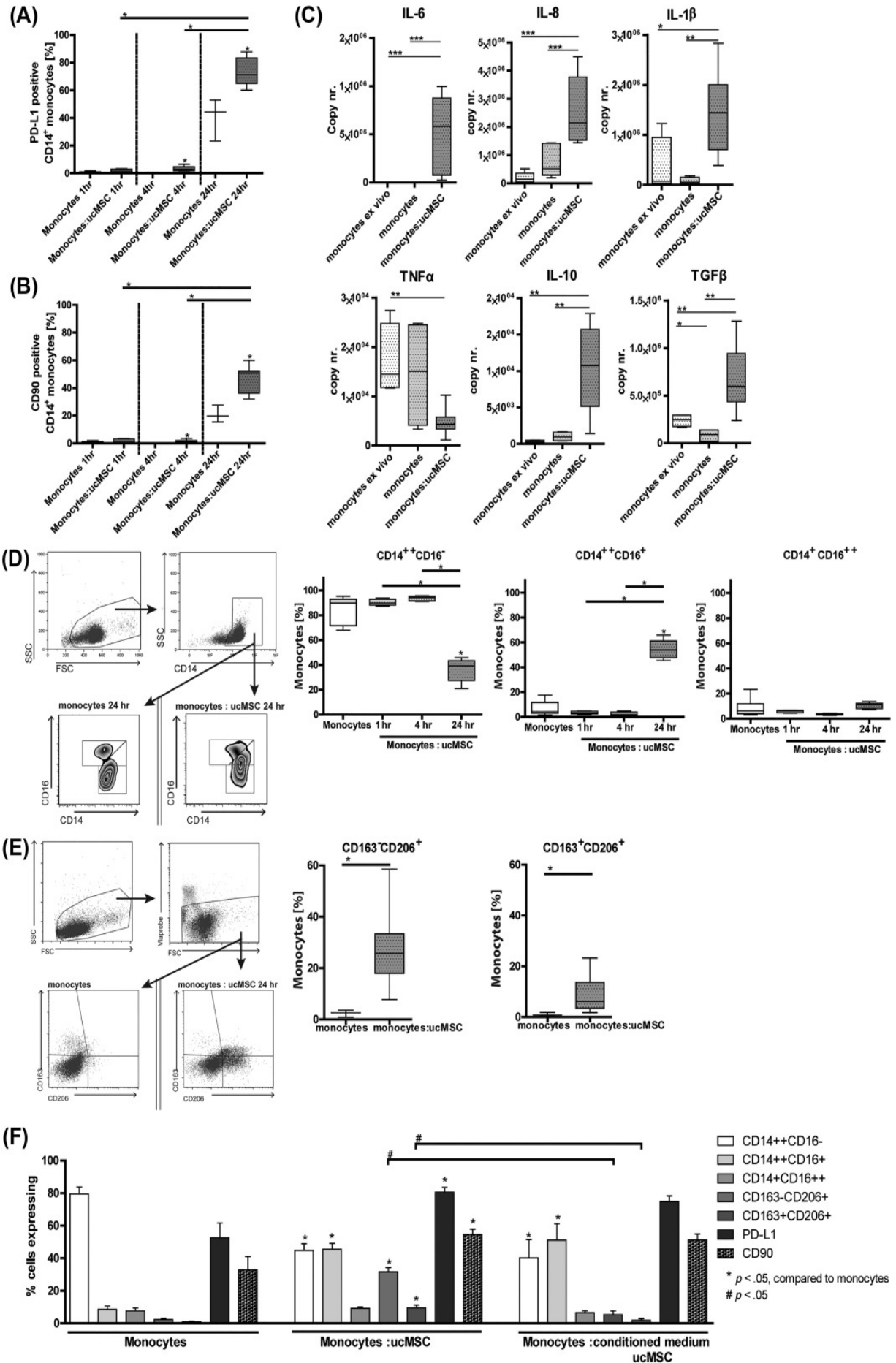


Figure 5. Human monocytes adapt phenotype upon phagocytosis of ucMSC *in vitro*. Protein expression of the surface proteins (A) PD-L1 and (B) CD90 on CD14⁺ monocytes is increased upon co-culture with ucMSC. * indicates significant difference ($p < 0.05$). (C) mRNA expression levels of IL-6, IL-8, IL1 β , TNF- α , IL10 and TGF- β in CD14⁺ monocytes increase upon co-culture with ucMSC. * indicates significant difference ($p < 0.05$). (D) Representative flow cytometry plot demonstrating changes in monocyte subset composition based on CD14 and CD16 expression 24h after co-culture with ucMSC. During co-culture, the frequency of CD14⁺⁺CD16⁻ monocytes decreased whereas CD14⁺⁺CD16⁺ monocytes increased. * indicates significant difference ($p < 0.05$). (E) Representative flow cytometry plot demonstrating increases in the frequency of CD163⁻CD206⁺ and CD163⁺CD206⁺ monocyte subsets after 24h of co-culture of monocytes with ucMSC. * indicates significant difference ($p < 0.05$). (F) Percentage of monocytes expressing CD14⁺⁺CD16⁺, CD14⁺⁺CD16⁻, CD14⁺CD16⁺⁺, CD163⁻CD206⁺, CD16⁺CD206⁺, PD-L1 and CD90 when monocytes are cultured alone, when monocytes phagocytosed ucMSC and when monocytes are cultured in ucMSC conditioned medium. * indicates significant difference compared to monocytes cultured alone ($p < 0.05$) and # indicates significant difference ($p < 0.05$). Results are shown as means \pm SEM ($n=3$).

Discussion

Previous work has demonstrated that intravenously administered MSC accumulate in the lungs and have a short survival time.^{15, 29, 32, 33} The present study shows that monocytes and neutrophils contribute to the clearance of MSC from the lungs by phagocytosing MSC. Subsequently, these cells migrate via the blood stream to other body sites, in particular to the liver. Our *in vitro* data show that phagocytosis of MSC induces phenotypic and functional changes in monocytes, which then modulate the adaptive immune cell compartment.

The brief presence and restricted distribution of intravenously administered MSC appears to be in contrast with the short-term and long-term effects of MSC administration observed in numerous pre-clinical studies and in a number of clinical trials.^{8, 12, 16-21} The short lifespan of MSC after intravenous infusion challenges the hypothesis that the effects of MSC are mediated via their secretome. MSC may lack time to secrete sufficient levels of immunomodulatory factors before they are cleared, although it is possible that disintegration of MSC leads to the release of intracellularly contained cytokines and growth factors. This phenomena might not be specific for MSC and may also be induced by other cell types as well. However, MSC have shown to be effective in several clinical trials as such we explored the fate of MSC after infusion into further depth. Previously, we showed that expression of the macrophage markers CD68 and F4/80 is significantly increased in the lungs of mice two hours after MSC infusion, suggesting recruitment of macrophages to the lungs after MSC infusion.³⁴ These cells are likely to play a key role in the effects of MSC infusion.

The data of the present study confirm that monocytic cells play a role in the clearance of infused MSC.^{35, 36} Braza et al. showed a similar phenomenon of phagocytosis of IV infused

MSC in the lungs by cells of the monocyte/macrophage lineage (F4/80+CD11c+). In their study different markers and terminology were used to define the phagocytosing cells of the monocyte/macrophage lineage, yet their results were in line with our data.

Recently, Dazzi et al. showed that for MSC-induced immunosuppression to occur, T cell induced cell death of MSC is essential, which triggers phagocytes to engulf MSC.³⁷ After phagocytosis of MSC, monocytes migrate to other body sites via the blood stream (summarized in Figure 7). In addition, some MSC may disintegrate and the remnants may be transported out of the lungs via the blood stream. We found accumulation of MSC remnants in the Kupffer cells of the liver. Kupffer cells line the liver sinusoids and are likely to encounter passing MSC remnants. Kupffer cells are professional clean-up cells through phagocytosis of cellular debris and may thus contribute to the clearance of MSC. The clean-up of infused MSC leaves a clear footprint in the monocyte compartment. We observed that monocytes that phagocytosed MSC were of a Ly6C⁻ regulatory phenotype. Ly6C⁻ monocytes containing remnants of MSC were observed in the lungs but also in the blood and in the liver of MSC treated animals. This demonstrates that MSC infusion induces the distribution of monocytes with immunoregulatory properties throughout the body. This is in line with previous findings by Miteva et al. where MSC were also seen to induce the distribution of anti-inflammatory monocytes in mice with Coxsackievirus B3-induced myocarditis.³⁸

It is however unclear why Ly6C⁻ monocytes specifically localize to the liver, but this may be part of an established clean-up route. It appears clear, however, that by recruitment of anti-inflammatory monocytes that phagocytosed MSC and by phagocytosis of MSC remnants by Kupffer cells, the liver is a target for MSC immune therapy.

The question remains whether Ly6C⁻ monocytes selectively phagocytose MSC, or whether Ly6C⁺ monocytes undergo phenotypic changes after phagocytosis of MSC. Our in vitro data suggest the latter. We showed that upon phagocytosis of ucMSC, human monocytes increased surface expression of the co-inhibitory molecule PD-L1 and polarized from CD14⁺⁺CD16⁻ classical monocytes towards CD14⁺⁺CD16⁺ intermediate monocytes. We have previously also observed these phenomena in our lab when using adipose derived MSC instead of umbilical cord derived MSC (data not shown). These phenomena when co-culturing monocytes with ucMSC was accompanied by an increased expression of CD206 on a subpopulation of monocytes. This is in accordance to what Cutler et al. observed when co-culturing ucMSC together with human adult PBMC.³⁹

Chapter 3

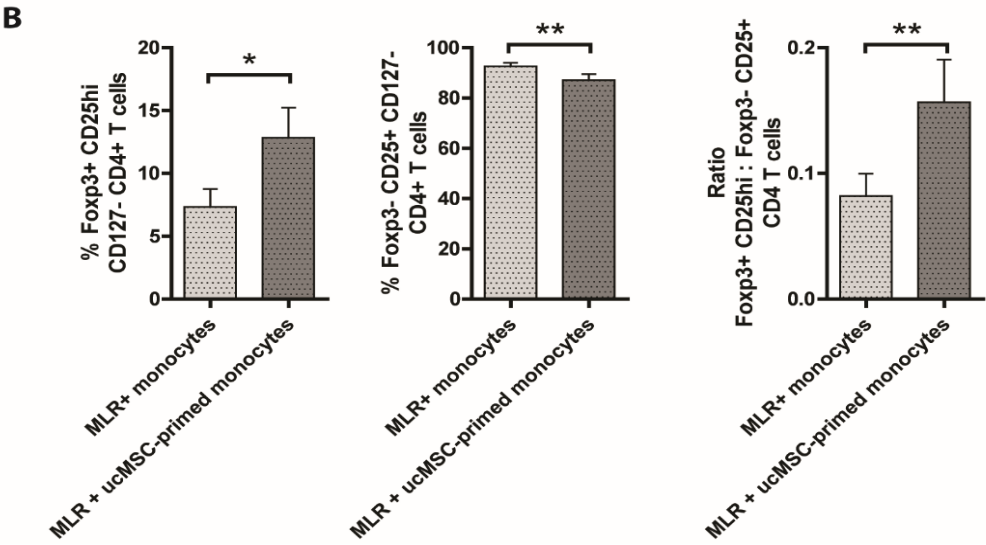
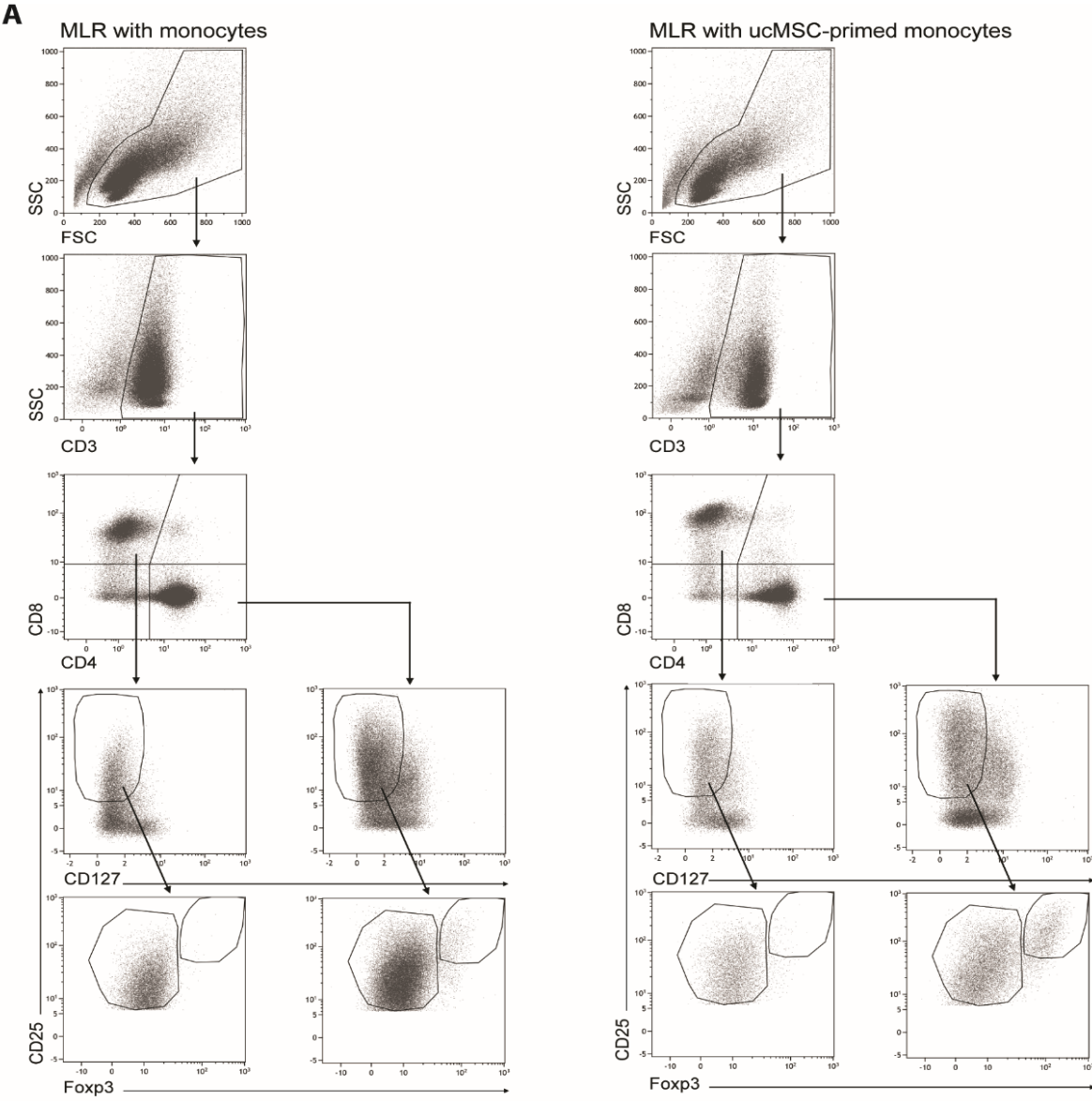


Figure 6. UcMSC primed monocytes induce regulatory T cells. CD14⁺ monocytes were co-cultured for 24h with or without ucMSC and subsequently separated from the ucMSC using MACS separation. Primed and unprimed monocytes were added to a mixed lymphocyte reaction. (A) Gating strategy of mixed lymphocyte reaction with primed monocytes after 7 days. (B) Frequencies of Foxp3-CD25⁺CD127-CD4⁺ activated T cells and Foxp3⁺CD25^{hi}CD127-CD4⁺ regulatory T cells of CD4⁺ T cells. Plots indicate means \pm SEM (n \geq 4). (C) Median fluorescence intensity of Foxp3 within Foxp3⁺CD25^{hi}CD127-CD4⁺ T cells. Plots indicate means \pm SEM (n \geq 4). * indicates significant difference ($p < 0.05$).

In our hands, upregulation of CD206 solely occurred when monocytes were able to phagocytose ucMSC and not by exposure to soluble factors that were secreted by ucMSC. CD206 is a known marker for alternatively activated monocytes.^{40, 41} Along with an increased CD206⁺ monocyte population, a population of CD206⁺CD163⁺ co-expressing monocytes was significantly increased upon phagocytosis of ucMSC. This again exclusively occurred when monocytes were able to phagocytose ucMSC. These CD206⁺CD163⁺ co-expressing monocytes have been described in literature as important cells for the generation of CD4⁺CD25^{hi}FoxP3⁺ T cells and as high IL-10 producing cells with the capacity to take up apoptotic cells.⁴²⁻⁴⁴ In our study, we observed significant increases in IL-10 production by monocytes upon co-culture with ucMSC, alongside a decrease in TNF α and increase in IL-6 and TGF β . This is well in conformity with earlier studies that demonstrated that phagocytosis of MSC induces an immunosuppressive phenotype in macrophages.^{23, 35} These cells produce increased amounts of IL-10 and IL-6 while their production of IL-12 and TNF- α decreases.^{45, 46} Other studies have shown different ways in which monocytes are immunomodulated by MSC in vitro, by the secretion of soluble factors.^{25, 44, 47} These studies were performed in different experimental settings such as whereby MSC were plastic adhered, which is in contrast to our setting as we used polypropylene tubes to avoid baseline activation of monocytes adhering to the plastic. Moreover, in vivo when MSC are infused they remain in suspension the first time frame, hence usage of polypropylene tubes more closely resembles more the in vivo setting.

Clearance of infused MSC leaves a phenotypical and functional footprint in the monocyte compartment. To examine whether these changes affected monocyte function, ucMSC-primed monocytes were added to mixed lymphocyte reactions. We were able to show that ucMSC-primed monocytes increased Foxp3⁺CD25^{hi}CD127-CD4⁺ regulatory T cells. Multiple studies have reported increased frequencies of regulatory T cells in experimental animal studies^{48, 49} and in patients treated with MSC⁵⁰⁻⁵³. It has furthermore been shown that immunosuppressive macrophages (M2) can induce regulatory T cells in vitro.⁵⁴ Our results give

insight in how MSC driven polarization of monocytic cells may mediate increasing regulatory T cell numbers after MSC infusion

Conclusion

In conclusion, we have demonstrated that the rapid clearance of infused MSC is largely mediated by phagocytosis by monocytes, which subsequently relocate from the lungs to the bloodstream and the liver. UcMSC-primed monocytes change their phenotype and function and change the course of immune responses. The described mechanisms are likely to play a role in the immunomodulatory response after MSC infusion in disease models and clinical trials. Future studies will determine whether monocyte polarization can be attributed to specific components of MSC. This could eventually lead to more defined therapies based on the most active components that can be produced in an efficient and controlled manner.

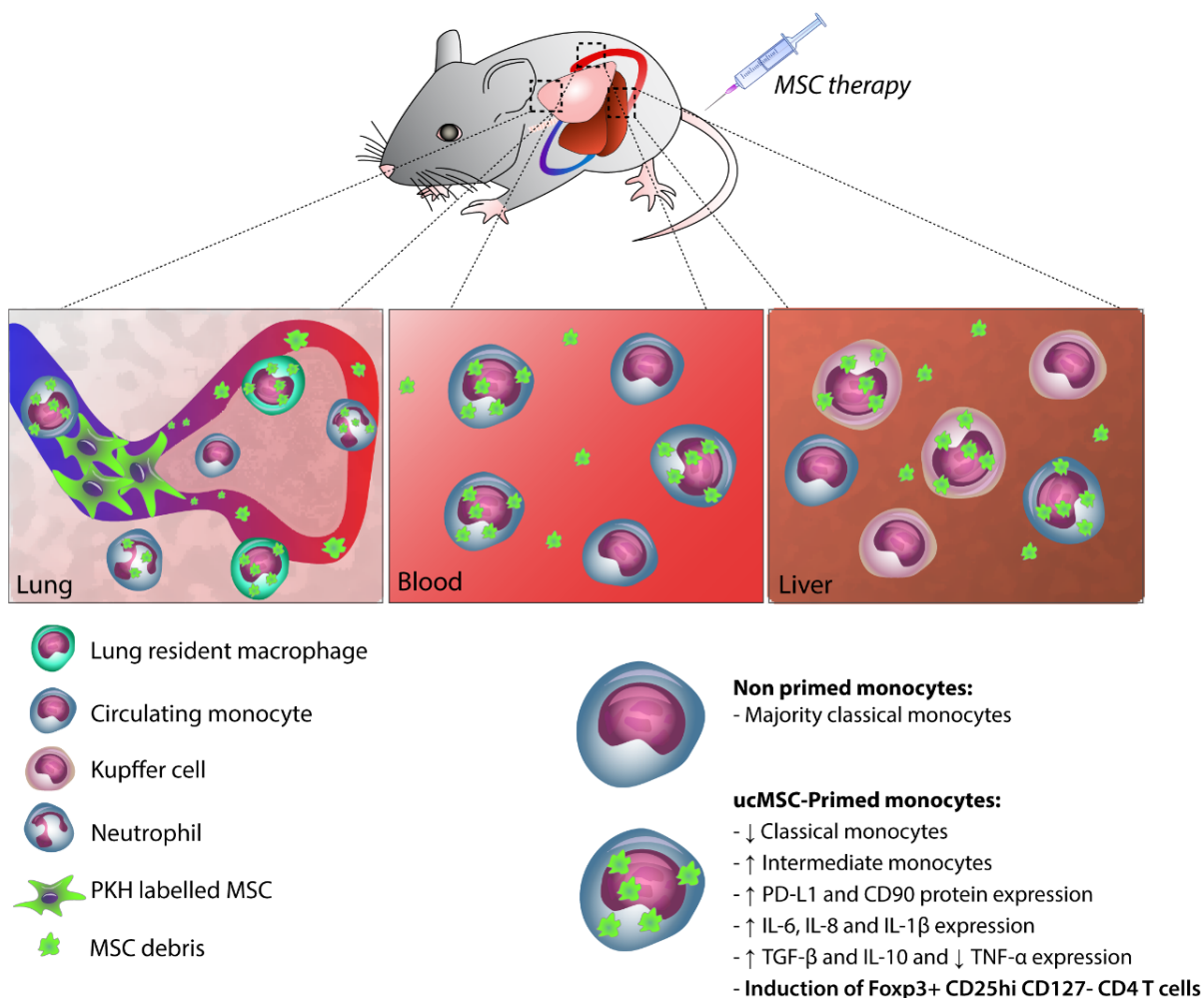
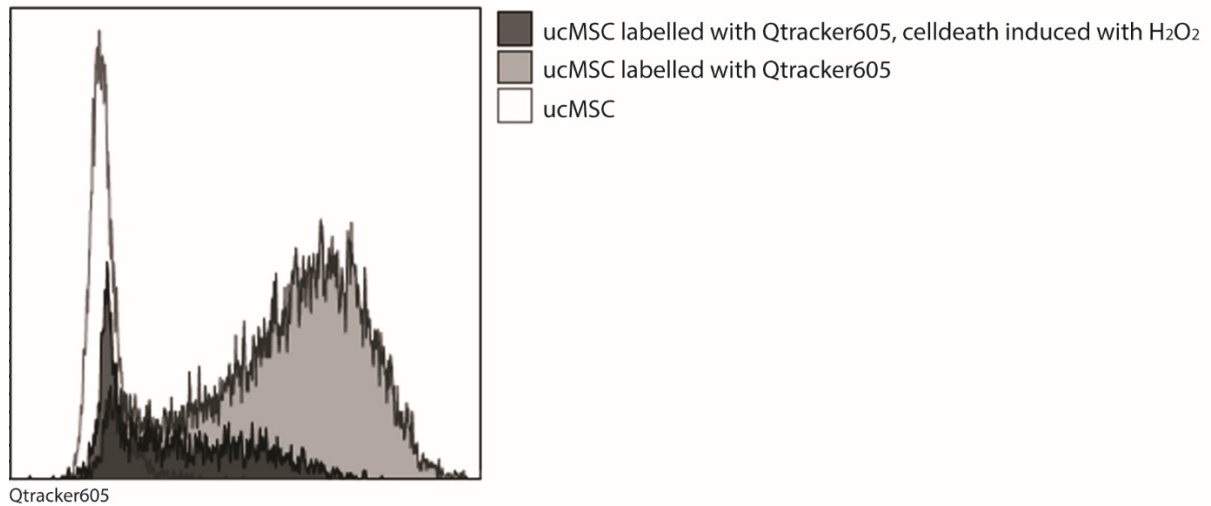
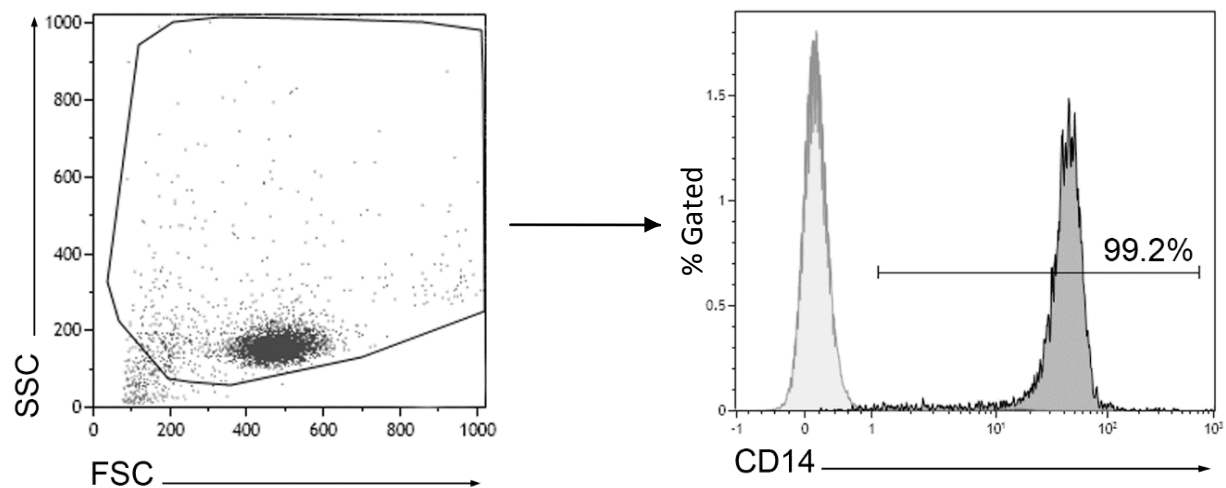


Figure 7. Overview of the interaction of monocytic cells with infused MSC. UCMSC get entrapped in the lungs after intravenous infusion and are rapidly cleared from the system through phagocytosis by neutrophils, lung resident macrophages and circulating monocytes. Monocytes containing ucMSC migrate via the blood stream to other sites, in particular to the liver. In addition, debris of ucMSC ends up in the liver where it is phagocytosed by liver-resident Kupffer cells. Phagocytosis of ucMSC induces an immunomodulatory phenotype in monocytes and ucMSC-primed monocytes induces Foxp3+CD25hiCD127-CD4+ regulatory T cells.

Supplementary Figures

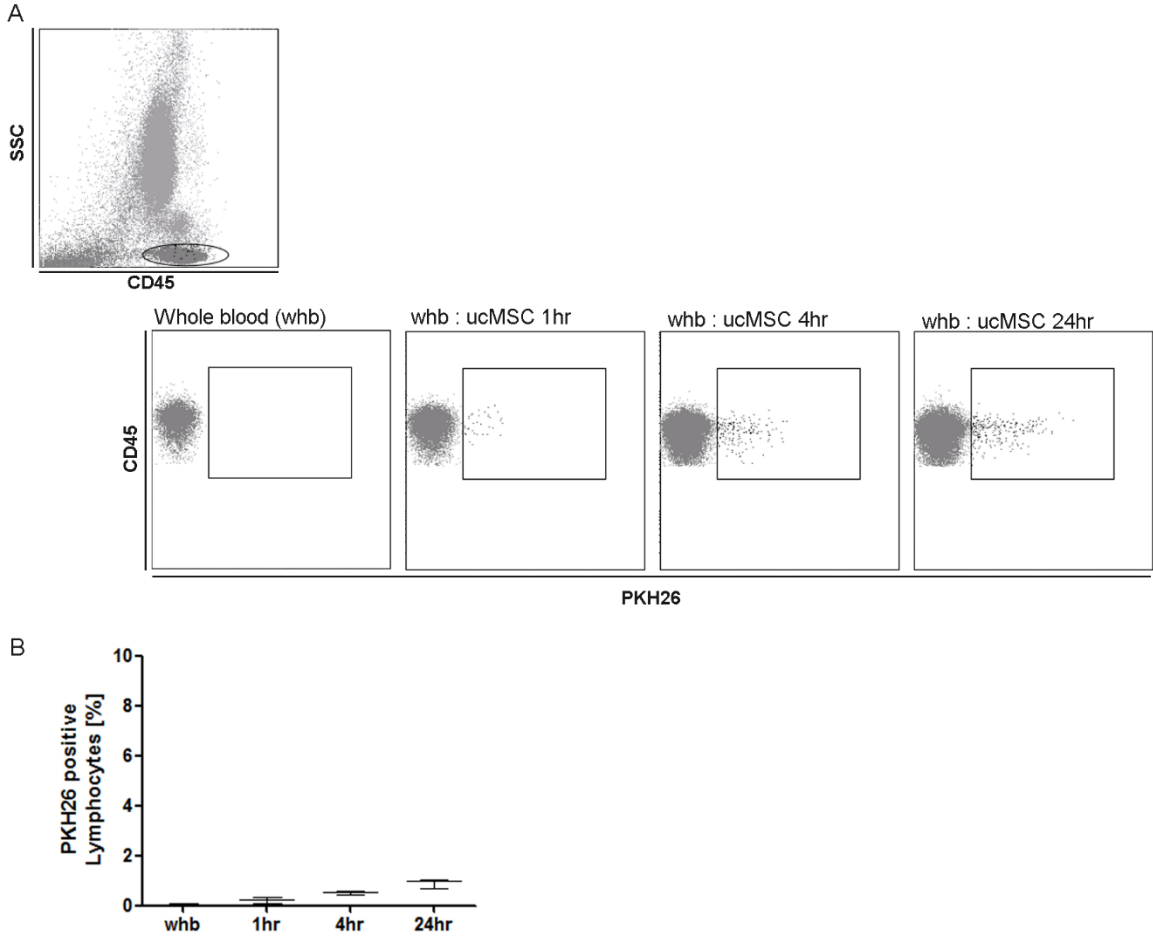


Supplementary Figure 1. ucMSC lose Qtracker beads after cell death. Flow cytometric plot showing unlabeled ucMSC (white), ucMSC labeled with Qtracker605 beads (light gray) and ucMSC labeled with Qtracker605 beads after induction of cell death by incubation with 50µM H₂O₂ (dark gray).



Supplementary Figure 2. Manual MACS separation of monocytes from MSC gives rise to a highly pure CD14+ population. Monocytes were MACS separated from the ucMSC by negative selection of CD73. Flow cytometric plot showing the purity of the isolated monocytes (>98%).

Chapter 3



Supplementary Figure 3. Phagocytosis of ucMSC by human lymphocytes in vitro is not significant. (A) Representative flow cytometry plot demonstrating of PKH26+ T-lymphocytes after addition of PKH26+ ucMSC to human whole blood. (B) Frequency of PKH26+ T-lymphocytes at t= 1, 4 and 24 hr after addition of PKH26+ labelled ucMSC to human whole blood. Plots indicate means \pm SEM. (n=4)

References

1. Gonzalez MA, Gonzalez-Rey E, Rico L, et al. Adipose-derived mesenchymal stem cells alleviate experimental colitis by inhibiting inflammatory and autoimmune responses. *Gastroenterology*. 2009;136:978-989.
2. Constantin G, Marconi S, Rossi B, et al. Adipose-derived mesenchymal stem cells ameliorate chronic experimental autoimmune encephalomyelitis. *Stem Cells*. 2009;27:2624-2635.
3. Popp FC, Eggenhofer E, Renner P, et al. Mesenchymal stem cells can induce long-term acceptance of solid organ allografts in synergy with low-dose mycophenolate. *Transpl Immunol*. 2008;20:55-60.
4. Roemeling-van Rhijn M, Khairoun M, Korevaar SS, et al. Human Bone Marrow- and Adipose Tissue-derived Mesenchymal Stromal Cells are Immunosuppressive In vitro and in a Humanized Allograft Rejection Model. *J Stem Cell Res Ther*. 2013;Suppl 6:20780.
5. Gonzalez-Rey E, Anderson P, Gonzalez MA, et al. Human adult stem cells derived from adipose tissue protect against experimental colitis and sepsis. *Gut*. 2009;58:929-939.
6. Augello A, Tasso R, Negrini SM, et al. Cell therapy using allogeneic bone marrow mesenchymal stem cells prevents tissue damage in collagen-induced arthritis. *Arthritis Rheum*. 2007;56:1175-1186.
7. Tobin LM, Healy ME, English K, et al. Human mesenchymal stem cells suppress donor CD4(+) T cell proliferation and reduce pathology in a humanized mouse model of acute graft-versus-host disease. *Clin Exp Immunol*. 2013;172:333-348.
8. Panes J, Garcia-Olmo D, Van Assche G, et al. Expanded allogeneic adipose-derived mesenchymal stem cells (Cx601) for complex perianal fistulas in Crohn's disease: a phase 3 randomised, double-blind controlled trial. *Lancet*. 2016;388:1281-1290.
9. Le Blanc K, Frassoni F, Ball L, et al. Mesenchymal stem cells for treatment of steroid-resistant, severe, acute graft-versus-host disease: a phase II study. *Lancet*. 2008;371:1579-1586.
10. Franquesa M, Hoogduijn MJ, Reinders ME, et al. Mesenchymal Stem Cells in Solid Organ Transplantation (MiSOT) Fourth Meeting: lessons learned from first clinical trials. *Transplantation*. 2013;96:234-238.
11. Bernardo ME, Ball LM, Cometa AM, et al. Co-infusion of ex vivo-expanded, parental MSCs prevents life-threatening acute GVHD, but does not reduce the risk of graft failure in pediatric patients undergoing allogeneic umbilical cord blood transplantation. *Bone Marrow Transplant*. 2011;46:200-207.
12. Hu J, Yu X, Wang Z, et al. Long term effects of the implantation of Wharton's jelly-derived mesenchymal stem cells from the umbilical cord for newly-onset type 1 diabetes mellitus. *Endocr J*. 2013;60:347-357.
13. Forbes GM, Sturm MJ, Leong RW, et al. A phase 2 study of allogeneic mesenchymal stromal cells for luminal Crohn's disease refractory to biologic therapy. *Clin Gastroenterol Hepatol*. 2014;12:64-71.
14. Eggenhofer E, Luk F, Dahlke MH, et al. The life and fate of mesenchymal stem cells. *Front Immunol*. 2014;5:148.
15. Eggenhofer E, Benseler V, Kroemer A, et al. Mesenchymal stem cells are short-lived and do not migrate beyond the lungs after intravenous infusion. *Front Immunol*. 2012;3:297.
16. Le Blanc K, Rasmusson I, Sundberg B, et al. Treatment of severe acute graft-versus-host disease with third party haploidentical mesenchymal stem cells. *Lancet*. 2004;363:1439-1441.
17. Xiao Y, Jiang ZJ, Pang Y, et al. Efficacy and safety of mesenchymal stromal cell treatment from related donors for patients with refractory aplastic anemia. *Cytotherapy*. 2013;15:760-766.

Chapter 3

18. Zhang Z, Lin H, Shi M, et al. Human umbilical cord mesenchymal stem cells improve liver function and ascites in decompensated liver cirrhosis patients. *J Gastroenterol Hepatol.* 2012;27 Suppl 2:112-120.
19. Tan J, Wu W, Xu X, et al. Induction therapy with autologous mesenchymal stem cells in living-related kidney transplants: a randomized controlled trial. *JAMA.* 2012;307:1169-1177.
20. Xu J, Wang D, Liu D, et al. Allogeneic mesenchymal stem cell treatment alleviates experimental and clinical Sjogren syndrome. *Blood.* 2012;120:3142-3151.
21. Gu F, Wang D, Zhang H, et al. Allogeneic mesenchymal stem cell transplantation for lupus nephritis patients refractory to conventional therapy. *Clin Rheumatol.* 2014;33:1611-1619.
22. Luk F, de Witte SF, Korevaar SS, et al. Inactivated Mesenchymal Stem Cells Maintain Immunomodulatory Capacity. *Stem Cells Dev.* 2016;25:1342-1354.
23. Lu W, Fu C, Song L, et al. Exposure to supernatants of macrophages that phagocytized dead mesenchymal stem cells improves hypoxic cardiomyocytes survival. *Int J Cardiol.* 2013;165:333-340.
24. Deng Y, Zhang Y, Ye L, et al. Umbilical Cord-derived Mesenchymal Stem Cells Instruct Monocytes Towards an IL10-producing Phenotype by Secreting IL6 and HGF. *Sci Rep.* 2016;6:37566.
25. Melief SM, Geutskens SB, Fibbe WE, et al. Multipotent stromal cells skew monocytes towards an anti-inflammatory interleukin-10-producing phenotype by production of interleukin-6. *Haematologica.* 2013;98:888-895.
26. Goncalves FDC, Luk F, Korevaar SS, et al. Membrane particles generated from mesenchymal stromal cells modulate immune responses by selective targeting of pro-inflammatory monocytes. *Sci Rep.* 2017;7:12100.
27. Ko JH, Lee HJ, Jeong HJ, et al. Mesenchymal stem/stromal cells precondition lung monocytes/macrophages to produce tolerance against allo- and autoimmunity in the eye. *Proc Natl Acad Sci U S A.* 2016;113:158-163.
28. de Witte SFH, Lambert EE, Merino A, et al. Aging of bone marrow- and umbilical cord-derived mesenchymal stromal cells during expansion. *Cytotherapy.* 2017.
29. de Witte SFH, Merino AM, Franquesa M, et al. Cytokine treatment optimises the immunotherapeutic effects of umbilical cord-derived MSC for treatment of inflammatory liver disease. *Stem Cell Res Ther.* 2017;8:140.
30. Tacke F, Randolph GJ. Migratory fate and differentiation of blood monocyte subsets. *Immunobiology.* 2006;211:609-618.
31. Ziegler-Heitbrock L. The CD14+ CD16+ blood monocytes: their role in infection and inflammation. *J Leukoc Biol.* 2007;81:584-592.
32. Kraitchman DL, Tatsumi M, Gilson WD, et al. Dynamic imaging of allogeneic mesenchymal stem cells trafficking to myocardial infarction. *Circulation.* 2005;112:1451-1461.
33. Fischer UM, Harting MT, Jimenez F, et al. Pulmonary passage is a major obstacle for intravenous stem cell delivery: the pulmonary first-pass effect. *Stem Cells Dev.* 2009;18:683-692.
34. Hoogduijn MJ, Roemeling-van Rhijn M, Engela AU, et al. Mesenchymal stem cells induce an inflammatory response after intravenous infusion. *Stem Cells Dev.* 2013;22:2825-2835.
35. Braza F, Dirou S, Forest V, et al. Mesenchymal Stem Cells Induce Suppressive Macrophages Through Phagocytosis in a Mouse Model of Asthma. *Stem Cells.* 2016;34:1836-1845.

36. Nemeth K, Leelahavanichkul A, Yuen PS, et al. Bone marrow stromal cells attenuate sepsis via prostaglandin E(2)-dependent reprogramming of host macrophages to increase their interleukin-10 production. *Nat Med*. 2009;15:42-49.
37. Galleu A, Riffo-Vasquez Y, Trento C, et al. Apoptosis in mesenchymal stromal cells induces in vivo recipient-mediated immunomodulation. *Sci Transl Med*. 2017;9.
38. Miteva K, Pappritz K, El-Shafeey M, et al. Mesenchymal Stromal Cells Modulate Monocytes Trafficking in Coxsackievirus B3-Induced Myocarditis. *Stem Cells Transl Med*. 2017;6:1249-1261.
39. Cutler AJ, Limbani V, Girdlestone J, et al. Umbilical cord-derived mesenchymal stromal cells modulate monocyte function to suppress T cell proliferation. *J Immunol*. 2010;185:6617-6623.
40. Murray PJ, Allen JE, Biswas SK, et al. Macrophage activation and polarization: nomenclature and experimental guidelines. *Immunity*. 2014;41:14-20.
41. Porcheray F, Viaud S, Rimaniol AC, et al. Macrophage activation switching: an asset for the resolution of inflammation. *Clin Exp Immunol*. 2005;142:481-489.
42. Svensson-Arvelund J, Mehta RB, Lindau R, et al. The human fetal placenta promotes tolerance against the semiallogeneic fetus by inducing regulatory T cells and homeostatic M2 macrophages. *J Immunol*. 2015;194:1534-1544.
43. Zizzo G, Hilliard BA, Monestier M, et al. Efficient clearance of early apoptotic cells by human macrophages requires M2c polarization and MerTK induction. *J Immunol*. 2012;189:3508-3520.
44. Melief SM, Schrama E, Brugman MH, et al. Multipotent stromal cells induce human regulatory T cells through a novel pathway involving skewing of monocytes toward anti-inflammatory macrophages. *Stem Cells*. 2013;31:1980-1991.
45. Kim J, Hematti P. Mesenchymal stem cell-educated macrophages: a novel type of alternatively activated macrophages. *Exp Hematol*. 2009;37:1445-1453.
46. Maggini J, Mirkin G, Bognanni I, et al. Mouse bone marrow-derived mesenchymal stromal cells turn activated macrophages into a regulatory-like profile. *PLoS One*. 2010;5:e9252.
47. Chen PM, Liu KJ, Hsu PJ, et al. Induction of immunomodulatory monocytes by human mesenchymal stem cell-derived hepatocyte growth factor through ERK1/2. *J Leukoc Biol*. 2014;96:295-303.
48. Casiraghi F, Azzollini N, Cassis P, et al. Pretransplant infusion of mesenchymal stem cells prolongs the survival of a semiallogeneic heart transplant through the generation of regulatory T cells. *J Immunol*. 2008;181:3933-3946.
49. Kavanagh H, Mahon BP. Allogeneic mesenchymal stem cells prevent allergic airway inflammation by inducing murine regulatory T cells. *Allergy*. 2011;66:523-531.
50. Jitschin R, Mougiakakos D, Von Bahr L, et al. Alterations in the cellular immune compartment of patients treated with third-party mesenchymal stromal cells following allogeneic hematopoietic stem cell transplantation. *Stem Cells*. 2013;31:1715-1725.
51. Ciccocioppo R, Bernardo ME, Sgarella A, et al. Autologous bone marrow-derived mesenchymal stromal cells in the treatment of fistulising Crohn's disease. *Gut*. 2011;60:788-798.
52. Xu L, Gong Y, Wang B, et al. Randomized trial of autologous bone marrow mesenchymal stem cells transplantation for hepatitis B virus cirrhosis: regulation of Treg/Th17 cells. *J Gastroenterol Hepatol*. 2014;29:1620-1628.

Chapter 3

53. Liang J, Zhang H, Hua B, et al. Allogenic mesenchymal stem cells transplantation in refractory systemic lupus erythematosus: a pilot clinical study. *Ann Rheum Dis.* 2010;69:1423-1429.
54. Schmidt A, Zhang XM, Joshi RN, et al. Human macrophages induce CD4(+)Foxp3(+) regulatory T cells via binding and re-release of TGF-beta. *Immunol Cell Biol.* 2016;94:747-762.

Chapter 4

Mesenchymal stromal cells are retained in the renal cortex independently of their metabolic state after renal intra-arterial infusion

Jesus M. Sierra-Parraga^{1,2}, Anders Munk³, Christine Andersen³, Stine Lohmann^{2,3}, Cyril Moers⁴, Carla C. Baan¹, Rutger J. Ploeg⁵, Merel Pool⁴, Anna K. Keller², Bjarne K. Møller⁶, Henri Leuvenink⁴, Martin J. Hoogduijn¹, Bente Jespersen³, Marco Eijken^{3,6}

¹Internal Medicine Department, University Medical Center Rotterdam, Erasmus MC, Rotterdam, the Netherlands;

²Department of Renal Medicine, Aarhus University Hospital, Aarhus, Denmark;

³Institute of Clinical Medicine, Aarhus University, Aarhus, Denmark;

⁴Department of Surgery – Organ Donation and Transplantation, University Medical Center Groningen, University of Groningen, Groningen, the Netherlands;

⁵Nuffield Department of Surgical Sciences and Oxford Biomedical Research Centre, University of Oxford, Oxford, UK;

⁶Department of Clinical Immunology, Aarhus University Hospital, Aarhus, Denmark.



Abstract

The regenerative capacities of mesenchymal stromal cells (MSC) make them suitable for renal regenerative therapy. The most common delivery route of MSC is via intravenous infusion, which is associated with off-target distribution. Renal intra-arterial delivery offers a targeted therapy but limited knowledge is available regarding the fate of MSC delivered via this route. Therefore, we studied the efficiency and tissue distribution of MSC after renal intra-arterial delivery to a porcine renal ischemia reperfusion model. MSC were isolated from adipose tissue of healthy male pigs, fluorescently labelled and infused into the renal artery of female pigs. Flow cytometry allowed MSC detection and quantification in tissue and blood. In addition, qPCR was used to trace MSC by their Y-chromosome. During infusion, a minor number of MSC left the kidney via the renal vein and no MSC were identified in arterial blood. Ischemic and healthy renal tissue were analyzed 30 minutes and 8 hours after infusion and $1-4 \times 10^4$ MSC per gram of tissue were detected, predominantly, in the renal cortex, with a viability greater than 70%. Confocal microscopy demonstrated mainly glomerular localization of MSC, but they were also observed in the capillary network around tubuli. The infusion of heat inactivated (HI)-MSC, which are metabolically inactive, through the renal artery showed that HI-MSC were distributed in the kidney in a similar manner as regular MSC, suggesting a passive retention mechanism. Long term MSC survival was analyzed by Y-chromosome tracing and demonstrated that a low percentage of the infused MSC were present in the kidney 14 days after administration, while HI-MSC were completely undetectable. In conclusion, renal intra-arterial MSC infusion limited off-target engraftment, leading to efficient MSC delivery to the kidney, most of them being cleared within 14 days. MSC retention was independent of the metabolic state of MSC, indicating a passive mechanism.

Introduction

Mesenchymal stromal cells (MSC) have regenerative properties which induce tissue regeneration in the injured kidney [1-3]. MSC secrete a variety of cytokines and growth factors that stimulate endothelial cell proliferation, enhance angiogenesis and reduce endothelium permeability [4-7]. Moreover, MSC are able to reduce inflammation through the secretion of immunoregulatory mediators and induce anti-inflammatory M2 macrophages [8-10].

Studies in rodents have shown that MSC can improve renal function in a transplant model [11] and restore renal structure and function in an acute kidney injury model [12]. A swine renal artery stenosis model showed that MSC are able to reduce fibrosis and inflammation of the renal medulla [13]. Moreover, in a porcine transplant model MSC treatment improved glomerular and tubular functions and protected the kidney from fibrosis [14].

As a result, several clinical trials are now trying to translate this success into an effective MSC therapy [15]. In these trials, the safety and efficacy of intravenous (IV) MSC infusion were investigated as a treatment for different renal diseases and to improve the outcome of kidney transplantation [2]. In the aforementioned animal and human studies, IV infusion of MSC was proven to be an easy and safe administration route. However, IV delivery of MSC has been shown to have some limitations. IV infused MSC do not specifically target the injured organ [16], which could lead to unwanted off-site effects. It has been shown that IV infusion of MSC leads to entrapment of MSC in the lung microvasculature, from where they are rapidly cleared by the immune system [17-19].

Intra-arterial infusion is a promising option to deliver MSC specifically to injured organs which increases MSC delivery efficiency compared to IV infusion [20,21]. This was demonstrated in a rat kidney transplantation model [22] and in kidney injury rat models of polycystic kidney disease [23] and glomerulonephritis [24]. Studies in an ovine model showed that administration of MSC through the renal artery leads to their engraftment in glomerular and tubular capillaries [25]. In swine models, renal intra-arterial delivery of MSC has been shown to reduce inflammation and fibrosis and improved revascularization, restoring renal function [13,26]. In an acute kidney injury monkey model, MSC infused through the renal artery were found in glomeruli and tubuli as well, and were able to restore renal function [27,28]. Moreover, a phase 1/2A human clinical trial has been carried out using renal intra-arterial infusion of autologous MSC treatment without reporting any adverse effects [29].

Chapter 4

Albeit renal intra-arterial MSC delivery is deemed feasible, the efficiency of MSC delivery is not known, which makes it difficult to study dose-dependent effects. In addition, the mechanisms behind the retention of MSC are unknown. To be able to better correlate renal intra-arterial based MSC therapy with observed effects in clinical and preclinical studies, more detailed knowledge regarding MSC retention and localization is crucial. These key questions require answering to further understand the role of exogenously administered MSC to the injured kidney and to explore the therapeutic use of MSC for kidney repair.

In the present study renal intra-arterial MSC infusion was investigated in a porcine ischemia-reperfusion injury kidney model. This model allows us to study MSC delivery in human sized kidneys making it translatable to studies in humans. The goal of the study was to determine the efficiency and tissue distribution of MSC delivered via the renal artery as well as to elucidate the mechanism responsible for MSC retention and survival in the kidney after infusion.

Materials and Methods

Institutional regulations

Female pigs of Danish Landrace and Yorkshire crossbreed weighing 40 kg were used. Animal care and experiments followed guidelines by the European Union (directive 2010/63/EU) and local regulations. The Animal Experiments Inspectorate approved the study (reference-number 2013-15-2934-00925 and 2017-15-0201-01367).

Isolation and expansion of MSC

Subcutaneous adipose tissue was collected from healthy 40-60 kg male Danish landrace pigs during surgery as a waste product. In total, 4 g fat was cut in small pieces and washed twice with 30 mL Dulbecco's phosphate buffered saline (DPBS) (ThermoFisher, Manhattan, NY, USA) by centrifugation at 850g for 5 min. Adipose tissue was dissociated in 10 mL RPMI-1640 medium (ThermoFisher) containing 150 U/mL collagenase type IV (ThermoFisher) in a GentleMACS Octo tissue dissociator (Miltenyi Biotec, Bergisch Gladbach, Germany) using protocol 37C-mr-ATDK-1. After dissociation, 10 mL culture medium was added and cells were pelleted at 650g for 10 min. Pellet was resuspended in 10 mL culture medium and filtered through a 70 µm cell strainer and seeded in culture flasks. Cells were cultured at 37°C and 5% CO₂ until they reached 80-90% confluency (about 7 days). Culture medium was replaced twice

a week and MSC were sub-cultured until passage 3 before use or cryostored in 50% serum, 10% DMSO in liquid N₂. MSC culture medium consisted of minimum essential medium (Sigma-Aldrich) supplemented with 15% fetal bovine serum (Sigma-Aldrich), 50 U/ml penicillin + 50 µg/ml streptomycin (ThermoFisher), and 2 mM L-glutamine (ThermoFisher).

MSC characterization

Morphology of MSC was observed with an axiovert 40 C microscope (Zeiss, Oberkochen, Germany) coupled to a Zeiss CanonSLR camera (Zeiss) and their fibroblastic appearance was confirmed (Figure 1A). MSC (p3) were characterized by the expression and absence of specific membrane markers. About 1×10^5 MSC in 100 µL DPBS were incubated for 30 minutes with 1 µL anti-human CD29 (APC, catalog #17-0299-42, Biolegend), 1µL CD44 (PE, catalog #17-0441-81, Biolegend), 1µL CD90 (BV421, catalog #561557, Biolegend), which are described to cross-react with swine species, and the absence of negative membrane markers was assessed with 5 µL anti-pig CD31 (FITC, catalog #MCA1746F, Bio-rad, Hercules, CA, USA) and 5 µL anti-pig CD45 (FITC, catalog #MCA1222F, Bio-rad). Next, cells were analyzed by multiparameter flow cytometry using a Novocyte flow cytometer (ACEA Biosciences, Inc., San Diego, CA, USA). All used MSC batches were >95% positive for CD29, CD44, CD90 and negative for CD31 and CD45 (Figure 1B and C). MSC size was measured directly after trypsinisation. MSC in suspension were transferred to a Burker-Turk counting chamber (ThermoFisher) and pictures were made under 100x magnification and analyzed by ImageJ software (National Institutes of Health, Bethesda, MD, USA) using plugins ij_Geodesics and Cell Magic Wand. The grid of the counting chamber was used as a size reference. For each cell the, maximum and minimum diameter was determined and the average diameter was used to express cell diameter. For each MSC batch cell diameter was determined of at least 100 cells. The size of infused MSC ranged from 10 to 30 µm and the median was 16-18 µm (Figure 1D and E).

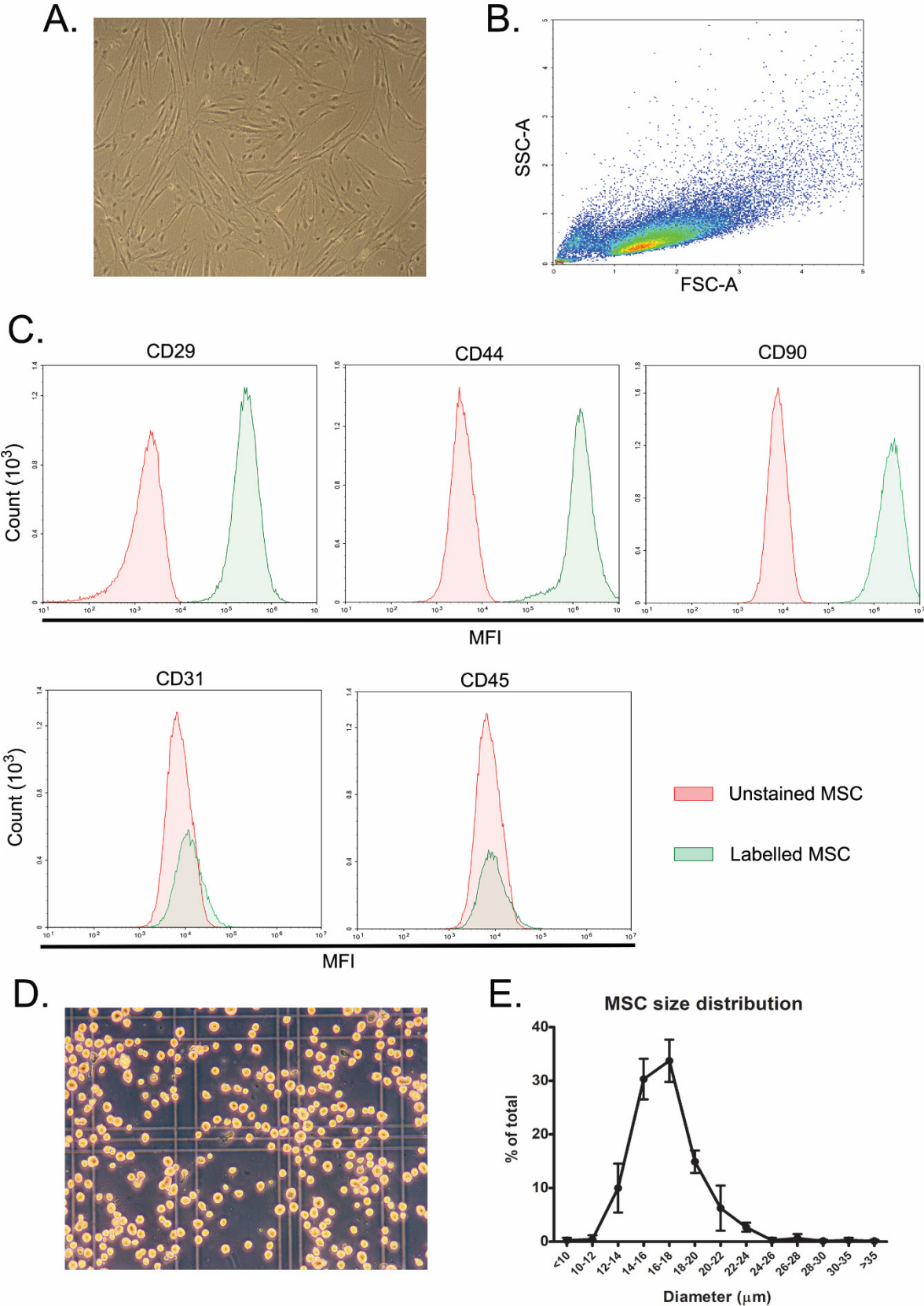


Figure 1. Porcine MSC characterization. (A) Fibroblast-like morphology of MSC. (B) Flow cytometry plot of forward and side scatter of MSC. (C) Expression level of CD29, CD44, CD90 CD31 and CD45. (D) Micrograph of trypsinized MSC in a Burkert-Turk chamber. (E) Size distribution of infused MSC.

MSC labelling

MSC were cultured until 90% confluency, trypsinized and labelled with Quantum dots (Qdot) 655 (ThermoFisher) using 1,5 μ L of the reagent per million MSC according to manufacturer's protocol immediately before the infusion. Fluorescence was measured prior to each infusion to establish the gating strategy to identify the MSC. For labelling with PKH-26 (Sigma), MSC were cultured as mentioned, trypsinized and labelling was performed following the manufacturer's protocol.

Heat inactivation of MSC

MSC were heat inactivated as previously described [30]. MSC were resuspended in DPBS (1-2 x 10⁶/mL) and incubated at 50° C for 30 minutes and cooled-down in ice for 5 minutes.

MSC administration

MSC were pelleted by centrifugation (440g, 5 min) after trypsinization, heat inactivation or labeling. MSC were resuspended in DPBS and filtered over a 70 μ m cell strainer. Before administration, cells were counted and visually inspected under a microscope in order to confirm a single cell solution.

Tissue dissociation

In total, 0.5 grams of renal tissue were cut in small pieces and dissociated using a GentleMACS Octo tissue dissociator (Miltenyi Biotec). Renal cortical tissue was dissociated in 2.5 mL RPMI 1640 (ThermoFisher) supplemented with 100 μ L enzyme D, 50 μ L enzyme R and 12.5 μ L enzyme A of a multi tissue dissociation kit 1 (Miltenyi Biotec) and run with protocol 37C_Multi_B. Renal medulla and lung tissue were dissociated in 2.5 mL buffer X supplemented with 25 μ L enzyme P, 25 μ L buffer Y, 50 μ L enzyme D and 10 μ L enzyme A of a multi tissue dissociation kit 2 (Miltenyi Biotec) and run with protocol 37C_Multi_E. After dissociation, 8 mL RPMI-1640 were added and the cell suspension was filtered through a 70 μ m cell strainer and centrifuged at 500 g for 7 minutes. Pellets were resuspended in 3 mL culture medium and analyzed immediately or cryo-preserved in 50% FBS, 10% DMSO.

Plastic adherent fraction of dissociated tissue

In total, 500 μ L cryo-preserved dissociated tissue was thawed and seeded in a T75 culture flask (Nunclon delta surface; Thermo Scientific) with 10 mL MSC medium and incubated for 1 day at 37°C and 5% CO₂. Medium was fully removed after 24 hours and cells were incubated for an additional 4 hours. Before trypsinization, cells were washed twice with PBS (without calcium and magnesium, ThermoFisher) and detached using 2 ml 0.05% Trypsin-EDTA (ThermoFisher). Cells were pelleted by centrifugation at 440g for 5 minutes and measured by flow cytometry or stored at -20°C for subsequent DNA isolation.

Y-chromosome PCR

DNA was isolated from 10 mg of kidney tissue or from cell pellets from the adherent fraction using a NucleoSpin Tissue DNA isolation kit (MACHEREY-NAGEL, Düren, Germany) according to manufacturer's protocol. DNA was eluted in 100 μ L water and Y-chromosome was detected by qPCR using primers directed to the male specific repeat (MSR) located on the porcine Y-chromosome as previously done by Gruessner et al. [31]. Primers directed to porcine S100C gene were used as a pig DNA control. Primer sequences were as follow: MSR forward 5'-CCA TCG GCC ATT GTT TTC CTG TTC A-3', MSR reverse 5'-CCT CTG TGC CCA CCT GCT CTC TAC A-3', S100C forward 5'-ATG CTG GAA GGG ACG GTA ACA ACA-3', and S100C reverse 5'-GCT CAG CTG CTG TCT TTC ACT CGT-3'. qPCR mix consisted of 0.5 μ L DNA, 10 pmol of each primer and 1x KiCStart SybrGreen qPCR ReadyMix (Sigma-Aldrich Life Science) in a final volume of 25 μ L. Samples were run in duplicate on a ABI 7300 (Perkin Elmer). The thermocycling program included an initial step of 2 minutes at 50° C. Subsequently 10 minutes at 95° C. Followed by a 40-time repeat two-step cycle consisting 95° C for 15 seconds and 60° C for 1 minute.

Anesthetics and surgical procedure

The pigs were sedated with intramuscular injection of Stresnil® (2.2mg/kg) to allow vein cannulation. Intravenous (IV) administration of Ketamine (6mg/kg) and Midazolam (0.5mg/kg) allowed intubation and ventilation keeping CO₂ between 4.5-5.5 kPa. Anesthesia was maintained using IV administrated Fentanyl (15 μ g/kg/h) and Propofol (3.5 mg/kg/h) preceded by a bolus of 7.5 μ g/kg (Fentanyl) and 1.875 mg/kg (Propofol). A bolus of 1.5 L Ringer Acetate was administrated within the first one and a half hours followed by a continuous infusion rate of 400 mL/h to maintain normal hydration and a mean arterial blood pressure \geq 60 mmHg in

all pigs. Introducers were inserted in the common carotid artery, external jugular vein and femoral artery (Radifocus® Introducer II, Terumo Europe, Leuven, Belgium). The experiments were conducted with or without renal ischemia.

MSC infusion during open surgery

The data presented in figures 2-4 were obtained by an open surgery procedure. Following a midline incision and retroperitoneal exposure of the left kidney, a catheter was positioned in the aorta over a guidewire in the femoral sheath. The catheter was further inserted into the left renal artery where positioning was controlled by palpation. Ischemic injury was performed by clamping the renal artery and vein for 60 minutes. After removing the clamps or directly after catheterization of healthy kidneys, 10 million MSC suspended in 25 mL DPBS were infused into the renal artery followed by a 5 mL DPBS flush both at a rate of 150 mL/h. In both healthy and ischemic kidneys, the renal artery catheter was removed after ten minutes when MSC administration was finished. Blood was collected simultaneously from the carotid artery and renal vein before, during and after MSC infusion. Bilateral nephrectomy was completed after either 30 minutes or 8 hours follow up and the pig was terminated using an IV overdose of pentobarbital (100mg/kg) while in general anesthesia. Both kidneys were weighted and cut longitudinally and horizontally through the medial line after retrieval. Kidney weight ranged from 90 to 110 grams in all pigs. One half of each kidney was used to obtain all tissue material used for analysis and the other one was embedded in PELCO® cryo-embedding compound (Ted Pella, Inc., Redding, CA, USA) and cryopreserved. Each experimental group consisted of 3 pigs.

Non-invasive MSC infusion

The data presented in figures 6 and 7 were obtained by a non-invasive MSC delivery method. Over a guidewire in the femoral introducer sheath, a catheter was introduced in the aorta and contrast agent (Iomeron 350mg/mL, total volume used 40 mL) was administered using X-ray to ensure the correct positioning of the catheter in the renal artery. Hereafter, 10 million MSC in 25 mL DPBS were infused into the renal artery followed by a 5 mL DPBS flush both at a rate of 150 mL/h. The renal artery catheter was removed after ten minutes, when MSC administration was finished.

Chapter 4

Bilateral nephrectomy was completed after 30 minutes (n=3) or 14 days follow up (n=8 and n=4 for MSC and heat inactivated (HI)-MSC infused kidneys, respectively) and the pig was terminated using an IV overdose of pentobarbital (100mg/kg) while in general anesthesia. Kidney weight ranged from 90 to 110 grams in all pigs.

MSC detection in kidney and blood by flow cytometry

Blood samples and renal tissue were analyzed using flow cytometry. Whole blood samples drawn from the renal vein and the carotid artery were directly analyzed. From the total dissociated kidney tissue, 400 μ L were analyzed by flow cytometry. The fluorescence was measured by excitation with a 405 nm laser and detection with the 660/20 BP, 650 LP filter set in a Novocyte flow cytometer (ACEA Biosciences, Inc., San Diego, CA, USA). To avoid low fluorescent cells from being measured and to speed up the measuring process a fluorescence threshold (median fluorescent intensity = 5000) was applied. Qdot-positive cells found in the cell suspensions were identified as the infused MSC. To confirm that the Qdot-positive cells found in dissociated renal tissue and in whole blood were indeed the infused MSC, simultaneous expression of CD29, CD44 and CD90 and absence of CD31 and CD45 was assessed as mentioned earlier for MSC characterization. The viability of MSC was assessed using the Zombie NIR™ Fixable Viability Kit (Biolegend). From the dissociated renal tissue 100 μ L were stained with Zombie NIR™ following the manufacturer's protocol and analyzed by flow cytometry. The total number of MSC in kidney tissue or blood was estimated from the number of events and the volume measured from each sample. Flow cytometry data was analyzed using NovoExpress software (ACEA Biosciences, Inc.).

Confocal microscopy of renal tissue

Kidney biopsies, containing both renal cortex and medulla, of 1 cm³ formalin-fixed and paraffin-embedded renal tissue biopsies were cut in 3 μ m thick slices. Images were obtained using a Leica SP5 confocal microscope (Leica microsystems, Wetzlar, Germany). Renal tissue auto-fluorescence was used to identify specific kidney structures such as glomeruli and tubules. Qdot 655 signal was detected by exciting the samples at a wavelength of 405 nm and measuring fluorescence emission at 655 nm. Tissue auto-fluorescence was measured at 420 nm to identify different renal structures. Images were analyzed using Fiji from ImageJ.

Cell localization by 3D cryo-imaging

Half kidneys were embedded in mounting medium for cryotomy (PELCO® cryo-embedding compound, Ted Pella Inc.) and frozen in liquid nitrogen. Frozen kidneys were kept at -80° C and shipped to BioInVision (OH, USA). At BioInVision, quantification of engrafted MSC was performed based on detection of fluorescent signal.

Statistical analysis

The Mann-Whitney test was used for comparison of mean numbers of MSC found in renal and lung tissue and MSC found in the blood outflow from the renal vein. The Kruskal-Wallis test was used when more than 2 groups were compared at the same time. Data were analyzed using GraphPad Prism version 5.00 for Windows (GraphPad Software, La Jolla, CA, USA).

Results

MSC quantification in blood and tissue

Qdot-labeled MSC showed a high fluorescent signal which allowed clear identification of the cells by flow cytometry (Sup. Figure 1A). To demonstrate the feasibility of a flow cytometry-based detection technique of relatively low numbers of MSC in large amounts of kidney and blood cells, Qdot-labelled MSC were mixed with dissociated renal tissue and whole blood in vitro. Results showed that Qdot-labeled MSC could be semi quantitatively measured in these samples (Sup. Figure 1B and C).

MSC detection after renal intra-arterial delivery

In total, 10 million Qdot-labelled MSC were infused in vivo through the renal artery to healthy or ischemic kidneys and 30 minutes after administration renal tissue was analyzed for the presence of Qdot-labelled MSC. We observed that MSC were successfully delivered to both healthy and ischemic kidneys (Figure 2A and D; Sup. Figure 3B and C). Measured MSC were in the order of $1-4 \times 10^4$ MSC per gram of dissociated cortical tissue. To demonstrate that MSC were stably retained in the kidney, the follow-up time of the ischemic group was extended to 8 hours. This demonstrated that the majority of MSC remained in the kidney at least up to 8 hours. The viability of MSC in the kidney tissue measured by flow cytometry ranged from 70 to 80% in all three conditions (Figure 2B). We observed that MSC found in the renal cortex had a bigger size than those found in the renal medulla (Figure 2C).

Qdot-labelled MSC were also detected in dissociated renal medulla, however, MSC numbers were 10-fold lower than those found in the renal cortex. Lung tissue contained numbers 100-fold lower compared to renal cortex, with an average of s200 MSC per gram of tissue (Figure 1D).

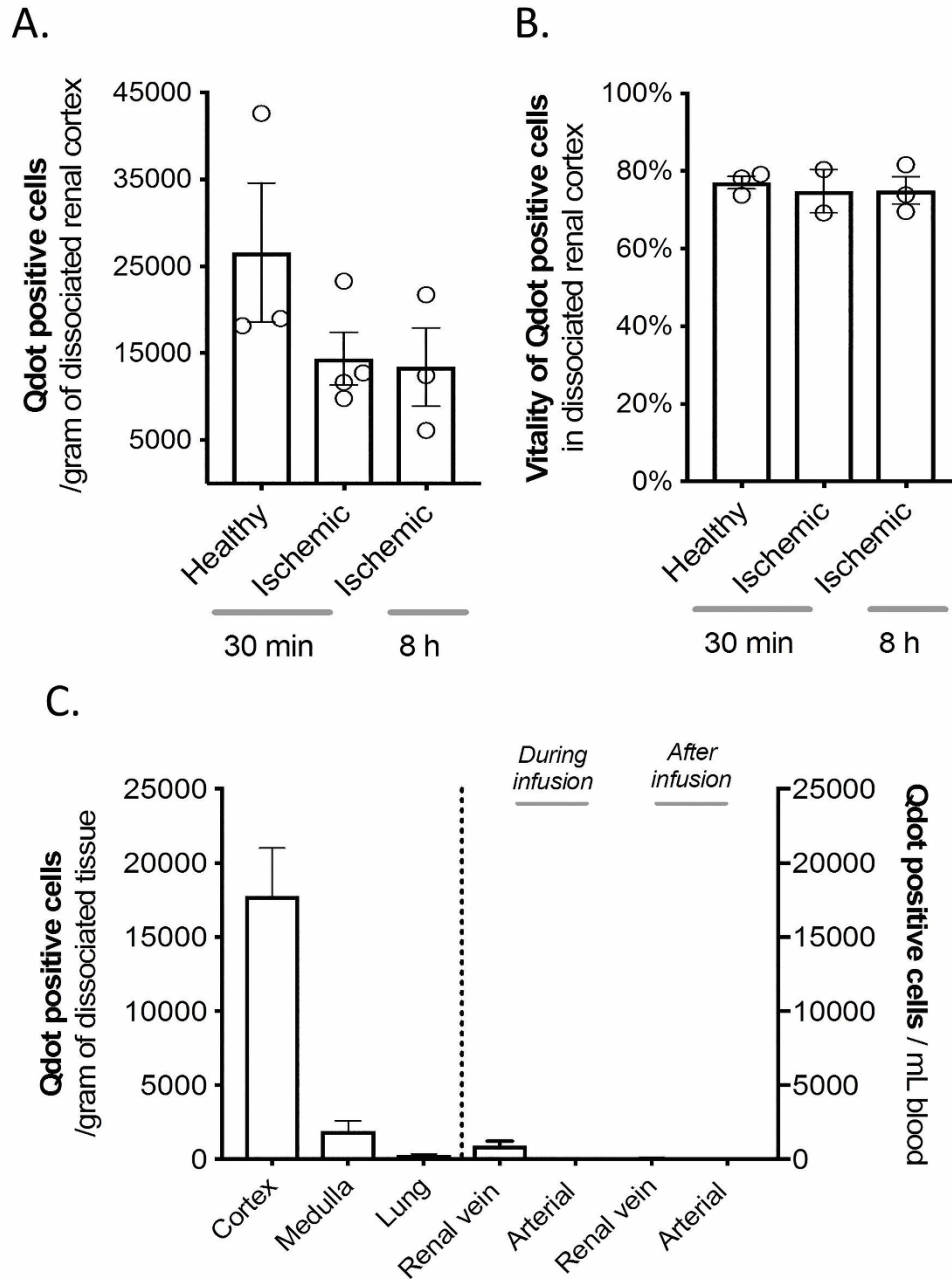


Figure 2. Intra-arterially delivered MSC are retained in the kidneys. (A) MSC per gram of renal cortical tissue of healthy and injured kidneys 30 minutes after infusion (n=3 and n=4, respectively) and of ischemic kidneys 8 hours after infusion (n=3). (B) Viability of MSC in healthy or ischemic renal cortical tissue after 30 min and in ischemic renal cortical tissue after 8 hours. (C) Size of MSC prior to infusion and MSC found in the renal cortex, renal medulla and venous outflow. (D) MSC per gram of renal cortex, renal medulla and lung. MSC per milliliter of whole blood drawn from the renal vein or the carotid artery.

During the experiments described above, blood samples from the renal vein and carotid artery were drawn to identify the presence of MSC passing through the kidneys. During infusion, an average of 500 MSC per mL were measured leaving the kidney through the renal vein. After the infusion stopped, hardly any MSC were found leaving the kidney (Figure 1D; Sup. Figure 2A). In blood samples from the carotid artery, no MSC were detected either during or after infusion (Sup. Figure 2B). The size of the MSC found in the renal vein outflow was smaller than those retained in the kidney, both in cortical and medullar tissue (Figure 2C).

Qdot-labelled MSC identified in blood and renal tissue were phenotyped to confirm MSC characteristics. Identified MSC expressed CD29, CD90 and CD105 and lacked the expression of CD31 and CD45 (Sup. Figure 4A-D).

Cortical localization of MSC after renal intra-arterial infusion was confirmed by 3D cryo-imaging

3D cryo-imaging was used to confirm the presence and localization of fluorescent MSC in the kidney. Kidneys were collected 30 minutes after administration of 10 million Qdot-labelled MSC and cryo-imaged. In figure 3A, a 3D volume rendering generated from brightfield data from the lateral and medial sides of the kidney are shown. Detected Qdot-positive MSC were pseudocolored in yellow and rendered along with brightfield data. MSC were mainly observed in renal cortical tissue (Figure 3B), supporting the data obtained by flow cytometry.

MSC are located mainly in glomerular structures

Confocal microscopy demonstrated that MSC were localised mostly to glomerular structures in the renal cortex. There was no clear difference regarding the location of MSC observed in healthy and ischemic kidneys. Pictures shown in Figure 4 were taken from healthy kidney tissue. Frequently, several MSC were observed in single glomeruli (Figure 4A-C). The frequency of MSC outside the glomerular structures was much lower. However, MSC could be identified around tubules both in the renal cortex and and medulla (Figure 4C and D, respectively).

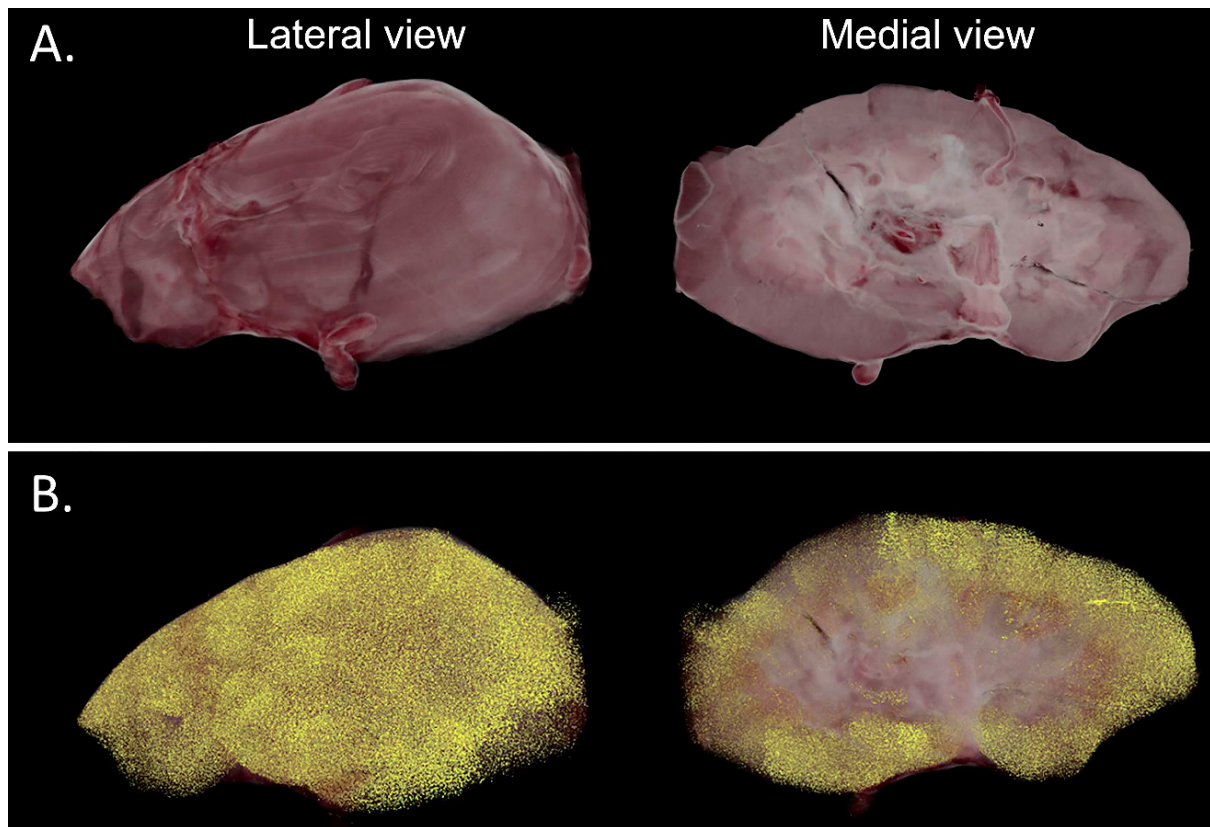


Figure 3. MSC are located mainly in renal cortex after infusion via the renal artery. (A) 3D volume rendering of half a kidney from the lateral and the medial side generated from brightfield data. (B) Detected Qdot-positive cells pseudo-colored in yellow and rendered along with brightfield volume from the lateral and medial side.

MSC stay in the kidney through a passive mechanism

In order to study the mechanism responsible for MSC retention in kidneys, we examined the retention of inactivated MSC in the kidney. HI-MSC were generated by heating MSC to 50°C for 30 minutes, which made them metabolically inactive and therefore they lost their ability to adhere (Figure 5).

Regular MSC or HI-MSC were infused in-vivo via the renal artery to healthy kidneys and MSC presence was assessed 30 minutes after administration by flow cytometry. HI-MSC were retained in similar numbers in the kidney as regular MSC (Figure 6A).

Viability analysis of retained MSC confirmed that regular MSC infused to the kidney remained alive in the renal cortex, whereas infused HI-MSC were indeed non-viable (Figure 6B). Dissociated renal tissue containing MSC was seeded in a culture dish to examine the adherent capacity of MSC in the tissue. Analysis of the adherent fraction of dissociated renal tissue demonstrated the presence of plastic-adherent Qdot-positive MSC, while only background

fluorescence was detected in the HI-MSC group (Figure 6C). Confocal microscopy and 3D cryo-imaging of HI-MSC infused kidneys confirmed that HI-MSC were located in the same renal structures as regular MSC (Figure 6D and E, respectively).

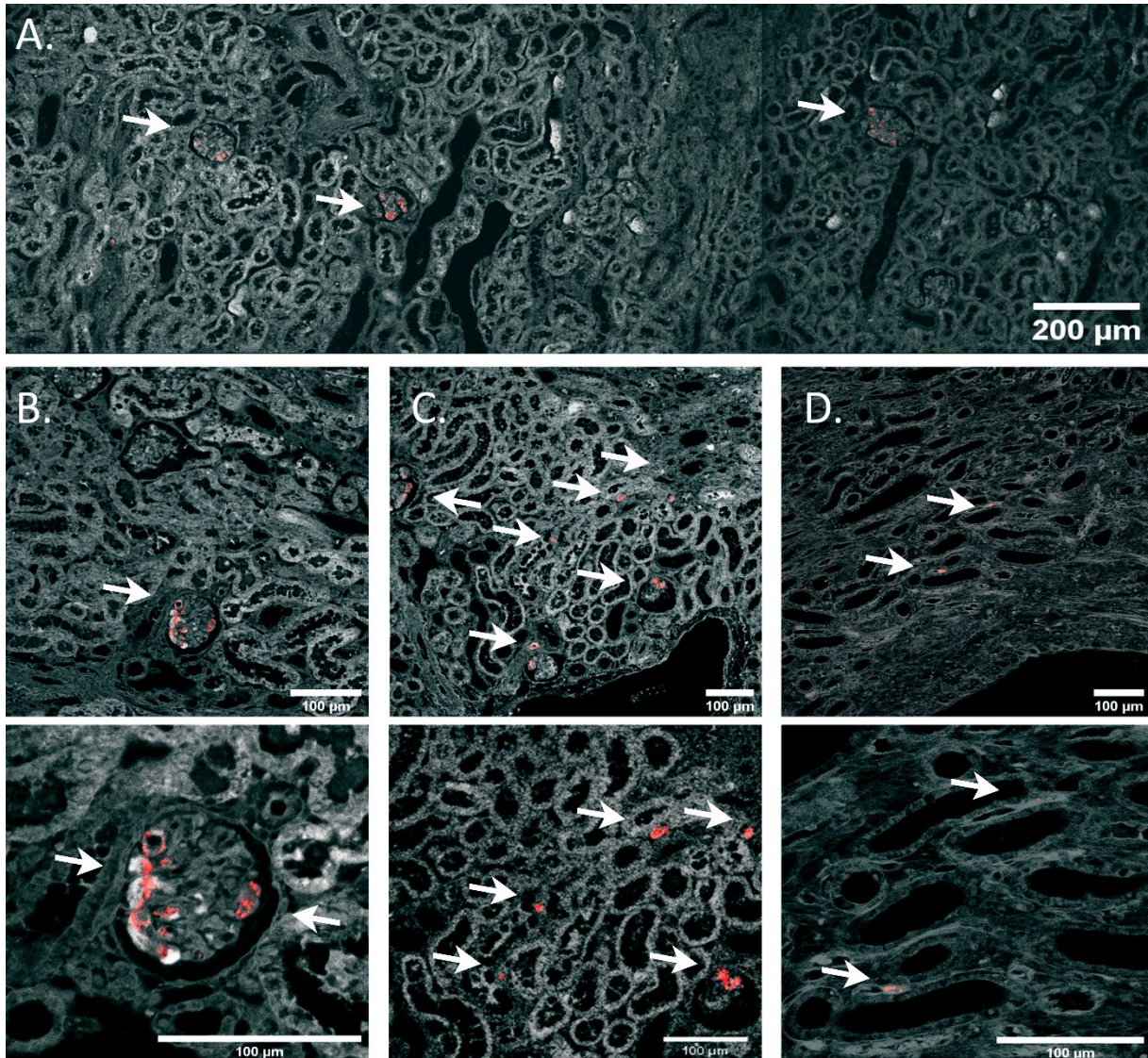


Figure 4. MSC are found primarily inside glomeruli. Micrograph of healthy renal tissue. Arrows depict Qdot 655 red fluorescence from MSC. Pictures were obtained from healthy renal tissue 30 minutes after fluorescent MSC infusion (A) Overview of renal cortical tissue overlaying renal tissue auto-fluorescence in grayscale and signal from Qdot 655 in red. (B) One single glomerulus occupied by several MSC. Zoomed in image of a glomerulus full of MSC. (C) Renal cortex with MSC found inside glomeruli and around tubules. Zoomed in image of MSC outside glomeruli. (D) Renal medulla with MSC found between tubuli. Zoomed in image of MSC around tubuli in renal medulla.

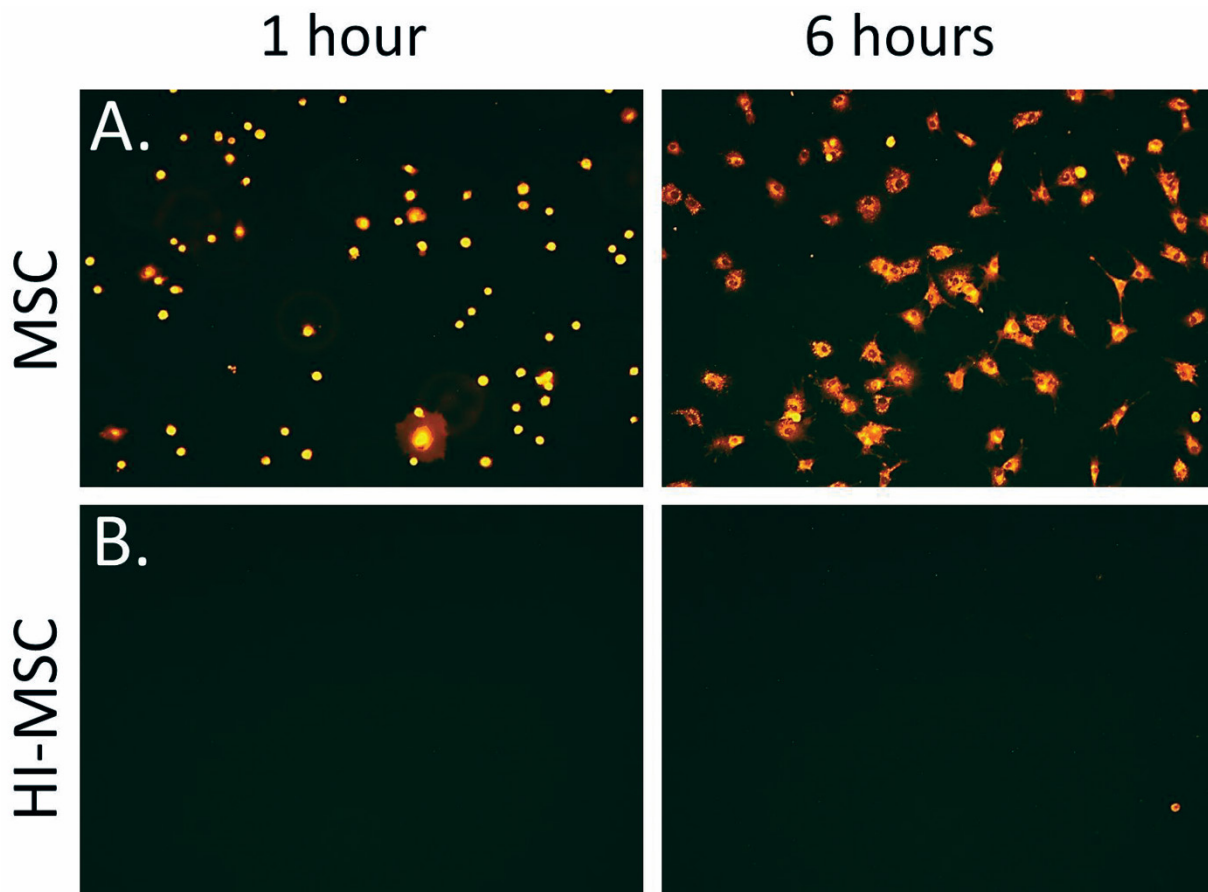


Figure 5. HI-MSC do not adhere to plastic in vitro. (A) PKH26-labelled MSC adhered to the culture flask 1 hour and 6 hours after seeding. (B) PKH26-labelled HI-MSC did not adhere to the culture flask 1 hour or 6 hours after seeding.

The majority of MSC are cleared from the kidney within 2 weeks

Male MSC were administered to female pigs which allowed male MSC tracing by a qPCR of a male specific repeat located on the pig Y-chromosome. First, renal tissue was analyzed for the presence of Y-chromosome in kidneys harvested 30 minutes after infusion of 10 million MSC or HI-MSC. This demonstrated that both MSC and HI-MSC infused kidneys contained high amounts of Y-chromosome 30 minutes after MSC delivery (Figure 7A).

The same experiment was repeated with a 14 days follow up. This showed that Y-chromosome could be detected 14 days after MSC infusion, whereas no such signal was detected in HI-MSC infused kidneys. Albeit Y-chromosome DNA was detected after 14 days, the average relative amount at day 14 was approximately 1% of the amount measured 30 minutes after infusion. Moreover, 3 out of 8 analyzed kidneys showed Y-chromosome DNA signal just above threshold. Viability of the detected MSC was demonstrated as previously described by analyzing the plastic adherent fraction of the dissociated renal tissue. This showed that

dissociated renal tissue isolated 14 days after MSC delivery contained living, plastic-adherent male MSC, whereas no male MSC could be found in the plastic adherent fraction of HI-MSC infused kidneys (Figure 7B).

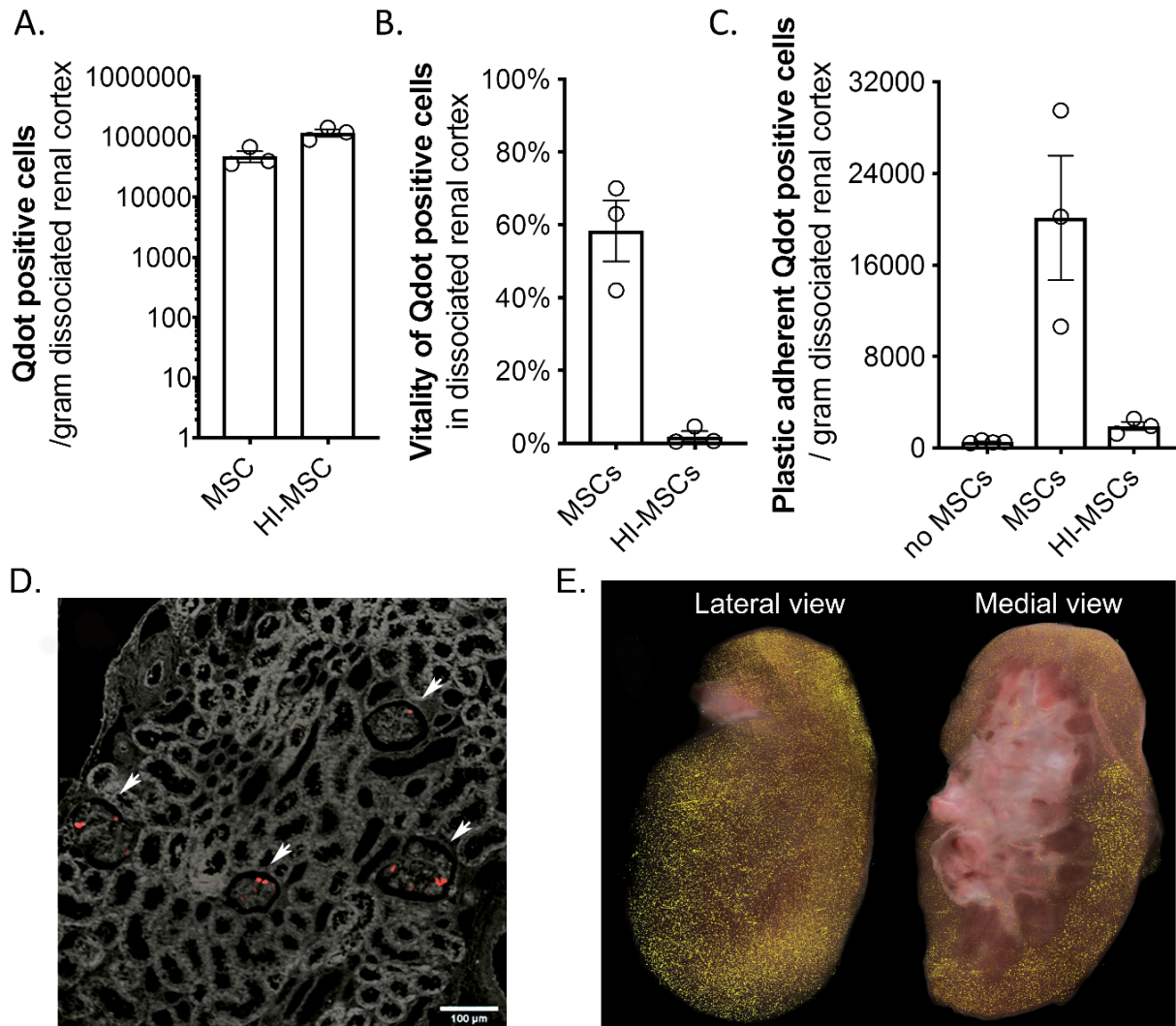


Figure 6. MSC stay in the kidney via a passive mechanism. (A) MSC and HI-MSC per gram of renal cortex 30 minutes after infusion in a healthy kidney (n=3). (B) Viability of MSC and HI-MSC in renal cortical tissue 30 minutes after infusion in a healthy kidney (n=3). (C) Plastic-adherent Qdot-positive MSC in dissociated kidney tissue after 1 day of culturing (n=3). (D) Arrows depict Qdot 655 red fluorescence from MSC. HI-MSC are located mostly inside glomeruli 30 minutes after infusion in healthy kidneys. (E) Detected Qdot-labelled HI-MSC are pseudo-colored in yellow and rendered along with brightfield volume from both the lateral and medial side.

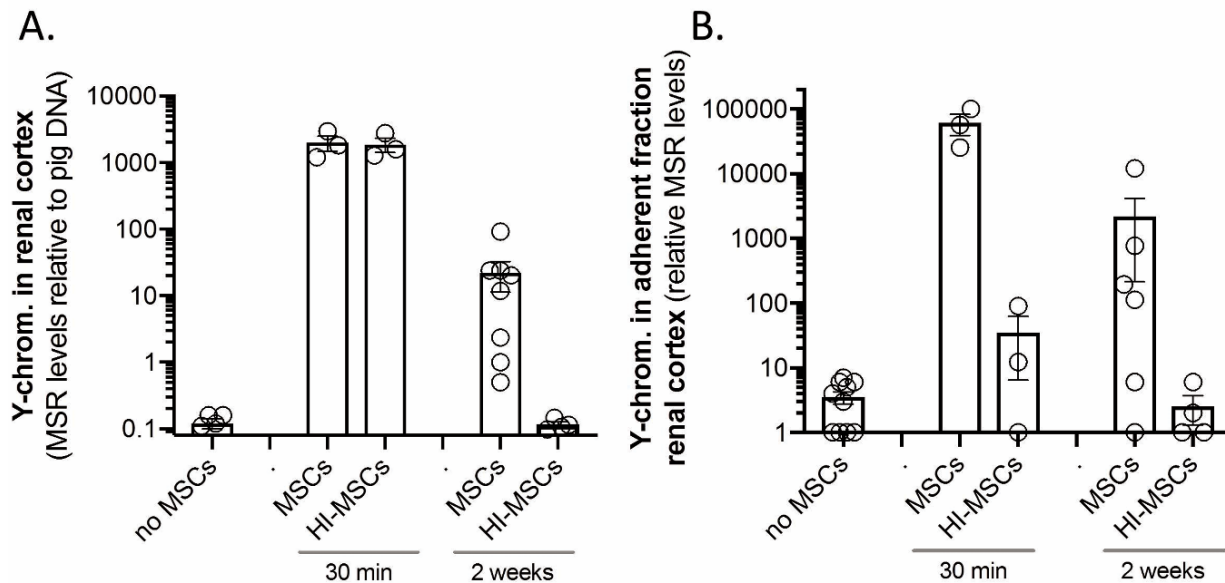


Figure 7. MSC are cleared from the kidney within 14 days. (A) Relative Y-chromosome compared to total pig DNA in kidney tissue 30 minutes after MSC or HI-MSC infusion (n=3) and 14 days after infusion of MSC (n=8) or HI-MSC (n=6). (B) Relative amount of Y-chromosome of the plastic-adherent cell fraction of dissociated kidney tissue isolated 30 minutes (n=3) and 14 days after infusion of MSC (n=6) and HI-MSC (n=4) after 1 day of culture.

Discussion

In this study we have tested the efficiency and tissue distribution of in-vivo MSC infusion through the renal artery in a porcine ischemia reperfusion injury model. We showed that targeted MSC delivery via the renal artery is a feasible route to deliver MSC to the kidney. Upon infusion, MSC are distributed throughout the kidney, located mostly in renal cortex and particularly inside glomeruli. MSC are retained in renal tissue presumably through a passive mechanism and after infusion they survive for at least 8 hours. The majority of MSC were cleared from the kidneys within two weeks.

We show that renal intra-arterial targeted infusion of MSC minimizes off-target delivery as only small numbers of MSC leave the kidney during infusion. Previous studies in animal models have simply associated the observed effects with the number of infused, but not delivered, MSC to the injured kidney [25,32,33]. In our study we actually quantify the number of MSC delivered to the target tissue which enables to correlate observed effects with the MSC dose in future studies. In order to do this, we used a semi-quantitative flow cytometric method which can be used to quantify MSC delivered to the kidney via renal intra-arterial infusion. Our approach using pre-labelled MSC in combination with flow cytometric analysis of dissociated kidney tissue allowed us to have a good estimate of the absolute amount of MSC that were retained in the kidney. Infusion of 10 million MSC to the kidney resulted in numbers

in the order of $1-4 \times 10^4$ MSC per gram of renal tissue delivered throughout the kidney, although the distribution was not completely homogenous. Extrapolation of measured concentrations of MSC using total kidney weight indicates that several million MSC were delivered per kidney. This number points out that a significant amount of MSC is not found back in the kidney. However, it should be noted that the measured numbers are a minimum value, as part of the MSC might be lost during the tissue dissociation and analysis process. It is still unknown whether this number of MSC is biologically relevant or therapeutically effective on the kidney. Therefore, our work paves the way for new studies to address this issue.

MSC were retained mostly in glomeruli as demonstrated also in other studies [24,25,32,33]. MSC are relatively large cells, so they might simply get entrapped in the microcapillaries of glomerular structures in a similar manner as MSC are entrapped in the lung's capillary network after intravenous infusion [17]. However, the size of MSC used in our experiments averaged $16 \mu\text{m}$ which is similar to some white blood cells which are able to pass through the microcapillaries of glomeruli. Red and white blood cells can deform by altering their cytoskeletal structure in order to be able to flow through microcapillaries [34-36]. However, MSC are originally tissue resident cells, which might be a reason not to have the same shape deformation capacities [37,38]. Moreover, HI-MSC were also retained in the same structures. These cells are not metabolically active and therefore unable to deform, which supports our hypothesis of a passive retention mechanism. We have shown that only bigger MSC were found in the renal cortex, while smaller MSC could pass through the glomerular microcapillaries and end up in the renal medulla or even left the kidney. In a rat model, infused MSC stayed in the kidney, whereas other infused cell type, of the same size, failed to stay in renal tissue [24]. This fact suggests that MSC are specifically retained by the kidney itself. In the case that MSC get stuck in the glomerular microcapillaries network, there might be some safety concerns as renal blood flow or function might be compromised. It has been reported in a rat model that after infusion of very high numbers of MSC, parenchymal perfusion decreased and it was restored to normality after 24 hours [32]. Furthermore, several murine pre-clinical studies showed improved function of injured kidneys after delivery of MSC through the renal artery with no adverse effects [23,24,39]. Besides, a human clinical trial has not reported serious adverse effects upon renal intra-arterial infusion of MSC and even showed, to some extent, improved kidney function [29].

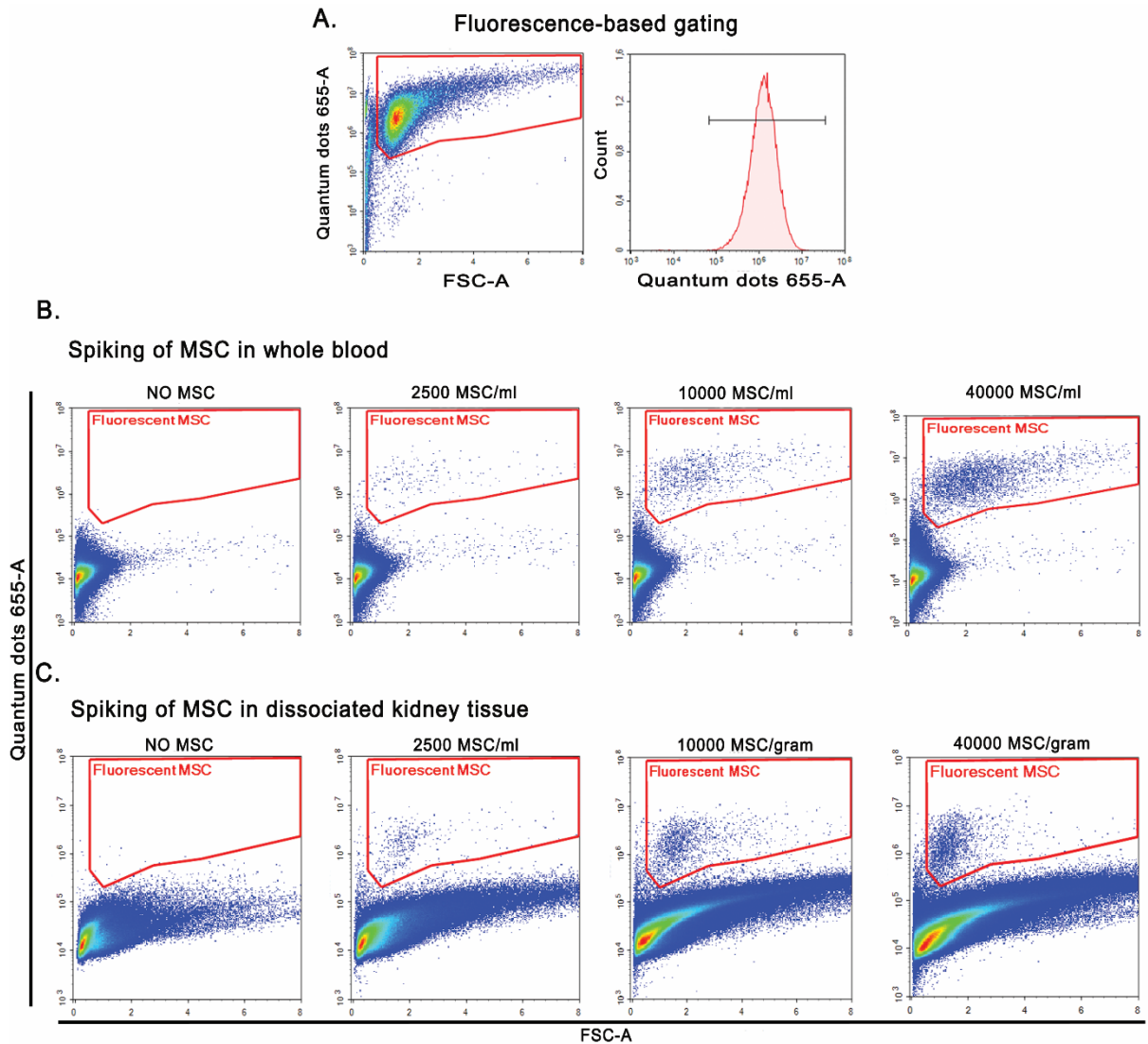
Chapter 4

MSC have been shown to be short lived after intravenous infusion [17,18,40]. However, renal intra-arterial infusion of MSC seems to ensure longer survival of MSC after infusion. In our study, MSC viability in the kidney 8 hours after infusion was around 70 to 80%. However, after 14 days, most MSC were cleared from the kidney. Nevertheless, large animal studies have shown the presence of MSCs up to 5 weeks after renal intra-arterial infusion [25], in contrast to our findings. In these large animal models, mostly autologous MSC are used [25-27,33], whereas rodent renal intra-arterial MSC infusion models usually employ allogeneic MSC [21,23,24]. In both cases, similar survival of infused MSC was observed, which suggests that the origin of MSC does not affect survival after delivery. From a logistic and translational point of view, the use of allogeneic MSC is more appealing as large numbers of therapeutic MSC should be readily available for treatment. Our results confirm that infusion of allogeneic MSC is feasible in large animal models and enables survival of MSC in renal tissue.

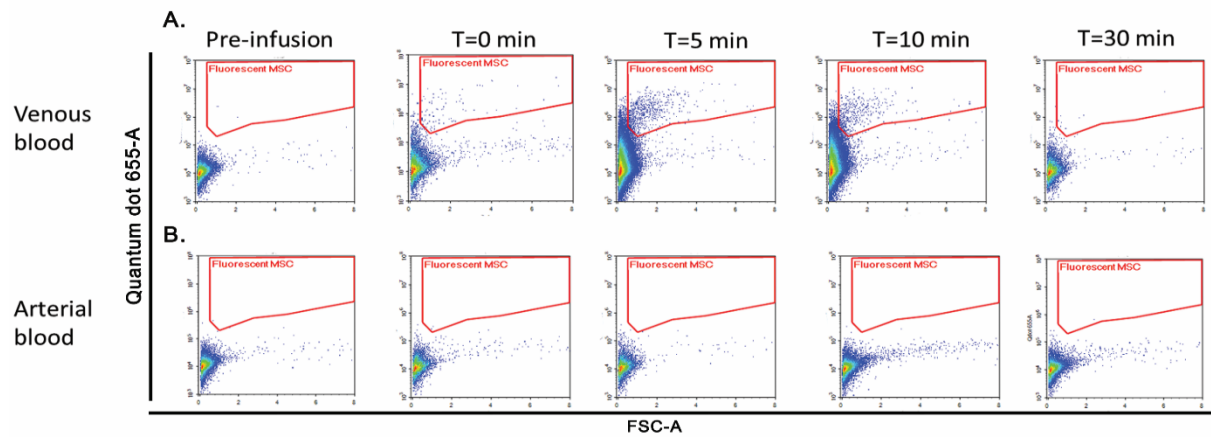
The mechanism behind MSC retention after renal intra-arterial infusion is, so far, poorly understood. Although we have shown that retention of MSC in the kidney is independent of the metabolic status of the infused MSC, they could be actively attached by the glomerular endothelium. It has been described that MSC can physically interact with endothelial cells via adhesion molecules present in their membrane, such as very late antigen 4 [41,42]. As HI-MSC maintain the proteins expressed on their membrane, they may still be able to interact with the endothelium through this mechanism. The elucidation of the mechanisms behind the effects of MSC is essential to further develop MSC therapies. However, conflicting data found in the literature defend both the paracrine secretion of cytokines [43,44] and the physical interaction with other cells [18,30] as the main mechanism of MSC action. This makes it difficult to draw a conclusion and therefore, additional experimentation is indeed needed.

Summarizing, renal intra-arterially infused MSC are delivered particularly to the glomeruli and survive for at least 8 hours after infusion. Their presence can potentially allow them to interact with injured tissue and elicit a regenerative response. To completely understand the potential of MSC therapy in kidneys, further studies are now starting in order to decipher the specific mechanisms of action of MSC after renal intra-arterial delivery, which will contribute to an improved MSC therapy for treatment of kidney injury.

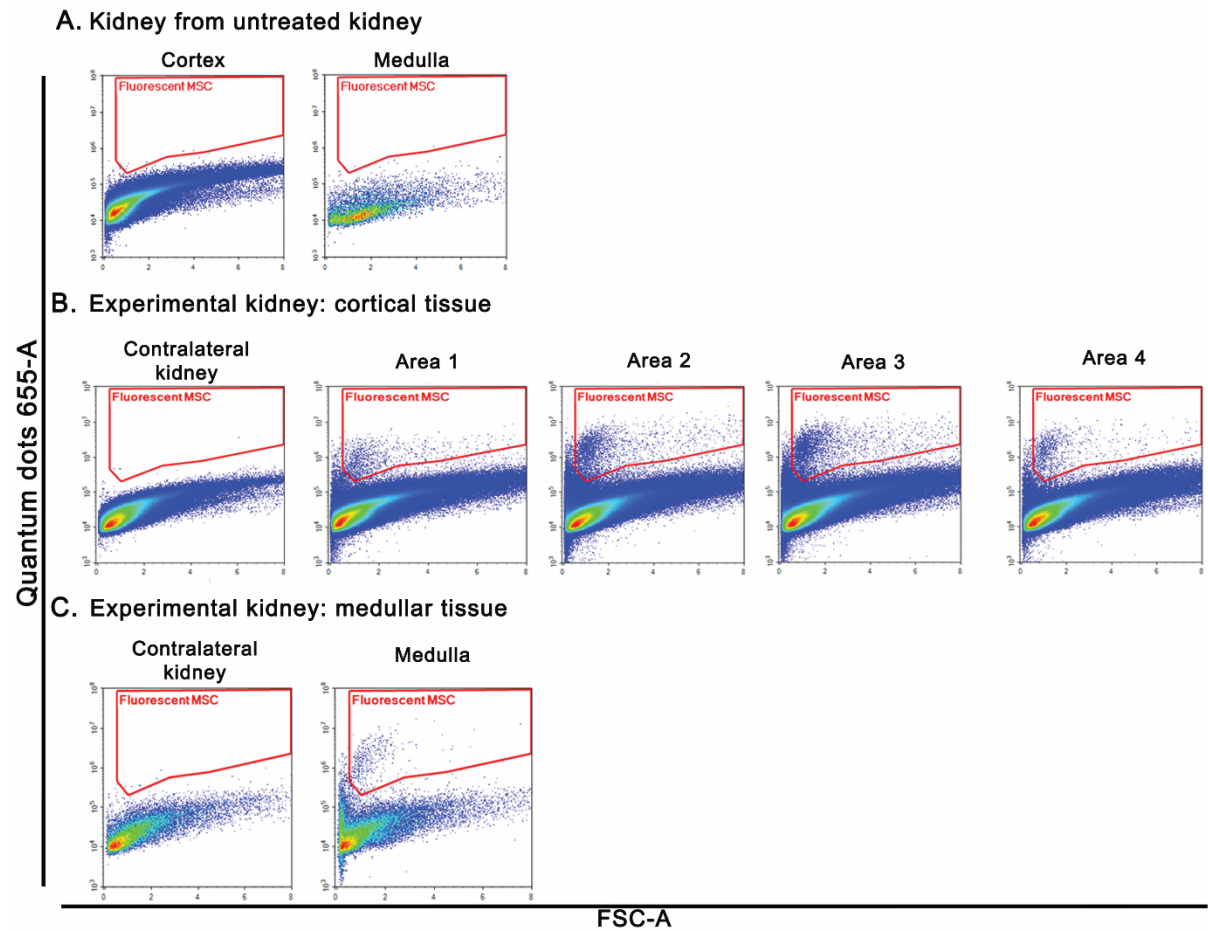
Supplementary figures



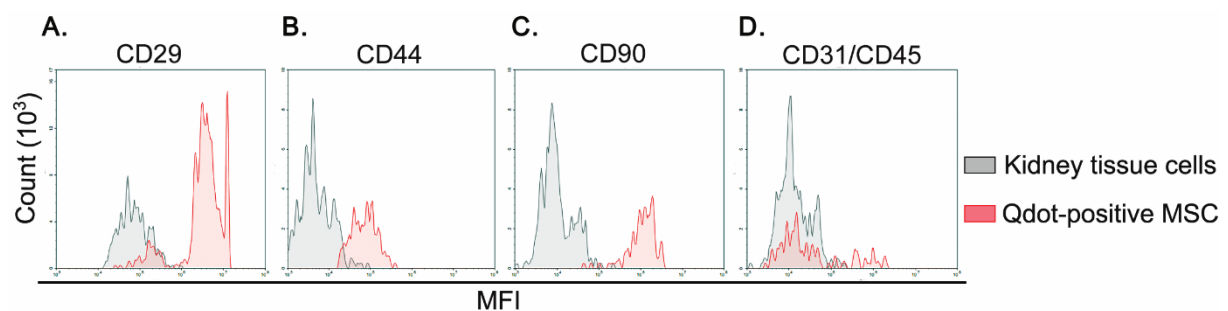
Supplementary Figure 1. MSC gating and quantification strategy. (A) Qdot 655 fluorescence-based gating of MSC prior to infusion. (B) Spiking of MSC in whole blood. (C) Spiking of MSC in dissociated renal tissue.



Supplementary figure 2. Cytometry plots of MSC found in venous and arterial blood. (A) MSC found in renal venous blood. (B) MSC detected in carotid arterial blood.



Supplementary figure 3. Cytometry plots of MSC found in renal cortex and medulla. (A) Renal cortex and medulla from a control kidney not infused with MSC. (B) Cytometry plots of renal cortex from a pig kidney infused with 10 million Qdot-labelled MSC and the contralateral kidney not infused with MSC. (C) Cytometry plots of renal medulla from a pig kidney infused with 10 million Qdot-labelled MSC and the contralateral kidney not infused with MSC.



Supplementary figure 4. MSC characterization. (A-C) Expression of CD29, CD44 and CD90, respectively, of Qdot positive MSC found in blood and dissociated kidney tissue. (D) Expression of CD31 and CD45 of Qdot positive MSC found in blood and dissociated kidney tissue.

References

1. Morigi M, C Rota and G Remuzzi. (2016). Mesenchymal Stem Cells in Kidney Repair. *Methods Mol Biol* 1416:89-107.
2. Peired AJ, A Sisti and P Romagnani. (2016). Mesenchymal Stem Cell-Based Therapy for Kidney Disease: A Review of Clinical Evidence. *Stem Cells Int* 2016:4798639.
3. Baraniak PR and TC McDevitt. (2010). Stem cell paracrine actions and tissue regeneration. *Regen Med* 5:121-43.
4. Morishita R, S Nakamura, Y Nakamura, M Aoki, A Moriguchi, I Kida, Y Yo, K Matsumoto, T Nakamura, J Higaki and T Ogihara. (1997). Potential role of an endothelium-specific growth factor, hepatocyte growth factor, on endothelial damage in diabetes. *Diabetes* 46:138-42.
5. Nakano N, R Morishita, A Moriguchi, Y Nakamura, SI Hayashi, M Aoki, I Kida, K Matsumoto, T Nakamura, J Higaki and T Ogihara. (1998). Negative regulation of local hepatocyte growth factor expression by angiotensin II and transforming growth factor-beta in blood vessels: potential role of HGF in cardiovascular disease. *Hypertension* 32:444-51.
6. Yang Y, QH Chen, AR Liu, XP Xu, JB Han and HB Qiu. (2015). Synergism of MSC-secreted HGF and VEGF in stabilising endothelial barrier function upon lipopolysaccharide stimulation via the Rac1 pathway. *Stem Cell Res Ther* 6:250.
7. Burlacu A, G Grigorescu, AM Rosca, MB Preda and M Simionescu. (2013). Factors secreted by mesenchymal stem cells and endothelial progenitor cells have complementary effects on angiogenesis in vitro. *Stem Cells Dev* 22:643-53.
8. Qi Y, D Jiang, A Sindrilaru, A Stegemann, S Schatz, N Treiber, M Rojewski, H Schrezenmeier, S Vander Beken, M Wlaschek, M Bohm, A Seitz, N Scholz, L Durselen, J Brinckmann, A Ignatius and K Scharffetter-Kochanek. (2014). TSG-6 released from intradermally injected mesenchymal stem cells accelerates wound healing and reduces tissue fibrosis in murine full-thickness skin wounds. *J Invest Dermatol* 134:526-37.
9. Geng Y, L Zhang, B Fu, J Zhang, Q Hong, J Hu, D Li, C Luo, S Cui, F Zhu and X Chen. (2014). Mesenchymal stem cells ameliorate rhabdomyolysis-induced acute kidney injury via the activation of M2 macrophages. *Stem Cell Res Ther* 5:80.
10. Bouffi C, C Bony, G Courties, C Jorgensen and D Noel. (2010). IL-6-dependent PGE2 secretion by mesenchymal stem cells inhibits local inflammation in experimental arthritis. *PLoS One* 5.
11. Iwai S, I Sakonju, S Okano, T Teratani, N Kasahara, S Yokote, T Yokoo and E Kobayash. (2014). Impact of ex vivo administration of mesenchymal stem cells on the function of kidney grafts from cardiac death donors in rat. *Transplant Proc* 46:1578-84.
12. Morigi M, B Imberti, C Zoja, D Corna, S Tomasoni, M Abbate, D Rottoli, S Angioletti, A Benigni, N Perico, M Alison and G Remuzzi. (2004). Mesenchymal stem cells are renotropic, helping to repair the kidney and improve function in acute renal failure. *J Am Soc Nephrol* 15:1794-804.
13. Ebrahimi B, A Eirin, Z Li, XY Zhu, X Zhang, A Lerman, SC Textor and LO Lerman. (2013). Mesenchymal stem cells improve medullary inflammation and fibrosis after revascularization of swine atherosclerotic renal artery stenosis. *PLoS One* 8:e67474.
14. Baulier E, F Favreau, A Le Corf, C Jayle, F Schneider, JM Goujon, O Feraud, A Bennaceur-Griscelli, T Hauet and AG Turhan. (2014). Amniotic fluid-derived mesenchymal stem cells prevent fibrosis and preserve renal function in a preclinical porcine model of kidney transplantation. *Stem Cells Transl Med* 3:809-20.
15. Reinders MEJ, C van Kooten, TJ Rabelink and JW de Fijter. (2018). Mesenchymal Stromal Cell Therapy for Solid Organ Transplantation. *Transplantation* 102:35-43.

Chapter 4

16. Gao J, JE Dennis, RF Muzic, M Lundberg and AI Caplan. (2001). The dynamic in vivo distribution of bone marrow-derived mesenchymal stem cells after infusion. *Cells Tissues Organs* 169:12-20.
17. Eggenhofer E, V Benseler, A Kroemer, FC Popp, EK Geissler, HJ Schlitt, CC Baan, MH Dahlke and MJ Hoogduijn. (2012). Mesenchymal stem cells are short-lived and do not migrate beyond the lungs after intravenous infusion. *Frontiers in Immunology* 3:297.
18. de Witte SFH, F Luk, JM Sierra Parraga, M Gargasha, A Merino, SS Korevaar, AS Shankar, L O'Flynn, SJ Elliman, D Roy, MGH Betjes, PN Newsome, CC Baan and MJ Hoogduijn. (2018). Immunomodulation By Therapeutic Mesenchymal Stromal Cells (MSC) Is Triggered Through Phagocytosis of MSC By Monocytic Cells. *Stem Cells* 36:602-615.
19. Fischer UM, MT Harting, F Jimenez, WO Monzon-Posadas, H Xue, SI Savitz, GA Laine and CS Cox, Jr. (2009). Pulmonary passage is a major obstacle for intravenous stem cell delivery: the pulmonary first-pass effect. *Stem cells and development* 18:683-692.
20. Sun JH, GJ Teng, ZL Ma and SH Ju. (2008). In vivo monitoring of magnetically labeled mesenchymal stem cells administered intravascularly in rat acute renal failure. *Swiss Med Wkly* 138:404-12.
21. Togel F, Y Yang, P Zhang, Z Hu and C Westenfelder. (2008). Bioluminescence imaging to monitor the in vivo distribution of administered mesenchymal stem cells in acute kidney injury. *Am J Physiol Renal Physiol* 295:F315-21.
22. Zonta S, M De Martino, G Bedino, G Piotti, T Rampino, M Gregorini, F Frassoni, A Dal Canton, P Dionigi and M Alessiani. (2010). Which Is the Most Suitable and Effective Route of Administration for Mesenchymal Stem Cell-Based Immunomodulation Therapy in Experimental Kidney Transplantation: Endovenous or Arterial? *Transplantation Proceedings* 42:1336-1340.
23. Franchi F, KM Peterson, R Xu, B Miller, PJ Psaltis, PC Harris, LO Lerman and M Rodriguez-Porcel. (2015). Mesenchymal Stromal Cells Improve Renovascular Function in Polycystic Kidney Disease. *Cell Transplant* 24:1687-98.
24. Kunter U, S Rong, Z Djuric, P Boor, G Muller-Newen, D Yu and J Floege. (2006). Transplanted mesenchymal stem cells accelerate glomerular healing in experimental glomerulonephritis. *J Am Soc Nephrol* 17:2202-12.
25. Behr L, M Hekmati, G Fromont, N Borenstein, LH Noel, M Lelievre-Pegorier and K Laborde. (2007). Intra renal arterial injection of autologous mesenchymal stem cells in an ovine model in the postischemic kidney. *Nephron Physiol* 107:p65-76.
26. Eirin A, XY Zhu, JD Krier, H Tang, KL Jordan, JP Grande, A Lerman, SC Textor and LO Lerman. (2012). Adipose tissue-derived mesenchymal stem cells improve revascularization outcomes to restore renal function in swine atherosclerotic renal artery stenosis. *Stem Cells* 30:1030-41.
27. Moghadasali R, M Azarnia, M Hajinasrollah, H Arghani, SM Nassiri, M Molazem, A Vosough, S Mohitmafi, M Najarasl, Z Ajdari, RS Yazdi, M Bagheri, H Ghanaati, B Rafiei, Y Gheisari, H Baharvand and N Aghdami. (2014). Intra-renal arterial injection of autologous bone marrow mesenchymal stromal cells ameliorates cisplatin-induced acute kidney injury in a rhesus Macaque mulatta monkey model. *Cytotherapy* 16:734-49.
28. Lee KW, TM Kim, KS Kim, S Lee, J Cho, JB Park, GY Kwon and SJ Kim. (2018). Renal Ischemia-Reperfusion Injury in a Diabetic Monkey Model and Therapeutic Testing of Human Bone Marrow-Derived Mesenchymal Stem Cells. *J Diabetes Res* 2018:5182606.
29. Saad A, AB Dietz, SMS Herrmann, LJ Hickson, JF Glockner, MA McKusick, S Misra, H Bjarnason, AS Armstrong, DA Gastineau, LO Lerman and SC Textor. (2017). Autologous Mesenchymal Stem Cells Increase Cortical Perfusion in Renovascular Disease. *J Am Soc Nephrol* 28:2777-2785.
30. Luk F, SF de Witte, SS Korevaar, M Roemeling-van Rhijn, M Franquesa, T Strini, S van den Engel, M Gargasha, D Roy, FJ Dor, EM Horwitz, RW de Bruin, MG Betjes, CC Baan and MJ Hoogduijn. (2016). Inactivated Mesenchymal Stem Cells Maintain Immunomodulatory Capacity. *Stem Cells Dev* 25:1342-54.

Passive Retention of MSC after Renal Intra-Arterial Infusion

31. Gruessner RW, BK Levay-Young, RE Nakhleh, JD Shearer, M Dunning, CM Nelson and AC Gruessner. (2004). Portal donor-specific blood transfusion and mycophenolate mofetil allow steroid avoidance and tacrolimus dose reduction with sustained levels of chimerism in a pig model of intestinal transplantation. *Transplantation* 77:1500-6.
32. Cai J, X Yu, R Xu, Y Fang, X Qian, S Liu, J Teng and X Ding. (2014). Maximum efficacy of mesenchymal stem cells in rat model of renal ischemia-reperfusion injury: renal artery administration with optimal numbers. *PLoS One* 9:e92347.
33. Behr L, M Hekmati, A Lucchini, K Houcinet, AM Faussat, N Borenstein, LH Noel, M Lelievre-Pegorier and K Laborde. (2009). Evaluation of the effect of autologous mesenchymal stem cell injection in a large-animal model of bilateral kidney ischaemia reperfusion injury. *Cell Prolif* 42:284-97.
34. Redenbach DM, D English and JC Hogg. (1997). The nature of leukocyte shape changes in the pulmonary capillaries. *Am J Physiol* 273:L733-40.
35. Li J, G Lykotrafitis, M Dao and S Suresh. (2007). Cytoskeletal dynamics of human erythrocyte. *Proc Natl Acad Sci U S A* 104:4937-42.
36. Ekpenyong AE, N Toepfner, C Fiddler, M Herbig, W Li, G Cojoc, C Summers, J Guck and ER Chilvers. (2017). Mechanical deformation induces depolarization of neutrophils. *Sci Adv* 3:e1602536.
37. Fraser JK, I Wulur, Z Alfonso and MH Hedrick. (2006). Fat tissue: an underappreciated source of stem cells for biotechnology. *Trends Biotechnol* 24:150-4.
38. Beltrami AP, L Barlucchi, D Torella, M Baker, F Limana, S Chimenti, H Kasahara, M Rota, E Musso, K Urbanek, A Leri, J Kajstura, B Nadal-Ginard and P Anversa. (2003). Adult cardiac stem cells are multipotent and support myocardial regeneration. *Cell* 114:763-76.
39. Jang MJ, D You, JY Park, K Kim, J Aum, C Lee, G Song, HC Shin, N Suh, YM Kim and CS Kim. (2018). Hypoxic Preconditioned Mesenchymal Stromal Cell Therapy in a Rat Model of Renal Ischemia-reperfusion Injury: Development of Optimal Protocol to Potentiate Therapeutic Efficacy. *Int J Stem Cells* 11:157-167.
40. Eggenhofer E, F Luk, MH Dahlke and MJ Hoogduijn. (2014). The life and fate of mesenchymal stem cells. *Front Immunol* 5:148.
41. Ruster B, S Gottig, RJ Ludwig, R Bistrrian, S Muller, E Seifried, J Gille and R Henschler. (2006). Mesenchymal stem cells display coordinated rolling and adhesion behavior on endothelial cells. *Blood* 108:3938-44.
42. Segers VF, I Van Riet, LJ Andries, K Lemmens, MJ Demolder, AJ De Becker, MM Kockx and GW De Keulenaer. (2006). Mesenchymal stem cell adhesion to cardiac microvascular endothelium: activators and mechanisms. *Am J Physiol Heart Circ Physiol* 290:H1370-7.
43. Brasile L, N Henry, G Orlando and B Stubenitsky. (2019). Potentiating Renal Regeneration Using Mesenchymal Stem Cells. *Transplantation* 103:307-313.
44. Kim HK, SG Lee, SW Lee, BJ Oh, JH Kim, JA Kim, G Lee, JD Jang and YA Joe. (2019). A Subset of Paracrine Factors as Efficient Biomarkers for Predicting Vascular Regenerative Efficacy of Mesenchymal Stromal/Stem Cells. *Stem Cells* 37:77-88.

Chapter 5

Reparative effect of mesenchymal stromal cells on endothelial cells after hypoxic and inflammatory injury

Jesus M Sierra-Parraga¹, Ana Merino¹, Marco Eijken^{2, 3}, Henri Leuvenink⁴, Rutger Ploeg⁵, Bjarne K. Møller³, Bente Jespersen^{2, 3}, Carla C. Baan¹, Martin J. Hoogduijn¹

¹ Internal Medicine Department, Sector Nephrology & Transplantation, University Medical Center Rotterdam, Erasmus MC, Rotterdam, the Netherlands.

² Department of Renal Medicine, Aarhus University Hospital, Aarhus, Denmark.

³ Department of Clinical Immunology, Aarhus University Hospital, Aarhus, Denmark.

⁴ Department of Surgery – Organ Donation and Transplantation, University Medical Center Groningen, University of Groningen, Groningen, the Netherlands.

⁵ Nuffield Department of Surgical Sciences and Oxford Biomedical Research Centre, University of Oxford, UK.

⁶ Department of Renal Medicine, Aarhus University Hospital, Aarhus, Denmark.



(Submitted to Stem Cells Research & Therapy)

Abstract

The renal endothelium is a prime target for ischemia reperfusion injury (IRI) during donation and transplantation procedures. Mesenchymal stromal cells (MSC) have been shown to ameliorate kidney function after IRI. However, whether this involves repair of the endothelium is not clear. Therefore, our objective is to study potential regenerative effects of MSC on injured endothelial cells and to identify the molecular mechanisms involved.

Human umbilical vein endothelial cells (HUVEC) were submitted to hypoxia and reoxygenation and TNF- α treatment. To determine whether physical interaction or soluble factors released by MSC were responsible for the potential regenerative effects of MSC on endothelial cells, dose-response experiments were performed in co-culture and transwell conditions and with secretome deficient MSC.

MSC showed increased migration and adhesion to injured HUVEC, mediated by CD29 and CD44 on the MSC membrane. MSC decreased membrane injury marker expression, oxidative stress levels and monolayer permeability of injured HUVEC, which was observed only when allowing both physical and paracrine interaction between MSC and HUVEC. Furthermore, viable MSC in direct contact with injured HUVEC improved wound healing capacity by 45% and completely restored their angiogenic capacity. In addition, MSC exhibited an increased ability to migrate through an injured HUVEC monolayer compared to non-injured HUVEC in vitro. These results show that MSC have regenerative effects on injured HUVEC via a mechanism which requires both physical and paracrine interaction. The identification of specific effector molecules involved in MSC-HUVEC interaction will allow targeted modification of MSC to apply and enhance the therapeutic effects of MSC in IRI.

Introduction

Ischemia-reperfusion injury (IRI) of a transplanted organ cannot be avoided and initiates an inflammatory cascade leading to organ dysfunction (1).

IRI especially impacts organs from donation after circulatory death and from expanded criteria donors with age higher than 60 years co-morbidities such as hypertension (2). The increasing use of organs from these donors enables enlarging the donor organ pool, but these organs tend to be more sensitive to injury which is associated with worse transplantation outcome (3, 4). IRI particularly leads to endothelial injury, resulting in their activation and the loss of endothelial wall integrity and function (5-8).

Mesenchymal stromal cells (MSC) may represent a unique cellular tool to repair damaged endothelium. MSC are adult multipotent cells present in most tissues in the adult human body (9, 10). These cells are known for their regenerative and anti-inflammatory properties, which have been explored in a number of small animal (11-13) and large animal (14-16) injury models. In these experimental models, MSC have been shown to have regenerative properties that may promote endothelial repair. For this reason, MSC are being studied as a therapeutic agent for kidney disease and transplantation in man (17). Several phase I trials have shown that MSC therapy is safe and suggest that their immunoregulatory and regenerative properties might lead to an improved kidney transplantation outcome (18-21). In most of these studies, the MSC were given via intravenous (IV) infusion which led to entrapment of MSC in the pulmonary capillaries that prevented MSC delivery to the injured kidney (22). Thus, direct MSC infusion to the injured tissue may be a better method to deliver MSC to the kidney. We have previously shown that infusion via the renal artery, MSC are delivered to the microvasculature of the kidney (23). The interaction with the kidney microvasculature is the starting point for the regenerative effects of MSC and therefore it is of key importance to understand the mechanisms of the interaction between MSC and endothelial cells. A better understanding of these interactions will enable us to optimize the potential regenerative effect of MSC therapy on endothelial injury. The first data about MSC delivery to the kidney during *ex situ* normothermic machine perfusion show a distribution of MSC to the renal microvasculature, with MSC localizing to the renal cortex (24). Although data suggest that MSC may possess renal regenerating effects after administration to the kidney (25), it is unknown whether this involves endothelial repair, and if so which mechanisms are involved.

Chapter 5

Here, we investigated the potential reparative effects of MSC on endothelial cells, which were subjected to hypoxic and inflammatory insults. We tested whether physical or paracrine interaction of MSC and endothelial cells was responsible for the regenerative effects of MSC and which molecules were involved.

Materials and Methods

Isolation and culture of MSC

MSC were isolated from subcutaneous adipose tissue from healthy human kidney donors (n=5) that became available during kidney donation procedures after obtaining written informed consent as approved by the Medical Ethical Committee of the Erasmus University Medical Centre Rotterdam (MEC-2006-190).

MSC were cultured at 37° C, 5% CO₂ and 20% O₂ in minimum essential medium- α (Sigma Aldrich, St. Louis, MO, USA) supplemented with penicillin (100 IU/ml), streptomycin (100 mg/ml) (1% P/S; Lonza), 2 mM L-glutamine (Lonza) and 15% fetal bovine serum (Lonza). MSC were used at passage 3-6.

Culture of HUVEC

Human umbilical vein endothelial cells (HUVEC) were purchased from Lonza (Basel, Switzerland) and cultured at 37° C, 5% CO₂ and 20% O₂ in endothelial growth medium 2 (EGM-2, Lonza). HUVEC were used at passage 3-6.

Immunophenotyping of MSC and HUVEC

HUVEC and MSC were phenotyped based on the expression of specific molecules on their cell surface. Damage and activation markers were also measured on the surface of HUVEC and MSC by flow cytometry (FACS Canto II, BD Biosciences, NJ, USA). Monoclonal antibodies conjugated with different fluorophores were used to measure the presence of these molecules.

Markers measured on MSC surface membranes were CD29 (Cat# 11-0299-42, eBioscience, Santa Clara, CA, USA), CD31 (Cat#555445, Becton Dickinson), CD38 (Cat# 562444, Becton Dickinson), CD44 (Cat# 553134, Becton Dickinson), CD45 (Cat#345809, Becton Dickinson), CD54 (Cat#559771, Becton Dickinson), CD62e (Cat#551145, Beckton Dickinson), CD73 (Cat# 550257, Becton Dickinson), CD144 (cat# 348510, Biolegend, San Diego, CA, USA), CD146

(Cat#747737, Becton Dickinson), TGF- β rII (Cat#FAB241P, R&D Systems, Minneapolis, MN, USA). PD-L1 (Cat# 557924, Becton Dickinson), HLA-II (Cat#347402, Becton Dickinson).

Markers measured on HUVEC membrane were CD31 (Cat#555445, Beckton Dickinson), CD54 (Cat#559771, Beckton Dickinson), CD62e (Cat#551145, Beckton Dickinson), CD105 (Cat# FAB10971F, R&D Systems), CD106 (Cat#744309, Beckton Dickinson), CD144, (cat# 348510, Biolegend, San Diego, CA, USA), CD146 (Cat#747737, Beckton Dickinson), Tie-2 (Cat# FAB3131N, R&D Systems), HLA-II (Cat#347402, Beckton Dickinson) and VEGF-r2 (Cat#560494, Beckton Dickinson). Data were analyzed using Kaluza Analysis 2.1 (Beckman Coulter).

In vitro hypoxia-reoxygenation injury model

HUVEC were cultured until complete confluence in EGM-2 medium (Lonza) at 37°C, 5% CO₂ and 20% O₂. Oxygen was enzymatically removed from culture medium using bovine catalase (0.43 mg/ml, Sigma) and glucose oxidase (0.125 mg/ml, Sigma) as previously described (26) to quickly remove all oxygen from the medium. Oxygen percentage was measured using an universal perfusion solution monitor (version 1.10, Hugo Sachs Elektronik -harvard Apparatus GmbH, March-Hugstetten, Germany). Culture medium was removed and cells were washed with PBS prior to the addition of hypoxic medium. Hypoxia was maintained by culturing HUVEC in a hypoxia incubator during 24 hours at 37°C, 5% CO₂ and 0-1% O₂. Additional file 1A shows that levels of oxygen were around 0% from the addition of the catalase and glucose oxidase and until O₂ measurement after 24 hours. After this time point, cultures were washed with PBS and normoxic culture medium supplemented with human recombinant 20 ng/mL tumor necrosis factor- α (TNF- α ; Peprotech, Rocky Hill, NJ, USA) was added for 24 hours to mimic the inflammatory response after ischemia-reperfusion (injured HUVEC).

HUVEC-MSC incubation

MSC were added to HUVEC to assess their effect on HUVEC injury observed after hypoxic and inflammatory injury. In order to study the effect of MSC on HUVEC, MSC were added to HUVEC in three different manners (Additional file 1D-F). Firstly, MSC were directly incubated with HUVEC for 24 hours after injuring HUVEC, allowing cell-to-cell physical and paracrine communication. Secondly, to determine the effect of physical MSC-HUVEC interaction, MSC were inactivated by warming them to 50° C during 30 minutes as previously described (22). After this procedure the metabolism of MSC is completely stopped and they lose their ability

Chapter 5

to secrete soluble factors, but the cell surface membrane and its associated proteins remain intact. Lastly, to assess the effect of cytokines and growth factor released by MSC on HUVEC, MSC were incubated with HUVEC in a transwell system. The transwell had a porous membrane of pore size 0.4 μm (Greiner Bio-One, Kremsmunster, Austria) that allows communication through soluble factors but prevents physical contact or cell migration. In all three conditions, the incubation of MSC with HUVEC started 24 hours after reoxygenation and culture with TNF- α to test their reparative role.

Assessment of HUVEC viability

HUVEC viability was assessed by Annexin-V (PE) and ViaProbe (PercP) staining using the Annexin-V apoptosis detection kit I (Beckton Dickinson, Franklin Lakes, NJ, USA) and measured by flow cytometry (Additional file 1B and C). Data were analyzed using Kaluza Analysis 2.1 software (Beckman Coulter, Brea, CA, USA).

Measurement of LDH release

HUVEC vitality was measured using a colorimetric assay to measure lactate dehydrogenase (LDH) release to the medium as a marker for cell injury. HUVEC were cultured in 96-well plates and an LDH activity assay kit (Sigma) was used according to the manufacturer's protocol. The results were obtained by measuring the absorbance of the reagent that is formed at 450 nm with a spectrophotometer (Victor2, PerkinElmer, Waltham, MA, USA).

Migration of MSC toward HUVEC monolayer

Migration of MSC towards injured HUVEC was assessed by culturing a monolayer of HUVEC in the lower well of a transwell system and injuring them as described above. MSC were added on top of a porous membrane with 3 μm pore size and cultured for 6 hours. After this, both upper and lower wells were trypsinized and cells counted by flow cytometry after staining them with CD31 antibody to discriminate endothelial cells from MSC. Stromal cell-derived factor 1 α (SDF-1 α , 10 ng/ml) was used as a positive control for MSC migration.

MSC adhesion to HUVEC

MSC adhesion to HUVEC was assessed under static and flow conditions. MSC were fluorescently labelled with PKH26 (Sigma) following the manufacturer's protocol in order to

enable later identification. HUVEC were injured as described above and MSC were added on top at a ratio of 1:2 or 1:10 and incubated for 10, 30 or 60 minutes. After these time points, supernatant was collected and wells were washed to eliminate all non-adherent MSC. Attached cells were trypsinized and analyzed by flow cytometry. Fluorescent signal detected by flow cytometry allowed the determination of the percentage of attached MSC by comparing this number to the initial number of added MSC.

To analyze MSC adhesion under flow conditions, HUVEC were seeded in Ibidi® μ -Slide I Luer slides (Gräfelfing, Germany) grown to complete confluence and injured as described above. Subsequently, the slide was connected to a rolling pump (REGLO Analog, Ismatec, Wertheim, Switzerland) and culture media was perfused at 37° C at a rate of 0.77 ml/min. PKH-labelled MSC were added to the perfusion system in different fashions: one time infusion of 200,000 MSC during flow, two times infusion of 100,000 MSC each during flow, one time infusion of 200,000 MSC followed by a 10 minutes stop in the flow to facilitate adhesion as in the adhesion experiment under static conditions or one time infusion of 200,000 MSC which was recirculated for 10 minutes. After each infusion, 10 additional minutes of flow were maintained. To analyze MSC adhesion to HUVEC during flow conditions, the slides were inspected by fluorescence microscopy to identify the adhesion of PKH-labelled MSC. To calculate the percentage of adherent MSC, the content of the slide was trypsinized and MSC were counted by flow cytometry using their fluorescence to identify them and comparing this number to the initial number of added MSC.

MSC-EC molecular interaction mechanism

In order to assess the role of specific adhesion molecules on MSC and HUVEC interaction, two molecules on the MSC cell surface were blocked. CD29 and CD44 were blocked by incubating MSC with CD29 polyclonal antibody (Cat# AF1778, R&D Systems) and CD44 polyclonal antibody (Cat# AF3660, R&D Systems) at a concentration of 2.5 μ g/ 10^6 MSC for 20 minutes. The effective blockage of these molecules was assessed by staining MSC with the previously described CD29 and CD44 antibodies and measuring fluorescence by flow cytometry. MSC with either blocked CD29, CD44 or both were added to a monolayer of injured HUVEC for 10, 30 or 60 minutes. After these time points, wells were washed to eliminate all non-adherent MSC. Attached cells were trypsinized and analyzed by flow cytometry. Fluorescent signal detected by flow cytometry allowed the determination of the percentage of MSC attached.

Measurement of oxidative stress

Oxidative stress of HUVEC was measured using CellRox reagent (ThermoFisher, Manhattan, NY, USA) according to the manufacturer's manual. Briefly, the cell-permeant CellROX reagent enters the cell and there it is oxidized by ROS, exhibiting red fluorescence. The production of ROS was quantified by measuring the fluorescence of oxidized CellRox inside the cell by flow cytometry. Data were analyzed using Kaluza Analysis 2.1 (Beckman Coulter).

Measurement of HUVEC monolayer permeability

HUVEC were grown to complete confluence on a transwell insert and cultured for 48 hours to allow the formation of tight intercellular junctions. The membrane of the insert had 0.4 μm size pores, which prevented cell migration but allowed soluble factor exchange with the lower well. FITC-conjugated dextran (100 mg/mL) diluted in PBS was added to the insert and incubated for 2 hours, while 200 μl of PBS was added to the lower well. HUVEC monolayer permeability was assessed by measuring the amount of FITC-conjugated dextran in the lower well after 2 hours by measuring fluorescence at 515nm with a spectrophotometer (Victor2, PerkinElmer).

Scratch assay

A scratch assay was performed on a confluent HUVEC monolayer. HUVEC were grown on 24-well plates until complete confluence and with the tip of a 200 μl pipette a scratch was made from top to bottom of the well, removing the cells in this area. After 2, 6- and 24-hours pictures were taken with an Axiovert 40 C microscope (Zeiss, Oberkochen, Germany) coupled to a Zeiss CanonSLR camera (Zeiss) to observe the closing of the scratched area. The size of the scratch area was measured using the plugin MRI Wound Healing Tool for Image J (National Institutes of Health, Bethesda, MD, USA).

Angiogenesis assay

A tube formation assay was performed to evaluate the effect of hypoxic and inflammatory injury on the angiogenic potential of HUVEC. Geltrex™ LDEV-Free Reduced Growth Factor Basement Membrane Matrix was kept at 4° C overnight prior to the experiment to allow complete thawing. At the start of the experiment, 50 μl Geltrex was added to each well of an ice-cold 96-well plate using cold pipette tips to avoid premature Geltrex solidification. The plates were incubated for 30 minutes at 37° C to allow Geltrex solidification. Cells were added

to the wells in a concentration of 2×10^4 per well. During 6 hours, pictures were taken hourly with an Axiovert 40 C microscope (Zeiss) coupled to a Zeiss CanonSLR camera (Zeiss) to evaluate the formation of tube-like structures. To evaluate the angiogenic capacity, the total length of the tubes formed during the assay was measured. The images were analyzed by Wimasis Image Analysis (Cordoba, Spain).

Migration of MSC through a HUVEC monolayer

This setup was modified to assess MSC transmigration through a HUVEC monolayer. HUVEC were grown on top of the porous membrane of the upper well of the transwell system. After injury, HUVEC monolayer confluence was checked by microscopy and MSC were added directly on top of the HUVEC monolayer and incubated for 6 hours. During this incubation, SDF-1 α (10 ng/ml) was added to the bottom well to elicit a chemotactic response for MSC. Both wells were trypsinized and cells counted by flow cytometry.

Results

MSC migrate and adhere to endothelial cells through CD29 and CD44

MSC migratory capacity towards endothelial cells was tested in a transwell system where MSC were added to the upper well and HUVEC grown to confluence in the lower well (Figure 1A). After 6 hours, 39% of MSC migrated towards non-injured HUVEC. Exposure of HUVEC to hypoxia and reoxygenation led to the migration of 61% of the added MSC towards HUVEC (Figure 1D).

The capacity of MSC to adhere to HUVEC was tested in static conditions, incubating MSC on a monolayer of HUVEC for 10, 30 and 60 minutes (Figure 1B). MSC showed an increased adhesion capacity to injured HUVEC compared to non-injured HUVEC at all time points (Figure 1E). Importantly, MSC also exhibited adhesion capacity to HUVEC under flow conditions (Figure 1C). HUVEC were cultured and injured in perfusion slides. Single or double infusions of MSC were administered to the perfusion slides, resulting in the adhesion of less than 30% of the added MSC. The recirculation of MSC in the same system enabled repeated contact of MSC with HUVEC, leading to 74% of the MSC to attach to injured HUVEC (Figure 1F).

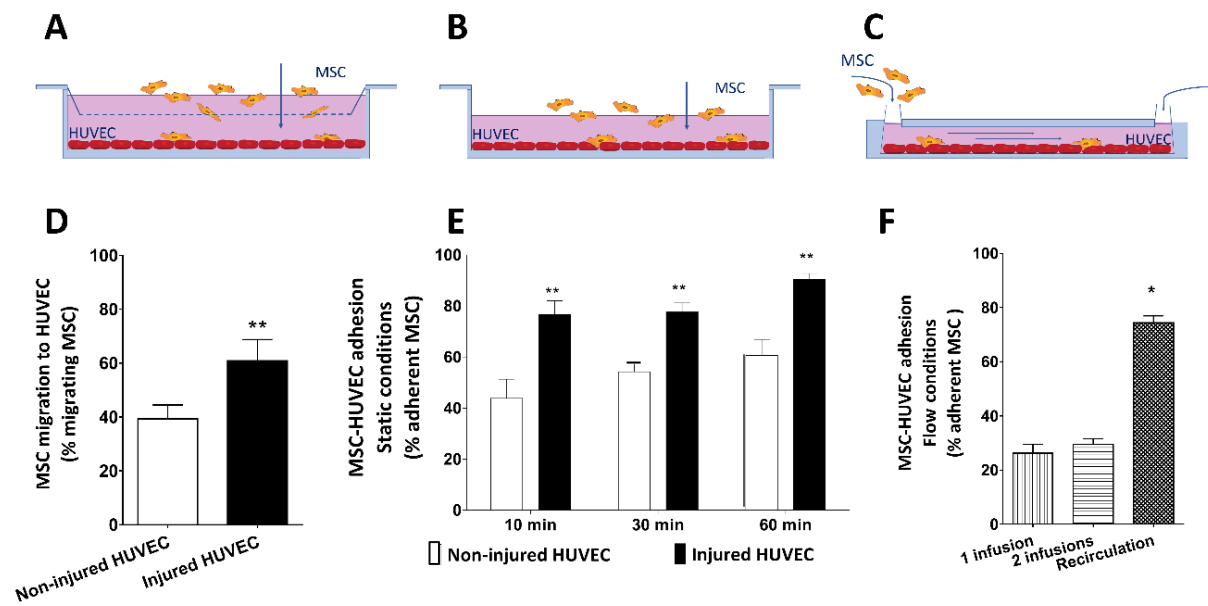


Figure 1. Migration and adhesion of MSC. A, migration of MSC is assessed by measuring the percentage of MSC able to migrate through a porous membrane towards (injured) HUVEC. B, adhesion of MSC to HUVEC in static conditions. MSC are added on a confluent monolayer of HUVEC and the percentage of MSC which adhered after 10, 30 and 60 minutes is assessed by flow cytometry. C, adhesion of MSC to HUVEC in flow conditions. HUVEC are grown and injured in a flow chamber. MSC were infused 1 time or 2 times during flow or 1 time and recirculated for 10 minutes. The percentage of MSC which adhered was assessed by flow cytometry. D, MSC showed an increased migratory capacity towards injured HUVEC compared to non-injured HUVEC. E, MSC show increased adhesion to injured HUVEC compared to non-injured HUVEC. F, MSC showed 28 % adhesion capacity to injured HUVEC during flow conditions after one- or two-times infusion. Recirculation of MSC yielded increased adhesion of MSC to injured HUVEC during flow conditions. Significance of the comparison between 1-time infusion and recirculation is shown. (n=5) Results are shown as mean \pm SD. ** p-value<0.01; * p-value<0.05.

The proposed mechanism for MSC and HUVEC interaction is depicted in figure 2A. Upon hypoxia and reoxygenation injury, CD62e and CD106 expression levels on HUVEC membrane were upregulated (Figure 2B). At the same time, their ligands, CD29 and CD44, were upregulated on the cell membrane of MSC after incubation with injured HUVEC (Figure 2C). In order to test the importance of these two molecules on MSC-HUVEC interaction, we blocked their binding sites on the surface of MSC. Blockage of CD29 and CD44 by blocking antibodies led to the inhibition of MSC adhesion to HUVEC (Figure 2D) without affecting the survival of MSC assessed by trypan blue (data not shown).

MSC decrease injury markers on endothelial cells after hypoxia-reoxygenation

To examine the effect of hypoxia-reoxygenation on endothelial cells, survival and metabolism of HUVEC was studied under hypoxic and inflammatory conditions. Several injury markers

were upregulated after this process including adhesion molecules CD54 and CD146, angiogenic receptors such as Tie-2 and VEGFR2, and HLA-II, which is typically upregulated on endothelial cells upon injury (Figure 3A-D). The release of ROS was increased after injury as well (Figure 3E).

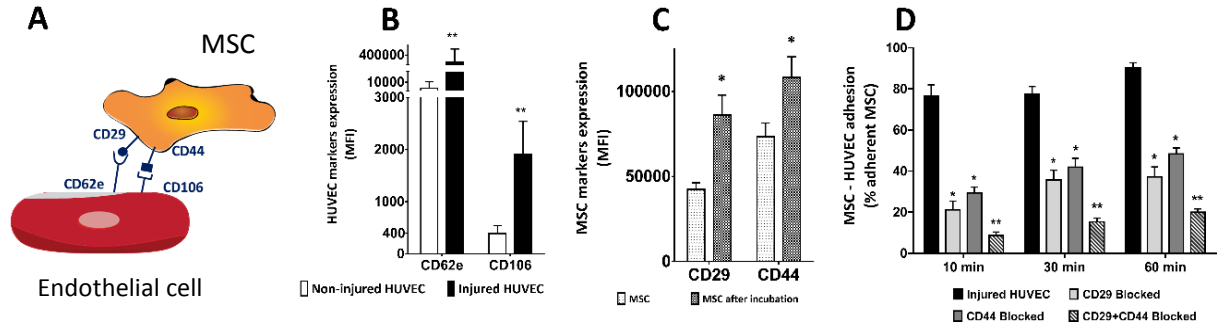


Figure 2. MSC-HUVEC adhesion mechanism. A, Schematic representation of the molecular mechanism for MSC and HUVEC interaction. B, the expression of CD62e and CD106 is upregulated on HUVEC membrane after hypoxia and reoxygenation. C, CD29 and CD44 adhesion molecules expression is increased on the surface of MSC after incubation with injured HUVEC. D, the blockage of CD29 and CD44 inhibits the adhesion of MSC to injured HUVEC. Significance of the comparison between injured HUVEC and the effect of blocking CD29 and/or CD44 is shown. (n=5) Results are shown as mean ± SD. ** p-value<0.01; * p-value<0.05.

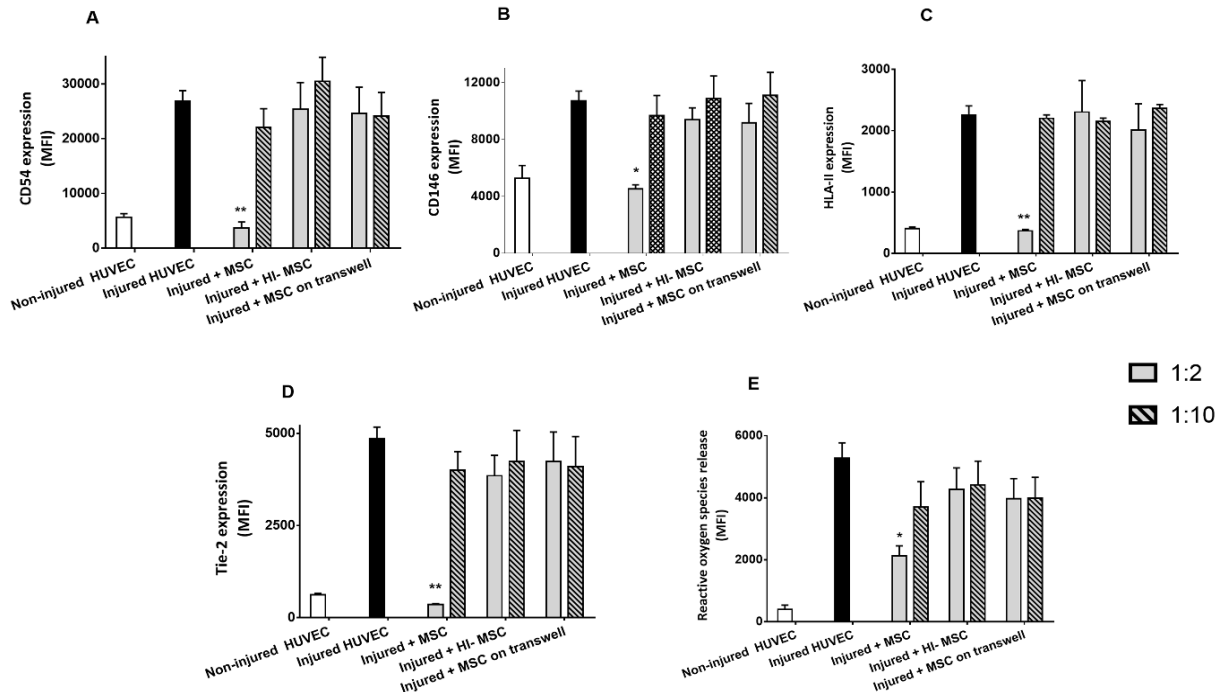


Figure 3. MSC reduce injury markers on injured HUVEC. A-D, the expression of CD54, CD146, HLA-II and Tie-2 on HUVEC membrane was increased after injury. After 24 hours incubation with MSC at a 1:2 ratio, membrane markers were decreased to non-injured levels. No effects of HI-MSC or MSC separated from HUVEC through a transwell were observed. E, production of ROS by HUVEC was increased by hypoxia and reoxygenation. After 24

Chapter 5

hours incubation with MSC at a 1:2 ratio, ROS levels in HUVEC were decreased by 60%. No effects of HI-MSC or MSC incubated through a transwell were observed. (n=5) Results are shown as mean \pm SD. Significance of the comparison between injured HUVEC and the effect of MSC is shown as ** p-value<0.01; * p-value<0.05.

Injured HUVEC were incubated with either MSC, HI-MSC that lost their ability to secrete factors, or with MSC on top of a transwell membrane for 24 hours at a 1:2 ratio, or at a 1:10 ratio. (Additional file 1D-F). Incubation with MSC at a 1:2 ratio decreased the expression of CD54, CD146, Tie-2 and HLA-II on injured HUVEC to levels close to uninjured HUVEC, whilst no effect was observed with MSC at a 1:10 ratio (Figure 3A-D). MSC also decreased ROS levels produced by HUVEC by 60% at a 1:2 MSC-HUVEC ratio (Figure 3E). When injured HUVEC were incubated with HI-MSC or with MSC separated through a transwell membrane, no effects on HUVEC surface markers or ROS levels were observed.

MSC improve injured endothelial cell wound healing, barrier and angiogenic function

To test the effect of hypoxia-reoxygenation on the permeability of a monolayer of HUVEC, a FITC-labelled dextran leakage assay was used to assess if the dextran leaked through injured HUVEC monolayers (Figure 4A). Hypoxia reoxygenation increased endothelial monolayer permeability, as demonstrated by a 3-fold increase in compared to non-injured HUVEC (Figure 4D). MSC reduced endothelial cell monolayer permeability by 60%, while HI-MSC and MSC separated from HUVEC with a transwell membrane failed to do so. No effects were observed of the lower MSC ratio (Figure 4D).

The ability of HUVEC to close a scratch in the monolayer, which is a measure of their wound healing capacity, sharply decreased after hypoxia and reoxygenation (Figure 4B). Incubation with the high MSC ratio was shown to stimulate the capacity of injured HUVEC to close a scratch by 45% whereas the low ratio of MSC improved this capacity by 17%. In addition, MSC incubated through a transwell had a small and dose-dependent effect on the scratch closing ability of HUVEC (Figure 4E).

Moreover, the angiogenic potential of HUVEC was measured by their capacity to form tubes *in vitro*, was decreased by 50% compared to non-injured endothelial cells (Figure 4C). The addition of MSC at a 1:2 ratio fully restored HUVEC angiogenic potential while at a 1:10 ratio MSC improved this capacity to 50% of the potential of non-injured HUVEC. HI-MSC did not elicit a reparative effect. In addition, the high dose of MSC separated from injured HUVEC via a transwell membrane improved their angiogenic capacity by 48% (Figure 4F).

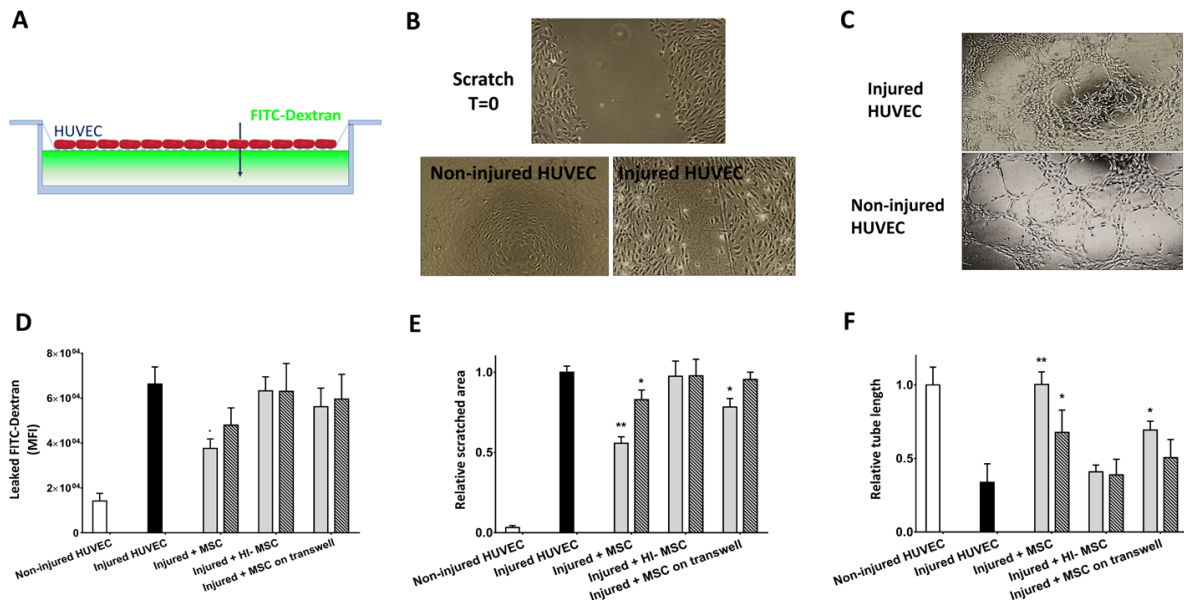


Figure 4. MSC repair wound healing capacity, barrier function and angiogenic properties of injured HUVEC. A, HUVEC monolayer permeability was increased after injury. MSC at a 1:2 ratio reduced HUVEC monolayer permeability by 44% after 24 hours of incubation. Incubation with HI-MSC or MSC through a transwell had no effect. B, hypoxia reoxygenation injury decreased the wound healing capacity of HUVEC measured by a scratch assay. After 24 hours incubation with MSC at a 1:2 ratio, MSC improved HUVEC capacity to close a scratched area by 45%. Secreted molecules by MSC during incubation through a transwell improved injured HUVEC wound healing by 22%. At a ratio of 1:10 MSC-HUVEC, wound healing capacity was improved by 17% by MSC. HI-MSC had no effect at any ratio. C, the total length of tube-like structures formed by HUVEC was measured to quantify angiogenic capacity. Hypoxia and reoxygenation injury decreased HUVEC angiogenic potential by half. After 24 hours of incubation with MSC at a 1:2 ratio, injured HUVEC fully recovered their angiogenic capacity. At a 1:10 ratio, MSC improved angiogenic potential of injured HUVEC by 50%. Secreted molecules by MSC at a 1:2 ratio led to a 48% recovery on injured HUVEC angiogenic potential. HI-MSC had no effect at any ratio. D, Schematic depiction of endothelial monolayer integrity. Added FITC-conjugated dextran leaks through an injured endothelial monolayer. E, Visual representation of non-injured (left) and injured (right) HUVEC angiogenic potential. F, Visual representation of HUVEC wound healing capacity. Top panel: A scratch is made to the endothelial monolayer at time point 0 h. Bottom left panel: Non-injured HUVEC completely close the scratch after 6 hours. Bottom right panel: Injured HUVEC are not able to completely close the scratch after 6 hours. (n=5) Results are shown as mean ± SD. Significance of the comparison between injured HUVEC and the effect of MSC is shown as ** p-value<0.01; * p-value<0.05.

MSC transmigrate through an endothelial monolayer in vitro

We went on examining the transmigration of MSC through a HUVEC monolayer as depicted in figure 5A, which would potentially allow MSC to provide regenerative signals to tissues underlying the endothelium. MSC did not show migratory capacity through an endothelial cell monolayer without a chemotactic signal underneath the endothelial monolayer (data not shown). Nonetheless, MSC were able to migrate through a HUVEC monolayer after adding SDF-1a to the lower well of the transwell system. After 6 hours, 38% of the added MSC migrated through a monolayer of HUVEC (Figure 5B). The migratory capacity of MSC was

enhanced when HUVEC were injured. These in vitro experiments indicate that MSC have the potential to pass the endothelium and migrate into tissues towards gradients of chemotactic signals.

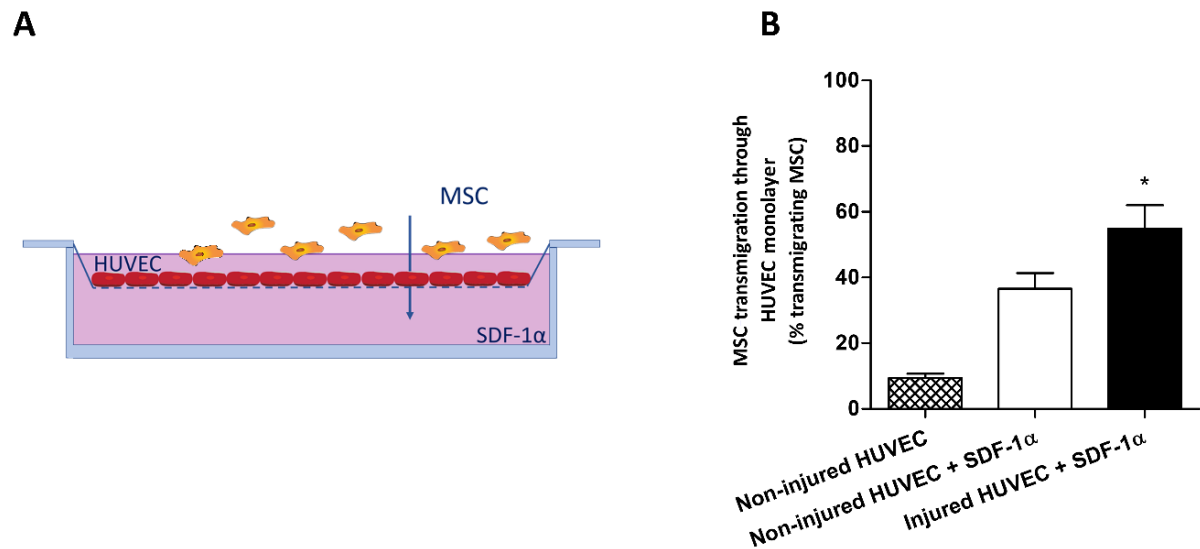


Figure 5. MSC transmigrate through an endothelial monolayer toward kidney injury chemokine SDF-1a. A, Schematic representation of the transwell assay to assess the capacity of MSC to transmigrate through a monolayer of endothelial cells. B, MSC showed the capacity to transmigrate through a confluent endothelial monolayer towards SDF-1a. Injury of HUVEC enhanced the transmigration capacity of MSC, resulting in 54 % of the added MSC transmigrating through the injured HUVEC monolayer after 6 hours. (n=5) Results are shown as mean \pm SD. Significance of the comparison between injured HUVEC + SDF-1 α and non-injured HUVEC + SDF-1 α is shown as * p-value<0.05.

Discussion

In this manuscript we described the reparative effect of MSC on HUVEC damaged by hypoxic and inflammatory conditions. The combination of physical and paracrine interaction of MSC with injured HUVEC proved to be key in restoring the wound healing and angiogenic potential of HUVEC as well as for the decrease in HUVEC oxidative stress and other injury markers. The migration of MSC towards injured HUVEC, their adhesion and subsequent transmigration through a HUVEC monolayer, in which CD29 and CD44 are key mediators, suggest that MSC are able to interact with endothelium after ischemia and reperfusion injury during the donation and transplantation procedures. The suppression of hypoxia-reoxygenation effects on HUVEC adhesion markers, the decrease in oxidative stress levels and the complete recovery of injured HUVEC angiogenic potential, suggest that MSC have the capacity to restore endothelial function.

We established a hypoxia and reoxygenation model *in vitro* to mimic endothelial inflammatory injury (1, 27, 28). The use of HUVEC was chosen based on their proven value for *in vitro* endothelial hypoxia-reoxygenation injury studies (29, 30). However, we realize that complementary studies on the regenerative effect of MSC on tissue-specific endothelial cells, such as microvascular endothelial cells in kidneys, will be necessary to confirm our results in organ-specific *in vitro* models.

Renal endothelial injury is correlated with kidney function loss (31, 32). In addition, in human renal IRI after donation and transplantation, endothelial permeability is increased and results in delayed graft function (33). Endothelial injury is associated with the release of pro-inflammatory factors and increased expression of adhesion molecules on endothelial cells after IRI, promoting immune cell recruitment and infiltration (34-37). Our data show that MSC decrease the expression of injury markers on injured HUVEC, reduce oxidative stress levels and endothelial permeability, suggesting that MSC could repair IRI effects on endothelium in a kidney transplantation setting.

The cytokines and adhesion molecules that are up-regulated upon endothelial injury can also promote MSC migration and adherence to endothelial cells (38, 39). We showed that MSC are able to migrate toward injured HUVEC and adhere in an inflammatory microenvironment under static and flow conditions. The latter is of relevance because MSC infused in the bloodstream have to interact with endothelial cells as they are transported by peripheral blood flow. We show that CD62e and CD106 expression levels, among others, are increased on HUVEC after hypoxic injury, and their ligands CD29 and CD44 (40, 41) are increased on MSC membrane after incubation with injured HUVEC. Blocking these two markers on the MSC surface resulted in a great inhibition of MSC adherence, suggesting that these molecules play a key role on MSC-HUVEC interaction (42, 43). Enhancing the expression of these two proteins during MSC *in vitro* culture could improve MSC delivery to endothelial cells (44). In addition, targeted delivery of MSC to the injured organ would be useful to improve their interplay with the injured tissue. Direct infusion through the renal artery or delivery during normothermic machine perfusion are plausible options to deliver cells specifically to the kidney and ensure MSC interaction with damaged renal endothelium during the organ preservation (24).

The fate of MSC after delivery to the kidney is currently unclear and there is little evidence about the invasion of MSC in tissues underlying the endothelium. Several publications show that after IV infusion, MSC die and are not detectable in the target organ within 24 hours (13,

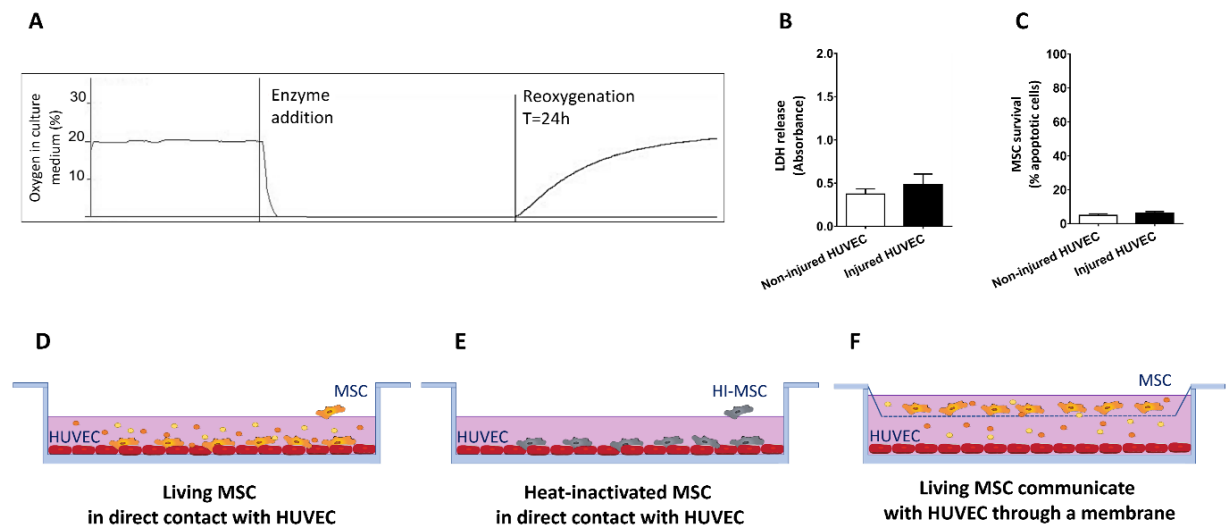
45, 46). Targeted infusion of MSC through the renal artery ensures high delivery efficiency of MSC to the kidney. However, the fate of MSC administered in this manner to the kidney is unclear. We previously reported a sharp decline in the number of MSC present in kidney biopsies at 2 weeks after administration of MSC (23). It is expected that MSC would not stay at the luminal side of microcapillaries, but that these cells are either removed by innate immune cells or migrate to other sides (13, 47). Previous reports suggested that MSC engraft in tubular and glomerular structures after infusion via the renal artery (15, 46), but these results remain controversial and have not been confirmed in recent studies. We observed in our *in vitro* experiments that MSC possess the capacity to migrate through endothelial cell layers which would suggest they are able to invade tissues. However, it has to be noted that *in vitro* experiments are performed at the most optimal conditions for cell activity and these are usually far from physiological conditions (concentration of triggering molecules, composition of the medium, etc.). Therefore, more studies are necessary to examine whether MSC harbor this property *in vivo*, which could be achieved for instance by real-time intravital tracking of MSC delivered to an animal model, visually unravelling the fate of MSC after infusion (48).

Likewise, the main mechanism behind the regenerative effects of MSC has been widely debated. In this study we show that the soluble factors secreted by MSC can promote the regeneration of injured HUVEC. However, the full regenerative potential of MSC required both physical and paracrine interaction between MSC and HUVEC. In this case, the *in vitro* setting is restricting many of the interactions occurring *in vivo*, which may be responsible for the actual observed MSC effect, as previously described (13).

Conclusion

We conclude that MSC harbor the capacity to control the damage associated with hypoxia reoxygenation injury on endothelial cells provided that they may interact physically and through secreted molecules. Our results suggest that MSC are a valuable therapeutic option to repair IRI and future studies will reveal whether and how MSC can be applied to repair organs prior to and after transplantation.

Additional files



Additional file 1. Hypoxia reoxygenation model and MSC-HUVEC interaction models. A, oxygen levels drop immediately to 0% after adding catalase and glucose oxidase to the culture medium. After 24 hours in a hypoxia incubator, the oxygen percentage in the medium remained 0% until contact with air was re-established. B and C, HUVEC did not die nor become apoptotic after culture in hypoxia and upon reoxygenation in the presence of TNF- α . D, MSC co-cultured with injured HUVEC allowing physical interaction and soluble factors secretion. E, Heat-inactivated (HI)-MSC co-cultured with injured HUVEC enabling only physical interaction, as HI-MSC lost their ability to secrete growth factors and cytokines. F, MSC co-cultured with injured HUVEC in a transwell system to avoid cell-to-cell contact but allow interaction through secreted molecules.

References

1. Malek M, Nematbakhsh M. Renal ischemia/reperfusion injury; from pathophysiology to treatment. *J Renal Inj Prev*. 2015;4(2):20-7.
2. Zhao H, Alam A, Soo AP, George AJT, Ma D. Ischemia-Reperfusion Injury Reduces Long Term Renal Graft Survival: Mechanism and Beyond. *EBioMedicine*. 2018;28:31-42.
3. Metzger RA, Delmonico FL, Feng S, Port FK, Wynn JJ, Merion RM. Expanded criteria donors for kidney transplantation. *Am J Transplant*. 2003;3 Suppl 4:114-25.
4. Aubert O, Kamar N, Vernerey D, Viglietti D, Martinez F, Duong-Van-Huyen J-P, et al. Long term outcomes of transplantation using kidneys from expanded criteria donors: prospective, population based cohort study. *BMJ : British Medical Journal*. 2015;351:h3557.
5. Basile DP, Yoder MC. Renal endothelial dysfunction in acute kidney ischemia reperfusion injury. *Cardiovasc Hematol Disord Drug Targets*. 2014;14(1):3-14.
6. Jankauskas SS, Andrianova NV, Alieva IB, Prusov AN, Matsievsky DD, Zorova LD, et al. Dysfunction of Kidney Endothelium after Ischemia/Reperfusion and Its Prevention by Mitochondria-Targeted Antioxidant. *Biochemistry (Mosc)*. 2016;81(12):1538-48.
7. Sutton TA, Mang HE, Campos SB, Sandoval RM, Yoder MC, Molitoris BA. Injury of the renal microvascular endothelium alters barrier function after ischemia. *Am J Physiol Renal Physiol*. 2003;285(2):F191-8.
8. Basile DP, Friedrich JL, Spahic J, Knipe N, Mang H, Leonard EC, et al. Impaired endothelial proliferation and mesenchymal transition contribute to vascular rarefaction following acute kidney injury. *Am J Physiol Renal Physiol*. 2011;300(3):F721-33.
9. Pittenger MF, Mackay AM, Beck SC, Jaiswal RK, Douglas R, Mosca JD, et al. Multilineage potential of adult human mesenchymal stem cells. *Science*. 1999;284(5411):143-7.
10. Fabre H, Ducret M, Degoul O, Rodriguez J, Perrier-Groult E, Aubert-Foucher E, et al. Characterization of Different Sources of Human MSCs Expanded in Serum-Free Conditions with Quantification of Chondrogenic Induction in 3D. *Stem Cells Int*. 2019;2019:2186728.
11. Morigi M, Introna M, Imberti B, Corna D, Abbate M, Rota C, et al. Human bone marrow mesenchymal stem cells accelerate recovery of acute renal injury and prolong survival in mice. *Stem Cells*. 2008;26(8):2075-82.
12. Semedo P, Palasio CG, Oliveira CD, Feitoza CQ, Goncalves GM, Cenedeze MA, et al. Early modulation of inflammation by mesenchymal stem cell after acute kidney injury. *Int Immunopharmacol*. 2009;9(6):677-82.
13. de Witte SFH, Luk F, Sierra Parraga JM, Gargasha M, Merino A, Korevaar SS, et al. Immunomodulation By Therapeutic Mesenchymal Stromal Cells (MSC) Is Triggered Through Phagocytosis of MSC By Monocytic Cells. *Stem Cells*. 2018;36(4):602-15.
14. Ebrahimi B, Eirin A, Li Z, Zhu XY, Zhang X, Lerman A, et al. Mesenchymal stem cells improve medullary inflammation and fibrosis after revascularization of swine atherosclerotic renal artery stenosis. *PLoS One*. 2013;8(7):e67474.
15. Eirin A, Zhu XY, Krier JD, Tang H, Jordan KL, Grande JP, et al. Adipose tissue-derived mesenchymal stem cells improve revascularization outcomes to restore renal function in swine atherosclerotic renal artery stenosis. *Stem Cells*. 2012;30(5):1030-41.
16. Baulier E, Favreau F, Le Corf A, Jayle C, Schneider F, Goujon JM, et al. Amniotic fluid-derived mesenchymal stem cells prevent fibrosis and preserve renal function in a preclinical porcine model of kidney transplantation. *Stem Cells Transl Med*. 2014;3(7):809-20.

17. Perico N, Casiraghi F, Remuzzi G. Clinical Translation of Mesenchymal Stromal Cell Therapies in Nephrology. *J Am Soc Nephrol*. 2018;29(2):362-75.
18. Reinders ME, de Fijter JW, Roelofs H, Bajema IM, de Vries DK, Schaapherder AF, et al. Autologous bone marrow-derived mesenchymal stromal cells for the treatment of allograft rejection after renal transplantation: results of a phase I study. *Stem Cells Transl Med*. 2013;2(2):107-11.
19. Perico N, Casiraghi F, Inrona M, Gotti E, Todeschini M, Cavinato RA, et al. Autologous mesenchymal stromal cells and kidney transplantation: a pilot study of safety and clinical feasibility. *Clin J Am Soc Nephrol*. 2011;6(2):412-22.
20. Perico N, Casiraghi F, Gotti E, Inrona M, Todeschini M, Cavinato RA, et al. Mesenchymal stromal cells and kidney transplantation: pretransplant infusion protects from graft dysfunction while fostering immunoregulation. *Transpl Int*. 2013;26(9):867-78.
21. Mudrabettu C, Kumar V, Rakha A, Yadav AK, Ramachandran R, Kanwar DB, et al. Safety and efficacy of autologous mesenchymal stromal cells transplantation in patients undergoing living donor kidney transplantation: a pilot study. *Nephrology (Carlton)*. 2015;20(1):25-33.
22. Luk F, de Witte S, Korevaar SS, Roemeling-van Rhijn M, Franquesa M, Strini T, et al. Inactivated mesenchymal stem cells maintain immunomodulatory capacity. *Stem Cells Dev*. 2016.
23. Sierra-Parraga JM, Munk A, Andersen C, Lohmann S, Moers C, Baan CC, et al. Mesenchymal Stromal Cells Are Retained in the Porcine Renal Cortex Independently of Their Metabolic State After Renal Intra-Arterial Infusion. *Stem Cells Dev*. 2019;28(18):1224-35.
24. Pool M, Eertman T, Sierra Parraga J, t Hart N, Roemeling-van Rhijn M, Eijken M, et al. Infusing Mesenchymal Stromal Cells into Porcine Kidneys during Normothermic Machine Perfusion: Intact MSCs Can Be Traced and Localised to Glomeruli. *Int J Mol Sci*. 2019;20(14).
25. Saad A, Dietz AB, Herrmann SMS, Hickson LJ, Glockner JF, McKusick MA, et al. Autologous Mesenchymal Stem Cells Increase Cortical Perfusion in Renovascular Disease. *J Am Soc Nephrol*. 2017;28(9):2777-85.
26. Huang Y, Zitta K, Bein B, Steinfath M, Albrecht M. An insert-based enzymatic cell culture system to rapidly and reversibly induce hypoxia: investigations of hypoxia-induced cell damage, protein expression and phosphorylation in neuronal IMR-32 cells. *Dis Model Mech*. 2013;6(6):1507-14.
27. Thurman JM. Triggers of inflammation after renal ischemia/reperfusion. *Clin Immunol*. 2007;123(1):7-13.
28. Abraham D, Distler O. How does endothelial cell injury start? The role of endothelin in systemic sclerosis. *Arthritis Res Ther*. 2007;9 Suppl 2:S2.
29. Luna C, Carmona A, Alique M, Carracedo J, Ramirez R. TNFalpha-Damaged-HUVECs Microparticles Modify Endothelial Progenitor Cell Functional Activity. *Front Physiol*. 2015;6:395.
30. Koo DD, Welsh KI, West NE, Channon KM, Penington AJ, Roake JA, et al. Endothelial cell protection against ischemia/reperfusion injury by lecithinized superoxide dismutase. *Kidney Int*. 2001;60(2):786-96.
31. Matthys E, Patton MK, Osgood RW, Venkatachalam MA, Stein JH. Alterations in vascular function and morphology in acute ischemic renal failure. *Kidney Int*. 1983;23(5):717-24.
32. Basile DP, Donohoe D, Roethe K, Osborn JL. Renal ischemic injury results in permanent damage to peritubular capillaries and influences long-term function. *Am J Physiol Renal Physiol*. 2001;281(5):F887-99.
33. Salmela K, Wramner L, Ekberg H, Hauser I, Bentdal O, Lins LE, et al. A randomized multicenter trial of the anti-ICAM-1 monoclonal antibody (enlimomab) for the prevention of acute rejection and delayed onset of

Chapter 5

graft function in cadaveric renal transplantation: a report of the European Anti-ICAM-1 Renal Transplant Study Group. *Transplantation*. 1999;67(5):729-36.

34. Szekanez Z, Koch AE. Mechanisms of Disease: angiogenesis in inflammatory diseases. *Nat Clin Pract Rheumatol*. 2007;3(11):635-43.
35. Opitz B, Puschel A, Beermann W, Hocke AC, Forster S, Schmeck B, et al. *Listeria monocytogenes* activated p38 MAPK and induced IL-8 secretion in a nucleotide-binding oligomerization domain 1-dependent manner in endothelial cells. *J Immunol*. 2006;176(1):484-90.
36. Ponte AL, Marais E, Gallay N, Langonne A, Delorme B, Herault O, et al. The in vitro migration capacity of human bone marrow mesenchymal stem cells: comparison of chemokine and growth factor chemotactic activities. *Stem Cells*. 2007;25(7):1737-45.
37. Fu X, Liu G, Halim A, Ju Y, Luo Q, Song AG. Mesenchymal Stem Cell Migration and Tissue Repair. *Cells*. 2019;8(8).
38. Tögel F, Isaac J, Hu Z, Weiss K, Westenfelder C. Renal SDF-1 signals mobilization and homing of CXCR4-positive cells to the kidney after ischemic injury. *Kidney Int*. 2005;67(5):1772-84.
39. Forte G, Minieri M, Cossa P, Antenucci D, Sala M, Gnocchi V, et al. Hepatocyte growth factor effects on mesenchymal stem cells: proliferation, migration, and differentiation. *Stem Cells*. 2006;24(1):23-33.
40. Zarbock A, Ley K, McEver RP, Hidalgo A. Leukocyte ligands for endothelial selectins: specialized glycoconjugates that mediate rolling and signaling under flow. *Blood*. 2011;118(26):6743-51.
41. Ley K, Laudanna C, Cybulsky MI, Nourshargh S. Getting to the site of inflammation: the leukocyte adhesion cascade updated. *Nat Rev Immunol*. 2007;7(9):678-89.
42. Ruster B, Gottig S, Ludwig RJ, Bistrrian R, Müller S, Seifried E, et al. Mesenchymal stem cells display coordinated rolling and adhesion behavior on endothelial cells. *Blood*. 2006;108(12):3938-44.
43. Segers VF, Van Riet I, Andries LJ, Lemmens K, Demolder MJ, De Becker AJ, et al. Mesenchymal stem cell adhesion to cardiac microvascular endothelium: activators and mechanisms. *Am J Physiol Heart Circ Physiol*. 2006;290(4):H1370-7.
44. Chou KJ, Lee PT, Chen CL, Hsu CY, Huang WC, Huang CW, et al. CD44 fucosylation on mesenchymal stem cell enhances homing and macrophage polarization in ischemic kidney injury. *Exp Cell Res*. 2017;350(1):91-102.
45. Eggenhofer E, Benseler V, Kroemer A, Popp FC, Geissler EK, Schlitt HJ, et al. Mesenchymal stem cells are short-lived and do not migrate beyond the lungs after intravenous infusion. *Front Immunol*. 2012;3:297.
46. Fischer UM, Harting MT, Jimenez F, Monzon-Posadas WO, Xue H, Savitz SI, et al. Pulmonary passage is a major obstacle for intravenous stem cell delivery: the pulmonary first-pass effect. *Stem Cells Dev*. 2009;18(5):683-92.
47. Meleshko A, Prakharenia I, Kletski S, Isaikina Y. Chimerism of allogeneic mesenchymal cells in bone marrow, liver, and spleen after mesenchymal stem cells infusion. *Pediatr Transplant*. 2013;17(8):E189-94.
48. Camirand G, Li Q, Demetris AJ, Watkins SC, Shlomchik WD, Rothstein DM, et al. Multiphoton intravital microscopy of the transplanted mouse kidney. *Am J Transplant*. 2011;11(10):2067-74.

Chapter 6

Effects of Normothermic Machine Perfusion Conditions on Mesenchymal Stromal Cells

Jesus M. Sierra Parraga¹, Kaithlyn Rozenberg², Marco Eijken^{3,4}, Henri G. Leuvenink⁵, James Hunter², Ana Merino¹, Cyril Moers⁵, Bjarne K. Møller³, Rutger J. Ploeg², Carla C. Baan¹, Bente Jespersen⁴, Martin J. Hoogduijn¹

¹Department of Internal Medicine, Erasmus MC, University Medical Center Rotterdam, The Netherlands

²Nuffield Department of Surgical Sciences and Oxford Biomedical Research Centre, University of Oxford, Oxford, United Kingdom

³Department of Clinical Immunology, Aarhus University Hospital, Denmark

⁴Department of Renal Medicine, Aarhus University Hospital, Aarhus, Denmark

⁵Department of Surgery – Organ Donation and Transplantation, University Medical Center Groningen, Groningen, The Netherlands



Abstract

Ex-situ normothermic machine perfusion (NMP) of transplant kidneys allows assessment of kidney quality and targeted intervention to initiate repair processes prior to transplantation. Mesenchymal stromal cells (MSC) have been shown to possess the capacity to stimulate kidney repair. Therefore, the combination of NMP and MSC therapy offers potential to repair transplant kidneys. It is however unknown how NMP conditions affect MSC. In this study the effect of NMP perfusion fluid on survival, metabolism and function of thawed cryopreserved human (h)MSC and porcine (p)MSC in suspension conditions was studied.

Suspension conditions reduced the viability of pMSC by 40% in both perfusion fluid and culture medium. Viability of hMSC was reduced by suspension conditions by 15% in perfusion fluid, whilst no differences were found in survival in culture medium. Under adherent conditions, survival of the cells was not affected by perfusion fluid. The perfusion fluid did not affect survival of fresh MSC in suspension compared to the control culture medium. The freeze-thawing process impaired the survival of hMSC; 95% survival of fresh hMSC compared to 70% survival of thawed hMSC. Moreover, thawed MSC showed increased levels of reactive oxygen species, which indicates elevated levels of oxidative stress, and reduced mitochondrial activity, which implies reduced metabolism. The adherence of pMSC and hMSC to endothelial cells was reduced after the thawing process, effect which was particularly profound in the perfusion fluid.

To summarize, we observed that conditions required for machine perfusion are influencing the behavior of MSC. The freeze-thawing process reduces survival and metabolism and increases oxidative stress, and diminishes their ability to adhere to endothelial cells. In addition, we found that hMSC and pMSC behaved differently, which has to be taken into consideration when translating results from animal experiments to clinical studies.

Introduction

As the outcome of kidney transplantation has improved, the demand for kidney transplantation has increased and the donor organ pool to date is too small to supply the current need for transplant organs. The shortage in available donor kidneys (1) has led to the use of expanded criteria donor organs, that includes kidneys from older donors or from donors with hypertension, suboptimal kidney function or death resulting from stroke (2). This has resulted in a higher decline rate at time of offering and may also lead to a poorer outcome of the transplantation (3).

Currently, several techniques are being employed to improve the quality of expanded criteria kidneys and discarded kidneys to make them suitable for transplantation, including machine perfusion. Hypothermic machine perfusion of donor kidneys implies connection of the organ to a pump that perfuses the organ with a solution that provides the required components needed to maintain viability while also removing waste products released as a result of the metabolism and perfusion injury of the organ.

A more physiological way to assess viability of donor organs is continuous perfusion at normothermic temperature at 37° C with proper oxygenation and in the presence of necessary nutrients. A few years ago, the clinical feasibility and safety of 1 hour normothermic machine perfusion (NMP) was demonstrated (4). Other groups decided to evaluate the feasibility of longer term NMP at 37° C, allowing more time to observe the kidney as well as intervene where possible. Recently, NMP has been successfully tested in a series of discarded donor kidneys for up to 24h (5,6). During NMP, using a bespoke red blood cell (RBC) enriched oxygenated and nutrient containing perfusate, the metabolism of the kidney resumes and allows monitoring during perfusion prior to transplantation (6,7). Application of NMP for assessment and targeted intervention (8) to improve kidney quality is appealing and the effect of the therapy can potentially be monitored before the organ is transplanted. Thus, NMP is postulated as a promising platform to reduce kidney damage and initiate regeneration prior to transplantation.

Mesenchymal stromal cells (MSC) are multipotent cells which are found in adult tissues where they support function and repair (9). The International Society for Cellular Therapy has established the minimum criteria that a cell must meet to be considered an MSC: in vitro attachment to plastic, expression of several cell surface markers including CD29, CD44, CD90, the absence of endothelial and hematopoietic markers and the capacity to differentiate into

Chapter 6

cell types of mesodermal origin (10). MSC provide growth factors to progenitor cells that boost their regenerative processes (11,12). More than 800 MSC-related studies are registered at <http://clinicaltrials.gov> on December 2018 and some of them have shown promising results in the treatment of kidney injury from different etiologies (13).

MSC are usually intravenously (IV) administered, which inevitably leads to accumulation in the lungs and poor delivery to target organs (14,15). Obviously, delivery of MSC to the target organ while perfused on an ex vivo stand-alone circuit may overcome this dilemma. The idea to combine NMP and MSC therapy has generated an interest in the area of kidney transplantation (16-18). It is however unknown whether MSCs are compatible with the conditions of NMP.

In addition, a significant difference exists between preparation of therapeutic MSC for pre-clinical versus clinical trials. In pre-clinical experiments, MSC are cultured in vitro and administered directly from the culture flask to laboratory animals when the cells are ready for infusion. In the human setting, large numbers of MSC are needed to treat a patient and cells are often produced at locations distant from the place of administration. This requires storage of cells in a frozen state and infusion following a delicate thawing process (13). Existing literature points out that frozen-thawed human MSC (hMSC) have an altered gene expression profile compared to cells directly retrieved from culture flasks (19), while it also has been shown that MSC immunoregulatory properties may be impaired by the freeze-thawing process (20). If the properties of MSC are impaired after the thawing process, this would mean that the results of human studies may not have the expected outcome.

It has been described that MSC from different species will exert the same actions through different mechanisms, which could affect the efficacy of MSC in various animal models (21,22). Human and non-human primate MSC (23,24) show marked similarities with respect to their biological properties, but it is unknown whether their therapeutic effects are comparable. Porcine models are very suitable for organ transplant and preservation studies due to the similarity in size and physiology between human and pig. It is however unknown whether MSC from human and pig behave in the same manner under NMP conditions.

With the questions above in mind, it is important to simulate conditions of NMP and assess their effect on MSC. We have evaluated the effect of the bespoke perfusate required for NMP

in combination with the condition of fresh versus frozen-thawed MSC in suspension using cells from porcine (pMSC) and from human (hMSC) origin.

Materials and Methods

Isolation and culture of human and porcine MSC and endothelial cells

hMSC were isolated from subcutaneous adipose tissue from healthy human kidney donors (n=5) that became available during kidney donation procedures after obtaining written informed consent as approved by the Medical Ethical Committee of the Erasmus University Medical Centre Rotterdam (MEC-2006-190). pMSC were isolated from subcutaneous adipose tissue (n=5) collected from male pigs, which were subjected to surgery for teaching purposes, as a waste product. hMSC and pMSC were isolated as described previously (25) and phenotypically characterized by the expression of CD29, CD44, CD90 and the absence of CD31 and CD45. Human umbilical vein endothelial cells (HUVEC) were purchased from Lonza (Basel, Switzerland) and porcine aortic endothelial cells (PAOEC) were purchased from Cell Applications Inc. (San Diego, CA, USA).

Both hMSC and pMSC were cultured in minimum essential medium- α (MEM- α) (Sigma Aldrich, St. Louis, MO, USA) supplemented with penicillin (100 IU/ml), streptomycin (100 mg/ml) (1% P/S; Lonza), 2 mM L-glutamine (Lonza) and 15% fetal bovine serum (FBS; Lonza). HUVEC were cultured in endothelial growth medium 2 (PromoCell, Heidelberg, Germany). PAOEC were cultured in porcine endothelial cell media (Cell Applications, Inc.). MSC were used at passage 3-6, HUVEC were used at passage 4-8 and PAOEC at passage 3-6.

Perfusion fluid

The perfusion fluid was an RBC-based solution with albumin as colloid adapted from NMP experiments used by several groups and allowing stable NMP of kidneys (4,26,27). The composition of the perfusion fluid is listed in Table 1.

Survival of MSC in perfusion fluid

MSC were trypsinized from the culture flasks at 90% confluency or thawed after cryopreservation and re-suspended either in complete culture medium or perfusion fluid at a concentration of 500,000 MSC/ml. MSC were incubated in perfusion fluid in polypropylene

tubes to avoid attachment of MSC to plastic. After 30 minutes or 2 hours in suspension, MSC were submitted to a RBC lysis process to remove the large amount of RBC present in perfusion fluid. MSC incubated in suspension with culture medium were also subjected to RBC lysis to treat both groups in the same way. Briefly, 3 ml of red blood cell lysis buffer (Invitrogen, Carlsbad, CA, USA) was added to MSC and incubated for 20 min at room temperature (RT). MSC were then washed with PBS and stained with Annexin-V (PE) and ViaProbe (PercP) to assess the number of early and late apoptotic cells. Perfusion fluid was also added to attached MSC and incubated for the same time and then trypsinized and stained as mentioned. Cells were analyzed by flow cytometry (FACS Canto II, BD Biosciences, NJ, USA) and data were analyzed using Kaluza Analysis 1.5a (Beckman Coulter, Brea, CA, USA).

Table 1. Composition of perfusion fluid.

| Component | Concentration |
|-----------------|----------------------|
| Red blood cells | (Hematocrit 0.4 L/L) |
| Sodium | (94.3 mmol/L) |
| Calcium | (1.46 mmol/L) |
| Potassium | (1.48 mmol/L) |
| Lactate | (5.33 mmol/L) |
| Bicarbonate | (26 mmol/L) |
| Albumin | (19.1 g/L) |
| Glucose | (2.93 mmol/L) |
| Mannitol | (15.87 mg/L) |
| Creatinine | (109.5 mg/L) |
| Amoxicillin | (43.5 mmol/L) |
| Clavulanic Acid | (16.1 mmol /L) |

Mitochondrial activity and oxidative stress of MSC

MSC metabolic activity was measured by a colorimetric assay based on the reduction of XTT (2,3-Bis-(2-Methoxy-4-Nitro-5-Sulfophenyl)-2H-Tetrazolium-5-Carboxanilide) by nicotinamide adenine dinucleotide (NADH) (ThermoFisher, Manhattan, NY, USA). The reagent is reduced by NADH produced during mitochondrial metabolism which results in a color change of the XTT

reagent detectable by a spectrophotometer. The concentration of the reagent is measured by absorbance measured at a wavelength of 450-500nm. This assay was performed on MSC that were in suspension for 30 and 120 min in perfusion fluid or culture medium and on attached MSC. In addition, oxidative stress of MSC was measured using CellRox reagent (ThermoFisher) according to the manufacturer's manual. CellRox is oxidized by reactive oxygen species (ROS) and emits a fluorescent signal that is measured by flow cytometry.

Proliferation of MSC

In order to assess the effects of perfusion fluid on cell proliferation, MSC were fluorescently labelled with carboxyfluorescein succinimidyl ester (CFSE) (ThermoFisher) which was added to the cells at a concentration of 5 mM. The cells were then incubated at 37° C for 15 minutes in the dark. Staining was stopped by the addition of twice the volume of FBS-containing culture medium and incubated for 5 min at RT. Cells were washed and exposed to perfusion fluid for 30 and 120 minutes at 37° C. After incubation with perfusion fluid, MSC were seeded in a 6-well plate with regular culture medium and proliferation was measured at 24, 48 and 72 hours by flow cytometry.

Release of cytokines

A custom-made Luminex Multiplex Assay (R&D Systems, Minneapolis, MN, USA) was designed to measure the release of the following cytokines and growth factors by hMSC after incubation with perfusion fluid:

Angiopoietin-1 (ANG-1), Angiopoietin-2 (ANG-2), epidermal growth factor (EGF), hepatocyte growth factor (HGF), interferon-gamma (IFN- γ), interleukin 10 (IL-10), interleukin 6 (IL-6), monocyte chemoattractant protein 1 (MCP-1), programmed death ligand 1 (PD-L1), platelet derived growth factor AA (PDGFAA), Thrombospondin-2, tissue inhibitor of metalloproteases 1 (TIMP-1), tumor necrosis factor alpha (TNF- α), soluble tumor necrosis factor receptor 1 (sTNF-RI) and vascular endothelial growth factor (VEGF).

Subconfluent (90%) cultures of hMSC were washed and cells were incubated in perfusion fluid for 30 and 120 minutes. Wells were washed again and culture medium was added. After 24 hours supernatants were retrieved and the array was performed according to the manufacturer's protocol. Fluorescence was measured on a Luminex 100/200 system

(Luminex, Austin, TX, USA) using Xponent software. Due to the lack of pig-specific reagents this assay was only performed in with hMSC.

Adhesion of MSC to Endothelial cells

Confluent monolayers of endothelial cells were cultured in 24-well plates. Culture medium was replaced by either a 1:1 mix of MSC and endothelial cell (EC) medium or perfusion fluid. 200,000 MSC were fluorescently-labelled with PKH26 (Sigma) and added to each well. After 10, 30, 60, 120 and 240 minutes supernatant was removed and wells were washed to eliminate all non-adherent MSC. Attached cells were trypsinized and analyzed by flow cytometry. Fluorescent signal detected by flow cytometry allowed the determination of the percentage of MSC attached.

Results

Cryopreserved MSC show reduced survival in perfusion fluid and medium

To examine the survival of MSC, fresh and cryopreserved MSC were incubated in suspension in perfusion fluid. Survival rates of freshly cultured and thawed pMSC were less than 40% after 30 minutes and decreased to 30% after 2 h in culture medium. Perfusion fluid had no negative impact on pMSC survival compared to culture medium except on thawed MSC after 30 min in perfusion (Figure 1A). hMSC were more resistant to suspension conditions than pMSC. Freshly cultured hMSC showed more than 95% survival in medium and in perfusion fluid. However, a significant decrease in survival to approximately 70% was observed for cryopreserved hMSC in perfusion fluid and in culture medium compared to fresh MSC. Perfusion fluid reduced survival of fresh hMSC after 2 hours only minimally when compared to regular culture medium (Figure 1B).

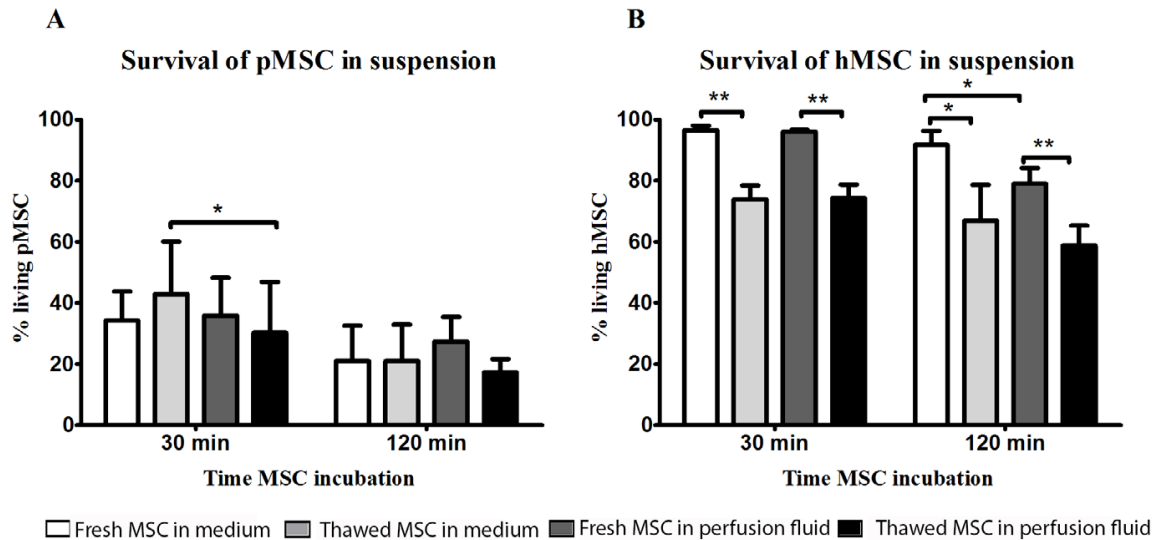


Figure 1. Effect of perfusion fluid on survival of fresh and thawed pMSC and hMSC in suspension. (A) Perfusion fluid had minimal effect on pMSC survival compared to medium. (B) Perfusion fluid had minimal effects on hMSC survival. Thawed hMSC showed a lower survival in suspension compared to fresh hMSC. Perfusion fluid reduced survival of hMSC after 2 hours. (n=5). Results are shown as means \pm SD. * p-value < 0.05; ** p-value < 0.01.

MSC show impaired adhesion to endothelial cells in perfusion fluid

To assess the function of surviving MSC in perfusion fluid, the capacity of MSC to adhere to EC was tested. In culture medium, fresh and thawed pMSC started to attach to PAOEC already 10 minutes after seeding. After 4 hours, almost 100% of freshly cultured pMSC were attached to PAOEC while only 80% of thawed pMSC adhered (Figure 2A). Perfusion fluid strongly reduced the capacity of pMSC to attach to PAOEC regardless if they were fresh or thawed cells. Fresh hMSC adhesion to HUVEC was higher than 95% after 4 h in culture medium. In perfusion fluid, 60% of fresh hMSC were able to attach after 4 h. Cryopreserved hMSC showed 80% attachment in culture medium after 4 hours and less than 50% of cryopreserved hMSC attached to HUVEC in perfusion fluid (Figure 2B). In general, thawed MSC showed a decreased capacity to attach to EC compared to fresh MSC, a difference that became more prominent in perfusion fluid.

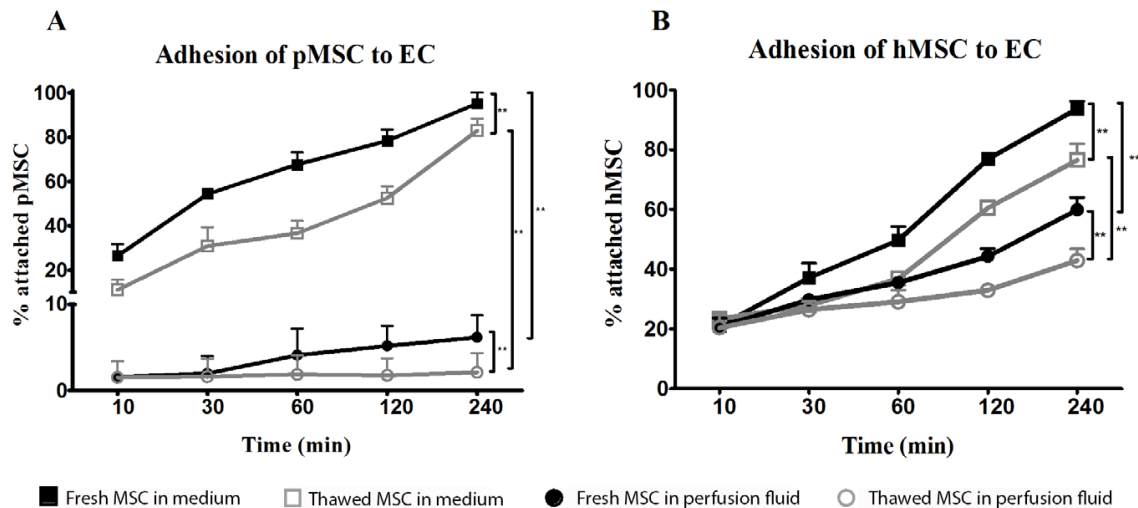


Figure 2. Adhesion of fresh and cryopreserved pMSC and hMSC to EC in medium and perfusion fluid. (A) pMSC attachment to PAOEC over time in culture medium. pMSC show reduced binding to PAOEC in perfusion fluid. Thawed pMSC showed a further reduced ability to bind to EC in perfusion fluid. (B) Thawed hMSC showed reduced attachment to HUVEC compared to fresh hMSC either in culture medium or perfusion fluid. (n=5) Results are shown as means \pm SD. ** p-value < 0.01.

Thawed MSC express higher levels of ROS

The reduced adhesion of thawed MSC to EC could be explained by higher oxidative stress of MSC after the thawing process. The accumulation of ROS derived from the thawing process might induce damage in thawed MSC. An increased production of ROS by thawed pMSC and hMSC was observed at 30 minutes and 2 hours after thawing both in medium and perfusion fluid (Figure 3A). Thawed hMSC produced a higher level of ROS than pMSC whereas ROS production in hMSC was boosted in perfusion fluid (Figure 3B). Thawed hMSC had elevated concentrations of ROS compared to fresh hMSC. These results indicate that freeze-thawing and perfusion fluid affects ROS production in pMSC and hMSC in the first hours after thawing.

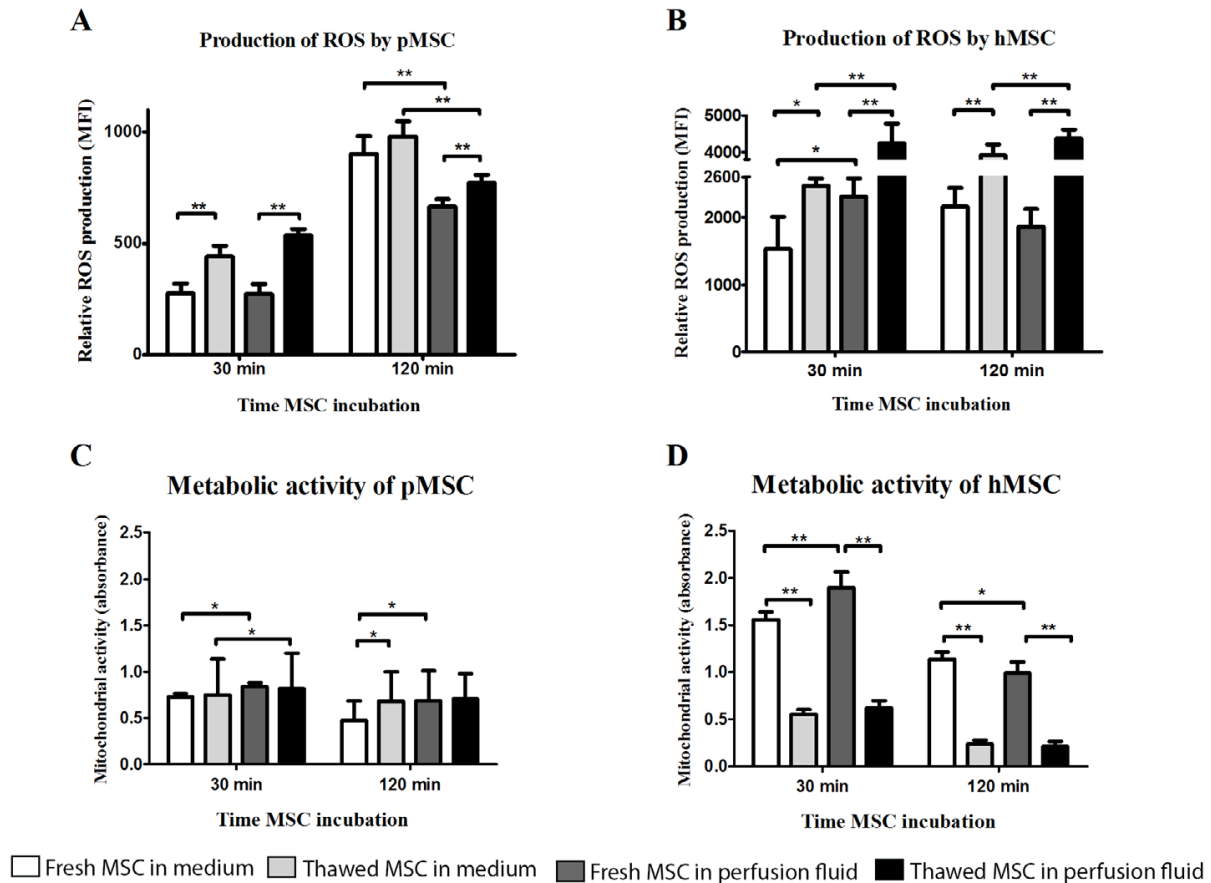


Figure 3. Perfusion fluid and thawing after cryopreservation increase ROS production and reduce metabolic activity in MSC. (A) ROS production in fresh and frozen-thawed pMSC suspended in culture medium or in perfusion fluid. (B) ROS production in fresh and in frozen-thawed hMSC suspended in culture medium or in perfusion fluid. (C) Metabolic activity measured by XTT reduction by NADH of fresh and frozen-thawed pMSC after 30 min and 2 h incubation in perfusion fluid. (D) Metabolic activity measured by XTT reduction by NADH of fresh and frozen-thawed hMSC after 30 min and 2 h incubation in perfusion fluid. (n=5) Results are shown as means \pm SD. * p-value < 0.05; ** p-value < 0.01.

Metabolic activity of mitochondria is reduced in thawed MSC

ROS production leads to mitochondrial damage which results in reduced metabolic activity of cells. It is possible that MSC survive in suspension but are less metabolically active, which may explain the different capacity of MSC to adhere to EC after thawing or in perfusion fluid. To determine the effect of perfusion fluid and the freeze-thawing procedure on MSC metabolic activity, the conversion of XTT to its reduced state by mitochondria was measured in MSC. pMSC mitochondrial activity showed to be very stable and was not affected by cryopreservation (Figure 3C). However, perfusion fluid induced a small increase in activity after 30 minutes. Fresh hMSC showed a 2-fold higher mitochondrial activity than pMSC. Furthermore, fresh hMSC were more active than their thawed counterparts. After 30 minutes

in perfusion fluid, fresh hMSC showed increased mitochondrial activity compared to culture medium (Figure 3D).

Freeze-thawing affects proliferation of hMSC but not pMSC

Proliferation of MSC was measured after initial incubation in suspension in perfusion fluid or medium for 30 min and 120 min, followed by 72 h culture in culture medium. Incubation in perfusion fluid did not affect pMSC proliferation (Figure 4A and B). Freshly cultured hMSC proliferated more than thawed hMSC after incubation in perfusion fluid or medium (Figure 4C and D).

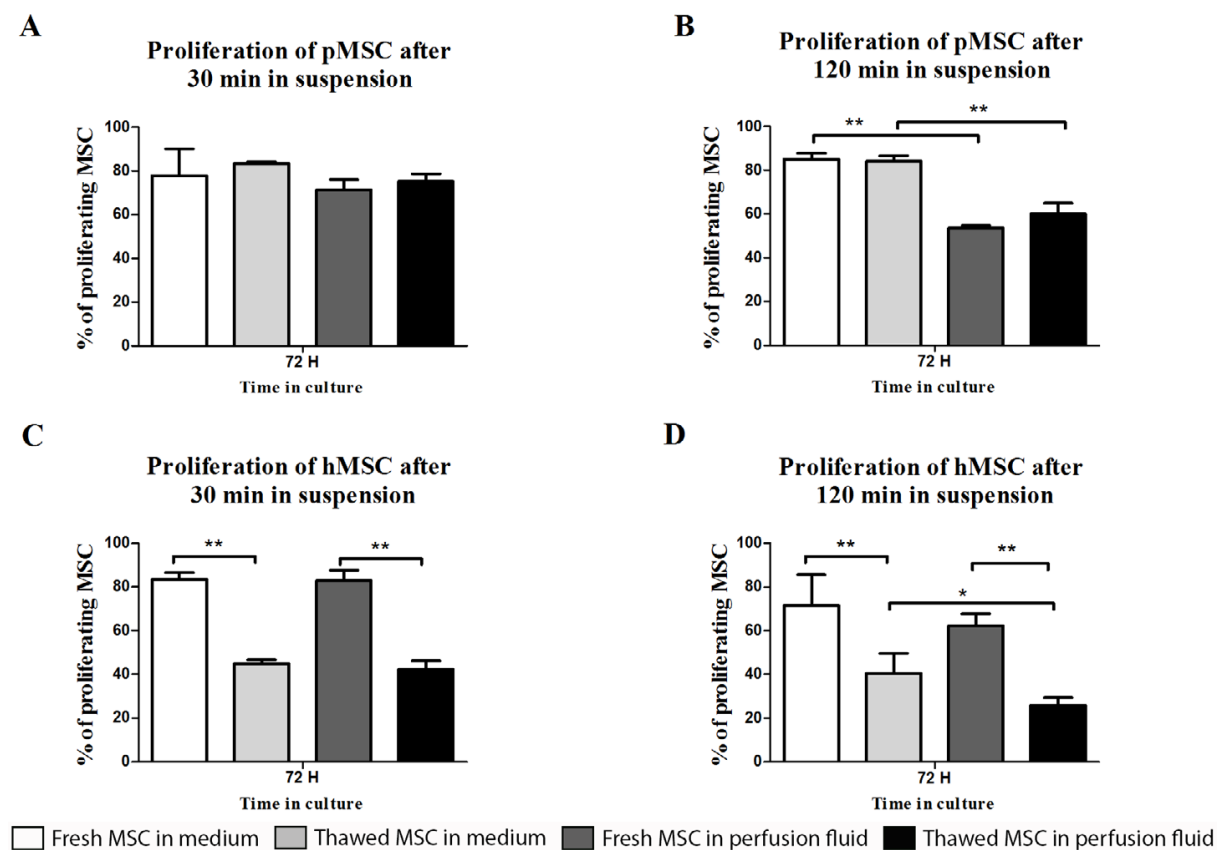


Figure 4. Effect of perfusion fluid and freeze-thawing on proliferation of MSC. pMSC and hMSC were incubated in perfusion fluid for 30 and 120 min and proliferation was measured after subsequent culturing in medium after 72h. (A) pMSC proliferation was not affected by incubation in perfusion fluid for 30 min. (B) pMSC in perfusion fluid proliferated less than pMSC in culture medium. (C-D) Fresh hMSC proliferated more than thawed hMSC and perfusion fluid did not have an effect on fresh hMSC proliferation. Thawed cells in perfusion fluid were the least proliferative. (n=5) Results are shown as means \pm SD. *p-value<0.05; ** p-value<0.01.

Perfusion fluid increases the proliferation of attached MSC

MSC are adherent tissue cells and the suspension conditions in the previous experiments may affect their phenotype and function. To examine how adherent MSC respond to perfusion fluid, morphology, survival, metabolic activity and proliferation of attached MSC were studied. The morphology of MSC in culture was not affected after 30 min or 2 h culture in perfusion fluid (Figure 5A-J). Adherent pMSC and hMSC showed increased survival in perfusion fluid compared to MSC in suspension. Survival of adherent pMSC was higher than 80% in culture medium and perfusion fluid (Figure 6A-B) compared to a maximum of 40% survival in suspension (Figure 1A). hMSC showed 78% survival after 2h in suspension in perfusion fluid, but when they were attached, survival after 2 hours was 93%. No differences in survival were observed between perfusion fluid and culture medium on attached MSC (Figure 6A-B). No significant effect of perfusion fluid on mitochondrial activity was observed for attached MSC, although there was a trend towards a decline in activity of pMSC and hMSC over time when cultured in perfusion fluid (Figure 6C-D). Pre-incubation of attached pMSC in perfusion fluid increased their proliferation after 24 h compared to culture medium. This effect was observed only after 120 min pre-incubation in perfusion fluid for hMSC (Figure 6E-F).

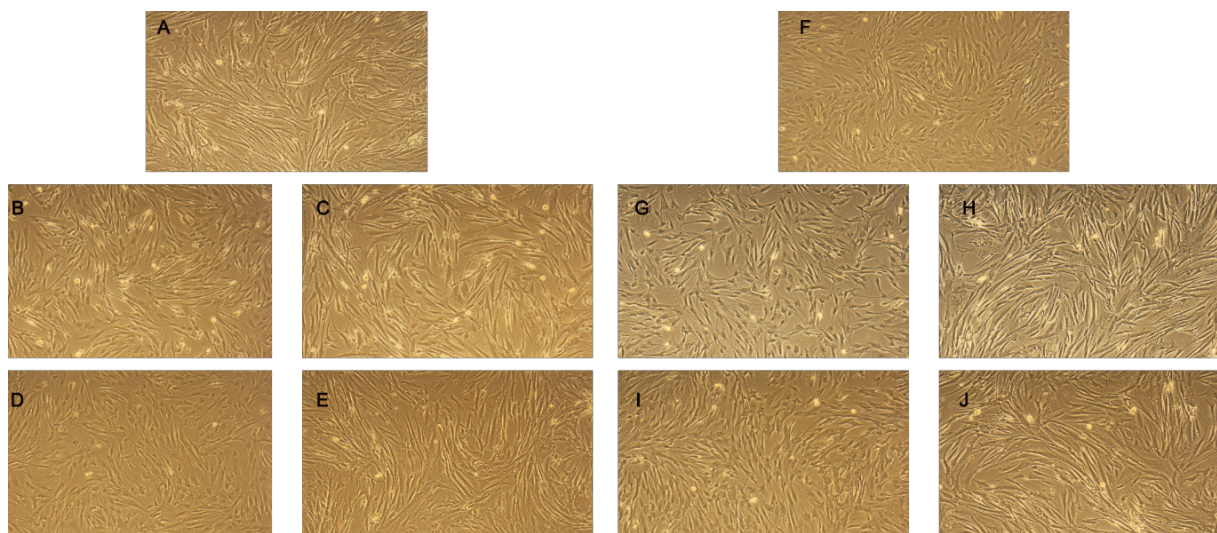


Figure 5. Effect of perfusion fluid on morphology of attached MSC. (A) pMSC in regular culture medium. (B, C) pMSC in culture medium or perfusion fluid respectively for 30 min. (D, E) pMSC cultured in culture medium or perfusion fluid respectively for 120 min. (F) hMSC in regular culture medium. (G, H) hMSC cultured in culture medium or perfusion fluid respectively for 30 min. (I, J) hMSC cultured in culture medium or perfusion fluid respectively for 120 min.

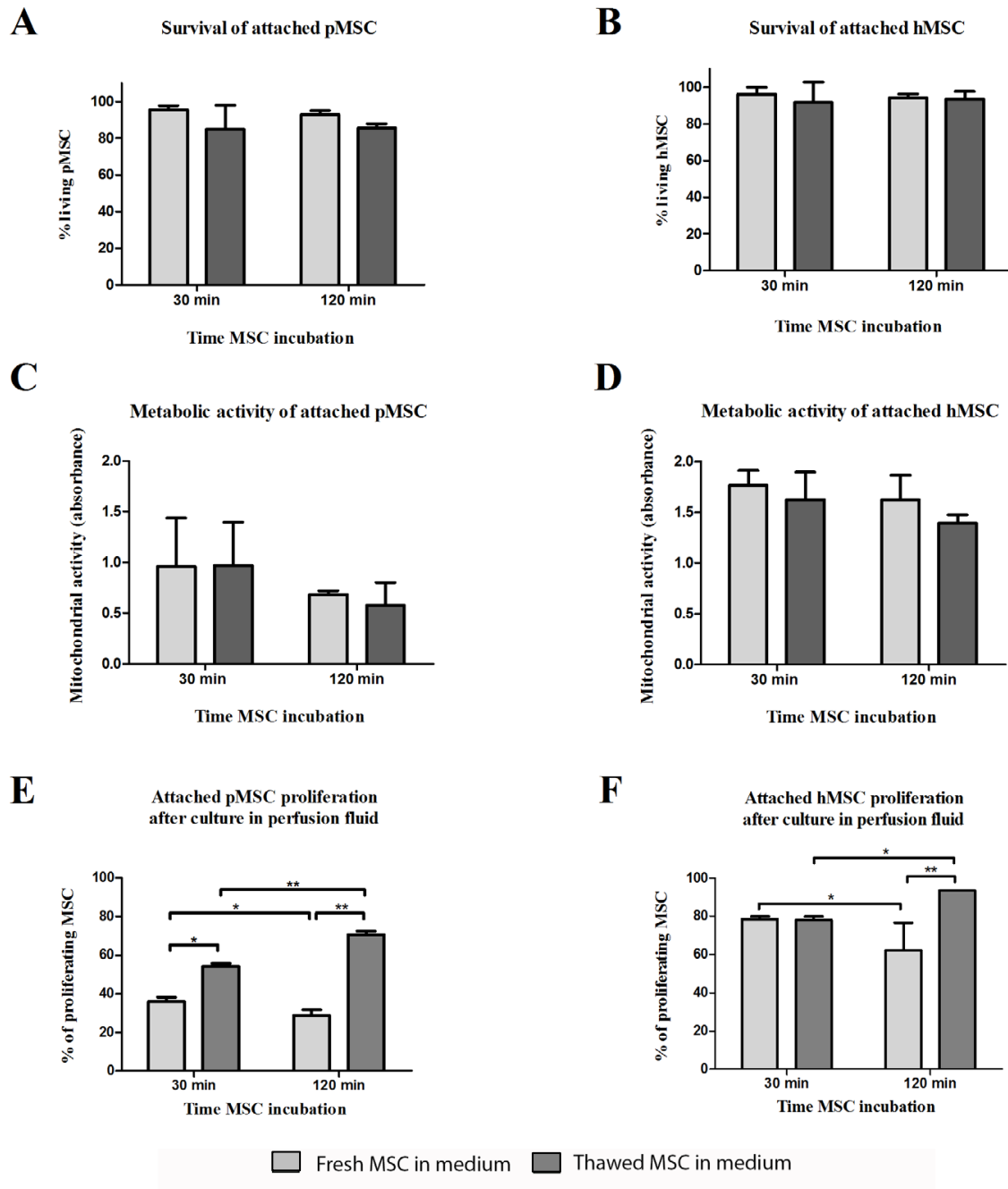


Figure 6. Effect of perfusion fluid on attached MSC. Survival of attached pMSC (A) and hMSC (B) after 30 minutes in perfusion fluid. (C, D) Metabolic activity of attached pMSC (C) and hMSC (D) after 30 minutes in perfusion fluid measured by reduction of XTT. (E, F). Proliferation of attached pMSC (E) and hMSC (F) after 30 in perfusion fluid. Cells were trypsinized and re-seeded in a culture flask. Proliferation after 24 h was determined by CFSE fluorescence. (n=5); Results are shown as means \pm SD. * p-value < 0.05; ** p-value < 0.01.

Secretory profile of MSC is not affected by culture in perfusion fluid

The secretion of growth factors and cytokines is an important mechanism of action of MSC. To examine whether perfusion fluid would preserve the secretory profile of adherent hMSC and furthermore whether perfusion fluid induced an inflammatory response in hMSC, hMSC

were incubated in perfusion fluid for 30 minutes and growth factor and cytokine secretion was analyzed. We observed that the secretion of the angiogenic factors VEGF, PDGF, ANG-1, HGF, Thr2 was unaffected in perfusion fluid (Figure 7A-E). Inflammatory cytokines IL-6 and MCP-1 were increased 2-fold and 10-fold respectively, in perfusion fluid (Figure 8A and B).

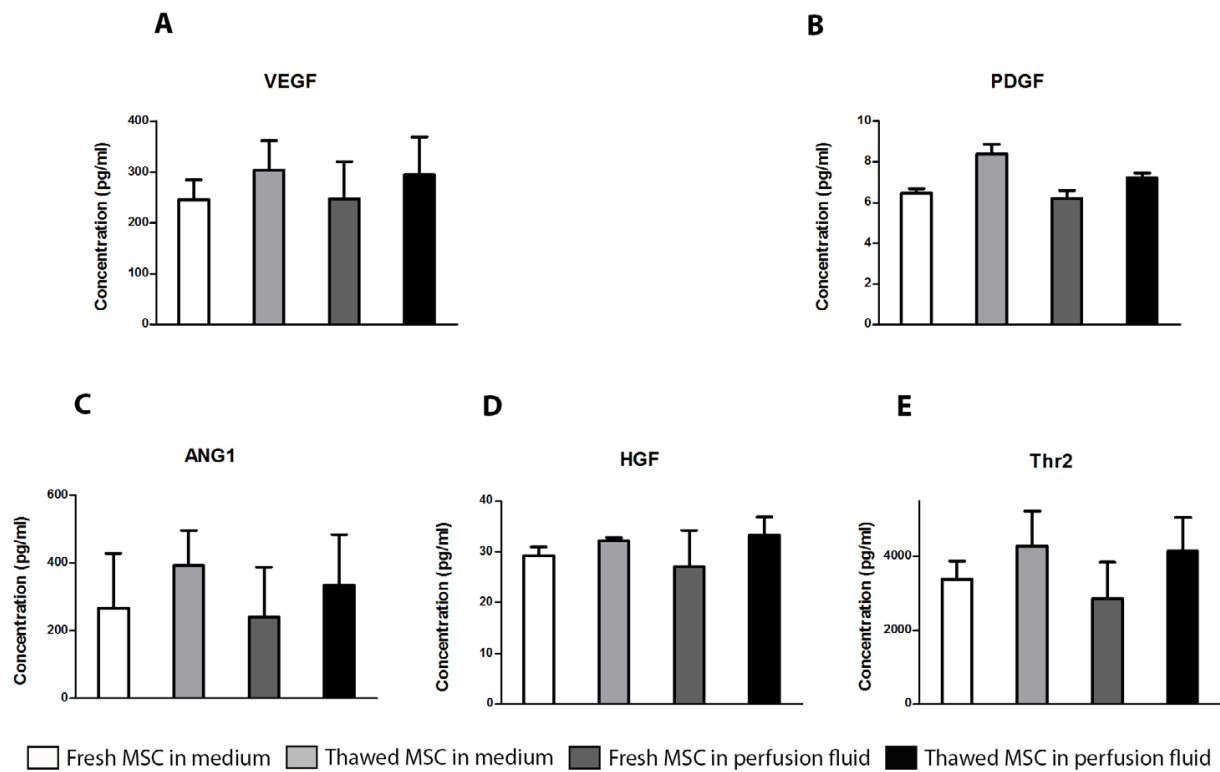


Figure 7. Production of angiogenic factors by hMSC in culture medium and perfusion fluid. MSC were incubated in perfusion fluid for 30 or 120 minutes, washed and replaced by culture medium for 24 h. The secretion of angiogenic and growth factors was not affected by perfusion fluid. (n=5) Results are shown as means \pm SD.

Discussion

In the present work we have assessed the effect of a period of incubation in a perfusion fluid required for robust longer-term ex vivo normothermic machine perfusion (NMP) of kidneys on MSC of both pig and human origin. Our work involved the use of cryopreserved MSC for logistic purposes, suspension conditions to deliver MSC via the renal artery using NMP and the use of an RBC-based perfusion fluid which may affect the survival and function of MSC. In order to mimic the conditions of a potential novel MSC therapy to stimulate the repair of injured kidneys while these are connected to NMP, MSC were thawed after cryopreservation and incubated in perfusion fluid in suspension. Actual infusion of MSC using NMP was not carried out as the purpose of the study was to assess the individual effect of each of the

mentioned conditions separately. In case that NMP conditions did not support MSC survival and function, future planned experimentation in the NMP setup could have been stopped, reducing economic and time costs. Nevertheless, the results of this study allow to take the next step and study MSC infusion through an NMP system, which is already planned to be carried out.

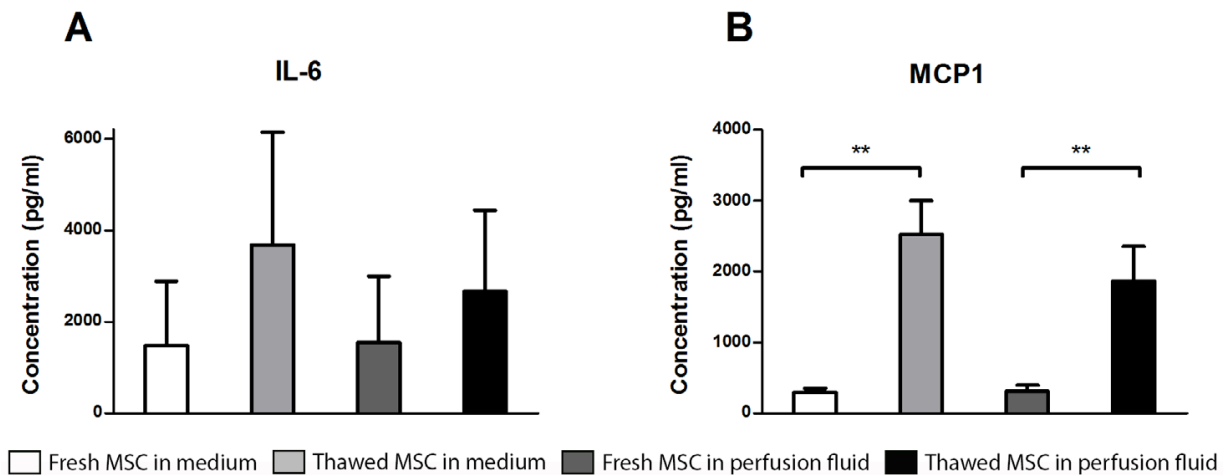


Figure 8. Production of inflammatory cytokines by hMSC in culture medium and perfusion fluid. MSC were incubated in perfusion fluid for 30 or 120 minutes, washed and replaced by culture medium for 24 h. The secretion of MCP-1 and IL-6 increased by perfusion fluid (A) The secretion of IL-6 show a tendency to increase by perfusion fluid. (B) The secretion of MCP-1 by MSC is increased after incubation in perfusion fluid. (n=5) Results are shown as means \pm SD. ** p-value < 0.01.

In the field of clinical MSC therapy, temporary cryopreservation and thawing along with vehicle solutions to deliver the therapy are important factors that can determine the success of MSC therapy (20,28-30). The handling time until administration will have an impact on the survival and function of MSC. Survival of MSC is affected by the composition of storage media (31) and cytokine secretion profile of MSC can be altered, affecting MSC properties such as angiogenic potential (32). Our results show that the particular perfusion fluid used for our experiment is not detrimental for the secretion of angiogenic factors by hMSC.

The bespoke NMP perfusion fluid used in this study supports the survival of pig and human MSC. However, the function and metabolism of these cells are affected by the suspension conditions MSC were kept in. Specifically, perfusion fluid inhibited the adhesion of pMSC in suspension to PAOEC and hMSC to HUVEC. MSC have the capacity to adhere to endothelial cells in vitro under flow conditions as previously shown, especially when endothelial cells have

been treated to recreate an inflammatory environment. Attachment of MSC to endothelial cells was shown to be reduced under flow compared to static conditions (33). Being in suspension in different clinically used storage solutions such as physiologic saline can influence the survival of MSC (31) and the composition of the solution that MSC are kept in modifies their metabolism and function (34,35). Therefore, it can be deduced that the effect of MSC therapy delivered to renal grafts during ex vivo NMP will depend, among other factors, upon the composition of the perfusion fluid. A recent study perfused kidneys for 24 h using NMP. They infused MSC at different concentrations however, after 24 h they found 95% of infused MSC back in their perfusion solution (36), which indicate a very diminished adhesion capacity of MSC towards endothelial cells. Our results are consistent with existing literature and indicate that the composition of the perfusion fluid as well as the infusion process affects the functional properties and delivery efficiency of the final MSC product. Therefore, further knowledge needs to be obtained regarding the effects of perfusion conditions on MSC delivery to the injured kidney.

Human and porcine MSC showed a negative response at several levels to cryopreservation, thawing and re-suspension in perfusion fluid. The effect of cryopreservation and thawing of hMSC has been a concern for the community as it can decrease the presumed efficacy of MSC therapy (19,28,30,37). Our results confirmed this concern. It has recently been published that freezing-thawing MSC increases the production of ROS and compromises membrane stability and homeostasis in pMSC (38), which is also supported by our data. Viability of MSC is a key factor for treatments that require an active role of MSC. However, inactive MSC have been shown to retain their immunomodulatory properties (14,39,40). Therefore, the aim of MSC therapy dictates the required characteristics of MSC.

In vivo, MSC are tissue resident cells and are found in perivascular niches in a wide variety of tissues (41-43). In vitro, MSC are strictly grown as adherent cells, and for this reason MSC are cultured allowing plastic adherence to expand them (10). We demonstrated that the poor performance of MSC in perfusion fluid was primarily due to the fact that they were in suspension. Survival of both pig and human MSC cultured in adherent conditions in perfusion fluid was higher than that of MSC kept in suspension, suggesting a protective effect of adherence. Mitochondrial activity, however, was similar in MSC in suspension and attached, suggesting that MSC are active also in suspension. Proliferation of pMSC was increased after

Chapter 6

exposure to perfusion fluid which could be a response to a specific component of the perfusion fluid (31). These results suggest that the nature of MSC make them more vulnerable when they are in suspension and therefore, it should be minimized when they are administered as therapy. Being in suspension in perfusion is, however, a transient condition in the process of MSC delivery using NMP. Presumably, when MSC are delivered to the injured kidney, the damaged tissue microenvironment will help the MSC to be retained and produce regenerative factors as previously shown (44-46). We have shown that after being in contact with perfusion solution MSC can recover, proliferate and be metabolically active. In addition, the secretory profile of angiogenic factor by hMSC is not affected by perfusion fluid. Therefore, this is a promising result that hints MSC maintain their reparative potential after delivery using NMP.

Cryopreservation, thawing and suspension of MSC are inevitable conditions to infuse GMP-grade MSC to kidney transplants via NMP. These conditions are necessary to bridge differences in time and location between MSC preparation and NMP. The disadvantageous effect of these conditions on MSC has to be taken into account for the evaluation of the suitability of MSC therapy for NMP. In order to improve the viability of MSC in NMP conditions, the composition of the perfusion fluid may be adapted to provide better support for MSC survival. Another possibility is to recover MSC after thawing under favorable conditions to improve the resistance of MSC to NMP. An alternative would be to take the loss of MSC under NMP conditions into account and use higher numbers of cells, although the effect of administering large numbers of non-viable MSC to the kidney is uncertain.

Pre-clinical work in the field of transplantation is often performed using porcine models to better understand the possible behaviors of new therapies in patients. Therefore, we investigated MSC of porcine and human origin in order to determine if results can be translated. The response to the thawing process as well as to suspension conditions and perfusion fluid was quite different between MSC from both origins for the parameters studied. We are aware that differences could be related not only to species but also to age and gender, as well as site of adipose tissue harvesting from the donor. However, our results indicate that caution should be taken when interpreting in vitro studies with porcine cells towards the behavior of human cells. A safe translation from swine pre-clinical models to clinical studies is challenging when results are not reproducible between species.

Summarizing, NMP conditions will affect MSC but show sufficient support of their function and survival to consider MSC administration through NMP as a viable option in pursuit of a potentially beneficial cell therapy for the regeneration of injured organs. After these essential preliminary experiments, further study is now underway to determine the best way of joining these two exciting techniques in an optimal manner.

References

1. Hippen, B., Ross, L.F., and Sade, R.M. (2009). Saving lives is more important than abstract moral concerns: financial incentives should be used to increase organ donation. *Ann Thorac Surg.* 88(4), 1053-1061. doi: 10.1016/j.athoracsur.2009.06.087.
2. Ojo, A.O. (2005). Expanded criteria donors: process and outcomes. *Semin Dial.* 18(6), 463-468. doi: 10.1111/j.1525-139X.2005.00090.x.
3. Nagaraja, P., Roberts, G.W., Stephens, M., Horvath, S., Kaposztas, Z., Chavez, R., et al. (2015). Impact of expanded criteria variables on outcomes of kidney transplantation from donors after cardiac death. *Transplantation.* 99(1), 226-231. doi: 10.1097/TP.0000000000000304.
4. Nicholson, M.L., and Hosgood, S.A. (2013). Renal transplantation after ex vivo normothermic perfusion: the first clinical study. *Am J Transplant.* 13(5), 1246-1252. doi: 10.1111/ajt.12179.
5. Weissenbacher, A., Lo Faro, L., Boubriak, O., Soares, M.F., Roberts, I.S., Hunter, J.P., et al. (2018). Twenty-four hour normothermic perfusion of discarded human kidneys with urine recirculation. *Am J Transplant.* doi: 10.1111/ajt.14932.
6. Hosgood, S.A., Thompson, E., Moore, T., Wilson, C.H., and Nicholson, M.L. (2018). Normothermic machine perfusion for the assessment and transplantation of declined human kidneys from donation after circulatory death donors. *Br J Surg.* 105(4), 388-394. doi: 10.1002/bjs.10733.
7. Kathis, J.M., Hamar, M., Echeverri, J., Linares, I., Urbanellis, P., Cen, J.Y., et al. (2018). Normothermic ex vivo kidney perfusion for graft quality assessment prior to transplantation. *Am J Transplant.* 18(3), 580-589. doi: 10.1111/ajt.14491.
8. Smith, S.F., Adams, T., Hosgood, S.A., and Nicholson, M.L. (2017). The administration of argon during ex vivo normothermic perfusion in an experimental model of kidney ischemia-reperfusion injury. *J Surg Res.* 218, 202-208. doi: 10.1016/j.jss.2017.05.041.
9. Pittenger, M.F., Mackay, A.M., Beck, S.C., Jaiswal, R.K., Douglas, R., Mosca, J.D., et al. (1999). Multilineage potential of adult human mesenchymal stem cells. *Science.* 284(5411), 143-147. doi: 10.1126/science.284.5411.143.
10. Dominici, M., Le Blanc, K., Mueller, I., Slaper-Cortenbach, I., Marini, F., Krause, D., et al. (2006). Minimal criteria for defining multipotent mesenchymal stromal cells. The International Society for Cellular Therapy position statement. *Cytotherapy.* 8(4), 315-317. doi: 10.1080/14653240600855905.
11. Kim, H.K., Lee, S.G., Lee, S.W., Oh, B.J., Kim, J.H., Kim, J.A., et al. (2018). A Subset of Paracrine Factors as Efficient Biomarkers for Predicting Vascular Regenerative Efficacy of Mesenchymal Stromal/Stem Cells. *Stem Cells.* doi: 10.1002/stem.2920.
12. Azhdari Tafti, Z., Mahmoodi, M., Hajizadeh, M.R., Ezzatizadeh, V., Baharvand, H., Vosough, M., et al. (2018). Conditioned Media Derived from Human Adipose Tissue Mesenchymal Stromal Cells Improves Primary Hepatocyte Maintenance. *Cell J.* 20(3), 377-387. doi:
13. Reinders, M.E.J., van Kooten, C., Rabelink, T.J., and de Fijter, J.W. (2018). Mesenchymal Stromal Cell Therapy for Solid Organ Transplantation. *Transplantation.* 102(1), 35-43. doi: 10.1097/TP.0000000000001879.
14. de Witte, S.F.H., Luk, F., Sierra Parraga, J.M., Gargasha, M., Merino, A., Korevaar, S.S., et al. (2018). Immunomodulation By Therapeutic Mesenchymal Stromal Cells (MSC) Is Triggered Through Phagocytosis of MSC By Monocytic Cells. *Stem Cells.* 36(4), 602-615. doi: 10.1002/stem.2779.
15. Eggenhofer, E., Benseler, V., Kroemer, A., Popp, F.C., Geissler, E.K., Schlitt, H.J., et al. (2012). Mesenchymal stem cells are short-lived and do not migrate beyond the lungs after intravenous infusion. *Frontiers in Immunology.* 3, 297. doi: 10.3389/fimmu.2012.00297.

16. Sierra-Parraga, J.M., Eijken, M., Hunter, J., Moers, C., Leuvenink, H., Moller, B., et al. (2017). Mesenchymal Stromal Cells as Anti-Inflammatory and Regenerative Mediators for Donor Kidneys During Normothermic Machine Perfusion. *Stem Cells Dev.* 26(16), 1162-1170. doi: 10.1089/scd.2017.0030.
17. Weissenbacher, A., and Hunter, J. (2017). Normothermic machine perfusion of the kidney. *Curr Opin Organ Transplant.* 22(6), 571-576. doi: 10.1097/MOT.0000000000000470.
18. Hamar, M., and Selzner, M. (2018). Ex-vivo machine perfusion for kidney preservation. *Curr Opin Organ Transplant.* 23(3), 369-374. doi: 10.1097/MOT.0000000000000524.
19. Hoogduijn, M.J., de Witte, S.F., Luk, F., van den Hout-van Vroonhoven, M.C., Ignatowicz, L., Catar, R., et al. (2016). Effects of Freeze-Thawing and Intravenous Infusion on Mesenchymal Stromal Cell Gene Expression. *Stem Cells Dev.* 25(8), 586-597. doi: 10.1089/scd.2015.0329.
20. Moll, G., Alm, J.J., Davies, L.C., von Bahr, L., Heldring, N., Stenbeck-Funke, L., et al. (2014). Do cryopreserved mesenchymal stromal cells display impaired immunomodulatory and therapeutic properties? *Stem Cells.* 32(9), 2430-2442. doi: 10.1002/stem.1729.
21. Lohan, P., Treacy, O., Morcos, M., Donohoe, E., O'Donoghue, Y., Ryan, A.E., et al. (2018). Interspecies Incompatibilities Limit the Immunomodulatory Effect of Human Mesenchymal Stromal Cells in the Rat. *Stem Cells.* doi: 10.1002/stem.2840.
22. Ling, W., Zhang, J., Yuan, Z., Ren, G., Zhang, L., Chen, X., et al. (2014). Mesenchymal stem cells use IDO to regulate immunity in tumor microenvironment. *Cancer research.* 74(5), 1576-1587. doi: 10.1158/0008-5472.can-13-1656.
23. Pogozhykh, O., Pogozhykh, D., Neehus, A.L., Hoffmann, A., Blasczyk, R., and Muller, T. (2015). Molecular and cellular characteristics of human and non-human primate multipotent stromal cells from the amnion and bone marrow during long term culture. *Stem Cell Res Ther.* 6, 150. doi: 10.1186/s13287-015-0146-6.
24. Izadpanah, R., Trygg, C., Patel, B., Kriedt, C., Dufour, J., Gimble, J.M., et al. (2006). Biologic properties of mesenchymal stem cells derived from bone marrow and adipose tissue. *J Cell Biochem.* 99(5), 1285-1297. doi: 10.1002/jcb.20904.
25. Hoogduijn, M.J., Crop, M.J., Peeters, A.M., Van Osch, G.J., Balk, A.H., Ijzermans, J.N., et al. (2007). Human heart, spleen, and perirenal fat-derived mesenchymal stem cells have immunomodulatory capacities. *Stem Cells Dev.* 16(4), 597-604. doi: 10.1089/scd.2006.0110.
26. Hosgood, S.A., and Nicholson, M.L. (2011). First in man renal transplantation after ex vivo normothermic perfusion. *Transplantation.* 92(7), 735-738. doi: 10.1097/TP.0b013e31822d4e04.
27. Hosgood, S.A., Barlow, A.D., Hunter, J.P., and Nicholson, M.L. (2015). Ex vivo normothermic perfusion for quality assessment of marginal donor kidney transplants. *Br J Surg.* 102(11), 1433-1440. doi: 10.1002/bjs.9894.
28. Moll, G., Geissler, S., Catar, R., Ignatowicz, L., Hoogduijn, M.J., Strunk, D., et al. (2016). Cryopreserved or Fresh Mesenchymal Stromal Cells: Only a Matter of Taste or Key to Unleash the Full Clinical Potential of MSC Therapy? *Adv Exp Med Biol.* 951, 77-98. doi: 10.1007/978-3-319-45457-3_7.
29. Francois, M., Copland, I.B., Yuan, S., Romieu-Mourez, R., Waller, E.K., and Galipeau, J. (2012). Cryopreserved mesenchymal stromal cells display impaired immunosuppressive properties as a result of heat-shock response and impaired interferon-gamma licensing. *Cytotherapy.* 14(2), 147-152. doi: 10.3109/14653249.2011.623691.
30. Chinnadurai, R., Garcia, M.A., Sakurai, Y., Lam, W.A., Kirk, A.D., Galipeau, J., et al. (2014). Actin cytoskeletal disruption following cryopreservation alters the biodistribution of human mesenchymal stromal cells in vivo. *Stem Cell Reports.* 3(1), 60-72. doi: 10.1016/j.stemcr.2014.05.003.
31. Nofianti, C.E., Sari, I.N., Marlina, Novialdi, and Pawitan, J.A. (2018). Temporary storage solution for adipose derived mesenchymal stem cells. *Stem Cell Investig.* 5, 19. doi: 10.21037/sci.2018.05.04.

Chapter 6

32. Parsha, K., Mir, O., Satani, N., Yang, B., Guerrero, W., Mei, Z., et al. (2017). Mesenchymal stromal cell secretomes are modulated by suspension time, delivery vehicle, passage through catheter, and exposure to adjuvants. *Cytotherapy*. 19(1), 36-46. doi: 10.1016/j.jcyt.2016.10.006.
33. Ruster, B., Gottig, S., Ludwig, R.J., Bistran, R., Muller, S., Seifried, E., et al. (2006). Mesenchymal stem cells display coordinated rolling and adhesion behavior on endothelial cells. *Blood*. 108(12), 3938-3944. doi: 10.1182/blood-2006-05-025098.
34. Xia, W., Li, H., Wang, Z., Xu, R., Fu, Y., Zhang, X., et al. (2011). Human platelet lysate supports ex vivo expansion and enhances osteogenic differentiation of human bone marrow-derived mesenchymal stem cells. *Cell Biol Int*. 35(6), 639-643. doi: 10.1042/CBI20100361.
35. de Witte, S.F.H., Lambert, E.E., Merino, A., Strini, T., Douben, H., O'Flynn, L., et al. (2017). Aging of bone marrow- and umbilical cord-derived mesenchymal stromal cells during expansion. *Cytotherapy*. 19(7), 798-807. doi: 10.1016/j.jcyt.2017.03.071.
36. Brasile, L., Henry, N., Orlando, G., and Stubenitsky, B. (2018). Potentiating Renal Regeneration using Mesenchymal Stem Cells. *Transplantation*. doi:
37. Chinnadurai, R., Copland, I.B., Garcia, M.A., Petersen, C.T., Lewis, C.N., Waller, E.K., et al. (2016). Cryopreserved Mesenchymal Stromal Cells Are Susceptible to T-Cell Mediated Apoptosis Which Is Partly Rescued by IFN γ Licensing. *Stem Cells*. 34(9), 2429-2442. doi: 10.1002/stem.2415.
38. Gurgul, A., Romanek, J., Pawlina-Tyszko, K., Szmatola, T., and Opiela, J. (2018). Evaluation of changes arising in the pig mesenchymal stromal cells transcriptome following cryopreservation and Trichostatin A treatment. *PLoS One*. 13(2), e0192147. doi: 10.1371/journal.pone.0192147.
39. Luk, F., de Witte, S., Korevaar, S.S., Roemeling-van Rhijn, M., Franquesa, M., Strini, T., et al. (2016). Inactivated mesenchymal stem cells maintain immunomodulatory capacity. *Stem Cells Dev*. doi: 10.1089/scd.2016.0068.
40. Galleu, A., Riffo-Vasquez, Y., Trento, C., Lomas, C., Dolcetti, L., Cheung, T.S., et al. (2017). Apoptosis in mesenchymal stromal cells induces in vivo recipient-mediated immunomodulation. *Sci Transl Med*. 9(416). doi: 10.1126/scitranslmed.aam7828.
41. Fraser, J.K., Wulur, I., Alfonso, Z., and Hedrick, M.H. (2006). Fat tissue: an underappreciated source of stem cells for biotechnology. *Trends Biotechnol*. 24(4), 150-154. doi: 10.1016/j.tibtech.2006.01.010.
42. Beltrami, A.P., Barlucchi, L., Torella, D., Baker, M., Limana, F., Chimenti, S., et al. (2003). Adult cardiac stem cells are multipotent and support myocardial regeneration. *Cell*. 114(6), 763-776. doi: 10.1016/S0092-8674(03)00687-1.
43. Griffiths, M.J., Bonnet, D., and Janes, S.M. (2005). Stem cells of the alveolar epithelium. *Lancet*. 366(9481), 249-260. doi: 10.1016/S0140-6736(05)66916-4.
44. Marquez-Curtis, L.A., and Janowska-Wieczorek, A. (2013). Enhancing the migration ability of mesenchymal stromal cells by targeting the SDF-1/CXCR4 axis. *Biomed Res Int*. 2013, 561098. doi: 10.1155/2013/561098.
45. Ryu, C.H., Park, S.A., Kim, S.M., Lim, J.Y., Jeong, C.H., Jun, J.A., et al. (2010). Migration of human umbilical cord blood mesenchymal stem cells mediated by stromal cell-derived factor-1/CXCR4 axis via Akt, ERK, and p38 signal transduction pathways. *Biochem Biophys Res Commun*. 398(1), 105-110. doi: 10.1016/j.bbrc.2010.06.043.
46. Talkenberger, K., Cavalcanti-Adam, E.A., Voss-Bohme, A., and Deutsch, A. (2017). Amoeboid-mesenchymal migration plasticity promotes invasion only in complex heterogeneous microenvironments. *Sci Rep*. 7(1), 9237. doi: 10.1038/s41598-017-09300-3.

Chapter 7

Infusing Mesenchymal Stromal Cells into Porcine Kidneys during Normothermic Machine Perfusion: Intact MSCs Can Be Traced and Localised to Glomeruli

Merel Pool¹, Tim Eertman¹, Jesus Sierra Parraga², Nils 't Hart³, Marieke Roemeling-van Rhijn⁴, Marco Eijken^{5,6}, Bente Jespersen^{5,6}, Marlies Reinders⁷, Martin Hoogduijn², Rutger Ploeg^{1,8}, Henri Leuvenink¹ and Cyril Moers¹

¹Department of Surgery—Organ Donation and Transplantation, University Medical Center, Groningen, the Netherlands

²Department of Internal Medicine, Erasmus Medical Center, Rotterdam, The Netherlands

³Department of Pathology, University Medical Center, Groningen, The Netherlands

⁴Department of Internal Medicine, University Medical Center, Groningen, The Netherlands

⁵Institute of Clinical Medicine, Aarhus University, Aarhus, Denmark

⁶Department of Renal Medicine, Aarhus University Hospital, Aarhus, Denmark

⁷Department of Internal Medicine (Nephrology), Leiden University Medical Center, Leiden, The Netherlands

⁸Oxford Transplant Centre, University of Oxford, Oxford, UK



Abstract

Normothermic machine perfusion (NMP) of kidneys offers the opportunity to perform active interventions, such as the addition of mesenchymal stromal cells (MSCs), to an isolated organ prior to transplantation. The purpose of this study was to determine whether administering MSCs to kidneys during NMP is feasible, what the effect of NMP is on MSCs and whether intact MSCs are retained in the kidney and to which structures they home. Viable porcine kidneys were obtained from a slaughterhouse. Kidneys were machine perfused during 7 h at 37 °C. After 1 h of perfusion either 0, 10^5 , 10^6 or 10^7 human adipose tissue derived MSCs were added. Additional ex vivo perfusions were conducted with fluorescent pre-labelled bone-marrow derived MSCs to assess localisation and survival of MSCs during NMP. After NMP, intact MSCs were detected by immunohistochemistry in the lumen of glomerular capillaries, but only in the 10^7 MSC group. The experiments with fluorescent pre-labelled MSCs showed that only a minority of glomeruli were positive for infused MSCs and most of these glomeruli contained multiple MSCs. Flow cytometry showed that the number of infused MSCs in the perfusion circuit steeply declined during NMP to approximately 10%. In conclusion, the number of circulating MSCs in the perfusate decreases rapidly in time and after NMP only a small portion of the MSCs are intact and these appear to be clustered in a minority of glomeruli.

Introduction

In an attempt to decrease waiting time for a donor kidney, donation after circulatory death (DCD) is starting to play a more prominent role in many transplant centres [1]. DCD is associated with an elevated risk of inferior early transplant outcome, as a result of the inevitable detrimental effect of warm ischaemia [2,3].

Preserving the function of ischaemically damaged kidney grafts is of vital importance for an effective transplantation. Pre-transplant machine perfusion could enable active organ conditioning and provides a platform for interventions prior to transplantation [4]. This is preferably done under near-physiological conditions, through (sub)normothermic machine perfusion at or just below 37 °C [5]. Normothermic machine perfusion (NMP) restores organ metabolism outside the body in absence of an allogeneic immune response prior to transplantation and this may reverse some effects of ischaemia. In addition, NMP may also allow for a better pre-transplant assessment of organ viability, compared to cold organ preservation techniques [6]. Finally, NMP could provide a platform for active interventions to an isolated organ prior to transplantation, such as administering cellular therapy.

Mesenchymal stromal cells (MSCs) could potentially improve the clinical outcome of kidney transplantations. MSCs are multipotent stromal cells that can be isolated from different tissue sources, including bone marrow and adipose tissue [7]. MSCs are defined by the following standard criteria: the potential to differentiate into osteoblasts, adipocytes and chondrocytes, adherence to plastic, the expression of surface markers CD105, CD90 and CD73, lack of expression of hematopoietic markers CD45, CD34 and endothelial marker CD31 [8,9]. MSCs have several attractive features, such as the modulation of innate immunity as well as adaptive immune responses [9,10]. In addition, MSCs are reported to facilitate repair of damaged tissue [10]. Current analyses suggest that treatment with MSCs will improve the outcome of cell and solid organ transplantation [11,12,13]. The desired immune modulating and regenerative effects can be achieved with either autologous or allogeneic MSCs [10]. So far, research has mainly focused on intravenous (IV) infusion of MSCs to kidney graft recipients after transplantation. These cells will most likely never reach the transplanted kidney, as studies show that IV infused MSCs do not migrate beyond the lungs [14]. In order for MSCs to be physically present in the injured target organ, direct infusion into the graft renal artery may be the solution. In addition, administering cellular therapy in a high concentration to only the isolated organ prior to transplantation could be advantageous, since the transplant recipient

will not be systemically exposed to most of these cells and, in the absence of a host immune response, the effect of therapy may commence earlier. NMP could be an ideal platform for such an intervention [15]. The purpose of this study was to determine whether administering MSCs during NMP is technically feasible, what the effect of NMP is on the survival of MSCs, whether intact MSCs can be detected in the kidney after NMP and to which renal structures these cells localise.

Results

Normothermic Machine Perfusion

Three successful pilots were performed prior to the start of this study. After these pilots, no experiments were excluded or repeated. In total, 12 experiments were performed with A-MSCs, 10 with pre-labelled BM-MSCs and one experiment was performed with FeraTrack labelled MSCs in an MRI scanner. During normothermic machine perfusion all kidneys were functional, as they consumed oxygen and glucose and produced urine. The addition of MSCs did not lead to any macroscopic changes of the kidney nor to changes in haemodynamics.

Characterisation of MSCs Using Fluorescence-Activated Cell Sorting (FACS)

FACS analysis showed that the analysed batch of passage 4 A-MSCs indeed expressed MSC markers CD105, CD73 and CD90 and lacked expression of lymphocyte marker CD45 and endothelial cell marker CD31 (**Appendix A, Figure A1**). The clinical grade BM-MSCs were provided by Leiden University Medical Center and were cultured and characterised at this GMP facility.

Renal Immunohistochemistry

No MSCs were seen at $t = 0$ using immunohistochemistry, at the control slides, and neither in the 100,000 or 1 million MSC groups at all time points ($n = 3$ per group). In the 10 million group, in $t = 360$ min biopsies multiple MSCs could be identified (**Figure 1**). These MSCs were located in the lumen of glomerular capillaries. None were seen in the tubules. The presence of undamaged MSC nuclei in histological biopsies suggests that MSCs were still intact after tissue engraftment.

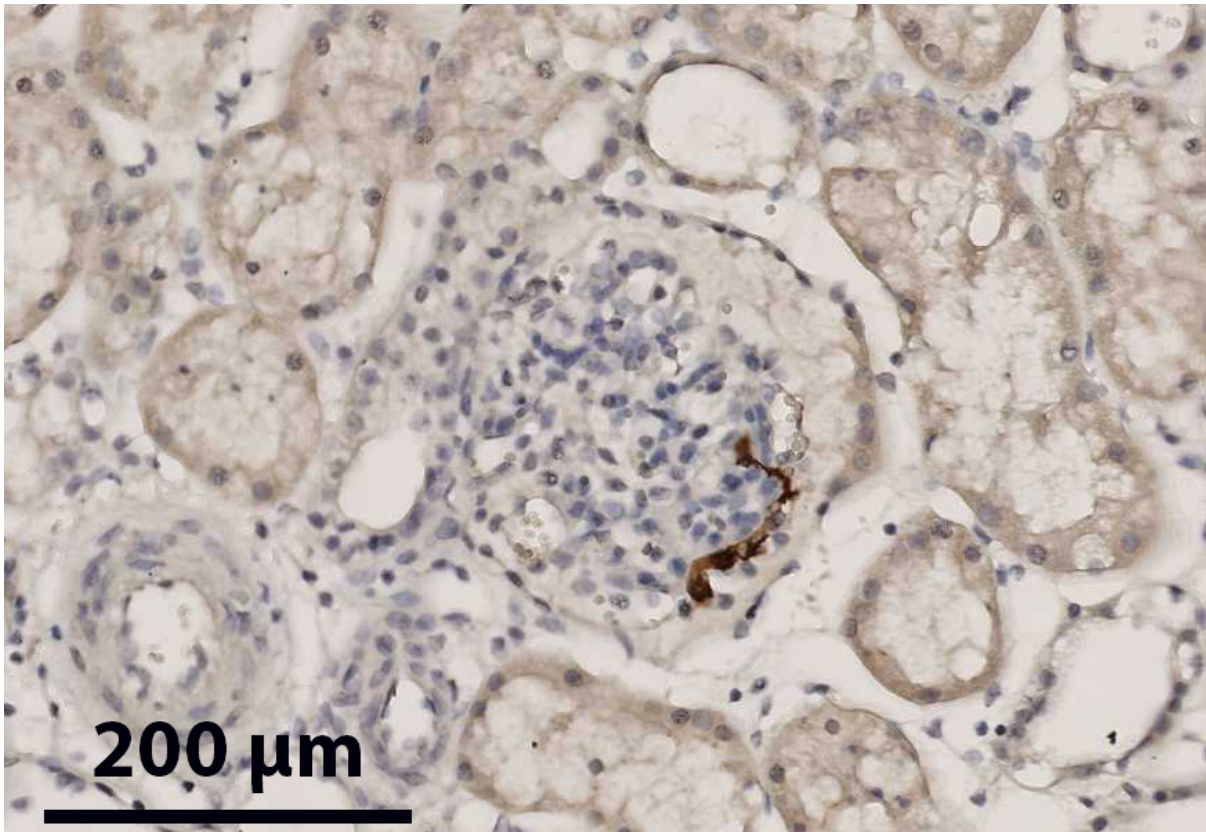


Figure 1. Red/brown immunohistochemical staining of MSCs in one glomerulus in a biopsy of the upper cortex of a kidney after NMP with 10^7 MSCs added.

Fluorescence Microscopy in the Experiments with Pre-labelled MSCs

For a more reliable detection, we decided to perform additional experiments in which MSCs were pre-labelled with Q-tracker 655 and PKH and infused in a perfusion system with and without a kidney ($n = 5$ per group). Selective detection of these fluorescent pre-labelled MSCs proved more straightforward compared to immunohistochemistry. Only a minority of glomeruli showed positive staining, however a striking finding was that fluorescent positive glomeruli often contained multiple MSCs, while most neighbouring glomeruli did not contain any MSCs at all. With confocal microscopy, the fluorescent emission wavelength of PKH26 (green) and Qtracker-655 (red) could be imaged separately. Most fluorescent hotspots were positive for both dyes. As PKH26 stains cell membranes and Qtracker-655 stains the cytoplasm, this finding indicates that these cells are likely to still be intact after NMP (**Figure 2**). We also consistently observed fluorescent hot spots in the glomeruli, which solely had positive PKH staining and no Q-tracker signal. As the intracellular Q-tracker label washes away, the outer membrane-bound PKH remains attached to membrane fragments when a cell breaks up. These hot spots most likely indicate disintegrated MSCs (**Figure 3**).

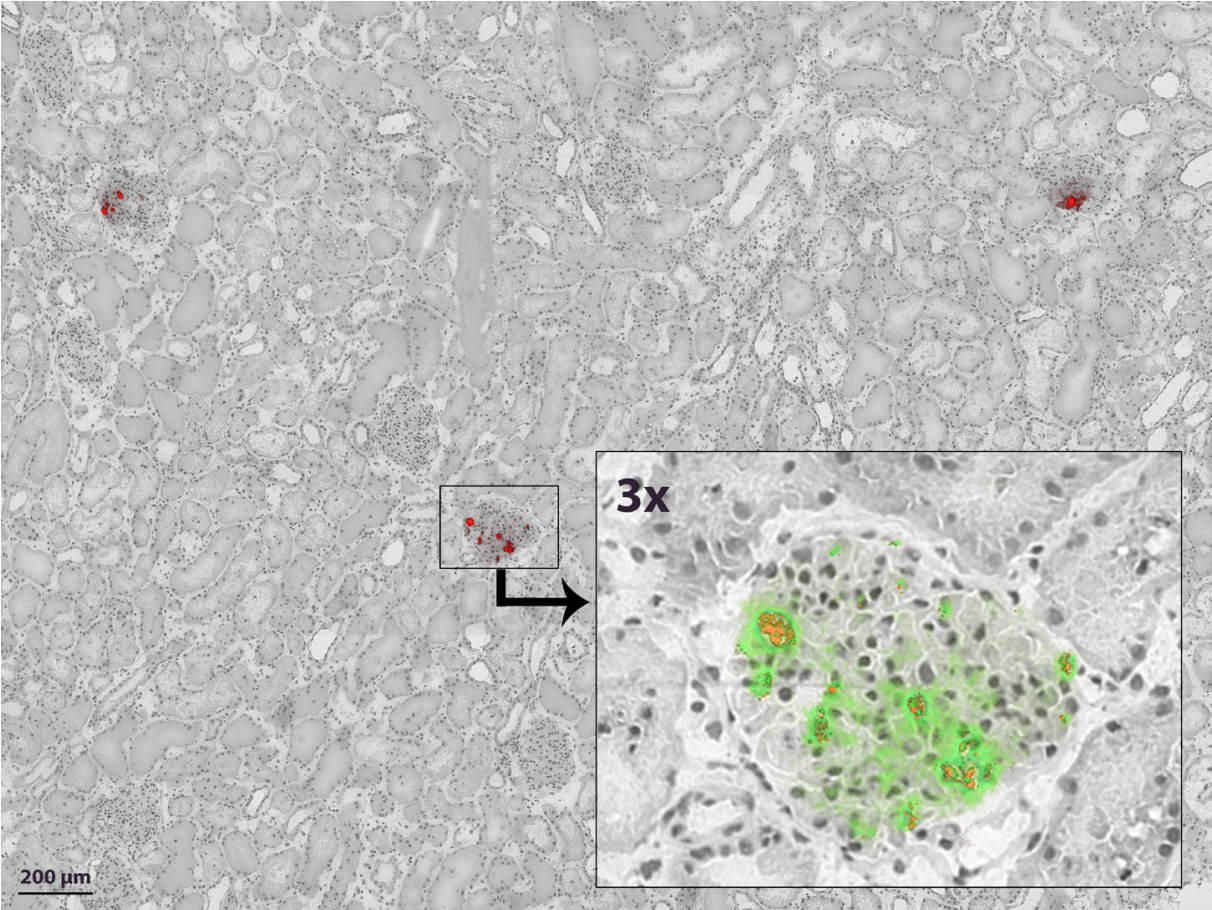


Figure 2. Glomerular PKH and Qtracker-625 fluorescence in cortical tissue after NMP with 10^7 MSCs added. Both fluorescent channels combined (red) in overview, showing that most glomeruli were negative and only a minority of glomeruli were positive for infused pre-labelled MSCs. In addition, some positive glomeruli contained more than one MSC. Inset shows a 3x magnified confocal fluorescence microscopy image with emission wavelengths of both dyes separated: PKH = green, Qtracker-625 = orange.

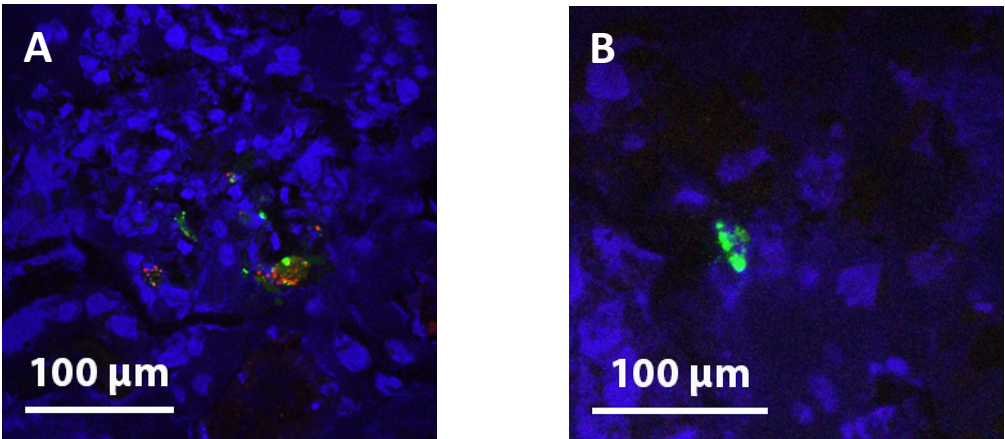


Figure 3. (A) Glomerular PKH (green) and Qtracker-625 (red), DAPI (blue) fluorescence in cortical tissue after NMP with 10^7 MSCs added indicating intact MSCs; (B) fluorescent hot spot in the glomeruli, which solely has positive PKH staining and no Q-tracker signal. Such findings could indicate disintegrated MSCs.

Detection of MSCs Using Flow Cytometry in the Experiments with Pre-labelled MSCs

Perfusate samples from the venous reservoir, as well as perfusate samples from the arterial line were analysed using flow cytometry to determine the isolated effect of machine perfusion on MSCs, while NMP was performed without a kidney in the circuit ($n = 5$). An example of the MSC detection using flow cytometry can be found in the **Appendix A, Figure A2. Figure 4** shows the number of circulating MSCs at each given time point. Results are shown as mean \pm SD. The MSCs were added at time point $t = 60$. The number of circulating MSCs in the reservoir initially dropped and then slightly increased again after a few hours of perfusion. After $t = 240$, the number of circulating MSCs in the venous reservoir decreased further. The yellow line, representing the number of circulating MSCs in the arterial line, shows similar results. Overall, during the perfusion the number of circulating MSCs seemed to be higher in the reservoir than in the arterial line. However, the number of cells circulating in the arterial line and in the venous reservoir were comparable at the end of each perfusion, and only approximately 10% of the number of cells that were initially infused were left.

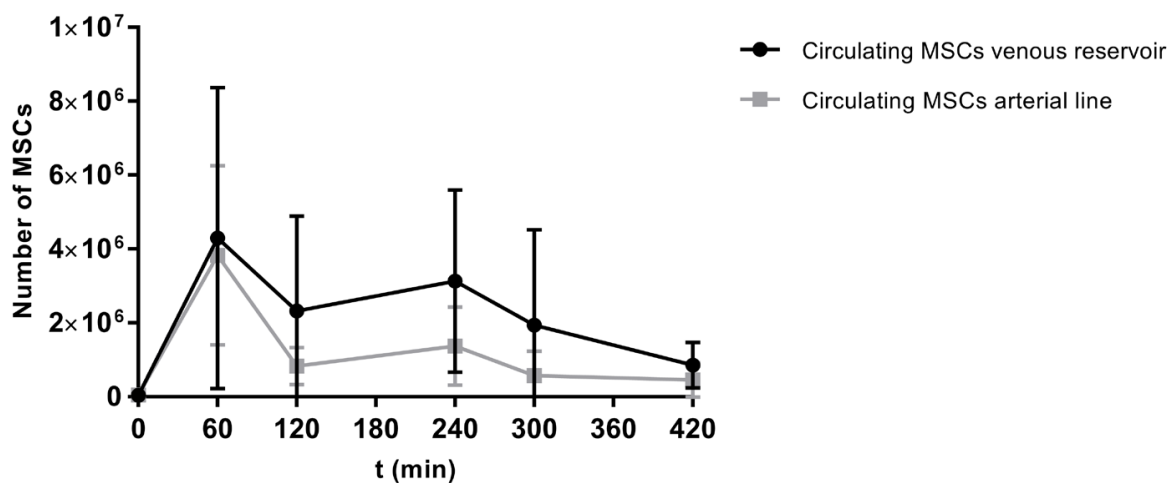


Figure 4. Graph of the MSCs circulating during NMP in the venous reservoir and the arterial line after the addition of 10 million MSCs at $t = 60$.

In the perfusions with a kidney in the circuit ($n = 5$), kidney biopsies were dissociated into single-cell suspensions to be able to detect MSCs that are retained in the kidney. Perfusate samples from the arterial line, as well as from the reservoir and urine samples, were also analysed to detect the presence of MSCs. Results obtained by flow cytometry showed a very small number of double labelled counts in the enzymatically disrupted biopsies. Reservoir samples taken immediately after arterial MSC infusion showed a relatively high number of

double labelled counts, which indicates that MSCs can travel through the kidney and are not fully retained at single pass. Reservoir samples taken at a later moment in time during the perfusion showed a lower level of circulating MSCs, indicating that the cells stop circulating over time. The arterial line perfusate samples showed very similar results (**Appendix A, Figure A3 and Figure A4**).

Detection of Iron Labelled MSCs during NMP in an MRI

The T2 weighted scans generated during and shortly after the infusion of the labelled MSCs during NMP confirmed that the MSCs can indeed be traced to the renal cortex. The most striking finding was that in a well-perfused kidney the distribution of the MSCs was very inhomogeneous (**Figure 5**).

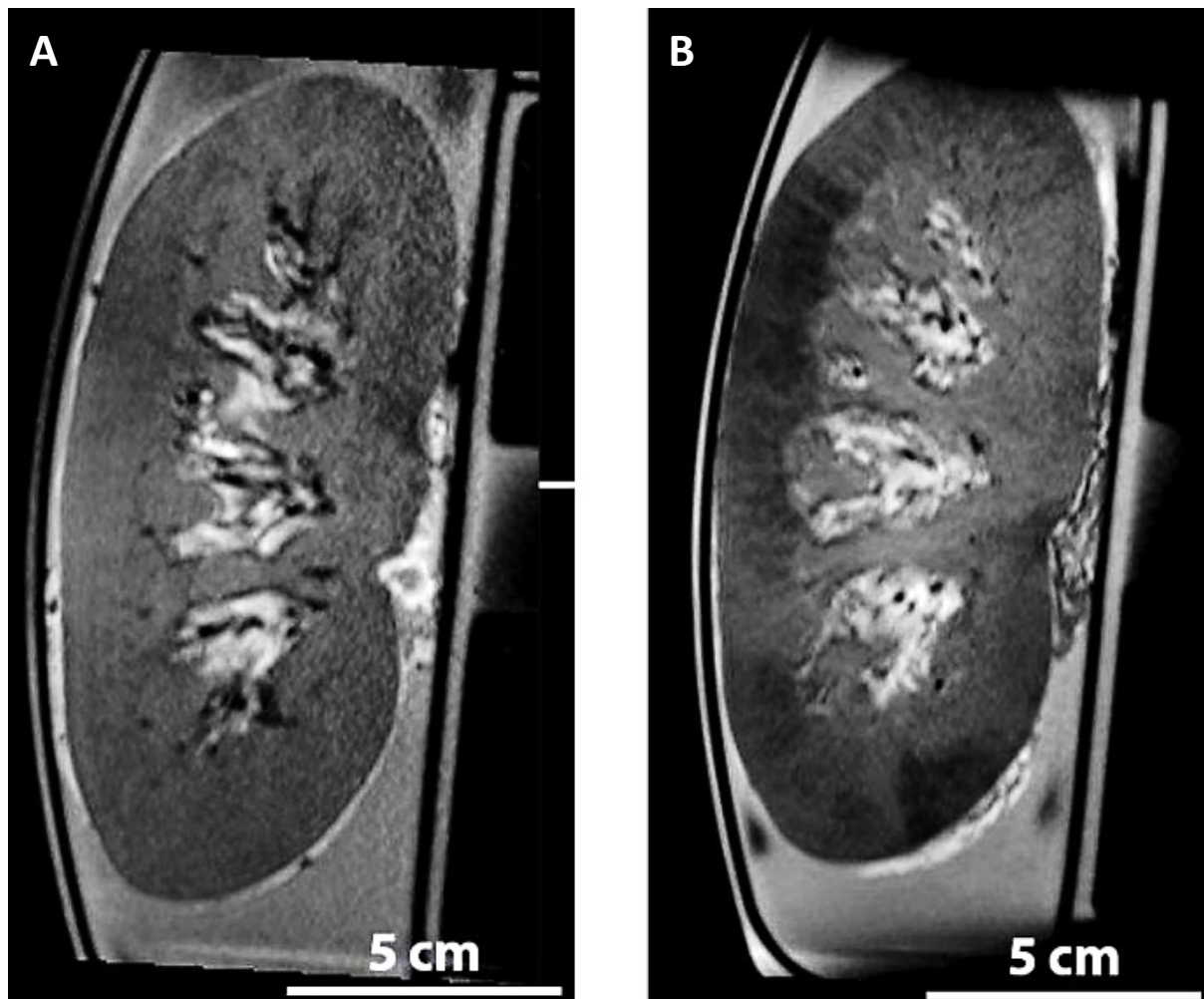


Figure 5. Anatomical, T2 weighted MRI sequence of a whole porcine kidney during normothermic ex vivo perfusion, in which water is typically displayed as white and iron (particles) will display as black. Examples of coronal reconstructions (**A**) baseline; (**B**) shortly after the infusion of 1 million FeraTrack labelled MSCs. The dark areas in the renal cortex represent the MSCs.

Discussion

To our knowledge, this is the first study in which human MSCs were administered during NMP of porcine kidneys. We added MSCs intra-arterially after 60 min of NMP and this did not lead to any changes in haemodynamics. On immunohistochemistry, it became apparent that after NMP most MSCs that were retained in the kidney were located inside the lumen of glomerular capillaries. These findings were confirmed with fluorescence microscopy of pre-labelled MSCs. As the capillary pores of glomeruli are significantly smaller than cultured MSCs it is quite plausible that the majority of cells remain inside the capillary lumen and do not migrate to other structures during perfusion [16,17,18]. Moreover, the relatively short NMP duration will most likely not allow for enough time to migrate to other structures. The finding that some glomeruli contained multiple fluorescent positive glomeruli, while most neighbouring glomeruli did not contain any at all, might be explained by anatomical heterogeneity in the microvasculature leading to MSCs following the path of least resistance during NMP.

Although we were able to determine the number of circulating MSCs in a perfusion set-up without a kidney, we have not fully succeeded in determining the exact number of intact MSCs, which are located in the kidney after several hours of NMP, using flow cytometry. Reliably counting even several millions of infused MSCs among the billions of native renal cells proved to be quite challenging. Although microscopy clearly showed intact MSCs in renal tissue after NMP, we could not convincingly count large numbers of MSCs localised in the kidney with flow cytometry. This could be due to the fact that there were too many kidney cells in the enzymatically digested samples and too few total counts could be made to detect a substantial number of MSCs. The small number of positive counts could also be explained by the negative effect of the inevitable enzymatic digestion of kidney tissue into a single-cell suspension (to allow flow cytometry), which is performed using collagenase. Recent research has shown that collagenase has a significant impact on quality as well as quantity of intact MSCs [19].

We found that, in the perfusate, the number of MSCs decreased during NMP. As this was seen in the experiments with and without a kidney, it is probably the result of cells being exposed to pressure and flow during the perfusion itself. The fact that MSCs are tissue-adherent by nature, but are forced in a continuous non-physiological suspension during perfusion, might also play a role in the cell death [20]. After all, MSCs are tissue-residing stromal cells that may not be particularly adapted to the conditions inside blood vessels or perfusion tubing. As the

cells decrease most rapidly during the final hours, shortening the perfusion time might result in better survival. Also, pre-conditioning, e.g. cytokine-activating, MSCs prior to ex vivo administration could be an interesting future refinement. However, there is evidence that the beneficial effects of MSCs do not solely rely on their viability [21,22].

A possible limitation of our study could be that we used human MSCs in a porcine kidney. This might have led to a xeno-effect. However, this is relatively unlikely as our plasma and leukocyte-free NMP system did not incorporate an actual immune system and only a small number of tissue resident leukocytes may have been present during NMP. Moreover, research has shown that mesenchymal stem cells are well tolerated in an allogeneic or xeno-setting. Hence, when the kidney is transplanted and the pre-transplant infused MSCs come into contact with the host immune system, this should not lead to any negative effects [23,24,25,26,27].

This study did not focus on the effect of MSCs on renal function during NMP. This was a deliberate decision, as we feel it is of the utmost important to first increase our fundamental knowledge about the localisation and structural integrity of MSCs during NMP of a kidney. In addition, renal function is usually only very minimal during ex vivo organ perfusion and thus not a reliable marker for organ viability [28]. The best setting to test such functional outcome is in experiments that also incorporate actual transplantation. Before transplantation experiments are conducted, we feel that the next step should be to investigate cytokine secretion and post-NMP viability of infused MSCs. Hence, when we start to transplant MSC-treated kidneys we will have a better understanding of what effects can be expected. As it is our hypothesis that ischaemia-reperfusion injury could be mitigated, and because post-transplant renal function is superior as a result of MSC infusion during NMP, we are planning future porcine studies in which kidneys are actually transplanted to allow a much longer follow-up and functional assessment in vivo.

In conclusion, this study showed that it is possible to add cultured MSCs during NMP to an isolated porcine kidney in such a way that MSCs reach and reside in the kidney, with at least a small proportion of the administered cells remaining structurally intact and detectable. We were able to visualise MSCs in glomerular capillaries after their administration to the NMP circuit, but only when infused numbers were as high as 10^7 . Transplant studies are needed to determine whether targeting ischaemically damaged donor kidneys with MSCs is indeed beneficial for graft function and survival. The present study has provided the first important

MSC are Delivered to Glomeruli after Infusion during NMP

insights in survival and localisation of culture-expanded MSCs during NMP, and can be considered a first step in establishing machine perfusion as a platform to administer cellular therapy to damaged donor kidneys. Thus, an exciting new window of opportunity might emerge to actively pre-condition isolated organs in a fully controlled setting and in the absence of an immune response, before they are transplanted.

Materials and Methods

Organ and Blood Retrieval

In this pre-clinical study, we utilised porcine kidneys, as they closely resemble human kidneys in anatomical and physiological characteristics [29]. Kidneys and autologous, heparinised whole blood were obtained from two local slaughterhouses. Kidneys underwent 30 min of warm ischemia before cold flush with UW-CS (Belzer UW cold storage solution, Bridge to Life Ltd, Columbia, SC, USA) and storage on melting ice (0–4 °C). Washed, leukocyte depleted autologous red blood cell concentrate was obtained by filtering, centrifuging and washing porcine blood.

Perfusion Setup

The perfusion circuit contained a pump unit (Medos Deltastream Pumpdrive DP2) with a centrifugal pump (both Medos Medizintechnik AG, Stolberg, Germany), an oxygenator/heat exchanger (Dideco Kids D100 neonatal oxygenator, Sorin LivaNova Nederland NV, Amsterdam, Netherlands, or Hilite 800 LT, Medos Medizintechnik AG, Stolberg, Germany) and a modified LifePort[®] organ chamber with SealRing cannula (Organ Recovery Systems, Itasca, IL, USA). Perfusate temperature was kept at 37 °C. The perfusate was oxygenated with carbogen (95% O₂/ 5% CO₂). Flow was monitored using an ultrasonic clamp-on flow probe (Transonic Systems Inc., Ithaca, NY, USA). Pressure was measured directly at the SealRing cannula using a clinical-grade pressure sensor (TruWave disposable pressure transducer, Edwards Lifesciences, Irvine, CA, USA) (**Figure 6**). The setup was primed with 500 mL Williams' Medium E (Gibco[®] William's Medium E + GlutaMAX™, Life Technologies Limited, Bleiswijk, Netherlands) supplemented with amoxicillin-clavulanate 1000 mg/200 mg (Sandoz B.V., Almere, Netherlands) and 40 gr of albumin (bovine serum albumin fraction V, GE Healthcare Bio-Sciences, Pasching, Austria) to obtain a physiological colloid concentration. After priming, 350 mL of pure red blood cells (RBCs) were added. The kidney was perfused in a pressure controlled, pulsatile sinusoid fashion at an arterial pressure of 120/80 mmHg during 7 h. Cold ischaemia time ranged from 3.5 to 5.0 h.

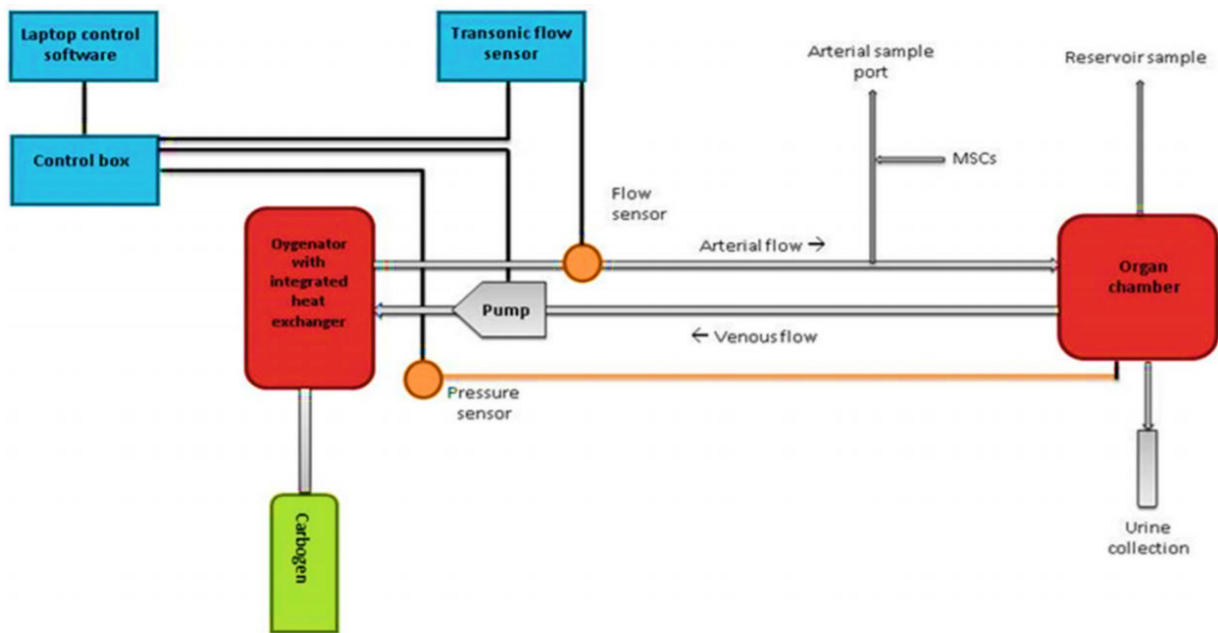


Figure 6. Schematic overview of the normothermic machine perfusion setup.

Isolation, Culture and Infusion of MSCs

Adipose tissue-derived MSCs were isolated from human perirenal fat, a clinical waste product of regular living donor nephrectomies in the University Medical Center Groningen. Informed consent was obtained from patients prior to organ donation. The choice to use human instead of porcine MSCs during this experiment was based on the idea that human MSCs would be easier to detect in the context of an abundance of porcine renal tissue. In addition, using human instead of porcine MSCs, means that we are testing the eventual clinical product. Due to the absence of circulating immune cells and antibodies, relevant xeno-effects are less likely to occur in an ex-vivo perfusion setup. The adipose tissue was mechanically disrupted and minced using a disposable scalpel knife. Next, the tissue was enzymatically digested using filtered 0.5 mg/mL collagenase type IV (Life Technologies), dissolved in RPMI medium (RPMI Medium 1640 + GlutaMAX™, Life Technologies) supplemented with 1% *p/s* (100 U/mL penicillin and 100 mg/mL streptomycin) during 30 min at 37 °C. After centrifugation at 700G for 7 min, the adipose tissue and medium were removed. The cell pellet was resuspended in minimal essential medium eagle-alpha (MEM- α) supplemented with 20% foetal bovine serum (FBS), 1% *p/s* and 2 mM L-glutamine (Life Technologies). The cells were then transferred to a cell culture flask and expanded at 37 °C. The culture medium was refreshed twice each week. The MSCs were trypsinised when they were 80% to 90% confluent. For each experiment, an MSC suspension from freshly trypsinised MSCs was prepared 1 h before infusion. Reportedly,

in humans, the most appropriate dose of MSCs is $0.4\text{--}10 \times 10^6$ MSCs per kilogram body weight, as this does not lead to any significant adverse effects [30]. However, there is evidence that higher doses of MSCs are also safe [31]. As the weight of porcine kidneys we obtained was in the order of 250 g, we chose two doses that were within the earlier mentioned range and one that was well above. The correct number of cells ($0, 10^5, 10^6$ or 10^7 , $n = 3$ per group) were dissolved in 5 mL of Williams' Medium E in a syringe. After 1 h of machine perfusion of the kidney, MSCs were added in a time span of 10 s via the arterial sample port, which was located very close to the renal artery. MSCs from passages 1 to 4 were used for these experiments.

Pre-labelling of MSCs

As we found that MSC visualisation by means of immunohistochemistry in the first four experimental groups yielded sub-optimal discrimination, we decided to improve the detection of MSCs by pre-labelling cells with two strongly fluorescent dyes. We decided to switch to BM-MSCs for these experiments to confirm that these cells behave in the same manner. Also, these cells proved easier to culture than A-MSCs. For this purpose, 10 additional experiments were performed using 10^7 bone-marrow derived pre-labelled MSCs. These BM-MSCs were provided by the Leiden University Medical Center (LUMC) and culture expanded by the Erasmus Medical Center Rotterdam. MSCs were double-labelled with PKH26 (Fluorescent Cell Linker kits, Sigma-Aldrich Chemie B.V., Zwijndrecht, Netherlands) and Qtracker 655[®] (Cell Labelling kits, Thermo Fisher Scientific, Landsmeer, Netherlands) prior to infusion, following the protocol provided by the manufacturers. In five experiments, these pre-labelled BM-MSCs were infused during 7 h NMP of a porcine kidney, following the same protocol as mentioned above. In the other five experiments, pre-labelled BM-MSCs were infused into a circulating NMP circuit, without a kidney present, to assess the isolated effect of NMP on the survival of MSCs. In these perfusions, an artificial resistance was connected to the arterial outflow tubing to obtain similar haemodynamics during NMP as observed in experiments with a kidney present.

Fluorescence-Activated Cell Sorting (FACS)

MSCs were immunophenotypically characterised by flow cytometry on a BD FACS Canto II (BD Biosciences). As the negative control we used 10^6 unstained MSCs. Test samples contained 10^6 MSCs with PE Mouse Anti-Human CD73, APC Mouse Anti-Human CD105, PerCP-Cy5.5

Mouse Anti-Human CD90, FITC Mouse Anti-Human CD31 and PerCP-Cy7 Mouse Anti-Human CD45 (all BD Biosciences). In addition, FACS analysis was used to determine the effect of NMP on the survival of MSCs during perfusion without a kidney with pre-labelled MSCs. For this purpose, hourly perfusate samples were taken. The MSCs could be identified by their fluorescence emission at two different wavelengths as a result of the PKH26 and Q-tracker 655 pre-labelling.

Flow cytometry was also performed on perfusate samples and enzymatically disrupted kidney biopsies from the experiments with pre-labelled MSCs with a kidney in the perfusion circuit. Of each sample, 1 million counts were obtained and analysed through flow cytometry.

Histology and Fluorescence Microscopy

A formalin fixed, paraffin embedded (FFPE) biopsy of the upper, lateral and lower renal cortex (T = 0; T = 180 and T = 360 min of NMP) was taken during the first 12 experiments. Visualisation of infused MSCs in the porcine renal tissue was performed at all three time points using a monoclonal mouse anti-human HLA Class I heavy chain (HC-10), rat anti-mouse polyclonal (RAMPO) and goat anti-rat polyclonal (GARPO) (all Sigma-Aldrich).

Cryopreserved cortical tissue biopsies (T = 420) of the additional experiments with pre-labelled MSCs were imaged with confocal microscopes: entire haematoxylin and eosin (HE)-stained slides were scanned in visual light to assess morphology (Leica SP8, Leica Microsystems, Wetzlar, Germany) and slides stained with mounting medium with 4,6-diamidino-2-phenylindole dihydrochloride (DAPI) (Vectashield mounting medium with DAPI, H-1200) (each only 4 µm apart from the corresponding HE-stained slide) were imaged at the emission wavelength corresponding to each of the fluorescent dyes, during excitation with the appropriate wavelength laser (LSM Zeiss 780 NLO, Carl Zeiss Microscopy, Jena, Germany). HE and fluorescence images were merged using Photoshop CC software (Adobe Systems Incorporated, San José, CA, USA).

Detection of Iron Labelled MSCs during NMP in an MRI

To visualise the distribution of MSCs in the kidney during NMP, 1 million BM-MSCs were labelled with FeraTrack Direct MRI contrast agent (Miltenyi Biotec, Leiden, the Netherlands). FeraTrack labels the MSCs with superparamagnetic iron oxide nanoparticles. During NMP in an MRI these labelled MSCs were infused whilst scanning in one porcine kidney.

Appendix A

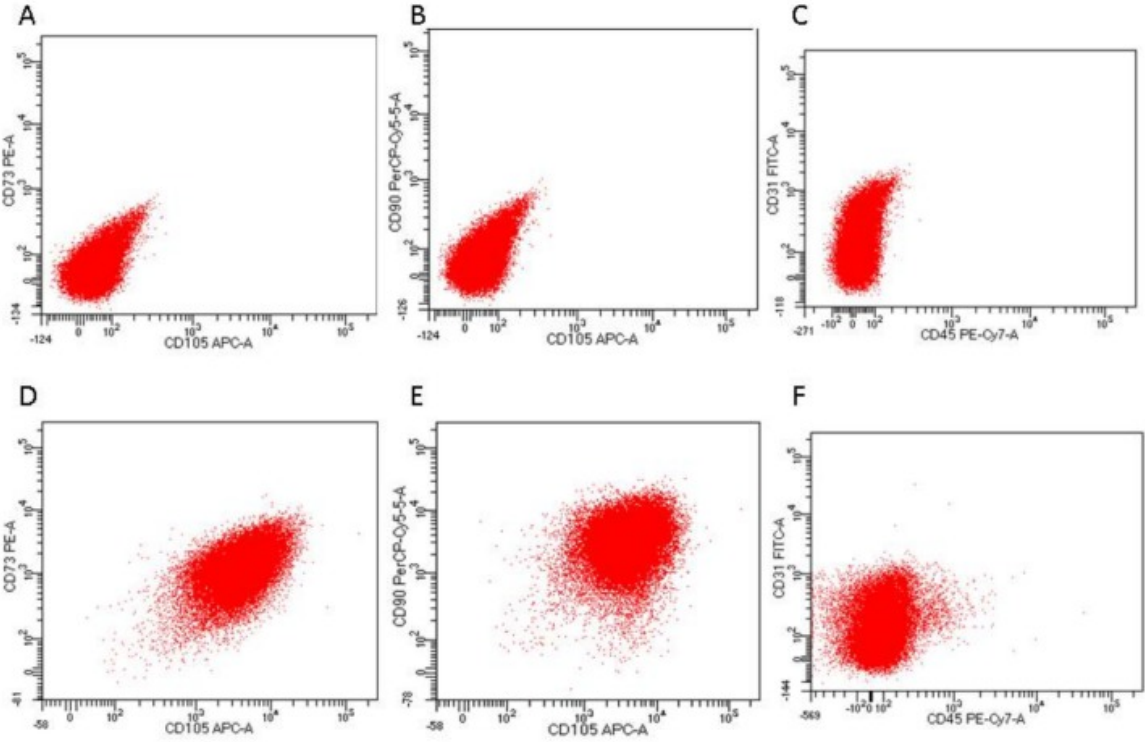


Figure A1. Characterisation of adipose tissue-derived MSCs. Flow cytometry analysis showed that unstained MSCs were negative for (A) CD73, (B) CD105, CD90, (C) CD31, and CD45. Stained MSCs were positive for (D) CD73, (E) CD105, CD90, and negative for (F) CD31, CD45.

MSC are Delivered to Glomeruli after Infusion during NMP

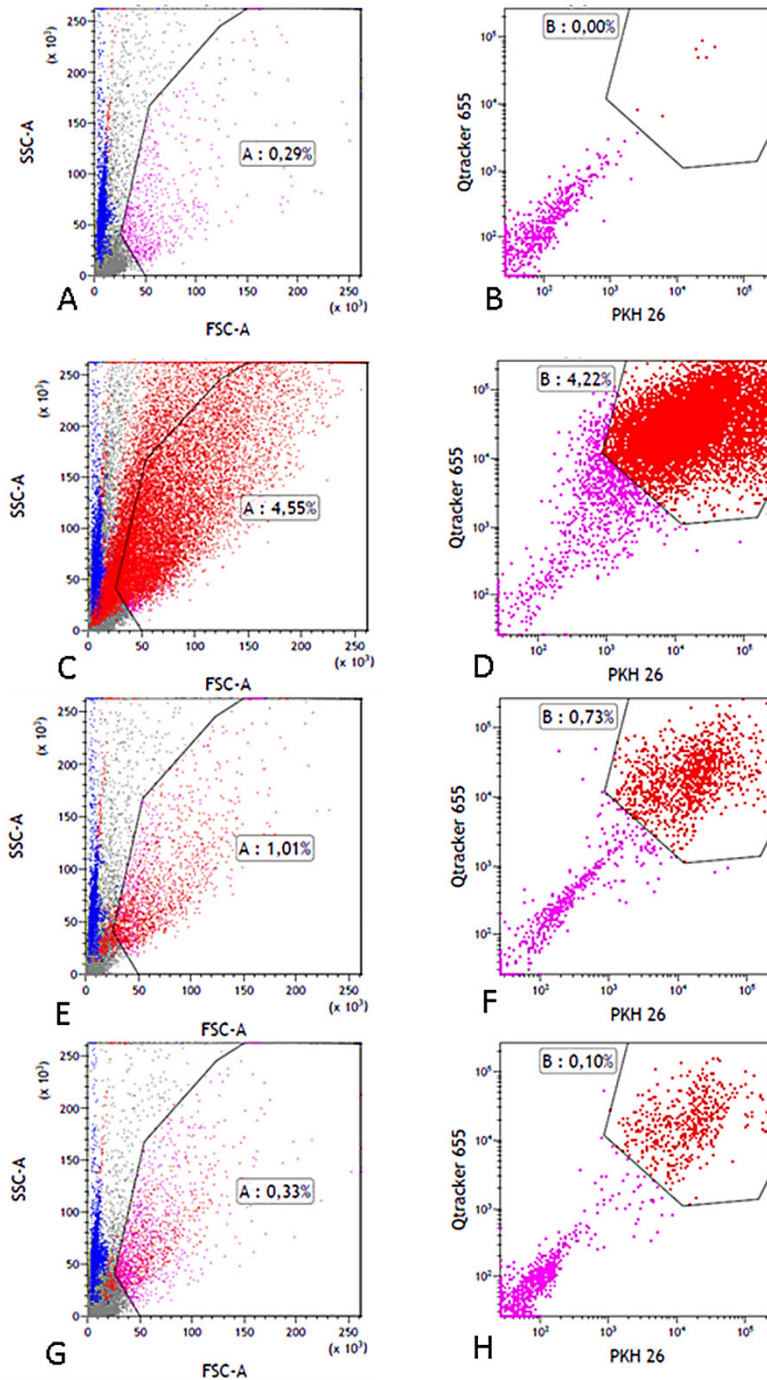


Figure A2. Example of flow cytometry results of perfusate reservoir samples. Cytograms of perfusate reservoir samples taken at different moments in time. Results shown in forward and side scatter cytograms and fluorescence signal strength cytograms of Qtracker655 and PKH26. (A) T = 0 sample moment, FSC-A, SSC-A cytogram, purple dots represent cells that fall within the MSC gating; 0.29% of all cells. (B) PKH26 and Qtracker655 cytogram of t = 0 sample, purple dots represent particles that fall in the auto fluorescence range. No dots visible in the MSC range gate. (C) T = 60 sample moment, FSC-A, SSC-A cytogram, purple dots represent cells that fall within the MSC gating; 4.55% of all cells. (D) PKH26 and Qtracker655 cytogram of t = 60 sample moment, purple dots represent particles that fall in the auto fluorescence range, red dots represent cells that fall within the MSC range gate; 4.22%. (E) T = 240 sample moment, FSC-A, SSC-A cytogram, purple dots represent cells that fall within the MSC gating; 1.01% of all the cells. (F) PKH26 and Qtracker655 cytogram of t = 240 sample moment, purple dots represent particles that fall in the auto fluorescence range, red dots represent cells that falls within the MSC range gate; 0.73%. (G) t = 420 sample moment, FSC-A, SSC-A cytogram, purple dots represent cells

that fall within the MSC gating; 0.33% of all counted cells. (H) PKH26 and Qtracker655 cytogram of t = 420 sample moment, purple dots represent particles that fall in the auto fluorescence range, red dots represent cells that fall within MSC gate range; 0.10%.

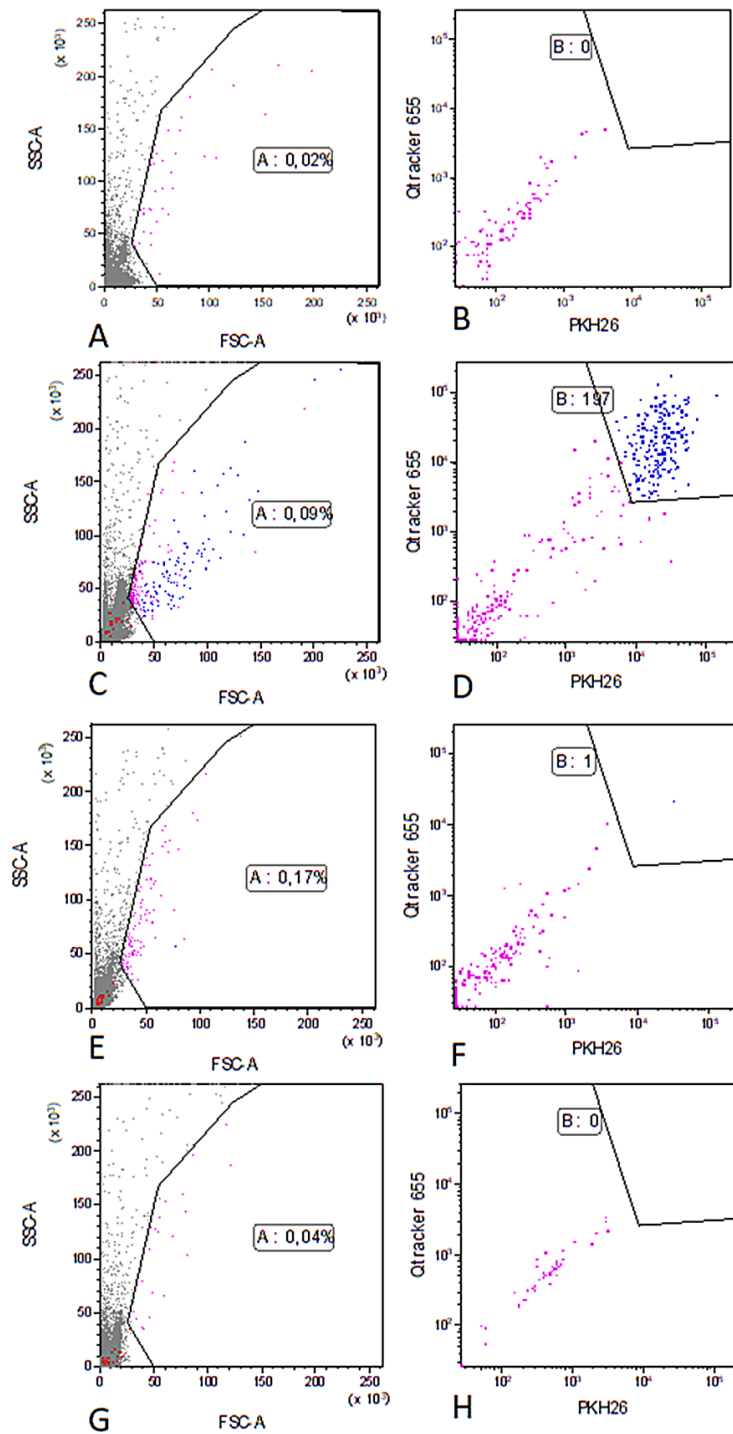


Figure A3. Example of flow cytometry results of reservoir samples. Results shown in forward and side scatter cytograms and fluorescence signal strength cytograms of Qtracker655 and PKH26. (A) T = 0 sample moment, FSC-A, SSC-A cytogram, purple dots represent cells that fall within the MSC gating; 0.02% of all cells. (B) PKH26 and Qtracker655 cytogram of t = 0 sample, purple dots represent particles that fall in the auto fluorescence range. No dots visible in the MSC range gate. (C) T = 60 sample moment, FSC-A, SSC-A cytogram, purple dots represent cells that fall within the MSC gating; 0.09% of all cells. (D) PKH26 and Qtracker655 cytogram of t = 60 sample moment, purple dots represent particles that fall in the auto fluorescence range, blue dots represent cells that fall within the MSC range gate; 0.22%. (E) T = 240 sample moment, FSC-A, SSC-A cytogram, purple dots represent cells that fall within the MSC gating; 0.17% of all the cells. (F) PKH26 and Qtracker655 cytogram of t = 240 sample moment, purple dots represent particles that fall in the auto fluorescence range, blue dot represents a cell that falls within the MSC range gate; 0.06%. (G) T = 420 sample moment, FSC-A, SSC-A cytogram, purple dots represent cells that fall within the MSC gating; 0.04% of all counted cells. (H) PKH26 and Qtracker655 cytogram of T = 420 sample moment, purple dots represent particles that fall in the auto fluorescence range, no dots visible in the MSC range gate.

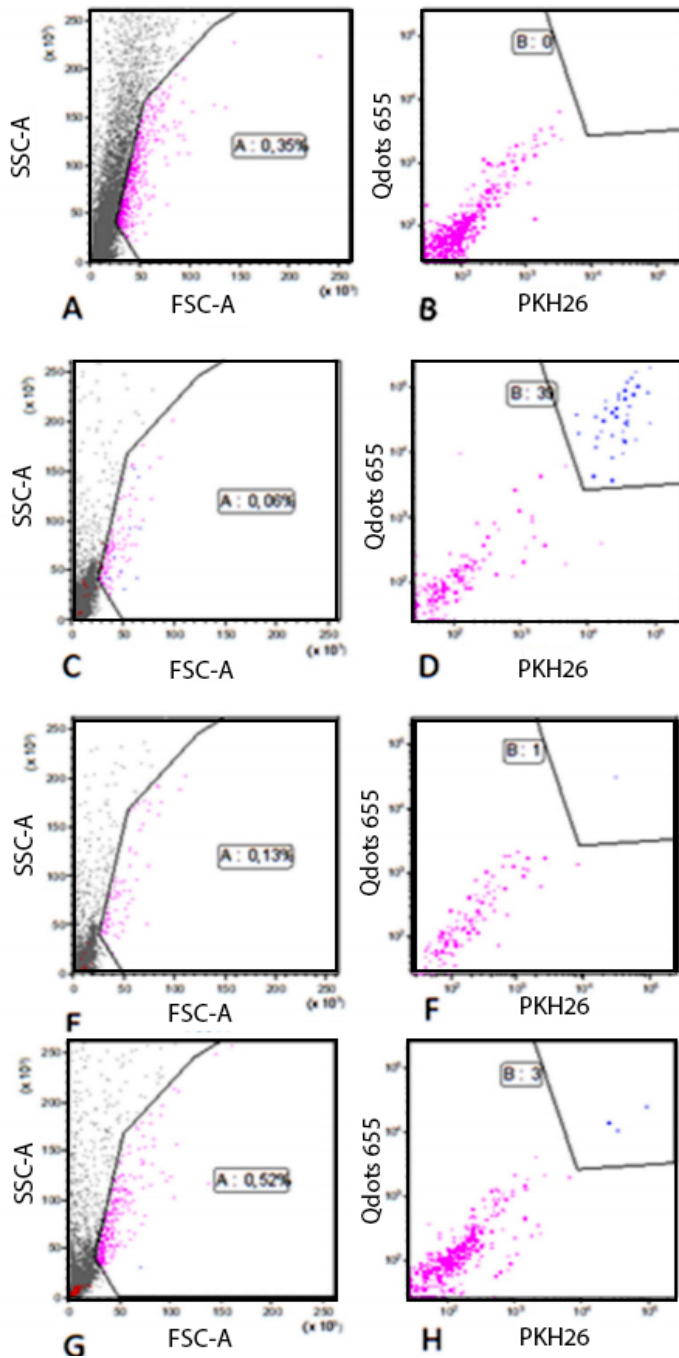


Figure A4. Example of flow cytometry results of arterial tubing samples. (A) T = 0 sample moment, FSC-A, SSC-A cytogram, purple dots represent cells that fall within the MSC gating; 0.35% of all counts. (B) PKH26 and Qtracker655 cytogram of T = 0 sample, purple dots represent particles that fall in the auto fluorescence range, no dots visible in the MSC range gate. (C) T = 60 sample moment, FSC-A, SSC-A cytogram, purple dots represent cells that fall within the MSC gating; 0.06% of all the cells. (D) PKH26 and Qtracker655 cytogram of T = 60 sample moment, purple dots represent particles that fall in the auto fluorescence range, blue dots represent cells that fall within the MSC range gate; 6.5% of the counted particles. (E) T = 240 sample moment, FSC-A, SSC-A cytogram, purple dots represent cells that fall within the MSC gating; 0.13% of all cells. (F) PKH26 and Qtracker655 cytogram of T = 240 sample moment, purple dots represent particles that fall in the auto fluorescence range, blue dot represents the cell that fall within the MSC range gate; 0.08% of the counted particles. (G) T = 420 sample moment, FSC-A, SSC-A cytogram, purple dots represent cells that fall within MSC gating; 0.52% of all counted cells. (H) PKH26 and Qtracker655 cytogram of T = 420 sample moment, purple dots represent particles that fall in the auto

fluorescence range, the blue dots represent cells with a double fluorescent label that fall within the MSC gating; 0.06% of the counted particles.

References

1. Moers, C.; Leuvenink, H.G.D.; Ploeg, R.J. Donation after cardiac death: Evaluation of revisiting an important donor source. *Nephrol Dial. Transpl.* 2010, 25, 666–673.
2. Moers, C.; Leuvenink, H.G.D.; Ploeg, R.J. Donation after cardiac death: Evaluation of revisiting an important donor source. *Nephrol Dial. Transpl.* 2010, 25, 666–673.
3. Nicholson, M.L.; Metcalfe, M.S.; White, S.A.; Waller, J.A.; Doughman, T.M.; Horsburgh, T.; Feehally, J.; Carr, S.J.; Veitch, P.S. A comparison of the results of renal transplantation from non–heart-beating, conventional cadaveric, and living donors. *Kidney Int.* 2000, 58, 2585–2591.
4. Hosgood, S.A.; van Heurn, E.; Nicholson, M.L. Normothermic machine perfusion of the kidney: Better conditioning and repair? *Transpl. Int.* 2015, 28, 657–664.
5. Bon, D.; Chatauret, N.; Giraud, S.; Thuillier, R.; Favreau, F.; Hauet, T. New strategies to optimize kidney recovery and preservation in transplantation. *Nat. Rev. Nephrol.* 2012, 8, 339–347.
6. Hosgood, S.A.; Barlow, A.D.; Yates, P.J.; Snoeijs, M.G.J.; van Heurn, E.L.; Nicholson, M.L. A pilot study assessing the feasibility of a short period of normothermic preservation in an experimental model of non heart beating donor kidneys. *J. Surg. Res.* 2011, 171, 283–290.
7. Kern, S.; Eichler, H.; Stoeve, J.; Klüter, H.; Bieback, K. Comparative analysis of mesenchymal stem cells from bone marrow, umbilical cord blood, or adipose tissue. *Stem Cells.* 2006, 24, 1294–1301.
8. Dominici, M.; Le Blanc, K.; Mueller, I.; Slaper-Cortenback, I.; Marini, F.; Krause, D.; Deans, R.; Keating, A.; Prockop, D.J.; Horwitz, E. Minimal criteria for defining multipotent mesenchymal stromal cells. The International Society for Cellular Therapy position statement. *Cytotherapy* 2006, 8, 315–317.
9. Casiraghi, F.; Remuzzi, G.; Perico, N. Mesenchymal stromal cells to promote kidney transplantation tolerance. *Curr. Opin. Organ. Transpl.* 2014, 19, 47–53.
10. De Vries, D.K.; Schaapherder, A.F.M.; Reinders, M.E.J. Mesenchymal stromal cells in renal ischemia/reperfusion injury. *Front. Immunol.* 2012, 3, 162.
11. Casiraghi, F.; Perico, N.; Cortinovis, M.; Remuzzi, G. Mesenchymal stromal cells in renal transplantation: Opportunities and challenges. *Nat. Rev. Nephrol.* 2016, 12, 241–253.
12. Franquesa, M.; Hoogduijn, M.J.; Reinders, M.E.; Eggenhofer, E.; Engela, A.U.; Mensah, F.K.; Torras, J.; Pileggi, A.; van Kooten, C.; Mahon, B.; et al. Mesenchymal Stem Cells in Solid Organ Transplantation (MiSOT) Fourth Meeting: Lessons Learned from First Clinical Trials. *Transplantation* 2013, 96, 234–238.
13. Reinders, M.E.J.; van Kooten, C.; Rabelink, T.J.; de Fijter, J.W. Mesenchymal Stromal Cell Therapy for Solid Organ Transplantation. *Transplantation* 2017, 102, 35–43.
14. Hoogduijn, M.J.; Roemeling-van Rhijn, M.; Engela, A.U.; Korevaar, S.S.; Mensah, F.K.; Franquesa, M.; de Bruin, R.W.; Betjes, M.G.; Weimar, W.; Baan, C.C. Mesenchymal stem cells induce an inflammatory response after intravenous infusion. *Stem Cells Dev.* 2013, 22, 2825–2835.
15. Sierra-Parraga, J.M.; Eijken, M.; Hunter, J.; Moers, C.; Leuvenink, H.G.D.; Møller, B.; Ploeg, R.J.; Baan, C.C.; Jespersen, B.; Hoogduijn, M.J. Mesenchymal stromal cells as anti-inflammatory and regenerative mediators for donor kidneys during normothermic machine perfusion. *Stem Cells Dev.* 2017, 26, 1162–1170.
16. Satchell, S.C.; Braet, F. Glomerular endothelial cell fenestrations: An integral component of the glomerular filtration barrier. *Am. J. Physiol. Ren Physiol.* 2009, 296, F947–F956.

MSC are Delivered to Glomeruli after Infusion during NMP

17. Ge, J.; Guo, L.; Wang, S.; Zhang, Y.; Cai, T.; Zhao, R.C.; Wu, Y. The Size of Mesenchymal Stem Cells is a Significant Cause of Vascular Obstructions and Stroke. *Stem Cell Rev.* 2014, 10, 295–303.
18. Scott, R.P.; Quaggin, S.E. The cell biology of renal filtration. *JCB* 2015, 209, 199–210.
19. Taghizadeh, R.R.; Cetrulo, K.J.; Cetrulo, C.L. Collagenase Impacts the Quantity and Quality of Native Mesenchymal Stem/Stromal Cells Derived during Processing of Umbilical Cord Tissue. *Cell Transplant.* 2018, 27, 181–193.
20. Mckee, C.; Chaudhry, G.R. Advances and challenges in stem cell culture. *Colloids Surfaces B Biointerfaces* 2017, 159, 62–77.
21. Eggenhofer, E.; Luk, F.; Dahlke, M.H.; Hoogduijn, M.J. The life and fate of mesenchymal stem cells. *Front. Immunol.* 2014, 5, 1–6.
22. Luk, F.; Korevaar, S.S.; Roemeling-van Rhijn, M.R.; Franquesa, M.; Strini, T.; van den Engel, S.; Garqesha, M.; Roy, D.; Dor, F.J.; Horwitz, E.M.; et al. Inactivated Mesenchymal Stem Cells Maintain Immunomodulatory Capacity. *Stem Cells Dev.* 2016, 25, 1342–1355.
23. Mansilla, E.; Marin, G.H.; Sturla, F.; Drago, H.E.; Gil, M.A.; Salas, E.; Gardiner, M.C.; Piccinelli, G.; Bossi, S.; Salas, E.; et al. Human mesenchymal stem cells are tolerized by mice and improve skin and spinal cord injuries. *Transplant. Proc.* 2005, 37, 292–294.
24. Toma, C.; Pittenger, M.F.; Cahill, K.S.; Byrne, B.J.; Kessler, P.D. Human mesenchymal stem cells differentiate to a cardiomyocyte phenotype in the adult murine heart. *Circulation* 2002, 105, 93–98.
25. Grinnemo, K.; Mansson, A.; Dellgren, G.; Klingberg, D.; Wardell, E.; Drvota, V.; Tammik, C.; Holgersson, J.; Ringdén, O.; Sylvén, C.; et al. Xenoreactivity and engraftment of human mesenchymal stem cells transplanted into infarcted rat myocardium. *J. Thorac. Cardiovasc. Surg.* 2004, 127, 1293–1300.
26. Mordant, P.; Nakajima, D.; Kalaf, R.; Iskender, I.; Maahs, L.; Behrens, P.; Coutinho, R.; Iyer, R.K.; Davies, J.E.; Cypel, M.; et al. Mesenchymal stem cell treatment is associated with decreased perfusate concentration of interleukin-8 during ex vivo perfusion of donor lungs after 18-hour preservation. *J. Hear. Lung Transplant.* 2016, 35, 1245–1254.
27. Li, J.; Ezzelarab, M.B.; Cooper, D.K. Do Mesenchymal Stem Cells Function Across Species Barriers? *Xenotransplantation* 2012, 19, 273–285.
28. Venema, L.H.; Brat, A.; Moers, C.; Hart, N.A.; Ploeg, R.J.; Hannaert, P.; Minor, T.; Leuvenink, H.G.D. Effects of oxygen during long-term hypothermic machine perfusion in a porcine model of kidney donation after circulatory death. *Transplantation* 2019, 1.
29. Bagul, A.; Hosgood, S.A.; Kaushik, M.; Kay, M.D.; Waller, H.L.; Nicholson, M.L. Experimental renal preservation by normothermic resuscitation perfusion with autologous blood. *Br. J. Surg.* 2008, 95, 111–118.
30. Chen, C.; Hou, J. Mesenchymal stem cell-based therapy in kidney transplantation. *Stem Cell Res. Ther.* 2016, 7, 16.
31. McDonald, C.A.; Oehme, D.; Pham, Y.; Kelly, K.; Itescu, S.; Gibbon, A.; Jenkin, G. Evaluation of the safety and tolerability of a high-dose intravenous infusion of allogeneic mesenchymal precursor cells. *Cytotherapy* 2015, 17, 1178–1187.

Chapter 8

Summary and general discussion



Summary

More and better-quality kidneys from deceased donors could minimize transplantation waiting lists for patients with end-stage kidney disease. Expansion of the organ donor acceptance criteria results in enlargement of the donor organ pool but may impact the transplantation outcome. In fact, marginal donor kidney transplantation is associated with a higher incidence of delayed graft function, as well as decreased graft and patient survival. In order to overcome this, innovative strategies are adopted to improve the quality and performance of donor kidneys as well as the transplantation outcome. The use of cold machine perfusion to preserve kidneys until transplantation has been proven to be better than static cold storage, improving the transplantation outcome. Extracorporeal organ perfusion platforms and particularly machine perfusion at body temperature allow conditioning and treatment of the perfused organ to improve its quality prior to transplantation. Specifically, normothermic machine perfusion (NMP) resuscitates the kidney's metabolism and opens the window to simultaneous perfusion and treatment as the function of the kidney is monitored. Therefore, this setting enables the possibility for cell therapy to treat organs on a pump. Mesenchymal stromal cells (MSC) have been proven to ameliorate kidney injury in animal models. Moreover, phase I clinical trials showed that MSC therapy is safe in patients with end stage renal disease and after transplantation. The mechanisms by which MSC mediate their immunoregulatory and tissue regenerative capacities are not completely understood. After intravenous (IV) infusion, the most commonly used method for MSC delivery, these cells exert immunomodulatory effects without migrating to the target organ and in spite of their short lifespan, they possess long-term immunoregulatory actions. In **chapter 3** it was demonstrated that after IV infusion, MSC are captured in the lung microvasculature when tested in a murine model. Moreover, 24 hours after infusion, more than 90 % of the infused MSC were dead and mainly present in the lungs with a low percentage in the liver. Dead MSC were phagocytosed by monocytes, as MSC membrane fragment-containing monocytes were detected in lungs, blood stream and liver, suggesting that monocytes transport MSC fragments from lung to liver. Upon MSC phagocytosis, monocytes underwent polarization towards a regulatory phenotype. *In-vitro*, these MSC-primed monocytes were able to induce regulatory T cells proliferation suggesting that this is one of the mechanisms through which MSC exert long-lasting immunomodulatory effect in spite of their short lifespan after IV infusion. To bypass the lung microvasculature barrier and explore a more targeted treatment for regeneration, a

different delivery route was tested in **chapter 4**. MSC were infused via the renal artery in a renal ischemia reperfusion injury (IRI) porcine model. The aim of this study was to evaluate the feasibility of this administration route and the fate of MSC after infusion. Immediately after administration, MSC were present in the renal cortex, particularly in the glomeruli, which contained different numbers of MSC. Also, MSC were found around tubular structures in renal cortex and medulla, presumably in the capillaries surrounding these structures. During renal intra-arterial infusion, a small percentage of MSC was not retained in the kidney and these cells were detected in the venous outflow. Analysis of lung tissue showed a hundred times lower amount of MSC than in the renal cortex, suggesting the suitability of this administration route to prevent off-target delivery. After ending intra-arterial infusion, MSC remained alive for at least 8 hours. After 2 weeks only 1 % of the infused MSC were detectable in the kidney. MSC were retained in the kidney through a passive mechanism which did not require MSC adhesion capacity, as inactivated MSC, that lost the ability to adhere, also retained in the kidney.

As MSC were delivered via intra-arterial infusion, the first cell type that they will interact with are the endothelial cells of the vascular bed. In **chapter 5**, the MSC regenerative properties were studied to assess their potential to reduce the effect of hypoxia and reoxygenation injury on endothelial cells. For this, cell-to-cell interaction and soluble factor secretion were studied. MSC displayed an active migratory and adhesive capacity to human umbilical vein endothelial cells (HUVEC) mediated by CD29 and CD44 present on the membrane of MSC. After endothelial injury, the combination of physical and paracrine interaction of MSC with HUVEC decreased injury markers on the endothelial cell membrane, oxidative stress levels and the permeability of the injured HUVEC monolayer. Moreover, MSC had the capacity to diminish the effect of hypoxic injury by improving HUVEC wound healing capacity and restoring their angiogenic potential. In addition, the secretome of MSC mildly repaired these two characteristics, though not to the same extent as physical and paracrine interaction of MSC and HUVEC combined. *In-vitro* experiments showed that MSC have the capacity to migrate through a monolayer of injured endothelial cells toward an injury chemokine secreted, e.g. by the kidney upon injury.

In **chapter 6** the reparative effects of MSC on endothelial cells were tested mimicking NMP conditions. Under these conditions, allogeneic MSC are cryopreserved and thawed, and kept in suspension in the perfusion solution used during kidney perfusion. MSC from human and

Chapter 8

porcine origin were studied, as the porcine model is a common and useful kidney transplantation model. Adipose tissue-derived human MSC survival was not affected by the freezing, defrosting cycle or as a result of being in suspension in perfusion fluid. However, the combination of cryopreservation and thawing and perfusion fluid composition decreased MSC survival and their capacity to adhere to endothelial cells. Regardless of these results, human MSC maintained their pro-angiogenic effect on endothelial cells in perfusion fluid, suggesting that they could be suitable for kidney treatment during machine perfusion. Adipose tissue-derived porcine MSC from subcutaneous adipose tissue were affected in a different manner by the same NMP conditions.

In **chapter 7**, MSC were infused during NMP into porcine kidneys for the first time. The aim of this study was to evaluate the feasibility of this administration method to deliver potentially therapeutic MSC to donor kidneys before transplantation. Infusion of labelled MSC showed a mainly cortical, heterogeneous distribution of MSC in well perfused kidneys. In addition, living MSC were observed in glomeruli at 6 hours after administration. Kidneys were metabolically active during perfusion as oxygen and glucose were consumed and urine was being produced. Thus, no macroscopic nor hemodynamic defects were observed in kidneys after MSC infusion during NMP.

Discussion

Mesenchymal stromal cells (MSC) have been extensively studied for their immunomodulatory and regenerative properties in the fields of kidney disease and transplantation [1-4]. The success of MSC treatment to ameliorate different conditions such as renal fibrosis or tubular atrophy in pre-clinical studies [5, 6] has led to the translation of these studies to patients [7-10]. In these clinical trials, it has been shown that MSC therapy is safe, while the regenerative capacities of MSC and the mechanisms of action after administration remained questionable and need further research.

In this thesis, the potential of MSC therapy delivered during normothermic machine perfusion (NMP) to regenerate damage produced by hypoxia-reoxygenation to donor kidneys was investigated. We evaluated the fate of MSC after intravenous infusion and administration via the renal artery *in-vivo* and *ex-vivo*, the mechanisms of action involved in their reparative effect on damaged endothelial cells and how the conditions necessary for infusion during NMP may affect the regenerative profile of MSC.

Intravenous (IV) infusion of MSC has been proven inefficient to deliver MSC to the kidney [11] as these cells are caught in the lung microvasculature [12]. Moreover, their short lifespan after entrapment challenged the understanding of the mechanisms involved in the immunomodulatory effects of MSC [13]. In chapter 3 of this thesis, it was demonstrated that MSC are phagocytosed by monocytes after IV infusion. This led to a phenotype shift in monocytes towards an anti-inflammatory phenotype. These monocytes induced the expansion of regulatory T cells [14], explaining the long-term immunomodulatory effect of MSC after IV administration. These results indicate that the short survival rate of MSC after entrapment in the lungs do not prevent their immunomodulatory effects. Although, it has been demonstrated in different models that MSC-mediated regeneration occurs when the injured tissue and MSC are in close proximity [15-19].

With the objective to ensure the delivery of MSC to the injured kidney, several studies have opted to infuse MSC through the renal artery [9, 20]. In chapter 4, the fate of MSC after renal intra-arterial infusion was studied. A semi-quantitative method to calculate numbers of MSC delivered to the kidney was developed, which enabled MSC delivery quantification, allowing better dosing studies to assess the therapeutic effect of MSC on injured kidneys. This is of importance as pre-clinical and clinical trials correlate the observed effects of MSC therapy with the infused dose of MSC, but these studies did not measure the actual number of cells in the

kidney. In line with previous studies [21, 22], chapter 4 showed that MSC are mainly delivered to the renal cortex and especially to glomeruli but also to the capillaries around the tubules in renal cortex and medulla after infusion via the renal artery. The efficacy of MSC therapy is directly correlated with the administered dose however, this is also a limitation as there is a limit to the number of MSC that can be safely infused [23, 24]. Therefore, it is of importance to study the maximum effective and safe dosage for MSC therapy in animal models. One of the hypotheses is that MSC migrate into the damaged interstitium after infusion and release regenerative factors leading to renal repair. The study by Allen *et al.* showed that MSC transmigrate through the endothelium *in-vivo* but the mechanisms involved are still not clear [25].

Upon infusion, MSC interact with the organ's vasculature. The capacity of MSC to bind to endothelial cells (EC) has been previously described [26], however, the specific pathways involved in MSC-EC communication have not been fully unraveled. In chapter 5 of this thesis it was determined that CD29 and CD44 are two mediators of MSC-EC interaction. These cell adhesion molecules are constitutively expressed on the MSC membrane [27]. It was described that these molecules also mediate the migration of MSC towards injured tissue [28]. Transmigration of MSC through endothelium towards the parenchyma has been reported to occur through mechanisms similar to leukocyte infiltration [26, 29]. Binding of MSC to endothelial cells involves E-selectin and vascular cell adhesion molecule 1 (VCAM-1), the respective ligands of CD29 and CD44 [30, 31]. Proof of this interaction comes from *in-vitro* studies demonstrating their involvement by blocking experiments [32]. Animal studies describe that also other molecules are involved in MSC transmigration suggesting that in patients, various molecules and pathways are involved in this interaction [26]. The development of animal models with tagged vascular adhesion molecules could be useful to identify the novel molecules and pathways responsible for MSC transmigration [33, 34], enabling improved MSC delivery efficiency after infusion. Preconditioning of MSC during *in-vitro* culture procedures or via genetic modification upregulate adhesion molecules on the membrane of MSC [35-37]. The stimulation of molecules involved in MSC-EC interplay may grant them increased adhesion to EC and possibly enhanced invasion of the damaged tissue and therefore potentially improve the immunoregulatory and regenerative effect of MSC. In the literature, there is no consensus about whether cell to cell recognition or the paracrine effect of MSC is the main mechanism behind the immunomodulatory and regenerative effects

of MSC. In chapter 5 it was demonstrated that both mechanisms are necessary for the regenerative action of MSC on hypoxic and inflamed endothelial cells. However, MSC have been shown to modulate the host immune response upon cell to cell interaction with monocytes [12, 38] or to promote renal repair via the release of their secretome in acute kidney injury [15]. This highlights that different mechanisms may be of importance for different reparative responses, depending on the type of cell and type of injury involved. Dissecting the mechanisms of action of MSC may allow the use of specific components of MSC for therapy, such as whole cells (chapter 5), conditioned medium [24] and natural [39] or artificial [40, 41] extracellular vesicles. The determination of the main MSC regenerative mechanism for each application may increase the effectivity of MSC therapy and avoid possible drawbacks.

In order to benefit from the regenerative properties of MSC, these cells were delivered *ex-vivo* via the renal artery to the kidney during NMP (chapter 7). MSC delivery efficiency and its possible beneficial and detrimental effects on kidney perfusion and renal function were monitored. Although MSC were mainly delivered to glomeruli in the renal cortex, this affected neither the hemodynamic profile nor the metabolism of the kidney during perfusion [42]. The possibility to infuse MSC during NMP allows loading of the kidney with MSC and may enable MSC-mediated renal repair due to the active metabolism of MSC in normothermic conditions. NMP initiates regenerative processes in the kidney, which can be monitored during perfusion without the need for intervention in the patient [43, 44]. On top of the beneficial effects of NMP, MSC therapy might further improve kidney quality and improve the transplantation outcome. As demonstrated in chapter 5, MSC are able to repair the injury that endothelial cells suffer after hypoxia and reoxygenation by decreasing the concentration of reactive oxygen species and recovering endothelial function. The use of MSC during *ex-vivo* perfusion of organs other than the kidney has been explored before. MSC administration during NMP of rat and porcine lungs led to the reduction of oxidative damage and concentration of pro-inflammatory cytokines [24, 45]. Additionally, MSC infused during porcine liver *ex-vivo* perfusion were retained in the liver and were metabolically active during the normothermic phase of the perfusion [46]. MSC administration during *ex-vivo* perfusion of discarded human kidneys has been shown to reduce the production of inflammatory cytokines by the kidney tissue and to promote renal regeneration [47]. This result led to the first in man trial testing a

Chapter 8

combination of allogeneic MSC therapy and a device-based continuous renal replacement therapy for the treatment of acute kidney injury (clinicaltrials.gov/NCT03015623).

The regenerative mechanisms of MSC described *in-vitro* are affected by external conditions required for MSC therapy during NMP. In order to deliver MSC therapy to donor kidneys during NMP, cells must be isolated from healthy individuals, which leads to donor differences, extensively expanded *in-vitro* and cryopreserved to ensure that the treatment is readily available. The effect of the conditions necessary to use MSC as a therapeutic product in the clinic have an impact on MSC phenotype and metabolism and might hinder MSC therapeutic properties [48-51], but it has not been fully explored yet. Phase I clinical trials using MSC as a therapeutic product have described the safety of MSC infusion to the patients. However, there is no strong data supporting MSC beneficial effects. This might be due, among other reasons, to the lack of standardization in MSC experimentation. The natural heterogeneity of MSC subpopulations is emphasized by the use of MSC from different sources. MSC from bone marrow, adipose tissue or umbilical cord are only some examples and MSC have been shown to display differences according to their origin. Moreover, MSC from elderly or sick individuals have been proven to be less effective [52, 53], forcing the use of allogeneic MSC of healthy individuals. However, MSC are not as immunoprivileged as previously thought and may elicit an immune response in the recipient [54, 55]. In addition, as mentioned before, *in-vitro* culture conditions are far from close to the conditions during clinical administration. The use of animal products and enzymatic treatments for MSC *in vitro* culture and testing is not compatible with the development of advanced therapy medical products [56], which requires that cellular therapeutic products are minimally manipulated, and therefore the approval from drug agencies to use and commercialize these products might be difficult. Since several exogenous factors may greatly impact MSC biological properties and eventually their therapeutic abilities, optimized protocols for MSC isolation and *ex vivo* preparation for clinical use need to be well established and standardized [57] as we intended to do in chapter 6.

For our project and most studies delivering MSC therapy, the effect of the cryopreservation time and the composition of the solution in which MSC therapy is delivered to patients is a concern as it may have detrimental effects on the success of the therapy [58, 59]. In chapter 6 the conditions necessary to infuse MSC during NMP were mimicked and the effect on MSC was assessed. In line with the literature, MSC had a different behavior after a cryopreservation and thawing cycle, compared to freshly cultured MSC. Also, the perfusion solution influenced

the survival and capacity of MSC to adhere to endothelial cells. One important consequence is a reduced adhesion capacity to endothelial cells, which may result in a decreased MSC-EC interaction.

However, these conditions and their effect on MSC properties cannot be avoided when developing an off-the-shelf GMP grade therapeutic product. *In-vitro* modification of MSC to increase the expression of adhesion molecules before storage might counteract this effect and rescue the physical interaction of MSC and endothelial cells. The modification of the perfusion solution is also an alternative. The composition of the perfused liquid is specifically designed to allow renal metabolism and function but it is not meant for MSC survival and function. Preconditioning of MSC and the adaptation of the cryopreservation and perfusion solutions might be an important step to pursue the use of MSC during NMP of donor kidneys.

Future perspectives

MSC are used for their immunoregulatory and regenerative properties in a wide range of applications. However, the underlying mechanisms of action in each of these applications remain unclear, which prevent us from advancing and improving MSC therapy. In this thesis, we describe a novel therapeutic option combining MSC and NMP to improve the quality of donor kidneys before transplantation by examining the fate of MSC after intravenous and intra-arterial infusion, their mechanisms of action and the possible drawbacks of this technique on MSC regenerative properties.

Our results suggest that infusion of MSC during NMP is a potential therapeutic option to repair kidneys on a pump. However, the conflicting efficacy data from large animal models demonstrated that in depth mapping of the effects of MSC is necessary to understand the beneficial effects of MSC therapy and also why some studies lack efficacy. Infusion of MSC during NMP delivers the cells to the kidney but no regenerative effect has been associated with MSC infusion yet. The determination of the most effective dose, which maintains the safety of MSC infusion is necessary to advance this technique. Likewise, the composition of the perfusion solution used during NMP must be optimized to support both renal function and MSC survival and metabolism. For instance, it should be evaluated if the use of a cellular oxygen carrier can provide adequate oxygen levels and prevent hypoxic conditions in both the kidney and MSC. Moreover, it is important to design a perfusion solution which enables a perfusion time long enough to allow MSC to start a regenerative action before the kidney is transplanted. At this point, the host immune system starts interacting with MSC allocated throughout the kidney, which may elicit an immune regulatory effect and decrease the extent of the inflammation but it may also lead to the clearance of MSC from the kidney. This interaction needs to be described to understand the short- and long-term fate of MSC after transplantation of the kidney. In addition, MSC modification for an enhanced expression and secretion of molecules of interest might lead to an improved therapeutic effect of MSC therapy, enabling the determination of specific pathways involved in MSC regenerative effect and counteracting the effect of the conditions concomitant with MSC infusion during NMP. A deeper understanding of the mechanism of action of MSC and the confirmation of the reparative effect of MSC in animal models will allow patients to receive better quality and better functioning kidneys treated with MSC during NMP.

Conclusions

- IV infused MSC do not reach the kidney.
- Immunomodulatory effect of MSC after intravenous infusion occurs indirectly, upon MSC phagocytosis by monocytes.
- MSC-primed monocytes induce the generation of regulatory T cell and promote long term immunoregulatory effects.
- Infusion of MSC via the renal artery is effective to deliver MSC to the renal cortex and medulla.
- Physical and paracrine interaction of MSC with endothelial cells repair the damage associated with hypoxia and reoxygenation.
- Cryopreservation and NMP solution composition impact MSC survival and metabolism but support their use as therapy for renal repair.
- MSC delivery during NMP is feasible and effective to deliver MSC to the kidney without altering renal function at the studied dose.

References

1. Reinders, M.E., et al., Autologous bone marrow-derived mesenchymal stromal cells for the treatment of allograft rejection after renal transplantation: results of a phase I study. *Stem Cells Transl Med*, 2013. 2(2): p. 107-11.
2. Abumoawad, A., et al., In a Phase 1a escalating clinical trial, autologous mesenchymal stem cell infusion for renovascular disease increases blood flow and the glomerular filtration rate while reducing inflammatory biomarkers and blood pressure. *Kidney Int*, 2020. 97(4): p. 793-804.
3. Reinders, M.E., et al., Autologous bone marrow derived mesenchymal stromal cell therapy in combination with everolimus to preserve renal structure and function in renal transplant recipients. *J Transl Med*, 2014. 12: p. 331.
4. Perico, N., et al., Mesenchymal stromal cells and kidney transplantation: pretransplant infusion protects from graft dysfunction while fostering immunoregulation. *Transpl Int*, 2013. 26(9): p. 867-78.
5. Franquesa, M., et al., Mesenchymal stem cell therapy prevents interstitial fibrosis and tubular atrophy in a rat kidney allograft model. *Stem Cells Dev*, 2012. 21(17): p. 3125-35.
6. Casiraghi, F., et al., Localization of mesenchymal stromal cells dictates their immune or proinflammatory effects in kidney transplantation. *Am J Transplant*, 2012. 12(9): p. 2373-83.
7. Perico, N., et al., Long-Term Clinical and Immunological Profile of Kidney Transplant Patients Given Mesenchymal Stromal Cell Immunotherapy. *Front Immunol*, 2018. 9: p. 1359.
8. Mudrabettu, C., et al., Safety and efficacy of autologous mesenchymal stromal cells transplantation in patients undergoing living donor kidney transplantation: a pilot study. *Nephrology (Carlton)*, 2015. 20(1): p. 25-33.
9. Pan, G.H., et al., Low-dose tacrolimus combined with donor-derived mesenchymal stem cells after renal transplantation: a prospective, non-randomized study. *Oncotarget*, 2016. 7(11): p. 12089-101.
10. Erpicum, P., et al., Infusion of third-party mesenchymal stromal cells after kidney transplantation: a phase I-II, open-label, clinical study. *Kidney Int*, 2019. 95(3): p. 693-707.
11. Eggenhofer, E., et al., Mesenchymal stem cells are short-lived and do not migrate beyond the lungs after intravenous infusion. *Front Immunol*, 2012. 3: p. 297.
12. de Witte, S.F.H., et al., Immunomodulation By Therapeutic Mesenchymal Stromal Cells (MSC) Is Triggered Through Phagocytosis of MSC By Monocytic Cells. *Stem Cells*, 2018. 36(4): p. 602-615.
13. de Witte, S.F.H., et al., Cytokine treatment optimises the immunotherapeutic effects of umbilical cord-derived MSC for treatment of inflammatory liver disease. *Stem Cell Res Ther*, 2017. 8(1): p. 140.
14. Xu, L., et al., Randomized trial of autologous bone marrow mesenchymal stem cells transplantation for hepatitis B virus cirrhosis: regulation of Treg/Th17 cells. *J Gastroenterol Hepatol*, 2014. 29(8): p. 1620-8.
15. Morigi, M., et al., Life-sparing effect of human cord blood-mesenchymal stem cells in experimental acute kidney injury. *Stem Cells*, 2010. 28(3): p. 513-22.
16. Berry, M.F., et al., Mesenchymal stem cell injection after myocardial infarction improves myocardial compliance. *Am J Physiol Heart Circ Physiol*, 2006. 290(6): p. H2196-203.
17. Akram, K.M., et al., Mesenchymal stem cells promote alveolar epithelial cell wound repair in vitro through distinct migratory and paracrine mechanisms. *Respir Res*, 2013. 14(1): p. 9.

18. Li, Q., et al., In vivo tracking and comparison of the therapeutic effects of MSCs and HSCs for liver injury. *PLoS One*, 2013. 8(4): p. e62363.
19. Carlsson, P.O., et al., Preserved beta-cell function in type 1 diabetes by mesenchymal stromal cells. *Diabetes*, 2015. 64(2): p. 587-92.
20. Saad, A., et al., Autologous Mesenchymal Stem Cells Increase Cortical Perfusion in Renovascular Disease. *J Am Soc Nephrol*, 2017. 28(9): p. 2777-2785.
21. Franchi, F., et al., Mesenchymal Stromal Cells Improve Renovascular Function in Polycystic Kidney Disease. *Cell Transplant*, 2015. 24(9): p. 1687-98.
22. Behr, L., et al., Intra renal arterial injection of autologous mesenchymal stem cells in an ovine model in the postischemic kidney. *Nephron Physiol*, 2007. 107(3): p. p65-76.
23. Cai, J., et al., Maximum efficacy of mesenchymal stem cells in rat model of renal ischemia-reperfusion injury: renal artery administration with optimal numbers. *PLoS One*, 2014. 9(3): p. e92347.
24. Mordant, P., et al., Mesenchymal stem cell treatment is associated with decreased perfusate concentration of interleukin-8 during ex vivo perfusion of donor lungs after 18-hour preservation. *J Heart Lung Transplant*, 2016. 35(10): p. 1245-1254.
25. Allen, T.A., et al., Angiopeliosis as an Alternative Mechanism of Cell Extravasation. *Stem Cells*, 2017. 35(1): p. 170-180.
26. Chamberlain, G., et al., Mesenchymal stem cells exhibit firm adhesion, crawling, spreading and transmigration across aortic endothelial cells: effects of chemokines and shear. *PLoS One*, 2011. 6(9): p. e25663.
27. Dominici, M., et al., Minimal criteria for defining multipotent mesenchymal stromal cells. The International Society for Cellular Therapy position statement. *Cytotherapy*, 2006. 8(4): p. 315-7.
28. Herrera, M.B., et al., Exogenous mesenchymal stem cells localize to the kidney by means of CD44 following acute tubular injury. *Kidney Int*, 2007. 72(4): p. 430-41.
29. Teo, G.S.L., et al., Mesenchymal stem cells transmigrate between and directly through tumor necrosis factor- α -activated endothelial cells via both leukocyte-like and novel mechanisms. *Stem cells (Dayton, Ohio)*, 2012. 30(11): p. 2472-2486.
30. Ruster, B., et al., Mesenchymal stem cells display coordinated rolling and adhesion behavior on endothelial cells. *Blood*, 2006. 108(12): p. 3938-44.
31. Ley, K., et al., Getting to the site of inflammation: the leukocyte adhesion cascade updated. *Nat Rev Immunol*, 2007. 7(9): p. 678-89.
32. Teo, G.S., et al., Mesenchymal stem cells transmigrate between and directly through tumor necrosis factor-alpha-activated endothelial cells via both leukocyte-like and novel mechanisms. *Stem Cells*, 2012. 30(11): p. 2472-86.
33. Camirand, G., et al., Multiphoton intravital microscopy of the transplanted mouse kidney. *Am J Transplant*, 2011. 11(10): p. 2067-74.
34. Winkler, F., et al., PECAM/eGFP transgenic mice for monitoring of angiogenesis in health and disease. *Sci Rep*, 2018. 8(1): p. 17582.
35. Chou, K.J., et al., CD44 fucosylation on mesenchymal stem cell enhances homing and macrophage polarization in ischemic kidney injury. *Exp Cell Res*, 2017. 350(1): p. 91-102.

Chapter 8

36. Ferreira, J.R., et al., Mesenchymal Stromal Cell Secretome: Influencing Therapeutic Potential by Cellular Pre-conditioning. *Front Immunol*, 2018. 9: p. 2837.
37. Philipp, D., et al., Preconditioning of bone marrow-derived mesenchymal stem cells highly strengthens their potential to promote IL-6-dependent M2b polarization. *Stem Cell Res Ther*, 2018. 9(1): p. 286.
38. Luk, F., et al., Inactivated mesenchymal stem cells maintain immunomodulatory capacity. *Stem Cells Dev*, 2016.
39. Bruno, S., et al., Renal Regenerative Potential of Different Extracellular Vesicle Populations Derived from Bone Marrow Mesenchymal Stromal Cells. *Tissue Eng Part A*, 2017. 23(21-22): p. 1262-1273.
40. Timaner, M., et al., Therapy-Educated Mesenchymal Stem Cells Enrich for Tumor-Initiating Cells. *Cancer Res*, 2018. 78(5): p. 1253-1265.
41. Goncalves, F.D.C., et al., Membrane particles generated from mesenchymal stromal cells modulate immune responses by selective targeting of pro-inflammatory monocytes. *Sci Rep*, 2017. 7(1): p. 12100.
42. Pool, M., et al., Infusing Mesenchymal Stromal Cells into Porcine Kidneys during Normothermic Machine Perfusion: Intact MSCs Can Be Traced and Localised to Glomeruli. *Int J Mol Sci*, 2019. 20(14).
43. Weissenbacher, A., et al., Twenty-four-hour normothermic perfusion of discarded human kidneys with urine recirculation. *Am J Transplant*, 2019. 19(1): p. 178-192.
44. Weissenbacher, A., et al., Urine Recirculation Improves Hemodynamics and Enhances Function in Normothermic Kidney Perfusion. *Transplant Direct*, 2020. 6(4): p. e541.
45. Pacienza, N., et al., Mesenchymal Stem Cell Therapy Facilitates Donor Lung Preservation by Reducing Oxidative Damage during Ischemia. *Stem Cells Int*, 2019. 2019: p. 8089215.
46. Versteegen, M.M.A., et al., First Report on Ex Vivo Delivery of Paracrine Active Human Mesenchymal Stromal Cells to Liver Grafts During Machine Perfusion. *Transplantation*, 2020. 104(1): p. e5-e7.
47. Brasile, L., et al., Potentiating Renal Regeneration Using Mesenchymal Stem Cells. *Transplantation*, 2019. 103(2): p. 307-313.
48. Czaplá, J., et al., The effect of culture media on large-scale expansion and characteristic of adipose tissue-derived mesenchymal stromal cells. *Stem Cell Res Ther*, 2019. 10(1): p. 235.
49. Laitinen, A., et al., The effects of culture conditions on the functionality of efficiently obtained mesenchymal stromal cells from human cord blood. *Cytotherapy*, 2016. 18(3): p. 423-37.
50. Chinnadurai, R., et al., Actin cytoskeletal disruption following cryopreservation alters the biodistribution of human mesenchymal stromal cells in vivo. *Stem Cell Reports*, 2014. 3(1): p. 60-72.
51. Gurruchaga, H., et al., Cryopreservation of Human Mesenchymal Stem Cells in an Allogeneic Bioscaffold based on Platelet Rich Plasma and Synovial Fluid. *Sci Rep*, 2017. 7(1): p. 15733.
52. Liu, M., et al., Adipose-Derived Mesenchymal Stem Cells from the Elderly Exhibit Decreased Migration and Differentiation Abilities with Senescent Properties. *Cell Transplant*, 2017. 26(9): p. 1505-1519.
53. Pachon-Pena, G., et al., Obesity Determines the Immunophenotypic Profile and Functional Characteristics of Human Mesenchymal Stem Cells From Adipose Tissue. *Stem Cells Transl Med*, 2016. 5(4): p. 464-75.
54. Joswig, A.J., et al., Repeated intra-articular injection of allogeneic mesenchymal stem cells causes an adverse response compared to autologous cells in the equine model. *Stem Cell Res Ther*, 2017. 8(1): p. 42.

55. Ankrum, J.A., J.F. Ong, and J.M. Karp, Mesenchymal stem cells: immune evasive, not immune privileged. *Nat Biotechnol*, 2014. 32(3): p. 252-60.
56. Ducret, M., et al., Production of Human Dental Pulp Cells with a Medicinal Manufacturing Approach. *J Endod*, 2015. 41(9): p. 1492-9.
57. Lukomska, B., et al., Challenges and Controversies in Human Mesenchymal Stem Cell Therapy. *Stem Cells Int*, 2019. 2019: p. 9628536.
58. Parsha, K., et al., Mesenchymal stromal cell secretomes are modulated by suspension time, delivery vehicle, passage through catheter, and exposure to adjuvants. *Cytotherapy*, 2017. 19(1): p. 36-46.
59. Moll, G., et al., Cryopreserved or Fresh Mesenchymal Stromal Cells: Only a Matter of Taste or Key to Unleash the Full Clinical Potential of MSC Therapy? *Adv Exp Med Biol*, 2016. 951: p. 77-98.

Chapter 9

Nederlandse samenvatting



Het gebrek aan voldoende donor nieren voor transplantatie leidt al jarenlang tot wachtlijsten voor patiënten met eindstadium nierziekte. De uitbreiding van de criteria waaraan orgaandonoren moeten voldoen om als acceptabele nierdonoren te worden beschouwd, resulteert in een toename van het aantal beschikbare organen. Echter, niertransplantatie met uitgebreide criteria donor organen is geassocieerd met een afname van transplantaat functioneren en overleving. Om orgaan functie van uitgebreide criteria donoren te verbeteren, worden verschillende strategieën onderzocht. Het gebruik van koude machine-perfusie van transplantaat organen is effectief gebleken om organen te preserven, maar is hoogstwaarschijnlijk niet voldoende om de functie van lage kwaliteit organen drastisch te verbeteren. Normotherme machine-perfusie (NMP) maakt metabolisme van organen mogelijk en kan gecombineerd worden met andere behandelingen waarbij de nierfunctie live gemonitord kan worden. NMP maakt het mogelijk om celtherapie toe te passen op nieren vóór transplantatie. Mesenchymale stromale cellen (MSC) zijn voorloper cellen voor bot, vet en kraakbeen en stimuleren daarnaast herstel van weefsels door grote hoeveelheden groeifactoren uit te scheiden. Tevens hebben MSC een sterk immuun regulerend effect. De hypothese is dat MSC een positief effect kunnen hebben voor de behandeling van nierziekten. De meest gebruikelijke toedieningstechniek voor MSC, intraveneuze infusie (IV), heeft echter verschillende nadelen. In **hoofdstuk 2** laten we zien dat na IV-infusie alle MSC worden vastgehouden in de microcapillairen van de longen, vanwege de grootte van de cellen. Na 24 uur zijn de MSC verdwenen. We hebben aangetoond dat monocyten in de bloedbaan MSC herkennen en fagocyteren. Door dit proces nemen MSC een regulerend fenotype aan dat de productie van regulatoire T-lymfocyten bevordert. Deze regulerende T cellen hebben een langere levensduur dan geïnfundeerde MSC en dit is mogelijk een van de mechanismen waardoor MSC een immunomodulerend effect op lange termijn kunnen hebben, ondanks hun korte overleving na IV infusie. Om te voorkomen dat MSC vast komt te zitten in de longen en te zorgen dat ze de transplantatie nier bereiken, heeft **hoofdstuk 3** de toediening van MSC via de nierslagader in een varkensmodel bestudeerd. De MSC bevonden zich voornamelijk in de glomeruli, de functionele eenheden van de nier cortex waar bloed wordt gefilterd, maar ook in de haarvaten rond de tubuli. De MSC werden op dezelfde manier vastgehouden als in de longen, waarschijnlijk doordat ze te groot zijn om door de capillairen te bewegen. Na aflevering in de nier werd waargenomen dat MSC ten minste acht uur in de nier overleefden, maar dat na twee weken minder dan 1% van de toegediende MSC in de nier aanwezig was.

Nadat een toedieningsroute was geïdentificeerd waarmee MSC in contact kunnen komen met beschadigd nierweefsel, was de volgende stap het bestuderen van het effect dat MSC op het weefsel hebben. Na infusie komen MSC in contact met het nierendotheel en daarom werden in **hoofdstuk 4** de regeneratieve effecten van MSC op endotheliale cellen die waren beschadigd door ischemie bestudeerd. We konden aantonen dat MSC in een in vitro model kunnen migreren naar beschadigde endotheelcellen en aan deze cellen binden, waarbij met name twee moleculen op het MSC-oppervlak, CD29 en CD44 een belangrijke rol spelen. Er werd waargenomen dat MSC schade-markers in aangetaste endotheelcellen zoals oxidatieve stress kunnen verminderen. Bovendien herstelden MSC de functie van beschadigde endotheelcellen, waardoor de stabiliteit van de endotheel cellagen werd verhoogd en hun capaciteit om bloedvaatjes te vormen werd hersteld. Evenzo werd onderzocht of de gunstige effecten van MSC op endotheel cellen te wijten waren aan binding tussen de cellen of aan de werking van de vele moleculen die MSC uitscheiden. We konden vaststellen dat de uitgescheiden moleculen op zichzelf een klein effect op endotheel cellen hadden, en dat beide mechanismen zijn nodig om een volledig regeneratief effect te verkrijgen. In **hoofdstuk 5** onderzochten we of de regeneratieve eigenschappen van MSC behouden blijven als we de MSC onderwerpen aan de condities van NMP. Deze condities omvatten cryopreservatie en ontdoing, suspensie condities en opname in de vloeistof waarmee de nier wordt geperfuseerd. Er werd aangetoond dat invriezen en ontdooien de overleving van MSC vermindert en hun vermogen om zich aan endotheelcellen te hechten verkleint. Bovendien remde de perfusievloeistof gedeeltelijk het hechtvermogen van MSC aan endotheelcellen. MSC behielden echter de regeneratieve eigenschappen onder deze omstandigheden, wat suggereert dat ze geschikt zijn voor de behandeling van nieren tijdens NMP. Om deze reden werden in **hoofdstuk 6** MSC voor het eerst toegediend aan varkensnieren met behulp van NMP. MSC werden toegediend aan het begin van nierperfusie en na 6 uur werd de lokalisatie van de MSC en effecten op de nier geanalyseerd. MSC vertoonden een heterogene verdeling ondanks een goede perfusie van de nier, en bevonden zich voornamelijk in de glomeruli in de niercortex. De nieren vertoonden geen macroscopische afwijkingen of hemodynamische veranderingen. De nieren waren metaboolactief wat werd aangetoond door zuurstof en glucose consumptie en urine productie tijdens de perfusie.

Samenvattend ondersteunen de resultaten van het onderzoek beschreven in dit proefschrift het gebruik van MSC om endotheelbeschadiging in de nier te behandelen tijdens

Chapter 9

reconditionering van de nier met behulp van NMP. Dit proefschrift toont aan dat de infusie van MSC via de nierslagader haalbaar is en bij de gebruikte cel hoeveelheid niet tot schade aan de nier leidt. Bovendien worden de mechanismen beschreven waarmee MSC interacteren met beschadigde endotheelcellen om hun regeneratieve effect uit te oefenen, evenals het feit dat deze mechanismen worden bewaard onder de omstandigheden van NMP. Als geheel opent de kennis die in dit proefschrift wordt gegenereerd de deur naar de ontwikkeling van een protocol voor het herstel van nieren tijdens NMP voorafgaand aan hun transplantatie.

Chapter 10

Dansk resumé



lere og bedre nyrer fra afdøde donorer kan forkorte ventelisterne til transplantation for patienter med terminalt nyresvigt. Udvidelse af kriterier for accept af afdøde donorer øger antal donororganer, men kan forringe transplantationsresultaterne. Transplantation med nyrer fra "marginale" donorer er forbundet med højere incidens af forsinket igangsætning af transplanterede nyrer og nedsat overlevelse af nyren og patienten. For at modvirke dette tages innovative strategier i brug mhp. at forbedre kvalitet og funktion af donornyrer og forbedre transplantationsresultater. Hypoterm maskinperfusion til præservasjon af nyrer indtil transplantation er vist at kunne forbedre transplantationsresultater sammenlignet med kold statisk opbevaring. Ekstrakorporale organperfusionsplatforme og særligt maskinperfusion ved legemstemperatur gør "konditionering" og behandling af det perfunderede organ mulig mhp. at forbedre organkvaliteten før transplantation. Specifikt kan normoterm maskinperfusion (NMP) "genoplive" nyremetabolismen og dermed åbne et vindue for behandling, samtidigt med at funktionen af organet monitoreres. Dette kan muliggøre celleterapi af organer under NMP. Mesenkymale stromale celler (MSC) er vist at kunne udbedre nyreskader i dyremodeller. Hertil kommer at fase I kliniske testninger viste, at MSC-terapi er sikker givet til patienter med terminalt nyresvigt og efter transplantation. Mekanismerne hvorved MSC medierer deres immunregulatoriske og vævsregenerative effekter er ikke fuldt ud forstået. Efter intravenøs (IV) infusion, som er den mest almindelige metode til MSC-administration, udøver cellerne immunmodulatoriske effekter uden nødvendigvis at migrere til målorganet. Selvom MSC har korte levetider, har de langtids-immunregulatoriske effekter. I **kapitel 3** blev det i en musemodel demonstreret, at efter IV infusion blev MSC fanget i lungernes mikrovaskulatur. Desuden blev det vist, at 24 timer efter infusionen var mere end 90% af de infunderede MSC døde, og MSC fandtes især i lungerne med en lille procentdel i leveren. Døde MSC blev fagocyteret af monocytter, idet membranfragmenter fra MSC kunne demonstreres i monocytter i lunger, blodet og leveren, hvilket tyder på, at monocytter transporterer MSC-fragmenter fra lunger til lever. Efter fagocytose af MSC polariserede monocytterne sig henimod en regulatorisk fænotype. *In-vitro*, var disse MSC-påvirkede monocytter i stand til at inducere regulatorisk T-celleproliferation tydende på, at dette er en mekanisme, hvorved MSC kan udøve langvarig immunmodulerende effekt, trods kort levetid af MSC efter IV indgift. For at undgå, at MSC fanges i lungernes mikrovaskulatur, og udforske en mere organmålrettet regenerationsterapi, blev en anden administrationsmåde undersøgt i **kapitel 4**. MSC blev infunderet via nyrearterien i en porcin

renal iskæmi-reperfusionmodel. Målet med dette stadium var at evaluere praktisk anvendelighed af denne administrationsvej og MSC-skæbne. Straks efter indgiften kunne MSC findes i renal cortex, navnlig i glomeruli, som indeholdt forskellige antal MSC. MSC kunne også påvises omkring tubulære strukturer i renal cortex og medulla, formentlig i kapillærer omkring disse strukturer. Under renal intraarterial infusion var der en lille procentdel af MSC, der ikke blev retineret i nyren, og disse celler kunne påvises i det venøse blod fra nyren. Analyse af lungevæv viste, at den organmålrettede behandling var lykkedes, idet indholdet af MSC i lungerne var minimalt. Efter afslutning af den intraarterielle infusion forblev MSC i live i mindst 8 timer. Efter 2 uger var kun 1 % af de infunderede MSC påviselige i nyren. MSC blev retineret i nyren ved en passiv mekanisme uafhængig af MSC's evne til at adhærere til andre celler, da inaktiverede MSC, som har mistet denne adhæsionsevne, også blev retineret i nyren.

Når MSC administreres intraarterielt, er den første celletype, de vil interagere med være endothelceller i karvæggen. I **kapitel 5** blev MSC's regenerative egenskaber studeret mhp. at vurdere, hvorvidt MSC kan reducere iskæmi-reperfusionsskader på endothelceller. Med dette formål blev celle til celle interaktion og sekretion af opløselige parakrine substanser studeret. MSC udviste aktive migratoriske og adhæsionsegenskaber i forhold til endothelceller fra human umbilikalvene (HUVEC), og det var medieret af CD29 og CD44 på MSC cellemembranen. Efter endothelskade, kunne kombinationen af fysisk og parakrin interaktion af MSC med HUVEC nedsætte skadesmarkører på endothelcellemembranen, oxidativt stress niveau og permeabilitet af et skadet HUVEC monocellelag. Ydermere havde MSC kapacitet til at mindske effekten af hypoksisk skade ved at forbedre HUVEC helingsevne, og MSC kunne genopbygge HUVECs angiogenetiske potentiale. Desuden reparerede secernerede substanser fra MSC på de to måder, men ikke så effektivt, som når der både var fysisk og parakrin interaktion mellem MSC og HUVEC. *In-vitro* forsøg viste, at MSC har kapacitet til at migrere gennem et monocellelag af skadede endothelceller henimod kemokiner, der f.eks. kunne være secerneret af nyrevæv udsat for iskæmisk skade.

I **kapital 6** blev MSC's reparative effekter på endothelceller testet ved at efterligne NMP omstændigheder. Under disse omstændigheder vil allogene MSC være kryopræservede og optøet og derefter holdt i suspension i nyreperfusionsvæsken. Både humane MSC og porcine MSC blev undersøgt, idet porcine modeller, herunder for nyretransplantation er hyppigt anvendte. Overlevelsen af fedtvævsderiverede humane MSC var ikke påvirket af nedfrysning og optøning eller af at være i suspension i perfusionsvæsken. Imidlertid blev MSC overlevelsen

Chapter 10

og cellernes evne til at adhærere til endothelceller forringet af kombinationen af cryopræservation og optøning. Trods disse resultater bevarede humane MSC deres pro-angiogenetiske effekt på endothelceller i perfusionsvæsken, hvilket tyder på, at MSC vil kunne anvendes til behandling af nyrer under maskinperfusion. Fedtvævsderiverede porcine MSC fra subcutis blev påvirket anderledes under de samme NMP-forhold.

I **kapitel 7** blev humane MSC for første gang infunderet i porcine nyrer under NMP for at studere gennemførlighed ved denne administrationsmetode. Infusion af mærkede MSC viste en heterogen fordeling af MSC især til cortex i velperfunderede nyrer. Levende MSC blev observeret i glomeruli 6 timer efter indgift. Nyrerne var metabolisk aktive, idet ilt og glucose blev forbrugt, og der var urinproduktion. Således blev der ikke observeret makroskopiske eller hæmodynamiske defekter i nyrerne efter MSC infusion under NMP.

Chapter 11

Resumen en español



El trasplante renal es el tratamiento óptimo para los pacientes con insuficiencia renal en fase terminal. Sin embargo, la falta de riñones disponibles para ser trasplantados a todos los pacientes incrementa su el tiempo que pasan en la lista de espera. Una solución para este problema ha sido ser menos estrictos con los criterios de donación del órgano, dando como resultado un aumento de órganos disponibles, pero también una disminución de la supervivencia del injerto.

Para superar este obstáculo, se han adoptado diferentes estrategias como el uso de la perfusión extracorpórea del riñón para preservar y reacondicionar el órgano antes del trasplante. Alguna de estas plataformas, como la perfusión extracorpórea normotérmica (NMP, por sus siglas en inglés), reanuda el metabolismo del riñón permitiendo su perfusión y la administración de tratamientos mientras que se monitoriza la función del riñón.

La terapia celular se basa en administrar células propias o de terceros a un tejido dañado para tratar una enfermedad a modo de medicamento. Uno de los tipos celulares mas utilizados son las células mesenquimales estromales (MSC, por sus siglas en inglés). Estas son células que se encuentran distribuidas por todos los tejidos del cuerpo y promueven la reparación de tejidos dañados de manera natural. Se ha demostrado que la terapia celular con MSC es útil para tratar enfermedades renales como la fibrosis renal o la atrofia tubular, así como como para mejorar el resultado del trasplante renal, como lo han demostrado una gran cantidad de estudios en modelos animales y ensayos clínicos.

La terapia celular con MSC se administra comúnmente por vía intravenosa y tiene efectos inmunomoduladores y regenerativos. En el **capítulo 3** demostramos que después de infundir MSC por vía intravenosa, la mayoría de células quedan retenidas en los pulmones, debido a su gran tamaño comparado con la red de microcapilares del pulmón. Después de 24 horas, los monocitos reconocen a las MSC y las fagocitan, adoptando un fenotipo regulador que activa la producción de linfocitos T reguladores. Este es, presumiblemente, uno de los mecanismos a través del cual las MSC ejercen un efecto inmunomodulador a largo plazo a pesar de su corta supervivencia tras su infusión. Para evitar que las MSC se queden atrapadas en los pulmones y asegurarnos que son entregadas al riñón, en el **capítulo 4** se estudió la administración de MSC a través de la arteria renal en un modelo porcino. Las MSC se localizaron principalmente en los glomérulos, la unidad funcional del córtex renal donde se filtra la sangre, pero también en los capilares alrededor de los túbulo. Las MSC fueron retenidas de manera similar a como lo son en los pulmones, a través de un mecanismo pasivo. Una vez en el riñón, se observó que

las MSC sobrevivieron durante al menos ocho horas y después de dos semanas, menos de un 1% de la cantidad infundida pudo ser detectada en el riñón. Una vez identificada una ruta de infusión que permite que las MSC entren en contacto con el tejido dañado del riñón, el siguiente paso fue estudiar el efecto que las MSC pueden tener en él. Después de su infusión, las MSC entraron en contacto con el endotelio del riñón y por ello en el **capítulo 5** se estudiaron los efectos regenerativos de las MSC sobre células endoteliales dañadas por la hipoxia y reoxigenación que tienen lugar durante el proceso de trasplante. Demostramos que las MSC pueden migrar hacia células endoteliales dañadas e interactuar con ellas principalmente a través de dos moléculas que se encuentran en su superficie, CD29 y CD44. Una vez en contacto con las células dañadas, se observó que las MSC pueden reducir marcadores de daño en las células afectadas como el estrés oxidativo. Además, las MSC consiguieron que las células endoteliales dañadas recuperaran su función incrementando la estabilidad de las monocapas endoteliales y restaurando su potencial angiogénico. Del mismo modo, se estudió si los efectos beneficiosos de las MSC se debían al contacto físico entre células o a la acción de las numerosas moléculas que secretan las MSC. Pudimos determinar que, en algunos casos, las moléculas secretadas tuvieron un pequeño efecto sobre el daño, pero ambos mecanismos son necesarios para obtener un efecto regenerativo completo.

En el **capítulo 6** investigamos si estas propiedades regenerativas de las MSC se mantienen cuando sometemos a las MSC a las condiciones necesarias para ser administradas durante NMP. Estas condiciones comprenden estar en suspensión, ser criopreservadas y descongeladas y estar en contacto con la solución con la que se perfunde el riñón, que permite la reactivación del metabolismo renal. El proceso de congelación y descongelación disminuye la supervivencia de las MSC y su capacidad de adherirse a las células endoteliales. Además, el líquido de perfusión inhibió parcialmente la capacidad de MSC de adherirse a células endoteliales. Sin embargo, las MSC conservaron sus propiedades regenerativas y pro-angiogénicas en estas condiciones, lo que sugiere que son adecuadas para el tratamiento de riñones durante NMP antes de ser trasplantados. Por este motivo, en el **capítulo 7** MSC fueron infundidas por primera vez en riñones porcinos administrándolas durante NMP. Las MSC fueron infundidas al comienzo de la perfusión del riñón y tras 6 horas se analizó la eficacia de este procedimiento. Se observó una distribución heterogénea de las MSC que se localizaron principalmente en el córtex renal, ocupando los glomérulos a pesar de una buena perfusión del riñón. A pesar de esto, los riñones no presentaron ninguna alteración macroscópica ni

Chapter 11

cambios hemodinámicos o metabólicos ya que estaban bien perfundidos y consumían oxígeno y glucosa y producían orina durante la perfusión.

En resumen, los resultados de la investigación descrita en esta tesis respaldan el uso de las MSC para tratar el daño endotelial en el riñón durante su reacondicionamiento mediante NMP. En esta disertación se demuestra que la infusión de MSC a través de la arteria renal es factible y efectiva. Por otra parte, se describen los mecanismos por los que las MSC interactúan con células endoteliales dañadas para ejercer su efecto regenerativo y que estos mecanismos son preservados en las condiciones de NMP, permitiendo su infusión a través de esta vía. En su conjunto, el conocimiento generado en esta tesis abre la puerta al desarrollo de una nueva técnica que combina la terapia celular con MSC y la NMP para la regeneración de riñones isquémicos antes de su trasplante.

Appendices

Curriculum vitae

PhD Portfolio

Listo f Publications

Acknowledgements



Curriculum vitae

Jesús María Sierra Párraga was born on 6 November 1992 in Córdoba, Spain. In 2010 he finished his secondary school studies at Medina Azahara Secondary School College in Córdoba. In the same year, he started his bachelor in Biotechnology at the Universitat Politècnica de València. During his studies, he specialized in the so-called red biotechnology, comprising the bio-pharmaceutical applications of animal and human research. Afterwards, he enrolled in the master program Translational



Biomedical Research at the Universidad de Córdoba. He performed his final internship under the supervision of prof. dr. Immaculada Concepción Herrera Arroyo and dr. Sonia Nogueras Martín at the department of Hematology and Cell Therapy at the Instituto Maimónides de Investigación Biomédica de Córdoba. In September 2015, he obtained his master degree. In May 2016, he started his joint PhD program at the Nephology and Transplantation laboratory of the Internal Medicine Department at Erasmus MC and the Department of Clinical Medicine at the Aarhus University in Aarhus, Denmark under the supervision of prof. dr. Carla C. Baan, prof. dr. Bente Jespersen and dr. Martin J. Hoogduijn. The results of his research are described in this thesis.

PhD portfolio

| | |
|-------------------------------|---|
| Name PhD student: | Jesús María Sierra Párraga |
| Erasmus MC department: | Internal Medicine, section Nephrology and Transplantation |
| Research school: | Postgraduate School Molecular Medicine |
| PhD period: | May 2016 – March 2020 |
| Supervisors: | Prof. dr. Carla C. Baan and Prof. dr. Bente Jespersen |
| Co-supervisor: | Dr. Martin J. Hoogduijn |

Congresses and meetings

| | |
|------|--|
| 2020 | International Society Cell & Gene Therapy Congress 2020. Paris, France. (Poster)** |
| 2020 | Dutch transplantation society Congress. Roermond, the Netherlands. (Oral) |
| 2019 | European Cell Therapy and Organ Regeneration Section from ESOT Congress. Copenhagen, Denmark. (Two oral) |
| 2019 | International Society Cell & Gene Therapy Congress 2019. Melbourne, Australia. (Two Posters) * |
| 2019 | Dutch transplantation society Congress. Amsterdam, the Netherlands. (Two oral) |
| 2019 | Science Days from Internal Medicine Department from Erasmus MC. Sint- Michielsgestel, the Netherlands. (Poster) |
| 2018 | The Transplantation Society Congress. Madrid, Spain. (Poster + Oral) |
| 2018 | Joint Dutch and Belgian transplantation societies Congress. Rotterdam, the Netherlands. (Two Oral) |
| 2018 | Science Days from Internal Medicine Department from Erasmus MC. Antwerp, Belgium. (Poster) |
| 2017 | European Society for Organ Transplantation Congress. Barcelona, Spain. (Pitch + Oral) |

PhD Portfolio

- 2017 European Hematology Society's Meeting on 'Scientific Meeting on Shaping the Future of Mesenchymal Stromal Cells Therapy. Amsterdam, the Netherlands. (Oral)
- 2016 Mesenchymal Stem Cells in Solid Organ Transplantation, MiSOT. Regensburg, Germany.

* Accepted for poster presentation; not presented.

** Presented by a colleague.

Awards

- 2019 Erasmus Trustfonds for Conference Participation.
- 2019 NTV training grant granted by Nederlandse Transplantatie Vereniging
- 2019 Novartis Transplantation Award 2019 for the best scored publication: Immunomodulation By Therapeutic Mesenchymal Stromal Cells (MSC) Is Triggered Through Phagocytosis of MSC By Monocytic Cells granted by the Dutch Transplantation Society.
- 2018 Mentor-Mentee award for the abstract: Monocytic Cells Phagocytose Therapeutic Mesenchymal Stem Cells, which Induces Polarization, Relocation and Immune Regulation granted during the TTS Congress 2018.
- 2017 Winner of Elevator Pitch session for an extended Oral presentation granted during ESOT Congress 2017.
- 2017 Travel grant for a term of Research at Health for international PhD students by Aarhus University.

Participation in educational courses

- 2019 Confocal microscopy training. *
- 2019 Responsible Conduct of Research. Graduate School of Health, Aarhus University.
- 2019 Epigeum online course on. Research Integrity - Biomedical Sciences.

- 2018 The SCORE PhD course: Stem cells, Organoids and Regenerative Medicine. *
- 2018 Integrity in Science for PhD students Erasmus MC. *
- 2017 The Monocytes: origins, destinations, functions and diagnostic targets. *
- * Erasmus MC, Rotterdam

Teaching activities

- 2016 - 2019 Introduction of our laboratory and main performed techniques to Master students (Infection and immunity Master).
- 2016-2017 Supervision of HLO student during final internship (9 months) at Dept. Internal Medicine, Erasmus Medical Centre, Rotterdam, the Netherlands.

Memberships

- 2016-present Dutch Transplantation Society
- 2016-present European Association for Organ transplantation
- 2016-present The Transplantation Society
- 2017 European Hematology Association

Miscellaneous

- 2020 Reviewer of scientific articles for Clinical and Translational Medicine
- 2019 Cover design for Stem Cells and Development Journal (Volume: 28 Issue 18: September 16, 2019)
- 2019 Reviewer of scientific articles for Scientific Reports

List of publications

- 2020 **Reparative Effect of Mesenchymal Stromal Cells on Endothelial Cells After Hypoxic and Inflammatory Injury.**
- Jesus M Sierra-Parraga, Ana Merino, Marco Eijken, Henri Leuvenink, Rutger J. Ploeg, Bjarne K. Møller, Bente Jespersen, Carla C. Baan, Martin J. Hoogduijn. (Submitted for publication in Stem Cells Translational Medicine)
- 2019 **First Report on Ex vivo Delivery of Paracrine Active Human Mesenchymal Stromal Cells to Liver Grafts During Machine Perfusion.**
- Verstegen, Monique M.A.^{1,*}; Mezzanotte, Laura^{2,*}; Ridwan, R. Yanto²; Wang, Kairong^{1,5}; de Haan, Jubi³; Schurink, Ivo J.¹; **Sierra Parraga, Jesús M.**⁴; Hoogduijn, Martin⁴; Kessler, Benedikt M.⁶; Huang, Honglei⁶; Hall, Sean R.R.⁷; IJzermans, Jan N.M.¹; Löwik, Clemens W.G.M.²; van der Laan, Luc J.W.¹; de Jonge, Jeroen¹ Transplantation: October 11, 2019 - Volume Online First - Issue - p doi: 10.1097/TP.0000000000002986.
- 2019 **Mesenchymal Stromal Cells Are Retained in The Renal Cortex Independently of Their Metabolic State After Renal Intra-Arterial Infusion.**
- Jesus M. Sierra-Parraga, Anders Munk, Christine Andersen, Stine Lohmann, Cyril Moers, Carla C. Baan, Rutger J. Ploeg, Merel Pool, Anna K. Keller, Bjarne K. Møller, Henri Leuvenink, Martin J. Hoogduijn, Bente Jespersen, Marco Eijken. Stem Cells Dev. 2019 Aug 1. doi: 10.1089/scd.2019.0105
- 2019 **Infusing Mesenchymal Stromal Cells into Porcine Kidneys During Normothermic Machine Perfusion: Intact Mscs Can Be Traced and Localised To Glomeruli.**
- Merel Pool, Tim Eertman, **Jesus Sierra Parraga**, Nils 't Hart, Marieke Roemeling-van Rhijn, Marco Eijken, Bente Jespersen, Marlies Reinders, Martin Hoogduijn, Rutger Ploeg, Henri Leuvenink, Cyril Moers. Int J Mol Sci. 2019 Jul 23;20(14). pii: E3607. doi: 10.3390/ijms20143607.

- 2019 **Towards Precision Medicine in Bronchiectasis: What Is the Role Of Neutrophilic Elastase Determination?**
- Oscullo Yopez G, **Sierra-Párraga JM**, Posadas Blázquez T, Martínez-García M^Á. Eur Respir J. 2019 Jun 13;53(6). pii: 1900765. doi: 10.1183/13993003.00765-2019. Print 2019 Jun.
- 2019 **Effects of Normothermic Machine Perfusion Conditions on Mesenchymal Stromal Cells.**
- Sierra Parraga JM**, Rozenberg K, Eijken M, Leuvenink HG, Hunter J, Merino A, Moers C, Møller BK, Ploeg RJ, Baan CC, Jespersen B, Hoogduijn MJ. Front Immunol. 2019 Apr 10; 10:765. doi: 10.3389/fimmu.2019.00765. eCollection 2019.
- 2018 **Immunomodulation by Therapeutic Mesenchymal Stromal Cells (MSC) Is Triggered Through Phagocytosis of MSC By Monocytic Cells.**
- de Witte SFH^{*}, Luk F^{*}, **Sierra Parraga JM**, Gargesha M, Merino A, Korevaar SS, Shankar AS, O'Flynn L, Elliman SJ, Roy D, Betjes MGH, Newsome PN, Baan CC, Hoogduijn MJ. Stem Cells. 2018 Apr;36(4):602-615. doi: 10.1002/stem.2779. Epub 2018 Feb 1.
- 2017 **Mesenchymal Stromal Cells as Anti-Inflammatory and Regenerative Mediators for Donor Kidneys During Normothermic Machine Perfusion.**
- Sierra-Parraga JM**, Eijken M, Hunter J, Moers C, Leuvenink H, Møller B, Ploeg RJ, Baan CC, Jespersen B, Hoogduijn MJ. Stem Cells Dev. 2017 Aug 15;26(16):1162-1170. doi: 10.1089/scd.2017.003